ANNUAL REVIEW

INSTITUTE FOR MOLECULAR SCIENCE

1991

ANNUAL REVIEW

INSTITUTE FOR MOLECULAR SCIENCE

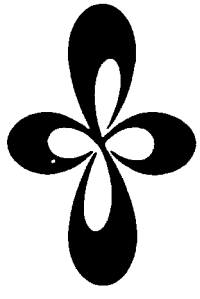

1991

Published by
Institute for Molecular Science
Okazaki National Research Institutes
Myodaiji, Okazaki 444, Japan
Phone 0564-54-1111
Telex 4537-475 KOKKEN J
Fax 0564-54-2254

IMS 1991

With the establishment of the Department of Vacuum UV Photoscience in April, 1991, Institute for Molecular Science reorganized its research departments. The new Department consists of the newly established laboratory, Laboratory of Reaction Dynamics and the two existing laboratories, Laboratory of Photochemistry and Laboratory of Interface Molecular Science. As the results IMS now consists of six research departments and seven research facilities.

Furthermore we are in the process of modifying the mission of the Equipment Development Center. A team of staff mostly from its machine shop is to develop original equipment for IMS — IMS Machines — in addition to their regular duties.

This is an important year from the viewpoint of the reorganization of the international cooperative research projects which IMS has been managing. The Japan-United States Cooperative Research Program on Solar Energy Conversion by Means of Photosynthesis which was implemented in 1981 is now extended for additional five years and, as the 15th Information Exchange Seminar, the Tenth Anniversary Symposium will be held in Okazaki in December, 1991. As to the Japan-United Kingdom Sicentific Cooperation implemented in 1981, the priority areas were reexamined in 1990. An increasing number of researchers are sent from UK with funds from the British Council. The Japan-Korea Scientific Cooperation implemented in 1984 is to be expanded through the new bilateral agreement on the Cooperation of Basic Scientific Research. In the field of molecular science, in addition to the existing long term exchange of scientists, short term (from two weeks to one month) exchanges will be started. Two new cooperative research projects between Japan and Spain and also between Japan and Israel will be added to the list of those that IMS has been managing.

In this year there has been large turnover of IMS staff. It is a great pleasure to announce that in coming March, 1992 seven graduated students in the Departments of Structural Molecular Science and Functional Molecular Science except to be awarded the first Ph. D. degrees from the Graduate University of Advanced Studies. Although it is a difficult task to accomplish two missions, the accumulation of the brilliant research achievements that erquire long, hard work and also the large turnover of personnel, it must continue to be done at IMS.

November, 1991

H. Inokuchi

Hiroo INOKUCHI
Director-General

CONTENTS

ORGANIZATION AND STAFF

Organization

The Institute for Molecular Science comprises twenty two research laboratories—each staffed by a professor, an associate professor, two research associates and several technical associates—, two research laboratories with foreign visiting professors, and six research facilities. The laboratories are grouped into six departments and one facility for coordination chemistry:

Department of Theoretical Studies	Theoretical Studies I
	Theoretical Studies II
	Theoretical Studies III[1)]
Department of Molecular Structure	Molecular Structure I
	Molecular Structure II[1)]
	Molecular Dynamics
Department of Electronic Structure	Excited State Chemistry
	Excited State Dynamics
	Electronic Structure[1)]
	Molecular Energy Conversion[2)]
Department of Molecular Assemblies	Solid State Chemistry
	Molecular Assemblies Dynamics
	Molecular Assemblies[1)]
Department of Applied Molecular Science	Applied Molecular Science I
	Applied Molecular Science II[1)]
	Physical Organic Chemistry[3)]
Department of Vacuum UV Photoscience	Photochemistry
	Chemical Dynamics
	Interface Molecular Science[3)]
	Synchrotron Radiation Research[2)]
Coordination Chemistry Laboratories	Synthetic Coordination Chemistry[3)]
	Complex Catalysis
	Functional Coordination Chemistry
	Coordination Bond[1)]
Research facilities are:	Computer Center
	Chemical Materials Center
	Instrument Center
	Low-Temperature Center
	Equipment Development Center
	Ultraviolet Synchrotron Orbital Radiation (UVSOR) Facility

1) Professors and associate professors are adjunct professors from other universities.
2) Research Laboratories with foreign visiting professors.
3) Professors, associate professors, and research associates, along with their positions, are transferred from other universities.

Scientific Staff

Hiroo INOKUCHI	**Professor, Director-General**

Department of Theoretical Studies

Theoretical Studies I

Keiji MOROKUMA	Professor
Iwao OHMINE	Associate Professor
Koichi YAMASHITA	Research Associate (–June '91)[1]
Masaki SASAI	Research Associate (–March '91)[2]
Nobuaki KOGA	Research Associate
Norihiro SHIDA	Research Associate
Yoshiaki AMATATSU	Technical Associate
Shinji SAITO	Technical Associate
Jerzy MOC	JSPS Post-doctoral Fellow (February '91–)
James L. ANCHELL	JSPS Post-doctoral Fellow (March '91–)
Djamaladdin G. MUSAEV	JSPS Post-doctoral Fellow (April '91–)
Simon MATHIEU	Post-doctoral Fellow
Xue-Kui LI	Post-doctoral Fellow (April '91–)
Hiroo FUKUNAGA	Visiting Research Fellow from Fuji Photo Film Co.
Tamiki KOMATSUZAKI	Graduate Student
Toshiaki FUJII	Graduate Student
Chizuru MUGURUMA	Graduate Student (April '91–)

Theoretical Studies II

Hiroki NAKAMURA	Professor
Keiichiro NASU	Associate Professor
Xin SUN	Adjunct Professor from Fudan University (July '90–July '91)
Masahiro IWAI	Research Associate (–June '91)
Kaoru IWANO	Research Associate
Masato SUZUKI	Technical Associate
Shoji TAKADA	Technial Associate (March '91–)
Itsuki BANNO	Technical Associate (April '91–)
Yasuji INADA	IMS Fellow (May '91–)
Masayoshi NAKANO	JSPS Post-Doctoral Fellow (April '91–)
Kee-Hag LEE	JSPS Post-Doctoral Fellow (June '91–)
Chayugan ZHU	Graduate Student (October '90–)
Kenichiro TSUDA	Graduate Student (April '91–)

Theoretical Studies III

Kizashi YAMAGUCHI	Adjunct Professor from Hokkaido University (April '91–)
Shinichi WATANABE	Adjunct Associate Professor from The University of Electro-Communications (April '91–)
Kenro HASHIMOTO	Research Associate (August '91–)
Kiyohiko SOMEDA	Research Associate

Department of Molecular Structure

Molecular Structure I

Shuji SAITO	Professor (April '91–)
Norio MORITA	Associate Professor
Asuka FUJII	Research Associate
Mitsutaka KUMAKURA	Technical Associate

Molecular Structure II

Takashi KUSHIDA	Adjunct Professor from Osaka Univ. (–March '91)
Hiroatsu MATSUURA	Adjunct Professor from Hiroshima Univ. (April '91–)
Tsutomu YABUZAKI	Adjunct Associate Professor from Kyoto Univ.
Takashi OGURA	Research Associate

Molecular Dynamics

Teizo KITAGAWA	Professor
Yasuo UDAGAWA	Associate Professor (–March '91)[3]
Keiji KAMOGAWA	Research Associate
Kazuyuki TOHJI	Research Associate (–March '91)[4]
Takanori MIZUSHIMA	Research Associate (–March '91)[5]
Tsuyoshi EGAWA	Research Associate (April '91–)
Misaki OKUNISHI	Research Associate
Shin-ichiro SATO	Technical Associate
Motoko ASANO-SOMEDA	IMS Fellow (–September '91)[6]
Shoji KAMINAKA	JSPS Post-doctoral Fellow
Hisashi HAYASHI	Graduate Student
Yasuhisa MIZUTANI	Graduate Student
Yoshinao SAKAN	Graduate Student
Satoshi TAKAHASHI	Graduate Student
Bhattacharjee RAMENDU	Visiting Scientist from St. Edmunds College, India (October '90–April '91)
James R. KINCAID	Visiting Scientist from Marquette Univ., USA (April '91–July '91)

Department of Electronic Structure

Excited State Chemistry

Keitaro YOSHIHARA	Professor
Yoshiyasu MATSUMOTO	Associate Professor
Hrvoje PETEK	Research Associate
Kyoichi SAWABE	Research Associate (December '90–)
Tohru KOBAYASHI	Technical Associate (–September '90)[7]
Shigeichi KUMAZAKI	Technical Associate (December '90–)
Hideki KANDORI	IMS Fellow
Takeshi SUZUMOTO	Visiting Research Fellow from Fuji Photo Film Co. Ltd.
Ryoji INABA	Graduate Student from the Univ. of Tokyo
Yutaka NAGASAWA	Graduate Student
Abderrazzak DOUHAL	JSPS Post-Dctoral Fellow
Bongsoo KIM	Visiting Scientist
Andrew BELL	JSPS Post-Doctoral Fellow
Klaus KEMNITZ	Visiting Scientist (March '91–)

Excited State Dynamics

Ichiro HANAZAKI	Professor
Nobuyuki NISHI	Associate Professor (–April '91)[8]
Masao TAKAYANAGI	Research Associate
Minoru SUMITANI	Research Associate (–September '90)[9]
Kazuhiko OHASHI	Research Associate (–August '91)[10]
Teruhiko NISHIYA	Technical Associate
Yoshihito MORI	Technical Associate (–March '91), Visiting Scientist (April '91–)
Prem K. SRIVASTAVA	Visiting Scientist
Pascal LABLANQUIE	Visiting Scientist
Nam-Soo LEE	Visiting Scientist from Chungbuk National University, Korea (December '90–February '91)
Anthony J. STACE	Visiting Scientist from The University of Sussex, U.K. (February '91–April '91)
Kazuhiro HONDA	Graduate Student
Takumi KOHNO	Graduate Student
Tetsuo SEKIGUCHI	Graduate Student
Tatsuo GEJO	Graduate Student
Noriaki OKAZAKI	Graduate Student

Electronic Structure

Michiya ITOH	Adjunct Professor from Kanazawa Univ.
Masaharu OKAZAKI	Adjunct Professor from Government Industrial Research Institute, Nagoya (—March '91)
Minoru SUMITANI	Adjunct Professor from Shizuoka Institute of Science & Technology (April '91—)
Kaoru SUZUKI	Research Associate

Molelcular Energy Conversion

Vaclav KUBEČEK	Visiting Associate professor from Technical University of Prague, Czechoslovakia (—September '91)

Department of Molecular Assemblies

Solid State Chemistry

Kyuya YAKUSHI	Professor
Kazushi KANODA	Associate Professor (April '91—)
Takashi IMAMURA	Research Associate (—March '91)[11]
Akito UGAWA	Research Associate
Ken-ichi IMAEDA	Technical Associate
Takashi IDA	Technical Associate (—March '91)[12]
Atsushi KAWAMOTO	IMS Fellow
Hideo YAMAKADO	Graduate Student
Kentaro IWASAKI	Graduate Student
Hideshi ISHII	Graduate Student from Univ. of Tokyo* (—August '91)

Molecular Assemblies Dynamics

Yusei MARUYAMA	Professor
Tamotsu INABE	Research Associate
Shinji HASEGAWA	Research Associate
Hajime HOSHI	Technical Associate
Shin-ichi SHAMOTO	Technical Associate (—March '91)[13]
Toshifumi TERUI	Graduate Student
Hironori OGATA	Graduate Student
Yoshihisa MORI	Graduate Student
Chikako NAKANO	Visiting Research Fellow
Kohji KAMIYA	Visiting Research Fellow (—August '91)[14]
Naoki NAKAMURA	Visiting Research Fellow from Toyota Motor Co. Ltd.

Molecular Assemblies

Satoshi HIRAYAMA	Adjunct Professor from Kyoto Institute of Technology (April '91—)
Kokichi OHSHIMA	Adjunct Associate Professor from Okayama Univ. (April '91—)
Takehiko MORI	Research Associate
Kenji FURUYA	Research Associate

Department of Applied Molecular Science

Applied Molecular Science I

Kazuhiro NAKASUJI	Professor
Kiyoshi ISOBE	Associate Professor
Koshiro TORIUMI	Reseach Associate (—March '91)[15]
Yoshiki OZAWA	Research Associate
Yasushi MORITA	Research Associate
Yoshihito HAYASHI	Technical Associate (—September '90)[16]
Jiro TOYODA	Technical Associate
Haruo AKASHI	JSPS Post-doctoral Fellow (—March '91)[17]
Ken-ichi SUGIURA	Graduate Student
Shotaro MATSUDA	Graduate Student from Ehime Univ. (April '91—December '91)
Youngkyu DO	Visiting Professor from Korea Advanced Institute of Science and Technology, Korea (December '90—February '91)
Tian-Wei ZHU	Visiting Professor from Innter Mongolia Normal Univ., China (March '91—August '91)

Bateer WANG	Visiting Professor from Innter Mongolia Normal Univ., China (March '91–August '91)
Kuming ZHAO	Visiting Professor from Innter Mongolia Normal Univ., China (March '91–August '91)

Applied Molecular Science II

Hideki SAKURAI	Adjunct Professor from Tohoku Univ. (–March '91)
Yumihiko YANO	Adjunct Professor from Gumma Univ. (April '91–)
Eiichi NAKAMURA	Adjunct Associate Professor from Tokyo Inst. of Tech. (–March '91)
Hiyoshizo KOTSUKI	Adjunct Associate Professor from Kochi Univ. (April '91–)
Hiroki OSHIO	Research Associate

Physical Organic Chemistry

Yuho TSUNO	Professor
Junji INANAGA	Associate Professor
Masaaki MISHIMA	Research Associate
Takeshi HANAMOTO	Research Associate
Yuji MIKATA	Graduate Student from Kyoto Univ.*
Kenji TAKEHARA	Graduate Student from Kyushu Univ.*
Katsuya SAKO	Graduate Student from Kyushu Univ.* (–March '91)
Yoshihiro SAEKI	Graduate Student from Kyushu Univ.*
Izumi AKASAKA	Graduate Student from Kyushu Univ.* (–March '91)
Yasuo YOKOYAMA	Graduate Student from Kyushu Univ.*
Yoshiyasu BABA	Graduate Student from Kyushu Univ.* (–March '91)
Kazuhide NAKATA	Graduate Student from Kyushu Univ.* (–March '91)
Yuichi SUGIMOTO	Graduate Student from Kyushu Univ.* (October '91–)

Department of Vacuum UV Photoscience

Photochemistry

Katsumi KIMURA	Professor
Kosuke SHOBATAKE	Associate Professor
Kiyohiko TABAYASHI	Research Associate
Katsuhiko OKUYAMA	Research Associate
Masahiko TAKAHASHI	Technical Associate
Martin COCKETT	JSPS Postdoctral Fellow (January '91–)
Kunikazu KONDO	Graduate Student from Nagoya Univ.* (–September '90)
Tatsuta MIYAKE	Graduate Student from Toyohashi Univ. of Technology* (April '90–March '91)
Hiroyuki OZEKI	Graduate Student
Haruhiko OHASHI	Graduate Student from Toyohashi Univ. of Technology*
Hiroshi YOSHIKAWA	Graduate Student
Yasuhiro IWANO	Graduate Student from Toyohashi Univ. of Technology* (April '90–March '91)

Chemical Dynamics

Koichiro MITSUKE	Associate Professor (April '91–)

Interface Molecular Science

Akira YOSHIDA	Professor (April '91–)
Shinri SATO	Associate Professor
Tatsuo MATSUSHIMA	Associate Professor from Hokkaido Univ. (–March '91)
Tadayoshi OHMORI	Research Associate from Hokkaido Univ. (–March '91)
Yuichi OHNO	Research Associate
Seigi MIZUNO	Research Associate (April '91–)
Yuji UKISU	Technical Associate
Kiyoshi NAGAI	Visiting Research Fellow (–November '90)[18]

Synchrotron Radiation Research

Xin SUN	Adjunct Professor from Fudan Univ., China (July '90–July '91)
Anvar A. ZAKHIDOV	Visiting Associate Professor from Uzbek Acad. of Sci., Tashkent USSR (December '90–October '91)

Coordination Chemistry Laboratories

Hitoshi OHTAKI	Director

Synthetic Coordination Chemistry

Yoshihiko KUSHI	Professor
Fumio KAWAIZUMI	Associate Professor
Tatsuya KAWAMOTO	Research Associate
Hideki MASUDA	Research Associate (–March '91)[19]
Matsuo NONOYAMA	Research Associate (April '91–)
Tamotsu SUGIMORI	Graduate Student from Nagoya Univ.
Hiroshi SHIMOMURA	Graduate Student from Osaka Univ.

Complex Catalysis

Hitoshi OHTAKI	Professor
Ei-ichi KIMURA	Adjunct Professor from Hiroshima Univ.
Ryuichi IKEDA	Adjunct Associate Professor from Nagoya Univ. (–March '91)
Kotaro OSAKADA	Adjunct Professor from Tokyo Institute of Technology (April '91–)
Kim A. BURKOV	Visiting Professor from Leningrad State Univ. (January '91–July '91)
Kiyohiko NAKAJIMA	Research Associate
Atsushi YAGASAKI	Technical Associate (–March '91)[20]
Kenji WAIZUMI	Technical Associate (April '91–)
Yusuke TAMURA	IMS Fellow (–March '91)[21]
Yasuhiro INADA	Graduate Student from Nagoya Univ.

Functional Coordination Chemistry

Koji TANAKA	Pofessor
Tamotsu TAKAHASHI	Associate Professor (January '91–)
Hirotaka NAGAO	Research Associate
Nobutoshi KOMEDA	Graduate Student from Osaka Univ.
Hiroaki TANAKA	Graduate Student (October '91–)
Hide KAMBAYASHI	Graduate Student (April '91–)

Coordination Bond

Masanobu HIDAI	Adjunct Professor from Univ. of Tokyo (–March '91)
Tasuku ITOH	Adjunct Professor from Tohoku Univ. (April '91–)
Toshio YAMAGUCHI	Adjunct Associate Professor from Fukuoka Univ. (–March '91)
Masatatsu SUZUKI	Adjunct Associate Professor from Kanazawa Univ. (April '91–)

Research Facilities

Computer Center

Keiji MOROKUMA	Director
Kazuo KITAURA	Associate Professor
Umpei NAGASHIMA	Research Associate
Kazuhiko HONDA	Technical Associate

Chemical Materials Center

Kazuhiro NAKASUJI	Director
Yoshiro YAMASHITA	Associate Professor
Shoji TANAKA	Research Associate
Masaaki TOMURA	Technical Associate
Masatoshi KOZAKI	Graduate Student (April '91–)

Instrument Center

Ichiro HANAZAKI	Director
Kiyokazu FUKE	Associate Professor
Keisaku KIMURA	Associate Professor (–March '91)[22]
Fuminori MISAIZU	Research Associate
Shunji BANDOW	Research Associate (November '90–)
Keizo TSUKAMOTO	Graduate Student (April '91–)
Masaomi SANEAKTA	Graduate Student (April '91–)

Low-Temperature Center

Yusei MARUYAMA	Director
Kunio AWAGA	Research Associate

Equipment Development Center

Teizo KITAGAWA	Director
Tadaoki MITANI	Associate Professor
Yoshihiro TAKAGI	Associate Professor (—March '91)[23]
Hiroshi OKAMOTO	Research Associate
Shuji ASAKA	Research Associate (January '91—)
Hiroshi KITAGAWA	Research Associate (April '91—)
Kaoru OKANIWA	Graduate Student

Ultraviolet Synchrotron Orbital Radiation Facility

Katsumi KIMURA	Director
Makoto WATANABE	Associate Professor
Goro ISOYAMA	Associate Professor
Masao KAMADA	Associate Professor
Eiji ISHIGURO	Adjunct Associate Professor from Osaka City Univ. (April '91—)
Kazuhiko SEKI	Adjunct Associate Professor from Hiroshima Univ. (—March '91)[24]
Atsunari HIRAYA	Research Associate
Shin-ichiro TANAKA	Research Associate
Shiro TAKANO	Research Associate
Hiroyuki HAMA	Research Associate (October '90—)
Eriko YAGASAKI	Graduate Student (April '90—March '91)
Sayumi HIROSE	Graduate Student (April '91—)
Akira OBA	Visiting Research Fellow from Hamamatsu Photonics* (April '90—March '91)

Technical Staff

Akira UCHIDA	Technical Division Head
Keiichi HAYASAKA	Technical Section Chief
Kusuo SAKAI	Technical Section Chief
Fumio NISHIMOTO	Computer Center (Unit Chief)
Fumitsuna TESHIMA	Computer Center
Kunihiko TANAKA	Computer Center
Sachiyo NOMURA	Chemical Materials Center
Takaya YAMANAKA	Instrument Center
Masahiro SAKAI	Instrument Center
Kiyonori KATO	Low-Temperature Center (Unit Chief)
Takashi TAKAYAMA	Low-Temperature Center
Toshio HORIGOME	Equipment Development Center (Unit Chief)
Hisashi YOSHIDA	Equipment Development Center
Masashi NAGATA	Equipment Development Center
Kouichi UCHIYAMA	Equipment Development Center
Norio OKADA	Equipment Development Center
Mitsukazu SUZUI	Equipment Development Center
Nobuo MIZUTANI	Equipment Development Center
Shinji KATO	Equipment Development Center
Osamu MATSUDO	UVSOR Facility (Unit Chief)
Toshi KINOSHITA	UVSOR Facility
Masami HASUMOTO	UVSOR Facility
Jun-ichiro YAMAZAKI	UVSOR Facility
Eiken NAKAMURA	UVSOR Facility

* Carries out graduate research of IMS on the Cooperative Education Program of IMS with graduate schools.

1) Present Address: Institute for Fundamental Chemistry, 34-4, Takano-Nishibiraki-cho, Sakyo-ku, Kyoto 606
2) Present Address: College of General Education, Nagoya Univ., Furo-cho, Chikusa-ku, Nagoya 464-01
3) Present Address: The Research Institute for Scientific Measurements, Tohoku Univ., 2-1-1, Katahira, Aoba-ku, Sendai 980
4) Present Address: Faculty of Engineering, Tohoku Univ., Aramaki, Aoba-ku, Sendai 980
5) Present Address: Dept. of Materials Science, Toyohashi Univ. of Technology, 1-1, Hibarigaoka, Tenpaku-cho, Toyohashi 441
6) Present Address: Dept. of Chemistry, Tokyo Institute of Technology, O-okayama, Meguro-ku, Tokyo 152
7) Present Address: The Institute of Physical and Chemical Research, Wako, Saitama 351-01
8) Present Address: Dept. of Chemistry, Faculty of Science, Kyushu Univ., 6-10-1, Hakozaki, Higashi-ku, Fukuoka 812
9) Present Address: Dept. of Material Science, Faculty of Science & Technology, Shizuoka Institute of Science & Technology, 2200-2, Toyosawa, Fukuroi, Shizuoka 437
10) Present Address: Dept. of Chemistry, Faculty of Science, Kyushu Univ., 6-10-1, Hakozaki, Higashi-ku, Fukuoka 812
11) Present Address: Dept. of Material Science, Faculty of Science, Himeji Institute of Technology, Harima Science Park City, Hyogo 678-12
12) Present Address: Dept. of Material Science, Faculty of Science, Himeji Institute of Technology, Harima Science Park City, Hyogo 678-12
13) Present Address: Dept. of Physics, Faculty of Science, Nagoya Univ., Furo-cho, Chikusa-ku, Nagoya 464
14) Present Address: Dept. of Chemistry, Faculty of Science, Nagoya Univ., Furo-cho, Chikusa-ku, Nagoya 464
15) Present Address: Dept. of Material Science, Faculty of Science, Himeji Institute of Technology, Harima Science Park City, Hyogo 678-12
16) Present Address: Dept. of Chemistry, Faculty of Science, Kanazawa Univ., 1-1, Marunouchi, Kanazawa 920
17) Present Address: Okayama Univ. of Science, 1-1, Ridai-cho, Okayama 700
18) Presnet Address: Komatsu Electronic Metals Co., LTD., 2612, Shinomiya, Hiratsuka, Kanagawa 254
19) Present Address: Dept. of Applied Chemistry Nagoya Institute of Technology, Gokiso-cho, Showa-ku, Nagoya 466
20) Present Address: Dept. of Chemistry, School of Science, Kwansei Gakuin Univ., Uegahara, Nishinomiya 662
21) Present Address: Cray Research Japan LTD., Ichibancho Eight-One Bldg., 4-th floor, 6-4, Ichiban-cho, Chiyoda-ku, Tokyo 102
22) Present Address: Dept. of Material Science, Faculty of Science, Himeji Institute of Technology, Harima Science Park City, Hyogo 678-12
23) Present Address: Dept. of Material Science, Faculty of Science, Himeji Institute of Technology, Harima Science Park City, Hyogo 678-12
24) Present Address: Dept. of Chemistry, Faculty of Science, Nagoya Univ., Chikusa-ku, Nagoya 464

COUNCIL

Hiroo INOKUCHI **Director-General**

Councillors

Chairman	Ikuzo TANAKA	President, National Institute for Academic Degrees
Vice-Chairman	Yutaka TOYOZAWA	Professor, Chuo University
	Hirotsugu AKAIKE	President, The Institute of Statistical Mathematics
	Hideaki CHIHARA	Executive Director, Japan Association for International Chemical Information
	Eiichi FUJITA	Professor Emeritus, Kyoto University
	Kenichi FUKUI	President, Institute for Fundamental Chemistry
	Sachio HAYAKAWA	President, Nagoya University
	Namio HONDA	Professor, Nagoya University of Commerce and Business Administration (–May '91)
	Sho ITO	Professor, Tokushima Bunri University (–May '91)
	Yoshikazu ITO	Chairman of The Board, Toray Industries, Inc. (June '91–)
	Kozo KUCHITSU	Professor, Nagaoka University of Technology
	Michio KURATA	Professor Emeritus, Kyoto University (–May '91)
	Yoshio MATSUNAGA	Professor, Hokkaido University (June '91–)
	Akira MIKAZUKI	Professor Emeritus, University of Tokyo
	Masatoshi MORITA	Chief Executive Officer, Toyota Central Research & Development Laboratories, INC (– May '91)
	Haruo NISHIHARA	President, Waseda University (–May '91)
	Kazuo SAITO	Professor, International Christian University
	Hideki SAKURAI	Dean of The Faculty of Science (June '91–)
	Hirotoshi SANO	President, Tokyo Metropolitan University (June '91–)
	Shinichi SASAKI	President, Toyohashi University of Technology (June '91–)
	Kenji TAMARU	Professor, Science University of Tokyo
	Teijiro YONEZAWA	Professor, Kinki University
	Peter DAY	Professor, Oxford University (June '91–)
	John C. POLANYI	Professor, University of Toronto
	Heinz A. STABB	President, Max-Planck Society for the Advancement of Science, F.R.G. (–May '91)

The Council is the advisory board for the Director-General. Two of the councillors are selected among distinguished foreign scientists.

Distinguished Research Consultants

Kenichi FUKUI	President, Institute for Fundamental Chemistry
Saburo NAGAKURA	President, The Graduate University for Advanced Studies
Kenji TAMARU	Professor, Science University of Tokyo
Yasutada UEMURA	Chancellor, Musashi Gakuen

Administration Bureau

Toshio UENO	Director-General, Administration Bureau
Satoshi FUJISAWA	Director, General Affairs Department
Yasuyoshi NONAKA	Director, Finance and Facilities Department
Nobuaki SHIMIZU	Head, General Affairs Division (—April '91)
Ryoichi ASANO	Head, General Affairs Division (April '91—)
Makoto SUZUKI	Head, Personnel Division
Tsunetaka GIMA	Head, Research Cooperation and International Affairs Division (—April '91)
Satoru TAMURA	Head, Research Cooperation and International Affairs Division (April '91—)
Masaaki TSUJITA	Head, Budge Division
Saigyo KAMIYAMA	Head, Accounts Division
Masakazu SASAKI	Head, Construction Division
Kunikatsu SHYOJI	Head, Equipment Division

BUILDINGS AND CAMPUS

The IMS campus covering 62,343 m^2 is located on a low hill in the middle of Okazaki City. The inequality in the surface of the hill and growing trees are preserved as much as possible, and low-storied buildings are adopted for conservation of the environment. The buildings of IMS are separated according to their functions as shown in the map. The Research Office Building and all Research Facilities except for the Computer Center are linked organically to the Main Laboratory Building by corridors. Computer Center, Library and Administration Buildings are situated between IMS and the neighboring National Institute for Basic Biology and National Institute for Physiological Sciences, because the latter two facilities are common to these three institutes.

The loding facility of IMS called Yamate Lodge, located within ten minutes' walk, has sleeping accommodations for 19 guests and two families. Mishima Lodge, located within four minutes' walk east of IMS can accommodate 68 guests and ten families. Scientists who visit IMS as well as the two other institutes can make use of these facilities. Foreign visiting scientists can also live at these lodgings with their families during their stays.

The Institute for Molecular Science

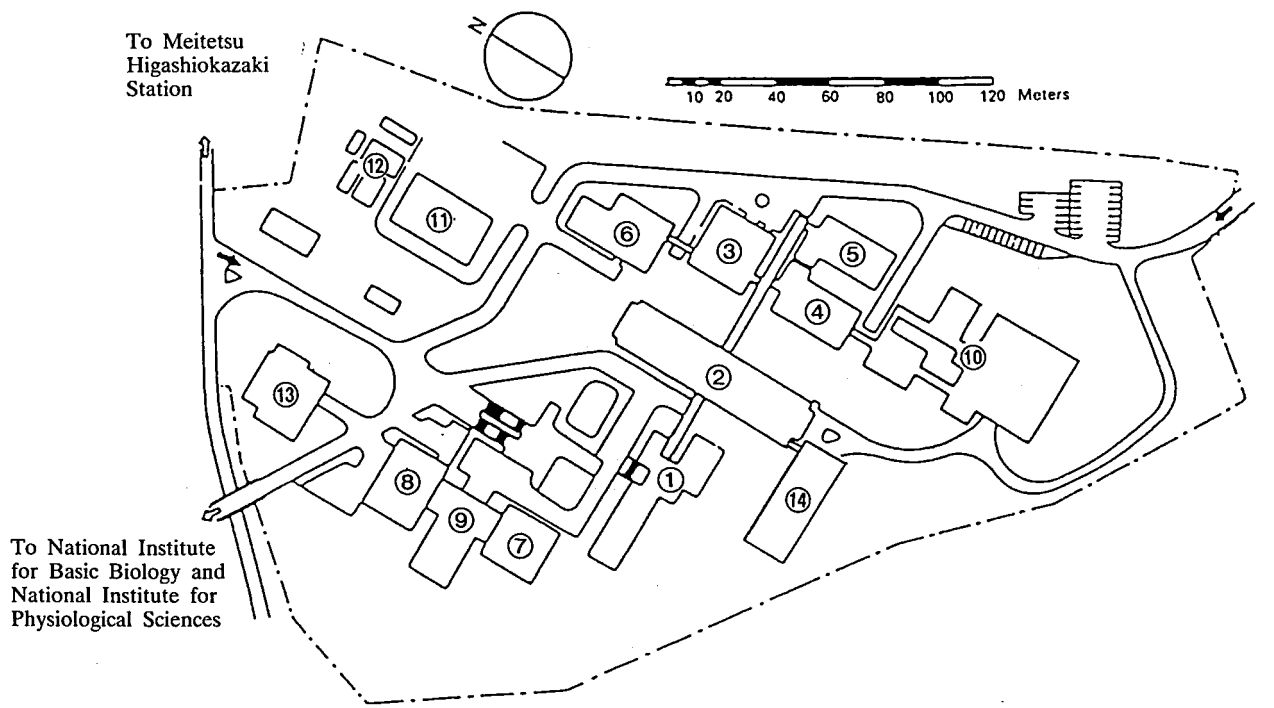

1. Research Office Building
2. Main Laboratory Building
3. Equipment Development Center
4. Instrument Center
5. Chemical Materials Center
6. Low-Temperature Center
7. Computer Center
8. Library
9. Central Administration
10. UVSOR Facility
11. Power Station
12. Waste-Water Disposition Facilities
13. Faculty Club
14. South Laboratory Building

Okazaki (population 300,000) is 260 km southwest of Tokyo, and can be reached by train in about 3 hours from Tokyo via New Tokaido Line (Shinkansen) and Meitetsu Line.
The nearest large city is Nagoya, about 40 km west of Okazaki.

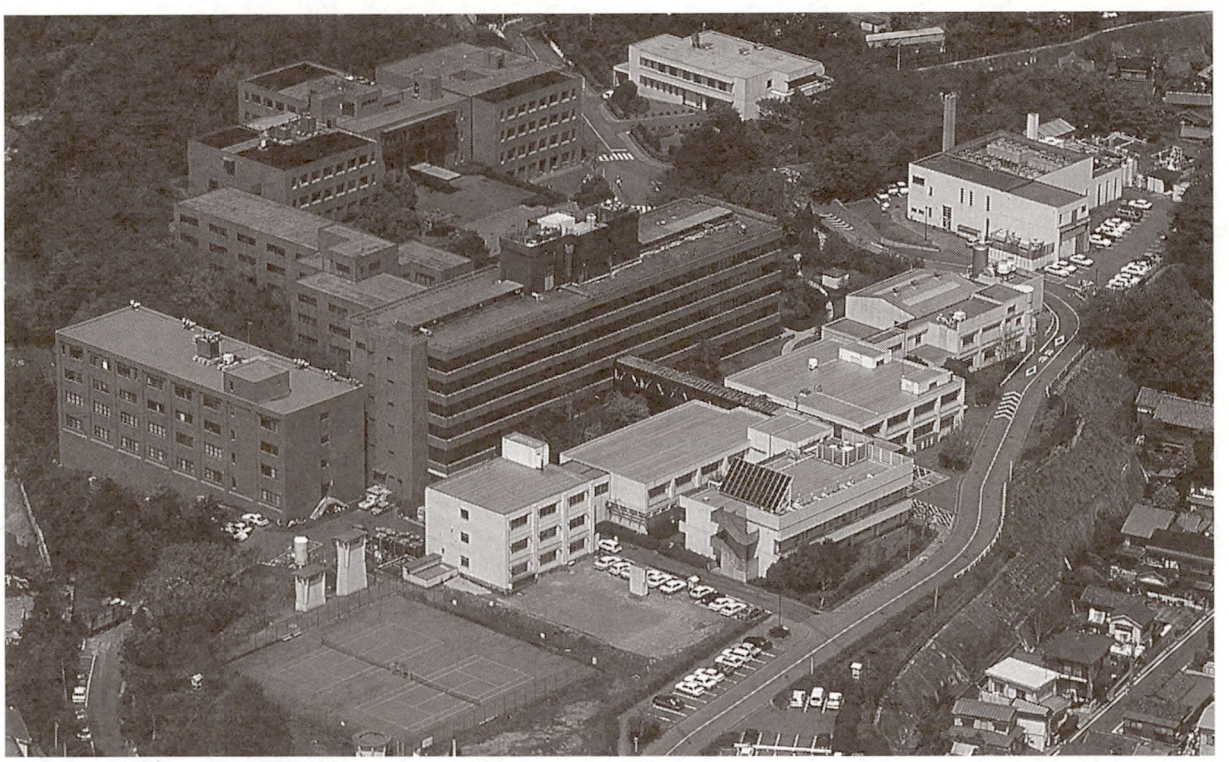

RESEARCH ACTIVITIES I
Department of Theoretical Studies

I—A Potential Energy Surfaces and Dynamics of Elementary Chemical Reactions

We have continued our studies in this field, calculating not only potential energy surface but also transition dipole and non-adiabatic coupling element as functions of nuclear coordinate. This activity has resulted in varieties of collaboration involving Dr. Claude LeForestier at University of Paris-Sud, Dr. Kosloff's group at Hebrew University, Dr. David Tanner's group at Notre Dame University and Dr. Bob Field's group at MIT. Dr. Yoshiaki Amatatsu spent a month at Jerusalem for collaboration. Dr. Koichi Yamashita, Research Associate of my group and the major driving force in our persuit in this field for the last seven years, has recently left our group to become Senior Scientist at the Institute for Fundamental Chemistry, a small private institute established for Dr. Kenichi Fukui in Kyoto. Kenro Hashimoto, Ph. D. from Keio University with Prof. Iwata, is a new Research Associate in my group and will continue our studies in this field.

I-A-1 Theoretical Study of the FHF^- Unimolecular Dissociation

Koichi YAMASHITA, Keiji MOKOKUMA, and Claude LEFORESTIER *(Univ. of Paris-Sud, France)*

Ab initio potential energy surface (PES) calculations of the ground-state unimolecular dissociation of PHF^- to the F^-+HF channel have been performed using the CEPA (coupled electron pair approach) method. The basis sets used were F[9s6p3dlf] and H[5s3pld] by van Duijneveldt augmented with diffuse and polarization functions. The global PES was fitted to the sixth-order Simons-Parr-Finlan analytical form and an ion-dipole attraction term was added to describe the long-range interaction. In order to treat large-amplitude vibrational motion which can break the anion, the hyperspherical coordinate system by Pack and Parker was used in three-dimensional (j=0) quantum mechanical calculations. The eigenstates over the dissociation threshold as well as of the bound states were calculated variationally using the grid method. It was found that quasi-bound vibrational states can exist over the dissociation threshold and we propose this reaction as a good candidate for spectroscopic studies of the vibrational levels of dissociating molecules.

I-A-2 Ab initio Study on the Excited Electronic States of NaI

Koichi YAMASHITA and Keiji MOROKUMA

Higher excited electronic states of NaI ($\Omega=0^+$, 0^-, 1, 2, 3) were studied by the ab initio spin-orbit CI method with the effective spin-orbit Hamiltonian. For the iodine atom the relativistic effective potential with spin-orbit parameters was used. To describe the valence space of iodine, uncontracted (3s,3p) primitive were used augmented with a polarization d and an anion p function. The Na (6s4p) valence basis sets were taken from McLean and Chandler's double-zeta contracted basis sets. To these, one d function was added. The potential energy curves of the low-lying states and the transition dipole moments between the ground $^1\Sigma^+$ and the excited states were calculated by the multireference SDCI and SECI method, respectively. The reference configurations were determined by distributing 6 electrons in 7 orbitals where Na 3s, 3p and I 5p orbitals are active. The calculations support the presence of a bound upper state for each of the spin-orbit $C0^+$, 0^-(III), 1(IV), 2(II), 3(I) electronic states, all correlating with covalent $Na(3^2P)$ + $I(5^2P_{3/2})$ dissociation. A possible candidate for a bound state which has been recently discovered experimentally by Bower et al.[1] and Bluhm et al.[2] was discussed based on the calculated spectroscopic properties and transition intensities of the electronic dipole allowed $C0^+$ and 1(IV) bound states.

Reference

1) R.D. Bower, P. Chevrier, P. Das, H.J. Foth, J.C. Polanyi, M.G. Prisant, and J.P. Visticot, *J. Chem. Phys.* **89**, 4478 (1988).
2) H. Bluhm, J. Linder and E. Tiemann, *J. Chem. Phys.* **93**, 4556 (1990).

I-A-3 Potential Energy Curves of Ground and Low-Lying Excited States of Bi_2

Toshiaki FUJII *(Grad. Univ. for Adv. Studies and IMS)*, **Koichi YAMASHITA, and Keiji MOROKUMA**

The electronic structure and reaction of the ground and excited states of Bi_2 have gained interests relating to the "femtosecond transition state spectroscopy."[1),2)] The potential energy curves of the ground and many low-lying excited states were determined by FV (full valence) CI calculation including the spin-orbit operator of Christiansen et al..[3)] We found large spin-orbit coupling in many states. For example, the contribution of the spin-free configurations of each multiplicity for the ground state in the equilibrium region is singlet : triplet : quintet=75% : 24% : 1%. Transition dipole moments as functions of the distance have also been evaluated. We are interested in the two dissociative channels, M and M', which are produced by the excitation from ground state with the 308 nm laser pulse and result in different dissociation limits. The assignments and characterization of these two channels have been carried out based on the energetics and transition properties.

Reference

1) J.H. Glownia, J.A. Misewich, and P.P. Sorokin, *J. Chem. Phys.* **92**, 3335 (1990)
2) R.M. Bowman, J.J. Gerdy, G. Roberts and A.H. Zewail, *J. Phys. Chem.* **95**, 4635 (1991)

3) R.B. Ross, J.M. Powers, T. Atashroo, W.C. Ermler, L.A. LaJohn and P.A. Christiansen, *J. Chem. Phys.* **93**, 6654 (1990)

I-A-4 Ab initio Potential Energy Surfaces and Classical Trajectory Studies of ICN* → I*+CN and I+CN

Yoshiaki Amatatsu, Keiji MOROKUMA, and Satoshi YABUSHITA *(Hiroshima Univ.)*

Following a preliminary study on qualitative features of potential energy surfaces (PESs)[1], contracted spin-orbit configuration interaction calculations have been performed to obtain the full 3-dimensional PESs of ICN. The molecular orbitals were determined by a state averaged MCSCF method with the relative weight of $X^1\Sigma^+$: $^1\Pi_x$: $_1\Pi_y$: $^3\Pi_x$: $^3\Pi_y$: $^3\Sigma^+$ ($\sigma \rightarrow \sigma^*$) = 1:1:1:3:3:3 with spin multiplicities taken into account. The $^3\Pi_0^+$ surface with respect to the C-I distance has a shallow well with its minimum inside the conical intersection, whereas the $^1\Pi_1$ surfaces are monotonically dissociative. Both $^3\Pi_0^+$ and $^1\Pi_1$ are double well functions with respect to bending angle.

Classical trajectory calculations have been carried out to exmine the photodissociation dynamics of ICN. The present calculations clearly show the I- and I*-channel selectivity in the rotational excitation that semi-quantitatively reproduces the experimental results. The excitation mechanism for I-channel product is different from that of CH_3I. In addition to the rotational excitation before transition as seen for CH_3I, a second excitation takes place after transition, which can be explained by an impact model. It has been found that molecules with initial important role in determining experimental quantum yield and giving rise to higher rotational products.

Reference

1) S. Yabushita and K. Morokuma, *Chem. Phys. Lett.* **175** 518 (1990).

I-A-5 Time-Dependent Quantum Mechanical Approaches to the Photodissociation Dynamics of ICN

Jiwen QIAN*, Carl J. WILLIAMS*, David J. TANNOR* *(*Univ. of Notre Dame. U.S.A.)*, **Yoshiaki AMATATSU, and Keiji MOROKUMA**

The ab initio calculated transition dipoles and non-adiabatic coupling elements from the ground to excited states as well as the potential energy surfaces (PESs) have been used to carry out a 3-dimensional (including bending) time-dependent quantum dynamics calculations. The transition dipoles for $^3\Pi_0^+ \leftarrow X^1\Sigma^+$ and $^1\Pi_1 \leftarrow {}^1\Sigma^+$ transitions are about ten times larger than others. The non-adiabatic coupling element between $^3\Pi_0^+$ and $^1\Pi_1$ can be fitted to a Lorentzian with a maximum at the crossing point, while that between two $^1\Pi_1$ surfaces shows an exponential decay with respect to the C-I distance.

I-A-6 Ab initio Potential Energy surfaces and Classical Trajectory Study of CH_3I and CD_3I Photodissociation

Yoshiaki AMATATSU and Keiji MOROKUMA

Using ab initio full 9-dimensional potential energy surfaces, classical trajectory calculations have been peformed to examine the photodissociation dynamics of methyl iodine. The qualitative aspects of the present results are similar to the previous ones[1] except for the I*-quantum yield. The I*-quantum yield (0.8) is closer to experimental ones (0.7-0.8) than that of 6-dimensional calculation (0.9). The origin of this decrease has been discussed in connection to the contribution of three C-H stretches to the potential coupling element. Isotope effects in the photodissociation dynamics is one of the interesting problems. Contrary to expectation, it has been found in many experiments that the I*-quantum yields in the photodissociation of CD_3I. The present theoretical result reproduces this tendency. The cause of this trend has been discussed.

Reference

1) Y. Amatatsu, K. Morokuma and S. Yabushita, *J. Chem., Phys.* **94** 4858 (1991).

I-A-7 Time-Dependent Quantum Mechanical Approach to the Photodissociation Dynamics of Methyl Iodide

Yoshiaki AMATATSU, Keiji MOROKUMA, Audrey D. HAMMERICH*, and Ronnie KOSLOFF* *(*The Hebrew Univ., Israel)*

A time-dependent quantum mechanical method has been applied to the photodissociation dynamics of CH_3I under the assumption of a collinear pseudo-triatomic system. The 2-dimensional potential functions used in this calculation were extracted from 9-dimensional potential functions of CH_3I (see I-A-XX) and were furthermore modified to reproduce the experimental total absorption spectrum. Non-adiabatic coupling elements between $^3Q_0$ and $^1Q_1$ surfaces, calculated by numerical differentiations of ab initio CI coefficients and with a maximum around the intersection region, have been used in the calculation.

I-A-8 Potential Energy Surface for Unimolecular Dissociation and Rearrangement Reactions of the Ground Electronic State of HFCO

Kenshu KAMIYA *(Univ. of Tokyo and IMS)* **and Keiji MOROKUMA**

[*J. Chem. Phys.* **94**, 7287 (1991)]

The potential energy surface of the HFCO molecule in its electronic ground state has been investigated with *ab initio* method, at levels up to MP4(SDTQ)/6-311G**//MP2/6-31G*. At the highest level, the barrier height for molecular dissociation (HFCO → HF+CO) was calculated to be 46.9 kcal/mol with a zero-point energy correction, in good agreement with an experimental estimate and a recent theoretical result. The intrinsic reaction coordinate (IRC) for molecular dissociation was traced and the coupling between the IRC and normal modes as well as that among the normal modes was analyzed along the IRC. The analysis is consistent with the mode specificity of recently observed quasi-stable vibrational states of HFCO above the dissociation limit. Almost all possible stationary points on the

potential surface of the HFCO system have been located, including the rearrangement and atomic dissociation products and transition states, as well as van der Waals complexes. These are compared with the H_2CO system. All the species that have an FO bond are unstable or non-existent, reflecting the weakness of the bond.

I-B Theoretical Studies of Spectroscopy and Structure

I-B-1 Theoretical Study of the Highly Vibrationally Excited HCP Molecule

Koichi YAMASHITA, Theresa KAVANAUGH *(MIT, U.S.A.)*, **Keiji MOROKUMA, and Claude LEFORESTIER** *(Univ. of Paris-Sud, France)*

We performed the ab initio potential energy surface (PES) and quantum mechanicl calculations to investigate the highly vibrationally excited HCP molecule. The ground state PES was calculated by using the MRSDCI method with the TZP basis set and fitted to the Murrell-Carter-Halonen analytical function. The calculation predicts that isomeric structure HPC is the transition state of hydrogen atom movement around the CP bond with a barrier height of 3.34 eV. Vibrationally excited states were calculated by using the DVR (discrete variable representation) method with the Jacobi coordinate system. The expectation values of Jacobi coordinates for each vibrational level of (0,n,0) and (0,n,1) (n is up to 28) allowed us an analysis on which part of the potential energy surface can be proved by a recent SEP (stimulated emission pumping) experiment by Chen et al.[1].

Reference

1) Y-T. Chen, D.W. Watt, and R.W. Field, *J. Chem. Phys.* **93**, 2149 (1990).

I-B-2 Solvent Effect on Vibrational Structure in the (n,π^*) Transition of Formaldehyde

Hiroo FUKUNAGA *(Fuji Photo Film Co. and IMS)* **and Keiji MOROKUMA**

The vibrational structures in the (n,π^*) excitation of formaldehyde complexed with one to several water molecules have been calculated theoretically and their temperature dependence have been examined. In these calculations, the configurations of formaldehyde-water complexes have been derived from Monte Carlo simulation based on an NTV ensumble, in which the ab initio fitted formaldehyde-water potential expressed in terms of r^{-1}, r^{-3}, and r^{-12} have been used in conjunction with the MCY water-water potential. The vibrational levels and their wave functions have been obtained by solving the Schrödinger equation with the effective intramolecular potential for each configuration. The ab initio electronic transition dipole moment of the complexes has been fitted to an analytical function and thereby the transition dipole moment of each vibronic transition has been evaluated by numerical integration.

I-B-3 On Incorrect Behavior of Single Annihilation Equation of Spin-projected UHF and UMP Energies

Nobuaki KOGA, Koichi YAMASHITA, and Keiji MOROKUMA

[*Chem. Phys. Lett.*, in press]

Approximate (i.e. single annihilation) equations for spin-projected UHF and UMP energy as well as $<S^2>$ expectation value for spin state S give *incorrect* results under the single projection, i.e. when only the next higher spin (S+1) contaminant is projected out. This originates from the fact that every time the annihilator operates, the wave functions of higher spin contaminants change sign. On the other hand, single annihilation equations with double projection of both S+1 and S+2 spin contaminants show correct behavior and are recommended for practical applications.

I-C Theoretical Studies of Reaction Mechanisms and Structure of Organic and Related Compounds

We have been involved in a cooperative Priority Area Grant from Ministry of Education in "Unusual Valency in Organic Chemistry." Dr. Jezy Moc, a JSPS Postdoctoral Fellow from the University of Wroclaw, Poland since February 1991, and Dr. Simon Mathieu, a Visiting Scientist from France, have been working on the structure and reactivity of model "organic hypervalent compounds" to elucidate similarities and differences between main group compounds and transition metal compounds. We have purchased two IBM/6000 workstations and have two more workstations on order. We have carried out a substantial fraction of work in this section and section I-D on workstations and are quite happy with them. We are also collaborating heavily with Prof. Eiichi Nakamura, organic chemist from the Tokyo Institute of Technology, and his students. We have learned a lot of organic chemistry from this collaboration.

I-C-1 Structural, Energetic and Electronic Properties of the Model Hypervalent Hydrides and Fluorides of P, As, Sb and Bi. Ab initio ECP Theoretical Study

Jerzy MOC and Keiji MOROKUMA

Systematic ab initio MO calculations employing effective core potentials on the central atoms have been carried out for the series of hypervalent hydrides and fluorides of formulas YH_4^-, YF_4^-, YH_5, YF_5, YH_6^-, where Y=P, As, Sb and Bi. Geometry optimizations for several structures have been done followed by the vibrational frequency analysis.

The structures corresponding to real minima for the species with coordination numbers 4, 5 and 6 were of C_{2v} (pseudo-trigonal bipyramidal), D_{3h} (trigonal bipyramidal) and O_h (octahedral) symmetries, respectively. The transition states for the Berry-like pseudorotation and inversion for the YH_4^- and YF_4^- molecules of C_{4v} (square pyramidal) and D_{4h} (square planar) symmetries, respectively, have been located. For the species with coordination numbers 5 and 6, the transition states corresponding to Berry pseudorotation and trigonal twist distortion possessed respetively the C_{4v} (square pyramidal) and D_{3h} (trigonal prism) symmetries. The final energy barriers for the molecular arrangements mentioned above have been predicted at the MP2 (fluorides) and MP4SDTQ (hydrides) levels of theory. The comparison of behaviour of the hydrides and fluorides has been made and the revealed periodic trends were discussed.

I-C-2 Theoretical Study of the Hypervalent Species Involving Seven Coordination

Jerzy MOC and Keiji MOROKUMA

In this project we focused on the prediction of structurally stable hypervalent molecules with seven coordination. The case of seven valence electron pairs is unique, i.e. the possible equilibrium structures range from D_{5h}, through a series of intermediate configurations of C_{2v}, C_2 or C_s symmetry, to C_{3v}. Peforming ab initio ECP calculations for the molecules of general formula YX_7^{-2}, where Y=P, As, Sb and X=H, F, Cl we investigated both the ligand substituent effect and the effect of the size of the central atom on the structural and thermodynamic stabilities of these hypervalent molecules.

I-C-3 Barriers to the $XH_6 \rightarrow XH_4 + H_2$ (X=S, Se and Te) Dissociation Reactions

Simon MATHIEU and Keiji MOROKUMA

Ab initio calculations have been performed for potential energy surfaces of the title reaction with effective core potentials for sulfur, selenium and tellurium. Valence electrons were described by a double-zeta basis set augmented by polarization and diffuse functions on all atomic centers. A zwitterionic XH_5^+/H^- like transition structure of C_s symmetry has been found at the HF level; its geometry is close to that of trigonal bipyramidal XH_5^+ interacting with the negative charged hydride in the equatorial plane. The imaginary frequency corresponds to the in-plane elimination of the H_2 molecule. The H_2 distance is 1.545Å (S), 1.508Å (Se) and 1.430Å (Te), which is far from the equilibrium distance of H_2 molecule (0.742Å, optimized with the same basis set). If we consider the reverse reaction, these large distances can be regarded to result from the charge transfer from the central atom into the σ^* MO of H_2. The barriers to dissociation at the MP2//HF level are very high: 57.18, 55.94 and 60.12 kcal/mol for SH_6 and TeH_6, respectively. The study of substituent effects is in progress for sulfur compounds. The presence of a σ donating group such as $-SiR_3$ is expected to lower the barrier by stabilizing the cationic charge deveoped at the SH_5^+ moiety in the transition state.

I-C-4 Structural Preference in MH_4OH ($M=Si^-$, P and S^+) Trigonal Bipyramids

Simon MATHIEU and Keiji MOROKUMA

As a general rule, the structural preference of trigonal bipyramids (TBP) is observed with the most electronegative group in the apical position. As an exception, PH_4OH was previously reported with a smaller basis set to prefer the hydroxyl group in the equatorial position by 2.7 kcal/mol over the apical position. Ab initio calculations have been performed with the standard 6-31G* bais set for the neutral phosphorane and for the cationic sulfurane and with the 6-31++G** basis set for the anionic siliconate. Geometry optimizations were carried out at the HF level and correlation effects were treated at the MP4 level of theory. Our MP4(SDTQ) results show that only slight structural preferences are observed for these three systems. For PH_4OH, the equatorial orientation of the hydroxyl is 0.31 kcal/mol more favorable than the apical one. SiH_4OH^- and SH_4OH^+ exhibit an apical preference for the hydroxyl by 0.85 and 0.49 kcal/mol, respectively. An analysis indicates that in all compounds, both hydroxyl and hydride interact stronger with the central atom in the equatorial site than in the apical one. The structural preference takes its origin in two opposite effects: the stronger equatorial preference of hydrogen over hydroxyl which tends to orientate the hydroxyl in the equatorial position and the geometry recorganization energy generated by the apical/equatorial ligand permutation which favours the equatorial orientation of hydroxyl.

I-C-5 Toward Theoretical Design of Tetracoordinate Silicon Compounds with High Reactivity to Hydrosilylation

Tadahiro OZAWA *(Kao Corp. and IMS)*, **Nobuaki KOGA, and Keiji MOROKUMA**

Our previous calculations for reactions 1 and 2 have shown that hydrosilylation of tetracoordinate silicon compound (TSC) is much more difficult than that of pentacoordinate compounds, supporting the experimental findings that hydrosilylation by TSC requires a catalyst.

$$H_2C=O + HSi(OH)_3 \rightarrow H_3C\text{-}OSi(OH)_3 \quad (E_{calc}^{\neq}=41.3 \text{ kcal/mole}) \quad (1)$$

$$H_2C=O + [HSi(OH)_4]^- \rightarrow [H_3C\text{-}OSi(OH)_4]^- \quad (E_{calc}^{\neq}=11.0 \text{ kcal/mole}) \quad (2)$$

Experimentally, highly reactive TSC has not been synthesized yet, and thus we try to design highly reactive TSC with an ab initio moleclar orbital method. By replacing OH groups of $HSi(OH)_3$ by hydrogens and fluorides, activation energy is changed to be 46.8 and 36.3 kcal/mole, respectively, suggesting that an electron-withdrawing substituent increases hydrosilylation ability of TSC. Such a substituent makes silicon more electropositive, to enhance bonding interaction between silicon and carbonyl oxygen. Further, we performed calculations by using silacyclopropene, $H_2SiCH{=}CH$, **(1)**, as a TSC, to obtain the lower activation energy of 31.3 kcal/mole. Deformation for **1** to reach the transition state structure is small, resulting in the lower activation energy, since **1** has a three-membered ring. These results suggest that properly deformed TSC with electron-

withdrawing substituents would undergo hydrosilylation easily. Therefore, we carried out the calculations with trifluorosilacyclopropene, FHSiCF=CF, (**2**), to find that the activation energy for **2** (21.0 kcal/mole) is a half of that for reaction 1, as expected. We suggest hydrosilylation of **2** may take place without catalyst.

I-C-6 Reversible Generation of Trimethylenemethanes by Mild Thermolysis of Dialkoxy Methylenecyclopropanes

Eiichi NAKAMURA*, Shigeru YAMAGO*, Satoshi EJIRI*, *(*Tokyo Inst. Tech.)* Andrea E. DORIGO, and Keiji MOROKUMA

[*J. Am. Chem. Soc.* **113**, 3183 (1991)]

Thermolysis of dialkoxy methylenecyclopropanes at 40–100°C has been studied with the aid of ^{13}C labeling, kinetic measurement, and stereochemical probes to show that the reaction reversibly generates zwitterionic dihydroxytrimethylenemethanes (TMMs) which behave in solution as relatively polarized species. Four-orbital four-electron CASSCF ab initio molecular orbital calculations of a model TMM species offered information about the structure and electronic properties of the dialkoxy TMMs.

I-C-7 Theoretical Studies of Heteroatom-Directed Carbometalation Reaction. Addition of MeCu and MeLi to Substituted Acetylenes

Eiichi NAKAMURA*, Yoshimitsu MIYACHI*, *(*Tokyo Inst. Tech.)* Nobuaki KOGA, and Keiji MOROKUMA

Ab initio theoretical studies of the additions of MeCu and MeLi to heteroatom-substituted acetylenes have shown that the regiochemistry of the heteroatom-directed carbometalation reactions are controlled by the electrostatic interaction between the metal and the acetylene fragment.

I-D Structure and Reactions of Transition Metal Complexes

Dr. Djamaladdin Musaev from the Institute of New Chemical Problems, Chernogolovka, USSR has joined our group in April 1991 as our third JSPS Postdoctoral Fellow and has been involved in structure and reactivity of bare transition metal carbenes. D. Nobuaki Koga continues his productive researh effort on reations of transition metal complexes, in collaboration with Prof. Xue-Kui Li, Visiting Scientist from Jilin University, and Mr. Endo and Mr. Kuribayashi, two industrial trainees.

I-D-1 Ab initio MO Study of Electronic and Geometrical Structures of the Complex $RhCH_2^+$

Djamaladdin G. MUSAEV, Nobuaki KOGA, and Keiji MOROKUMA

The electronic and geometrical structures of the complex $RhCH_2^+$ have been investigated by using ab initio UMP4(SDTQ) and CASSCF methods with a 17 electron ECP for Rh and basis sets: (5s5p4d)/[3s3p3d](Rh) + (9s5pld)/[4s2pld](C) + (4s)/[2s](H).

It has been found that the complex $RhCH_2^+$ has three electronic states $^1A_1$, $^3A_1$ and $^3A_2$, which are close to each other in energy. Among these states the singlet $^1A_1$ is the ground state, but triplets $^3A_1$ and $^3A_2$ lie about 3–5 kcal/mol higher than the ground state. All these electronic states of $RhCH_2^+$ are results of interaction of the ground state of $Rh^+(d^8, {}^3F)$ with the excited $^1A_1$-state of CH_2. Therefore, we refer this complex to the class of metal-carbene or "Fischer" type complexes. The $^3B_1$ state, which is the lowest among states arising from interaction of the ground state of $Rh^+(d^8, {}^3F)$ with the ground $^3B_1$-state of CH_2, lies about 37 kcal/mol higher than the $^1A_1$-state.

I-D-2 Ab initio MO Study of the Mechanism of Reaction $RhCH_2^+ + H_2 \rightarrow Rh^+ + CH_4$

Djamaladdin G. MUSAEV, Nobuaki KOGA, and Keiji MOROKUMA

The mechanism of reaction

$$RhCH_2^+ + H_2 \rightarrow RhCH_4^+ \rightarrow Rh^+ + CH_4 \qquad (1)$$

has been investigated by using ab initio UMP4(SDTQ) and CASSCF methods with a 17 electron ECP for Rh and basis sets: (5s5p4d)/[3s3p3d](Rh) + (9s5pld)/[4s2pld](C) + (4s)/[2s](H) for $^1A_1$- and $^3A_1$-states of $RhCH_2^+$. It has been found that reaction (1) is exothermic by about 31 kcal/mol for $^3A_1$-state, but is endothermic by about 10 kcal/mol for $^1A_1$-state of $RhCH_2^+$. For both electronic states, this reaction is symmetry allowed only in C_s-symmetry or less and the energetically most favorable path for reaction (1) is attack of the molecule H_2 to the C atom. But it probably does not take place in moderate temperature for the ground $^1A_1$-state, because of a considerable (36 kcal/mol) activation barrier. The more favorable path is to cross over from the ground state to the excited $^3A_1$-state, requiring about 5 kcal/mol, and then to go over a small (about 5–10 kcal/mol) activation barrier, giving an ion-molecule complex $Rh^+ \cdot CH_4$, which is stable by about 12 kcal/mol relative to the dissociation limit $Rh^+ + CH_4$.

I-D-3 Ab initio MO Study of Electronic and Geometrical Structure of the Complex $CoCH_2^+$

Djamaladdin G. MUSAEV, Nobuaki KOGA, and Keiji MOROKUMA

The electronic and geometrical structures of the complex $CoCH_2^+$ have been investigated by using ab initio 10 electron-10 orbital CASSCF with the 9 electron ECP for Co and basis sets: (3s3p5d)/[2s2p2d](Co) + (9s5p)/[3s2p](C) + (4s)/[2s](H).

It has been found that the nearly degenerate $^3A_1$ and $^3A_2$ states are the ground states for this complex. Next low-lying electronic states are $^1A_1$ and $^3B_1$ states, lying about 15 and 21 kcal/mol above the ground states. The ground states are results of interaction of the ground state of $Co^+(d^8, {}^3F)$ with

the excited $^1A_1$-state of the CH_2 group. Therefore, this complex can be classified as a metal-carbene or "Fischer" type complex.

The results for this complex have been compared with those for the $RhCH_2^+$ complex.

I-D-4 Carbonyl Insertion into Pd-H Bond of $HPd(R)(CO)(PH_3)$ (R=CH_3, H) and Comparison with that into Pd-CH_3 Bond. Ab Initio MO Study

Nobuaki KOGA and Keiji MOROKUMA

[*New J. Chem.*, in press]

We studied carbonyl insertion into the Pd-H bond (hydride migratory insertion) of $HPd(R)(CO)(PH_3)$ (R=CH_3 and H) theoretically using the ab initio MO methods and compared it with carbonyl insertion into the Pd-CH_3 bond (methyl migratory insertion). Comparison at the MP2//RHF level shows that the hydride migratory insertion is more endothermic, but has a lower activation barrier than the methyl migratory insertion. The larger endothermicity is ascribed to the Pd-H bond which is stronger than the Pd-CH_3 bond. The smaller activation barrier is due to the fact that the spherical hydrogen is orbital is more suitable for the three-centered interaction at the transition state than the more directional carbon sp^3 hybrid orbital of the methyl group. Though $Pd(CHO)(CH_3)(PH_3)$ is an equilibrium structure, $Pd(CHO)(H)(PH_3)$ is not; electron correlation makes the simple hydride migratory insertion of $Pd(H)_2(CO)(PH_3)$ up-hill. Therefore, we studied the reaction of $Pd(H)_2(CO)(PH_3)$ with the MP2 geometry optimization to show that the insertion and reductive elimination of hydride and the resultant formyl group takes place as one combined step with the low activation barrier. The energetics obtained shows that carbonyl insertion into the Pd-H bond of the present model systems can take place easily, regardless of whether the hydride migration is simple or couples with reductive elimination.

I-D-5 Ab initio Potential Energy Surface for SiH Bond Oxidative Addition to Coordinatively Unsaturated $RhCl(PH_3)_2$

Nobuaki KOGA and Keiji MOROKUMA

We have previously studied potential energy surface for methane CH bond activation by $RhCl(PH_3)_2$ (1), reaction 2, to find that coordinatively unsaturated 1 activates CH bond easily and that electron correlation effect is important in calculating energetics. As an extension, we studied SiH bond oxidative addition to 1 (reaction 1), to compare its potential energy surface with that for reaction 2.

$$SiH_4 + RhCl(PH_3)_2 \rightarrow HRhCl(PH_3)_2(SiH_3) \quad (1)$$

$$CH_4 + RhCl(PH_3)_2 \rightarrow HRhCl(PH_3)_2(CH_3) \quad (2)$$

Because of the importance of correlation effect, in the present study we determined the structures of the stationary points for reactions 1 and 2 at the RMP2 level. While for reaction 2 a C_{2v} CH_4 complex and the transition state (TS) between this complex and the product are located, the C_{2v} SiH_4 complex is found to be the TS connecting $HRhCl(PH_3)_2(SiH_3)$ and its enantiomer and the TS for SiH bond oxidative addition does not exist. This difference originates from the fact that reaction 1 is more exothermic than reaction 2 by about 40 kcal/mol calculated at the RMP2 level. In order to clarify why reaction 2 is so exothermic, we calculated at the RMP level the differences in the bond energy between CH and SiH bonds as well as between RhC and RhSi bonds, to find that the RhSi bond is 20 kcal/mol stronger than the RhC bond and that the SiH bond is 16 kcal/mol weaker than the CH bond at the RMP2 level. These two factors make reaction 1 much more exothermic.

I-D-6 Effect of Phosphine on H_2 Oxidative Addition to $Pt(PR_3)_2$ (R=H, Me, and t-Bu). Ab Initio MO Study

Nobuaki KOGA and Keiji MOROKUMA

H_2 *cis* oxidative addition to $Pt(PR_3)_2$ (eq.1) has been studied theoretically by several groups including ourselves, using PH_3 as a model phosphine.

$$H_2 + Pt(PR_3)_2 \rightarrow H_2Pt(PR_3)_2 \quad (1)$$

Though *cis* addition is symmetry allowed, experimentally only the *trans* product has been observed in the reactions with bulky phosphines such as $P(t\text{-}Bu)_3$. Therefore, it is necessary to carry out calculations on the reaction with a bulky phosphine, in order to investigate what actually takes place in the experiments. We have studied reaction 1 with H, Me, and t-Bu as R by geometry optimization at the RHF level. Potential energy profiles of *cis* addition for R=H and Me are very similar to each other; the activation barriers are low (13–15 and 5–6 kcal/mol at the RHF and the MP2 level, respectively) and the reactions are exothermic by 10 and 18 kcal/mol at the RHF and the MP2 level, respectively. On the other hand, H_2 *cis* addition with R=t-Bu is very different in energetics; the reaction is 17 kcal/mol endothermic and the activation barrier is 34 kcal/mol at the RHF level. While *cis* addition is unfavorable, *trans*-$H_2Pt(P(t\text{-}Bu)_3)_2$ is much more stable than *cis*-$H_2Pt(P(t{=}Bu)_3)_2$ by 30 kcal/mol. Further calculations suggest that the dissociative mechanism is responsible to the trans product, in which *cis* addition at first takes place with dissociation of one $P(t\text{-}Bu)_3$, followed by *cis-trans* isomerization and re-association of the phosphine. Endothermicity of *cis* H_2 addition to $Pt(P(t\text{-}Bu)_3)_2$ is ascribed to the steric repulsion between two bulky phosphines and the weak Pt-H bond in the product.

I-D-7 Ab Initio MO Study on the Structure and Bonding in $H_4Os(PH_3)_3$ and $H_5Os(PH_3)_3^+$

Xue-Kui Li *(Jilin Univ. and IMS)*, **Nobuaki KOGA, and Keiji MOROKUMA**

The structures of $H_4Os(PH_3)_3$ and $H_5Os(PH_3)_3^+$ have been studied with an ab initio MO method. We determined the geometries of the several isomers of these complexes and of the transition states between the isomers at the RHF level under the effective core potential approximation. Also, based on the analysis of bonding between hydrides and Os, we have discussed the relative stabilities of isomers having η^1-H_2 and η^2H_2 coordination forms as well as polyhydride forms. The optimized classical structure of

$H_4Os(PH_3)_3$ corresponds well with the experimentally determined structure of $H_4Os(PMe_2Ph)_3$.

I-D-8 A Theoretical Study on Hydrozirconation

Jun ENDO *(Mitsubishi Petrochemical Co. and IMS)*, **Nobuaki KOGA, and Keiji MOROKUMA**

Hydrozirconation (reaction 1) can be considered to be a simple model reaction of olefin polymerization by zirconocene/methyl-aluminoxane system.

$$Cp_2Zr(H)Cl + C_2H_4 \rightarrow Cp_2Zr(C_2H_5)Cl \quad (1)$$

$$Cp_2Zr(H)Cl + C_2H_2 \rightarrow Cp_2Zr(C_2H_3)Cl \quad (2)$$

Following our previous study, we analyzed difference of reactivity between ethylene (eq.1) and acetylene (eq.2). There are two possible reaction paths; the one is olefin attack to Zr between Cl and H (path 1), and the other is olefin attack from the site opposite to Cl (path 2). As in reaction 1, path 1 is more favorable than path 2 in reaction 2. At the RHF level, the exothermicities for reaction 2 (38 and 36 kcal/mol for paths 1 and 2, respectively) are larger than those for reaction 1 (24 and 21 kcal/mol, respectively), whereas the activation energies for reaction 2 (16 and 29 kcal/mol for paths 1 and 2, respectively) are similar to those for reaction 1 (15 and 28 kcal/mol for paths 1 and 2, respectively). The electron correlation effect, taken into account by the MP2 calculations at the RHF structures, lowers the activation energy by 20 and 11 kcal/mol for paths 1 and 2, respectively. To investigate why this Zr complex does not bring about olefin polymerization experimentally, we also performed calculations for reaction 3.

$$Cp_2Zr(CH_3)Cl + C_2H_4 \rightarrow Cp_2Zr(C_3H_7)Cl \quad (3)$$

The activation energy of path 1 for this reaction was 44 and 27 kcal/mol at the RHF and the MP2 level, respectively. This high activation energy was ascribed to the large deformation energy of the Zr complex at the transition state structure.

I-D-9 A Theoretical Study on Isotactic Propylene Polymerization with Silylene-Bridged Zirconocene Catalyst

Hiroshi KURIBAYASHI *(Sumitomo Chemical Co. and IMS)*, **Nobuaki KOGA, and Keiji MOROKUMA**

It has been reported recently that some silylene-bridged zirconocene complexes catalyze propylene polymerization to give highly isotactic polypropylene. In this study, in order to clarify the origin of regio- and stereo-selectivity in this polymerization, we calculated the potential energy profile for the following model reactions (eq.1) by the ab initio MO method combined with molecular mechanics (MM).

$$[Zr]R'^{+} + C_2H_3R'' \rightarrow [Zr]R'(C_2H_3R'')^{+} \rightarrow [Zr]C_2H_3R'R''^{+} \quad (1)$$

$$[Zr] = [H_2Si(C_5H_{4-n}R_n)_2]Zr$$

First, we have optimized the structures of the reactant, the intermediate, the transition state, and the product for the ethylene insertion into Zr-CH_3 bond (R=R″=H and R′=CH_3) at the RHF/3-21G (Zr:ECP, Cp:STO-3G) level. We obtained the reasonably low activation barrier of 16.7 and 6.0 kcal/mol at the RHF and the RMP2 level, respectively, relative to the ethylene complex.

Further, we carried out MM calculations by introducing the methyl substituents on olefin and/or Cp ligands and keeping the remaining structures to be those for ethylene insertion calculated by the ab initio MO method. The calculated selectivities are in good agreement with the experimental trends. We found that selectivities were determined by the steric effects at the transition state.

I-E Theoretical Studies of Chemical Reactions on Solid Surfaces

Jim Anchell, Ph.D. from University of Wisconsin, came to our group in March 1991 as a JSPS Postdoctoral Fellow to restart our surface reaction project, which has been temporarily slowed down by departure of Mr. Sawabe, who finished his PhD and became a Research Associate in experimental surface chemistry.

I-E-1 Ab initio Study of the Adsorption and Absorption of Hydrogen on the Surface of Ni (111)

James ANCHELL and Keiji MOROKUMA

Adsorption and subsequent absorption of H on a three-fold hollow site on the surface of Ni (111) has been studied with the *ab initio* MO method. A nineteen atom cluster has been used to model the Ni-surface, where we have employed a one-electron model potential on all nickel atoms. Double-zeta plus polarization basis sets were employed for hydrogen and seven nickel atoms nearest the adsorption and absorption site. At the level of fourth-order Moller-Plesset perturbation our model predicts that the perpendicular distance of H above the three-fold hollow at equilibrium is 1.22Å; the adsorption energy is 56 kcal/mole; the barrier to absorption is 35 kcal/mole, and that once absorbed the barrier to desorption is 17 kcal/mole. We also find that when a first hydrogen is preabsorbed into the three-fold hollow site, the adsorption energy for a second hydrogen atom at the same site is reduced by 42 kcal/mole. Using a Morse potential fit to our energy profile, we find A_1 vibrational stretching frequencies at the adsorption and absorption site of 1097 cm^{-1} and 815 cm^{-1}, respectively.

I—F Structures and Reactions of Manybody Chemical Systems

Electronic structure and dynamical behavior of large systems such as liquids and polymers are investigated theoretically. (a) Collective motions and fluctuations in liquid and cluster (b) Chemical reactions and energy relaxations in liquid and clusters, and (c) Electronic structures and dynamical behaviors of polyenes, are analyzed.

I-F-1 Long Time Fluctuation of Liquid Water; $1/f$ Spectrum of Energy Fluctuation in Hydrogen Bond Network Rearrangement Dynamics

Masaki SASAI, *(Nagoya Univ.)* **Iwao OHMINE, and Ramakrishna RAMASWAMY** *(Jawaharlal Nehre Univ. and IMS)*

The power spectrum of the potential energy fluctuation of liquid water is examined and found to yield so called $1/f$ frequency dependence (f is frequency). This is in sharp contrast to spectra of simple liquids (for example, liquid argon), which exhibit a near white spectrum. This indicates that there exists an extended multiplicity of hydrogen bond network relaxations in liquid water. A simple model of cellular dynamics is proposed to explain this frequency dependence. On the other hand, the cluster dynamics of argon also involves energy fluctuations of a $1/f$ type, resulting from various relaxation processes at core and surface.

I-F-2 Potential Energy Surfaces for Water Dynamics II: Vibrational Mode Excitations, Mixing and Relaxations

Iwao OHMINE and Hideki TANAKA *(Kyoto Univ.)*

[*J. Chem. Phys.* **93**, 8138 (1990)]

Multidimensional properties of the potential energy surface are explored in terms of vibrational mode excitations. The vibrational mode dynamics, especially mechanism of mode relaxation and structure transitions, is analyzed. It shows very strong excitation energy dependence and mode dependence. There exist very low energy paths involving single or few water molecule displacements at almost every inherent structures, indicating that certain facile molecular movements occur even in very low temperature states. Different energy excitations of a low frequency mode result in different inherent structure transitions; transitions caused by high energy excitations involve many large molecular displacements.

I-F-3 Relaxations, Fluctuations, Phase Transitions and Chemical Reactions in Liquid Water

Iwao OHMINE and Masaki SASAI

[*Prog. Thepr. Phys. Supplement* **108**, 61 (1991)]

Fluctuations and collective motions in liquid water and their effects on chemical reactions dynamics are analyzed. Liquid water is a 'frustrated' system with multiple random hydrogen bond network structures, and has anomalous microscopic and macroscopic properties. Rearrangement dynamics of the hydrogen bond network induce collective motions of water molecules and energy fluctuations. Vibrational motions of photoexcited molecules strongly resonate to these water fluctuations, and thus energy dissipation processes in liquid water are extremely fast. Time scale, spatial scale and energy scale of the collective motions are analyzed by examining potential energy surfaces involved. A model of hydrogen bond network based on the functional integral method is presented and spatial and energy scales of fluctuations are discussed. Instability of hydrogen bond network is studied to understand the physical origin of these microscopic and macroscopic anomalies of liquid water.

I-F-4 The Argon Cluster Dynamics in the Melting Region

Norihiro SHIDA and Iwao OHMINE

The melting in argon clusters has been investigated within the molecular dynamics simulation framework; A new characterization has been proposed to represent the global shapes of multi-dimensional potential energy surfaces. Statistical properties, such as Lyapnov exponents, Kolmogorov (metric) entropies and fractal dimensions, have also been calculated to see the extent of the phase space by the melting. We have been investigating the relationship between these statistical properties and the global shapes of potential energy surfaces.

We have been investigating a new characterization to symbolize the global shapes of potential energy surfaces, by using high energy stationary points where the Hessian matrices have more than two negative eigenvalues, in addition to local minima and saddle points. Local minima and saddle points are valuable reference points to calculate the intrinsic observables. In contrast, high energy stationary points are important to characterize the global shapes of potential energy surfaces, such as valleies, ridges or cliffs. We have found such stationary points in Ar_7 by using the gradient extremal method and each point on the trajectories has been assigned to either of these stationary points. The number of points assigned to each stationary point have been examined against the temperatures in the melting region.

I-F-5 Dynamics of Water Clusters and Energy Relaxation of an Excess Electron in Water Clusters

Shinji SAITO and Iwao OHMINE

Dynamical behavior of an excess electron in an attachment process is investigated. To fully take into account of the electronic non-adiabatic transitions, the time-dependent Schrödinger equation of the excess electron in water molecules is solved with the Pechukas' method combined with the classical Molecular Dynamics technique. Temperature- and cluster size- dependences of the energy flow and effects of specific water motional modes on the non-adiabatic transition are being analyzed.

Dynamics of water clusters without an excess electron at various temperatures has also been studying. The melting temperature, the dielectric relaxation, the structural fluctuation etc., are explored.

I-F-6 Proton Transfer in Water; Analysis for Potential Energy Surface

Tamiki KOMATSUZAKI and Iwao OHMINE

Proton transfer(PT) in liquid water is investigated. To examine the existence of cooparative PTs (proposed by Grotthus, Davydov et al) in hydrogen network, we are investigating the hydrated structures of $(H_2O)_nH^+$ (n=3,5,7,8) and the potential surface for the cooparative

2-proton transfer. The activation energy of concerted PT is found to be less than KT in a certain structure. The barrier heights are very sensitive to surrounding water structure. Very long range (through bond) interactions are be included to obtain correct potential energy surface.

To construct a realistic potential function for PT in water which includes the internal freedom and many body effect, a detail analysis of interaction energy components of $(H_2O)_nH^+$ (n=1,2,3) was made within Hartree-Fock approximation; we used the energy decomposition scheme (Morokuma and Kitaura) where the interaction energy are devided into electrostatic, polarization, charge transfer, exchange repulsion and their coupling terms). The amount of 3-body effect between $2H_2O$ and H_3O^+ in $H_7O_3^+$ were estimated to be about 4 ~ 12 kcal/mol. These values depend strongly on molecular geometry. The most-dominant contribution to the 3-body effect is the charge transfer term rather than the polarization term, unlikely water clusters.

The validity of polarization model of hydrated proton by Stillinger and David who reduced the hydrated proton to the aggregate of ionic species (polarizable O_2^- and bare H^+) were also investigated.

I—G Theoretical Studies of Chemical Reaction Dynamics

Clarification of the reaction mechanisms and development of illuminating good approximate theories are our ultimate purposes of the theoretical reaction dynamics studies. We are pursuing to employ hyperspherical coordinates for triatomic systems. We have also analyzed a reaction in cluster, prototypical model of reactions in liquid, by using the recently proposed decoupling surface analysis method.

I-G-1 Reaction Dynamics of D + H_2 → DH + H: Effects of Potential Energy Surface Topography and Usefulness of the Constant Centrifugal Potential Approximation

Shoji TAKADA, Akihiko OHSAKI *(Miyazaki Univ.)*, **and Hiroki NAKAMURA**

[*J. Chem. Phys.* in press]

Two findings are reported for the D + H_2 → DH + H reaction on the basis of the exact quantum mechanical calculation for $J = 0$, where J is total angular momentum. First, with use of the Liu-Siegbahn-Truhlar-Horowitz (LSTH) surface and the Varandas surface, we demonstrate that a rather small difference in potential energy surface (PES) induces a surprisingly large effect on reaction dynamics. Two origins of the discrepancy are pointed out and analyzed: (1) Non-collinear conformation in the reaction zone contributes to the reaction significantly despite the fact that the minimum energy path and the saddle point are located in the collinear configuration. (2) A difference in the distant part of PES also causes a discrepancy in the reaction dynamics indirectly, although this effect is much smaller than (1). Secondly, we investigate the validity of the constant centrifugal potential approximation (CCPA) based on the accurate results for $J = 0$. The use of CCPA to estimate total cross section and rate constant is again proved to have practical utility as in the cases of the sudden and adiabatic approximations.

I-G-2 Application of the Decoupling Surface Analysis to Intracluster Reaction

Kiyohiko SOMEDA and Hiroki NAKAMURA

In order to grasp the qualitative features of chemical reaction dynamics, we have proposed the decoupling surface analysis based on a canonical transformation in phase space.[1] This is confined at present to a classical mechanical framework, but is applicable to large reaction systems. Our final goal is to understand reactions in solution. As a prototypical model to the reactions in solution we have studied a reaction in cluster. We have chosen the reaction Cl + Cl_2 in Ar_{52}. The chlorine atoms are placed in the central collinear conformation in the icosahedral symmetry Ar_{55} cluster. The decoupling surface is constructed and the local frequencies $\Omega_1(\varepsilon, \tau)$ as a function of energy ε and time τ are analyzed for each vibrational mode. The symmetric stretch mode of Cl_3 has a strong effect on the reaction, but is almost isolated from the solvent motions. The bending vibrations and translation modes are naturally mixed with the solvent modes and split into stable and unstable branches.

Reference

1) Kiyohiko Someda and Hiroki Nakamura, *J. Chem. Phys.* **94**, 4260 (1991).

I-G-3 Semiclassical Approach to Charge-Transfer Processes in Ion-Molecular Collisions

Hiroki NAKAMURA

[*Adv. Chem. Phys.* in press]

Basic mechanisms of nonadiabatic electronic transitions associated with charge transfer are summarized and their qualitative characteristics are discussed. These are the Landau-Zener and Rosen-Zener type of nonadiabatic transitions, and the transitions induced by Coriolis (rotational) coupling, spin-orbit interaction, and the coupling due to the electron momentum transfer or the ETF (electron translation factor) in charge transfer. It is shown that the semiclassical theory can be utlized to analyze all these transitions uniformly by introducing the new (dynamical-state) representation. Qualitative discussions are also presented for reactive transition, or particle rearrangement by emphasizing the role of the potential ridge, the watershed diving the reactant and product valleys. The basic formulae for the two-state nonadiabatic electronic transitions are also summarized and the dynamical-state representation is explained mathematically in more detail. One of the important generalizations of the one-dimensional two-state semiclassical theories is the multichannel curve crossing problem. With use of the two-state theories a general formalism is described for the multi-level system involing closed channels.

The simplified treatment, i.e., the BFG (Bauer-Fisher-Gilmore) model, for the vibronic transitions in ion-molecule collisions is also briefly touched upon. Some of the numerical applications reported so far are presented together. After briefly summarizing the historical orbiting model of ion-polar molecule collisions and the classical S-matrix theory for reaction, the hyperspherical coordinate approach is explained and is demonstrated to be powerful for grasping the reaction mechanisms. A simple semiclassical generalization of the trajectory surface hopping method is proposed. Essential idea is to use the well developed one-dimensional semiclassical theories on the curvilinear one-dimensional classical trajectories. Other desirable challenging problems to be developed in future are also briefly discussed.

I—H Theoretical Studies of Highly Excited States of Molecules

Highly excited states show various intriguing properties and participate in a variety of dynamic processes. We believe that they will open a new challenging world of science. The ultimate purpose of our studies is to find the new collective motions in these states and understand their participating dynamics.

I-H-1 Doubly Excited States of Hydrogen Molecules

Masahiro IWAI and Hiroki NAKAMURA

Various doubly excited states (first kind of superexcited states) of hydrogen molecule ($^{1,3}\Sigma_{g,u}$, $^{1,3}\Pi_{g,u}$ and $^{1}\Delta_{g}$) are calculated by using the Feshbach projection operator method based on the H_2^+ orbitals. The resonance energies and autoionization widths are estimated as a function of internuclear distance. Information on these quantities is inevitable to investigate various dynamic processes. Role of electron correlation in these states is also analyzed in comparison with the collective motion in the corresponding doubly excited states of He in the united atom limit. Interesting transition is observed from the strongly correlated collective motion in He to the independent particle picture in the separated atom limit.

I-H-2 Anharmonic Collective Vibrational Modes in ABA Triatomic Molecules

Masahiro IWAI and R.D. LEVINE *(The Fritz Haber Research Center, Israel)*

[*Phys. Rev.* **A42**, 3991, (1990)]

An algebraic Hamiltonian for two coupled anharmonic (Morse-type) oscillators admits an exact symmetry at a finite value of the coupling constant. The two symmetry-adapted modes are neither local nor normal, yet are independent. The explicit discussion is given for two coupled stretch modes but the same symmetry is found also when the two stretches are in addition coupled to the bend mode.

I—I Theory of Nonadiabatic Transition

Nonadiabatic transition is one of the very basic mechanisms of state (phase) change in various fields of physics and chemistry. We are currently interested in developing good analytical formulae for various cases of nonadiabatic transitions and also in nonadiabatic tunneling in one-dimensional periodic system.

I-I-1 Nonadiabatic Tunneling in One-Dimensional Finite Periodic System

Hiroki NAKAMURA

Nonadiabatic tunneling in one dimensional finite periodic potential system is analyzed. Conditions for complete resonant transmission and reflection, and for acceleration of transmission are derived. Theoretical possibility of controlling transmission (switching) is discusses by considering electronic coupling as a control parameter. This could be a prototypical model of electron or proton transfer occurring in chemical and biological systems. Or if we could synthesize such a molecular system, this could be a kind of molecular element.

I-I-2 Semiclassical Theories for the Linear Curve Crossing Problems

Chaoyuan ZHU and Hiroki NAKAMURA

The linear curve crossing problems are thoroughly reinvestigated. Stokes line structure and transition point distribution are analyzed in the whole range of the two parameters. Relations among the Stokes constants are obtained and the scattering matrices are expressed in terms of one Stokes constant. Exact expression for this Stokes constant is derived, and the new better approximate expressions for the scattering matrices are obtained for the high and low energy limiting cases.

I—J Theory for High-Tc Superconductivity

To clarify the origin of Cu-O type high-temperature super-conductivities, we theoretically study their microscopic electronic structures and the natue of electron-phonon couplings in these materials. We are especially interested to clarify the effects of anharmonicity of lattice vibrations on the isotopic shift of Tc.

I-J-1 Suppressed Metal-Insulator Transitions, Enhanced Superconductivity and Reduced Isotope Effect by Quartic Anharmonicity of Phonon in Peierls-Hubbard Model

Keiichiro NASU

A quasi two-dimensional Peierls-Hubbard model with anharmonic phonons has been studied, so as to clarify the competition between the metallic state and the charge- or spin-density wave (CDW or SDW) states, as well as the isotope effect on the super-conducting (SP) transition temperature Tc of this system. The anharmonicity is assumed to be a local quartic one, like a hardcore repulsion. This theory is based on the mean field approximation for electrons and a variational method for phonons. Because of an interplay between the quantum fluctuation of phonons and this hardcore type anharmonicity, the Peierls distortion is excessively suppressed. Thus, the metallic state becomes more stable than the CDW, even when the electron-phonon coupling is very strong. This interplay is shown to suppress the SDW, too, and relatively enhances the SP state. Tc due to this anharmonic phonon has no isotope effect, and amounts to around 50K ~ 100K. Recent optical measurements on Cu-O type ceramics are also discussed in connection with this local anharmonicity.

I-J-2 The Effect of Electron Interaction on Two-Dimensional Peierls Instability

Jin NAN LIU *(Fudan Univ.)*, **Xin SUN** *(Fudan Univ. and IMS)*, **and Keiichiro NASU**

The effect of electron interaction on two-dimensional Peierls instability is studied by means of electron correlation function. Our theory deals with full electron interaction rather than only the on-site repulsion, so that its results are more physical. Meanwhile, our method can avoid the uncertainty caused by the finite-size effects. The results show, in contrast to the one-dimensional case, the two-dimensional half-filled electron-lattice system has a normal behavior under the electron-electron interaction, that the dimerization is reduced by the electron interaction. The weaker is the screening of the interaction, the larger is the reduction.

I-J-3 New Approach to the Local Polaron Model in Fluctuating-Valence System

Haung ZHENG *(Shanghai Jiao Tong Univ. and IMS)* **and Keiichiro NASU**

The local polaron problem, in which a local f-electron hybridized with conduction electrons in a wide band, coupling to a local phonon mode, is solved by a new variational approach. The nonadiabatic effects due to finite phonon frequency ω are treated through a variational polaron wave function, in which the softening of the phonon frequency as a result of electron phonon interaction is taken into consideration by means of the squeezing transformation. We have found that the quantum fluctuation of the phonon mode gradually smooth out the abrupt transition of the f-level occupancy, when the effective f-level increases across the Fermi energy. There is a critical value of ω, above which the transition becomes continuous. In order to improve our treatment for the degenerate case when ω is small, the method of the "orthogonality catastrophe theorem" is used, and an energy-dependent form for the local potential of conduction electrons has been introduced. Our results show that the transition of the f-level occupancy should be continuous for finite ω, although it becomes steeper and steeper with decreasing ω. Besides, it is pointed out that because of the quantum fluctuation of the phonon mode, a significant renormalization of the virtual f-level width never occurs even if the conditions of previous authors for its occurence are satisfied.

I—K Nonlinear Excitations in Halogen-Bridged Mixed-Valence Metal Complexes

To clarify the nonlinear lattice relaxation process of optical elementary excitations in one-dimensional charge density wave state, we study singlet excitons, self-trapped excitons, solitons and polarons in one-dimensional halogen-bridged mixed-valence metal cmplexes.

I-K-1 Nonlinear Lattice Relaxation Process of Exciton in Quasi One-Dimensional Halogen-Bridged Mixed-Valence Metal Complexes; Self-Trapping, Solitons and Polarons

Masato SUZUKI and Keiichiro NASU

Self-trapped exciton(STE), solitons and Polarons of a one-dimensional extended Peierls-Hubbard model are investigated, so as to clarify the lattice relaxation paths of photogenerated excitons in halogen-bridged mixed-valence metal complexes. This theory takes into account the lattice distortion of halogen ions in the direction perpendicular to the chain, as well as a parallel one. It is mainly based on the adiabatic approximation for phonons and the mean field theory for interelectron interactions, but is also reinforced by taking into account the electron-hole correlation to obtain the exciton. Potential surfaces relevant to the relaxation of the excition have been finally clarified in terms of various nonlinear excitations. This result can explain various rather dispersed experiments from an unified point of view, such as photo-absorption and luminescence spectra, the Stark effect and the ESR data. The origins of the photo-induced absorption are concluded to be the polarons.

I—L Optical Nonlinearity of Low Dimensional Materials

To clarify the higher order optical activities of low dimensional solids, we calculate frequency dependence of third order optical susceptibility

I-L-1 Frequency Dependence of Third Harmonic Generation of Polyacetylene

Xin SUN *(Fudan Univ. and IMS)*, **Keiichiro NASU, and Chang GIN WU** *(Center of Theoretical Physics, Trieste)*

The frequency dependence of the third harmonic generation of the trans-polyacetylene is quantitatively interpreted by considering the bands of finite chain and the damping of excitation. Our theory shows there are two distinct peaks in the spectrum of the third harmonic generation. The first one around 0.6eV comes from the three-photon resonant transition between the edges of valence band and conduction band; the second one around 0.9eV is produced by the two-photon transitions from the levels in the valence band to the levels in the conduction band. The momentum-dependent damping is essential to determine the position of the second peak. The theoretical results agree well with the experimental data.

RESEARCH ACTIVITIES II
Department of Molecular Structure

II—A Laser Investigation of Autoionizing and Predissociating States of Atoms and Small Molecules

Highly excited electronic states of molecules and atoms play important roles in inelastic collision processes including chemical reactions. In those states of molecules, many dissociation and ionization channels are generally open and strongly compete with each other, so that dominating channels tend to differ from state to state. Therefore, 'state-resolved' measurements of dynamical behaviors of those highly excited states are expected to give us a lot of knowledge on the complicated channel competition, which may provide useful information on photochemical reactions. In atoms, on the other hand, doubly excited states are of particular interest because they do not only play an important role in photoionization processes but they also intrinsically involve electron correlation effects, which may lead to cooperative electronic motions. In this study, with the above interest, highly excited states of molecules and atoms are spectroscopically investigated through laser multiphoton and/or multistep excitation methods with the aid of some theoretical analyses.

II-A-1 Detection of Nitrogen Atoms Produced by Predissociation of Superexcited Rydberg States of NO

Asuka FUJII and Norio MORITA

[*Chem. Phys. Lett.*, **182**, 304 (1991)]

Predissociation processes of superexcited states (neutral states above the first ionization threshold) of the NO molecule have been investigated by detecting the fragment nitrogen atom. A two-color double resonance technique is used to produce the superexcited Rydberg states. The molecule is excited to the $A^2\Sigma^+$ (v=1,N) state by a laser, and then successively excited to the superexcited Rydberg states (v=1, n=7−17, l=s, p and f) by another laser. Nitrogen atoms resulting from predissociation of the Rydberg states are detected by (2+1)REMPI (resonance-enhanced multiphoton ionization) with the third laser. Scanning the second excitation laser, fragment-yield spectra of the nitrogen atom have been obtained (Fig.1 (c) and (d)). As a result, the N(^{2}D) production, which was predicted by theoretical calculations, has been confirmed. Moreover, the unexpected generation of N(^{4}S) has been observed. We have also obtained a two-color fluorescence dip spectrum of the intermediate A state (Fig.1(a)) and a two-color MPI spectrum (NO^+ yield) (Fig.1(b)). The former corresponds to an absorption specrum in the A→nl transition, and the latter reflects an autoionization cross section of each Rydberg state. Each of these four spectra is quite different in intensity distribution. This shows that the competition between autoionization and predissociation processes strongly depends on both the principal and angular momentum quantum numbers of the Rydberg electron.

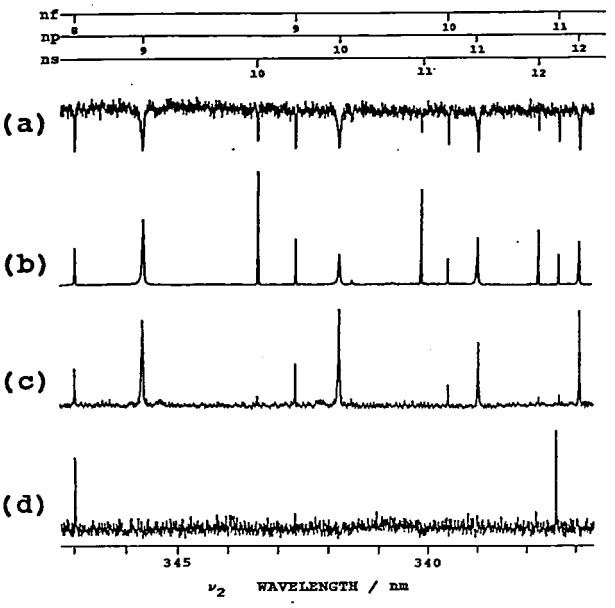

Figure 1. Four kinds of excitation spectra of the NO molecule, obtained by detecting (a) fluorescence from the $A^2\Sigma^+$ state (fluorescence dip spectrum due to the absorption in the A→nl transition, (b) NO^+, (c) N(^{2}D) and (d) N(^{4}S). They are all displayed as functions of excitation laser wavelength scanned over transitions from the $A^2\Sigma^+$ (v=1, N=0) to nl Rydberg states.

II-A-2 Rotational Dependence of Predissociation in the Superexcited 7f Rydberg State (v=1) of NO

Asuka FUJII and Norio MORITA

Rotational dependence of predissociation processes in the superexcited 7f Rydberg state (v=1) of NO has been studied by means of resonance-enhanced multiphoton ionization (REMPI). Several rotational levels of the 7f Rydberg state are selectively excited by using a two-color double resonance technique, and fragement nitrogen atoms generated by the predissociation are detected with the REMPI method. The rotational coupling in the 7f state can be described by Hund's case (d), and the projection of the orbital angular momentum onto the axis of core rotation, L, is well defined. As a result of the experiment, it has been found that the rotational levels having odd L generate both N(^{2}D) and N(^{4}S) atoms by predissociation, while the even L levels

produce only N(^{2}D) atoms. The odd L rotational levels have Σ^+-type parity, and the even L levels have Σ^--type parity. Therefore, the experimental results indicate that the predissociation to the N(^{4}S) atom occurs via the $A'^2\Sigma^+$ state, which is the only Σ^+ symmetry state dissociating to N(^{4}S). In addition, we have found that the autoionization efficiency of the odd L rotational levels is much smaller than that of the even L levels. Moreover, remarkable line-broadening in the odd L levels was reported[1]. These facts suggest that the predissociation process is much faster than the autoionization process in the odd L levels.

Reference

1) D.T. Biernacki, S.D. Colson and E.E. Eyler, *J. Chem. Phys.*, **89**, 2599 (1988).

II-A-3 R-Matrix Calculation of Doubly Excited $^1S^e$ States of Ca Atom below 6s Threshold

Norio MORITA

[*J. Phys. B*, submitted]

By an eigenchannel R-matrix calculation of the final state multichannel quantum-defect parameters in LS coupling, the photoexcitation spectrum of doubly excited $^1S^e$ states of atomic calcium from the 4p ionization threshold up to the 6s threshold has been obtained with the initial state fixed to the 4s4p state. The spectrum is calculated in both ways using the length- and velocity-form dipole-matrix elements, and agreement between both results is good enough to support the correctness of the calculation. Moreover, using the isolated-core-excitation formula, excitation spectra of the 6sns Rydberg series from the 4sn's states have been calculated and compared with the experimental data. The calculated result is in good agreement with the experimental data except in the lowest observed state, i.e. 6s9s. The latter disagreement has been discussed under a consideration of strong channel interactions.

II—B Laser Cooling of Neutral Atoms

Light has no mass but has momentum, so that an atom can be accelerated or decelerated when the atom absorbs or emits light. On the other hand, a strong radiation field can modify the internal energy of an atom, so that an atom in an inhomogeneous radiation field receives a force. Using those mechanisms, the translational motion of a neutral atom cannot only be controlled but also be cooled to an extremely low temperature by laser radiation. As an atom is cooled and its temperature goes down to a nanokelvin region, its translational de Broglie wavelength becomes a macroscopic size. At this stage, a macroscopic quantum-mechanical collective motion of an atomic assembly can be expected to occur in a very thin gas. Taking a main interest in this point, we have been studying the laser cooling of neutral atoms. Besides this interest, when neutral atoms are controllable by lasers, there will be many applications in various research fields.

II-B-1 Laser Cooling of a Helium Atomic Beam

Mitsutaka KUMAKURA and Norio MORITA

[*Jpn. J. Appl. Phys.* **30**, L1678 (1991)]

Laser cooling of a helium atomic beam in the $2s^3S_1$ metastable state has been demonstrated. The atomic beam is produced by supersonic expansion with a nozzle at the liquid-nitrogen temperature and excited to the metastable state by electron bombardment. Using a homemade single-mode LNA ($La_{1-x}Nd_xMgAl_{11}O_{19}$) laser resonant with the $2s^3S_1$-$2p^3P_2$ transition (λ=1.083 μm), the velocity components perpendicular to the atomic beam are decelerated by irradiation of the laser beam from four directions at right angles with the atomic beam (transverse cooling), and then the velocity component along the atomic beam is decelerated by a counter-propagating laser beam with the Zeeman-tuning technique (longitudinal cooling). To monitor the velocity distribution, the Doppler profile of the $2p^3P_2$-$3d^3D_3$ transition (λ=588 nm) is observed. Figure 1 shows the result. The velocity distribution without the longitudinal cooling is shown in Fig.1(a). Figures 1(b)—1(e) show four different cases of the applied magnetic field. With the present Zeeman-tuning solenoid, the longitudinal cooling is effective to the metastable atoms having velocities slower than 980 m/s. Therefore, the atoms belonging to the slower component of the initial double-peaked velocity distribution are cooled, while the faster component is left uncooled. Adjusting the magnetic field to achieve the optimum cooling, the most probable velocity of the metastable helium atoms, which is initially 750 m/s, is decreased to 90 m/s (Fig.1(e)).

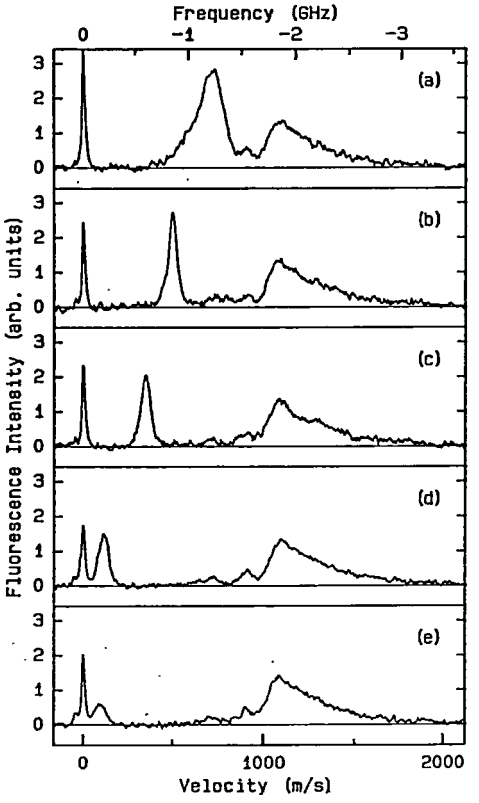

Figure 1. The laser cooling of the longitudinal velocity: (a) the velocity distribution without longitudinal cooling, (b) the one observed when the magnetic field is forced to diminish rapidly to zero at the midway point of the Zeeman-tuning solenoid, (c) the same as (b) except that the diminishing point of the magnetic field is shifted further downstream than for (b), (d) the one observed when the complete magnetic field is applied, and (e) the same as (d) except that the magnetic field is adjusted so as to achieve the minimum velocity.

II—C Molecular Science of Biomolecules and Their Model Compounds

Elucidation of the structure-function relationship of proteins is a current subject of this group. The primary technique to be used for this project is the stationary and time-resolved resonance Raman and absorption spectroscopies. The main themes that we want to explore are 1) mechanism of oxygen activation by enzymes, 2) electron- and proton transfers through proteins and their coupling in the energy transducing membrane, 3) the primary process of photoreceptor proteins, 4) dynamical features of higher order protein structures. In category (1), we have treated reaction intermediates of cytochrome *c* oxidase, cytochrome P-450, chloroperoxidase, and horseradish peroxidase by using the mixed-flow transient Raman apparatus and Raman/absorption simultaneous measurement system. We also examined model compounds such as Fe^{IV}=O porphyrin and its π cation radical. For (2), we have investigated bacteriorhodopsin and cytochrome *c* oxidase, while for (3) we have found the structural difference between P_r and P_{fr} forms of phytochrome and their model compounds. For (4), we succeeded in observing the UV- (200—240 nm) excited time-resolved resonance Raman spectra of proteins in the time resolution of 10 ns and applied it to elucidate the quaternary structure change of hemoglobin. Furthermore, the pump/probe time-resolved Raman system by using two 10-ns visible lasers was set up and applied to pursue photodissociation of the CO adduct of myoglobin, hemoglobin and their mutants. In these experiments dynamical features of protein structures are explored.

II-C-1 Unusual CO Binding Geometry in Abnormal Subunits of Hemoglobin M Boston and Hemoglobin M Saskatoon

Masako NAGAI *(Kanazawa Univ.)*, **Yoshimasa YONEYAMA** *(Kanazawa Univ.)*, **and Teizo KITAGAWA**

[*Biochemistry* **30**, 6495-6503 (1991)]

To clarify the role of the proximal histidine (F8-His), distal His (E7-His), and E11 valine (E11-Val) in ligand binding of hemoglobin (Hb), we have investigated the resonance Raman (RR) spectra of the carbonmonoxide adduct of Hbs M (COHb M) in which one of these residues was genetically replaced by another amino acid in either α or β subunit. In the fully reduced state, all Hbs M gave ν_3 at ~ 1472 cm^{-1} and $\nu_{Fe\text{-}His}$ at 214—218 cm^{-1}, indicating that they

have a pentacoordinate heme and the heme iron is bound to either E7-His or F8-His. The porphyrin skeletal vibrations of the COHb M were essentially unaltered by replacements of E7- or F8-His with tyrosine (Tyr) and of E11-Val by glutamic acid (Glu). The ν_{CO}, $\nu_{Fe\text{-}CO}$, and $\delta_{Fe\text{-}C\text{-}O}$ frequencies of COHb M Iwate (αF8His→Tyr), COHb M Hyde Park (βF8His→Tyr), and COHb M Milwaukee (βE11Val→Glu) were nearly identical with those of COHb A. In contrast, the RR spectra of COHb M Boston (αE7His→Tyr) and COHb M Saskatoon (βE7His→Tyr) gave two new Raman bands derived from the abnormal subunits, $\nu_{Fe\text{-}CO}$ at 490 cm^{-1} and ν_{CO} at 1972 cm^{-1}, in addition to those from the normal subunits at 505 cm^{-1} ($\nu_{Fe\text{-}CO}$) and 1952 cm^{-1} (ν_{CO}). The CO adduct of the abnormal subunits exhibited apparently no photodissociation upon illumination of CW laser with a stationary cell under which the normal subunit exhibited complete photodissociation. From the normal coordinate analysis, the Fe-C-O bond in the abnormal subunits of Hb M Boston and Hb M Saskatoon was suggested to be linear perpendicular against the heme plane.

II-C-2 Observation of the O-O Stretching Raman Band for Cytochrome P-450$_{cam}$ under Catalytic Conditions

Tsuyoshi EGAWA, Takashi OGURA, Ryu MAKINO *(Keio Univ.)*, **Yuzuru ISHIMURA** *(Keio Univ.)*, **and Teizo KITAGAWA**

[*J. Biol. Chem.* **266**, 10246-10248 (1991)]

Dioxygen stretching (ν_{oo}) Raman band was observed for the oxy form of *Pseudomonas putida* cytochrome P-450 (P-450$_{cam}$) generated at room temperature under catalytic conditions, that is, in the presence of D-camphor, β-NADH, putidaredoxin, and putidaredoxin reductase, by using the mixed flow transient Raman apparatus. At the same time the visible absorption spectra were monitored for the transient species. It was found that the ν_{oo} frequency is little altered by binding of putidaredoxin to P-450$_{cam}$, although the reduction rate of the oxy form becomes faster. Another intermediate with an oxygen isotope-sensitive band was not found in a time region until 2 s after mixing of the reduced enzyme with oxygen.

II-C-3 Resonance Raman Study on Intact Pea Phytochrome and Its Model Compounds: Evidence for Proton Migration during the Phototransformation

Yasuhisa MIZUTANI *(Grad. Univ. Adv. St.)*, **Satoru TOKUTOMI** *(NIBB)*, **Katsuhiro AOYAGI** *(Fukushima National College of Tech.)*, **Keisuke HORITSU** *(Tokyo Kasei Univ.)*, **and Teizo KITAGAWA**

[*Biochemistry* in press (1991)]

Resonance Raman (RR) scattering from intact pea phytochrome was observed in resonance with the blue band at ambient temperature. The relative populations of the red-light absorbing form (P_r) and far-red-light absorbing form (P_{fr}) under laser illumination were estimated from the absorption spectra. The most prominent RR band of P_r obtained by 364-nm excitation under 740-nm pumping exhibited a frequency shift between H_2O and D_2O solutions, but that of P_{fr} obtained by 407-nm excitation under 633-nm pumping did not, indicating a distinct difference in a protonation state of their chromophores. Since the protonation level of a whole molecule of intact phytochrome remains unchanged between P_r and P_{fr}, this observation indicates migration of a proton from the chromophore of P_r to the protein moiety of P_{fr}. As model compounds octaethylbiliverdin (OEBV-h_3), its deuterated and ^{15}N derivatives, and their protonated forms were also studied with both RR and ^1H- and ^{15}N-NMR spectroscopies. The RR spectrum of the protonated form, for which the protonation site was determined to be C-ring pyrrole nitrogen by NMR, displayed a deuteration shift corresponding to that of P_r, suggesting a similar protonated structure for the pyrrolic rings of P_r. The RR spectral difference between OEBV-h_3 and OEBV-d_3 and that between H_2O and D_2O solutions of P_{fr} suggested that the N-H protons of the A-, B- and D-rings of intact phytochrome are replaced with deuterons in D_2O. A role of the 7 kDa segment of phytochrome is discussed on the basis of RR spectral differences between the intact and large phytochromes.

II-C-4 Time-Resolved Resonance Raman Investigation of Cytochrome Oxidase Catalysis: Observation of a New Oxygen-Isotope Sensitive Raman Band

Takashi OGURA, Satoshi TAKAHASHI *(Grad. Univ.)*, **Kyoko SHINZAWA-ITOH** *(Himeji Inst. of Tech.)*, **Shinya YOSHIKAWA** *(Himeji Inst. of Tech.)*, **and Teizo KITAGAWA**

[*Bull. Chem. Soc. Jpn.* **64**, 2901-2907 (1991)]

The reduction of dioxygen by cytochrome oxidase has been investigated, in the time interval between 0.1 and 5.4 ms after initiation of the reaction, by using time-resolved resonance Raman spectroscopy combined with the Artificial Cardiovascular System [Ogura et al., Biochemistry 28, 8022-8027 (1989)]. At 0.5 ms we observed a new oxygen-isotope sensitive Raman band at 356 cm^{-1} for $^{16}O_2$, which shifted down to 341 cm^{-1} for $^{18}O_2$. The temporal behavior of this band was found to be very close to that of another oxygen-isotope sensitive band at 788 cm^{-1} which had been assigned previously to the Fe(IV)=O stretching mode of the ferryloxo intermediate [Ogura et al., J. Biol. Chem., 265, 14721-14723 (1990)]. However, the fact that the 788 cm^{-1} band shifts to a higher frequency (802 cm^{-1}) in ^2H_2O, taken together with the present detection of two oxygen-isotope sensitive bands, prompts us to suggest an alternative assignment; namely, that these bands arise from the O^--O^- (788 cm^{-1}) and Fe(III)-O^- (356 cm^{-1}) stretching modes of the Fe(III)-O^--O^--H intermediate. This conclusion forces a reconsideration of the currently accepted view of cytochrome oxidase catalysis.

II-C-5 Time-Resolved UV Resonance Raman Study on Bohr Effects of Hemoglobin

Shoji KAMINAKA and Teizo KITAGAWA

[*J. Am. Chem. Soc.* in press]

Effects of Bohr protons on the quaternary structure dynamics were investigated for photodissociation of carbonmonoxy hemoglobin (COHb) by using time-resolved UV resonance Raman spectroscopy. The 218-nm excited Raman spectra reproduced the quaternary structure-dependent spectral change of the Trp bands reported by us previously (J. Am. Chem. Soc. (1990), **112**, 23). However, in the present study, a newly designed sample-flowing system was used successfully to prevent photodissociated deoxyHb from recombining with CO. This allowed determination of the final point of the change. The intensity of a Trp band at 1011 cm^{-1} relative to a Phe band at 1003 cm^{-1} was used for monitoring the quaternary structure change. At pH 7.4 the intensity change began at 5 μs after photolysis and ended at 20 μs. A two state change was observed and there was no evidence for intermediate state, contrary to the recent report by Su et al. [J. Am. Chem. Soc. (1989), **111**, 3457]. At pH 5.8, where Bohr protons are attached, the change was significantly faster; it was already finished at 10 μs and remained unchanged after that. The relative intensity values and, therefore, the amount of change, were not altered by binding of the Bohr protons, indicating that the structural changes are similar and only the rate is altered by Bohr protons. The likely mechanism of the quaternary structure change, based on the present observations, is discussed.

II-C-6 Observation of the Cu_A-Ligand Stretching Resonance Raman Band for Cytochrome *c* Oxidase

Satoshi TAKAHASHI *(Grad. Univ.)*, **Takashi OGURA, Kyoko ITOH-SHINZAWA** *(Himeji Inst. of Tech.)*, **Shinya YOSHIKAWA** *(Himeji Inst. of Tech.)*, **and Teizo KITAGAWA**

A new Raman system using a CCD (Charge Coupled Device) detector was constructed and successfully applied to observe resonance Raman spectra of cytochrome *c* oxidase in resonance with the 830 nm absorption. The spectra yielded the amide bands and side chain modes of aromatic residues of protein irrespective of the oxidation state. However, additional resonance Raman bands were observed around 330 cm^{-1} only for the oxidized enzyme. The intense band at 330 cm^{-1} was insensitive to deuteration of the protein and therefore assigned to Cu-S(Cys) stretching mode, while the weak feature at 356 cm^{-1} was shifted to 350 cm^{-1} in D_2O and assigned to Cu-N(His) stretching mode.

II-C-7 Site-Directed Mutagenesis in Hemoglobin: Functional Role of Tyrosine-42(C7)α at the α1-β2 Interface

Kiyohiro IMAI *(Osaka Univ., MRC in U.K.)*, **Kenzo FUSHITANI** *(Osaka Univ.)*, **Koichiro ISHIMORI** *(Osaka Univ., Kyoto Univ.)*, **Teizo KITAGAWA, Yoshinao WADA** *(Osaka Medical Center)*, **Hideki MORIMOTO** *(Osaka Univ.)*, **Isao MORISHIMA** *(Kyoto Univ.)*, **Daniel T.-b. SHIH** *(MRC in U.K.)*, **and Jeremy TAME** *(MRC in U.K.)*

[*J. Mol. Biol.* **218**, 769-778 (1991)]

To clarify the functional role of Tyr-42(C7)α, which forms a hydrogen bond with Asp-99(G1)β at the α1-β2 interface of human deoxyhaemoglobin, we engineered two artificial mutant haemoglobins (Hb), in which Tyr-42α was replaced by Phe (Hb Phe-42α) or His (Hb His-42α), and investigated their oxygen binding properties together with structural consequences of the mutations by using various spectroscopic probes. Like most of the natural Asp-99β mutants, Hb Phe-42α showed a markedly increased oxygen affinity, a reduced Bohr effect and diminished co-operativity. Structural probes such as ultraviolet-region derivative and oxy-minus-deoxy difference spectra, resonance Raman scattering and proton nuclear magnetic resonance spectra indicate that, in Hb Phe-42α, the deoxy T quaternary structure is highly destabilizied and the strain imposed on the Fe-N^{ϵ} (proximal His) bond is released, stabilizing the oxy tertiary structure. In contrast with Hb Phe-42α, Hb His-42α showed an intermediately impaired function and only moderate destabilization of the T-state, which can be explained by the formation of a new, weak hydrogen bond between His-42α and Asp-99β. Spectroscopic data were consistent with this assumption. The present study proves that the hydrogen bond between Tyr-42α and Asp-99β plays a key role in stabilizing the deoxy T strucure and consequently in co-operative oxygen binding.

II-C-8 Site-Directed Mutagenesis in Hemoglobin: Functional and Structural Role of Inter- and Intra-subunit Hydrogen Bonds as Studied with 37β and 145β Mutations

Koichiro ISHIMORI *(Kyoto Univ.)*, **Kiyohiro IMAI** *(Osaka Univ.)*, **Gentaro MIYAZAKI** *(Osaka Univ.)*, **Teizo KITAGAWA, Yoshinao WADA** *(Osaka Medical Center)*, **Hideki MORIMOTO** *(Osaka Univ.)*, **and Isao MORISHIMA** *(Kyoto Univ.)*

In order to clarify the functional and structural role of intra- and intersubunit hydrogen bonds in human hemoglobin (Hb A), we prepared two artificial β chain mutant hemoglobins by site-directed mutagenesis. The mutant Hb Phe-37β, in which Trp-37β is replaced by Phe to remove the intersubunit hydrogen bond between Asp-94α and Trp-37β at the α1-β2 interface in deoxy Hb A, showed a markedly increased oxygen affinity and almost completely diminished Bohr effect and cooperativity. However, ^{1}H-NMR data indicated that the structure of deoxy Hb Phe-37β is rather similar to that of deoxy Hb A. The enhanced tetramer-to-dimer dissociation previously observed in Hb Hirose (Trp-37β → Ser) together with our observation of the effects of organic phosphate on the structure and function of Hb Phe-37β suggested that large part of the abnormal properties of Hb Phe-37β observed for dilute solutions appears to result from partial dissociation into $\alpha\beta$ dimers rather than direct destabilization of the T-quaternary structure in the deoxygenated state. Thus, the primary and direct role of the hydrogen bond between Asp-94α and Trp-37β is to stabilize the tetrameric assembly, and thereby this hydrogen bond indirectly contributes to stabilization of the T-quaternary structure.

The other mutant Hb Phe-145β has a Phe residue at the

145β site and lacks the intrasubunit hydrogen bond formed between Tyr-145β and the carbonyl group of Val-98β in deoxy Hb A. Although this hydrogen bond has been considered to fix the phenolic group of Tyr-145β in a pocket between the F and H helices, to strengthen the salt bridges formed by His-146β, and thereby to stabilize the T quaternary structure, Hb Phe-145β exhibited only mild functional and structural alterations. This result led us to conclude that the van der Waals contacts between the benzene ring of Tyr-145β and the tyrosine pocket, rather than the hydrogen bond between Tyr-145β and Val-98β, makes a major contribution to the stabilization of the T-quaternary structure.

The present NMR spectra of deoxygenated Hb Phe-37β and Hb Phe-145β further showed that the exchangeable proton resonance observed at 6.4 ppm for deoxy Hb A originates from the intersubunit hydrogen bond between Asp-94α and Trp-37β, although it has previously been assigned to the intrasubunit hydrogen bond between Val-98β and Tyr-145β.

II-C-9 A New Model for Dioxygen Binding in Hemocyanin. Synthesis, Characterization, and Molecular Structure of the μ-η^2:η^2 Peroxo Dinuclear Copper(II) Complexes, [Cu(HB(3,5-R_2pz)$_3$)]$_2$(O_2) (R=iPr and Ph)

Nobumasa KITAJIMA *(Tokyo Inst. of Tech.)*, **Kiyoshi FUJISAWA** *(Tokyo Inst. of Tech.)*, **Chisato FUJIMOTO** *(Tokyo Inst. of Tech.)*, **Yoshihiko MORO-OKA** *(Tokyo Inst. of Tech.)*, **Shinji HASHIMOTO, Teizo KITAGAWA, Koshiro TORIUMI, Kazuyuki TATSUMI** *(Osaka Univ.)*, **and Akira NAKAMURA** *(Osaka Univ.)*

[*J. Am. Chem. Soc.* in press.]

The synthesis and characterization of μ-η^2:η^2 Peroxo dinuclear copper(II) complexes which show many similarities to oxyhemocyanin (or oxytyrosinase) in their physicochemical properties are presented. The low temperature reaction of a di-μ-hydroxo dinuclear copper(II) complex [Cu(HB(3,5-iPr_2pz)$_3$)]$_2$($OH)_2$ **(8)** with H_2O_2 gave a μ-peroxo complex [Cu(HB(3,5-iPr_2pz)$_3$)]$_2$(O_2) **(6)**. Complex **6** was also prepared by dioxygen addition to a copper(I) complex Cu(HB(3,5-iPr_2pz)$_3$) **(9)**. The preparation of an analogous peroxo complex [Cu(HB(3,5-Ph_2pz)$_3$)]$_2$(O_2) **(7)** was accomplished by the similar dioxygen treatment of a copper(I) acetone adduct Cu(Me_2CO) (HB(3,5-Ph_2pz)$_3$) **(10)**. The reaction of **6** with CO or PPh_3 causes release of dioxygen, resulting in formation of the corresponding copper(I) adduct, Cu(CO) (HB3,5-iPr_2pz)$_3$) **(11)** or Cu(PPh_3) (HB(3,5-iPr_2pz)$_3$) **(12)**. Crystallography was performed for **6**-6(CH_2Cl_2), **8**-1.5(CH_2Cl_2), and **11**. Compound **6**-6(CH_2Cl_2) crystallizes in the monoclinic space group $C_{2/c}$ with a=26.36(2) Å, b=18.290(2) Å, c=29.29(2) Å, β=114.59(6)°, V=7915(9) Å^3, and z=4. The refinement converged with the final R(R_w) value, 0.101 (0.148) for 3003 reflections with $F \geq 3\sigma(F_o)$. Compound **8**-1.5(CH_2Cl_2) crystallizes in the triclinic space group $P\bar{1}$ with a=16.466(4) Å, b=16.904(5) Å, c=14.077(3) Å, α=112.92(2)°, β=99.21(2)°, τ=90.76(2)°, V=3550(2) Å^3, Z=2, and the final R(R_w) factor, 0.082 (0.105) for 7226 reflections with $F \geq 3\sigma(F_o)$. Compound **11** crystallizes in the monoclinic space group, $P_{21/a}$ with a=16.592(3) Å, b=19.144(4) Å, c=10.352(2) Å, β=106.71(2)°, V=3149(1) Å^3, Z=4, and the final R(R_w) value 0.083 (0.074) for 5356 reflections with $F \geq 3\sigma(F_o)$. The X-ray analysis of **6**-6(CH_2Cl_2) definitely established the μ-η^2:η^2 coordination structure of the peroxide ion for the first time. This unusual side-on structure is entirely novel for a d-block element transition metal-dioxygen complex. Both **6** and **7** show remarkable characteristics which are very similar to those known for oxyhemocyanin and oxytyrosinase: complex **6**; diamagnetic, ν(O-O), 741 cm^{-1}, 349 nm (ε, 21000), 551 nm (ε, 790), Cu–Cu, 3.56 Å: complex **7**; diamagnetic, ν(O-O), 759 cm^{-1}, 355 nm (ε, 18000), 542 nm (ε, 1040). These properties are all consistent with those of an analogous complex, [Cu(HB(3,5-Me_2pz)$_3$)]$_2$(O_2) **(5)**, of which the characterization and reactivities were reported already. The magnetic and spectroscopic features of **5-7** and their biological relevance are discussed in detail. Furthermore, simple interpretations of the electronic state of the $N_3Cu(O_2^{2-})CuN_3$ chromophore is provided based on extended Hückel MO calculations. The close resemblance between the μ-η^2:η^2 peroxo complexes **5-7** and oxyhemocyanin led us to propose a new model for dioxygen binding in hemocyanin; dioxygen is simply bound at the middle of the two copper ions in the μ-η^2:η^2 mode. With this structural model, the existence of an endogeneous bridging ligand, which has been generally supposed to account for the diamagnetism of oxyhemocyanin, is no longer necessary.

II—D Vibrational Spectroscopy on Short-lived States and Solution Structure

Raman spectroscopy reveals the vibrational spectrum of molecule which is sensitive to geometrical as well as electronic structures. When the wavelength of the probe beam is tuned within the absorption band of a molecule, resonance enhancement of Raman intensity makes it possible to detect Raman scattering from excited molecules or reaction intermediates even if their life times are short and thus their population are considerably small. We take the advantage of resonance Raman effect to explore the structures of metalloporphyrins in an excited triplet state and of intermediates of photoreduction of iron-porphyrins. On the other hand, the array detector combined with an optical fiber enabled us to construct a double beam Raman spectrometer and thus to observe a precise difference spectrum. Accordingly, we have applied it to evaluate relative magnitudes of intermolecular interactions and to explore the concentration-dependent cluster structures in a binary mixture of liquid samples.

II-D-1 Resonance Raman Spectra of Copper Porphyrins in the Excited Triplet States

Motoko ASANO, Shin-ichiro SATO, and Teizo KITAGAWA

Resonance Raman spectra of several meso-substituted copper porphyrins in the excited triplet states were measured by using a pump-probe technique and differences between their excited state structures are discussed.

Copper porphyrin has an unpaired electron in the metal d_σ orbital. The interaction between electrons in the central metal ion and porphyrin π-orbitals makes porphyrin triplets split into sublevels of trip-doublets and trip-quartets. Fluorescence from S_1 states is quenched by prompt intersystem crossing to the lowest excited triplet states and phosphorescence is observed with the lifetime of 10—100 ns in solution even at room temperature. Some meso-substituted copper porphyrins exhibit red-shifted emission spectra in fluid solution from those in rigid medium and an extend of the shift depends on the meso-substituents. In order to reveal an origin of medium dependence of emission spectra, structural differences in T_1 states among those copper porphyrins in solution were investigated.

The triplet state resonance Raman spectra of TPPCu (TPP: tetraphenylporphin) in benzene solution show a strong band of meso-substituent phenyl mode (ν_{8a}) at 1596 cm^{-1} with 3 cm^{-1} downshift from the ground state and a moderate intensity ν_1(Cm-Ph) band at 1300 cm^{-1}, which is 65 cm^{-1} upshifted from the ground state frequency. On the other hand, TMPCu(TMP:tetramesitylporphin), which shows slightly red-shifted emission in solution, displayed less intense ν_{8a} with no shift from the ground state and ν_1 with an upshift of 33 cm^{-1}. With TFPPCu (TFPP: tetrapentafluorophenylporphin), a phenyl band was not strong and showed no shift. Torsional distortion of phenyl rings toward coplanar structure in the lowest excited triplet states can not fully explain little frequency shifts of phenyl mode. Planar structure of porphyrin macrocycle might be deformed in the excited triplet states depending upon meso-substituents.

II-D-2 Time-Resolved Resonance Raman Spectra of Photoreduction Intermediates of Iron (III)-Octaethylporphyrin Complex

S. SATO, K. KAMOGAWA, K. AOYAGI *(Fukushima Natl. Coll. of Tech.)*, **and T. KITAGAWA**

Octaethylporphyrinato-iron (III)-(2-methylimidazole)-(methanol) [(OEP)Fe(III)(2-MeIm)(MeOH)] was previously found to be photoreduced to the five coordinate (OEP)Fe(II)(2-MeIm) in the absence of oxygen upon illumination of laser light at warelengths shorter than 450 nm.

In this study, the TR^3 experiments were carried out with two ns pulse lasers ($\Delta\tau$=7—17 ns) operated at 10 Hz, a polychromator, and a diode array detector. The probe beam was shifted by a home-made H_2 Raman shifter. Sample was stirred magnetically in a cuvettee. In order to reveal small spectral differences between successive transient spectra, we developed a new device; a single computer (NEC PC9801RX) controls firing of two pulse lasers so that they could have a given delay time (Δt_d) and also timing of reading data of the detector. This device enabled us to measure the probe-only spectrum and three different pump/probe spectra with different Δt_d for an identical setting of the sample at a few sec periods in turn; each spectrum was obtained as accumulation of spectra obtained from 100—200 cycles of 3.2 sec exposure in this study. Thus the probe-only spectrum can be always monitored as a standard during the TR^3 experiments. We emphasize that this device allows us to pursue reliably an intensity change between the transient spectra.

Previously we reported that intensity of the Fe-(MeOH) stretching band of (OEP)Fe(III)(2-MeIm)(MeOH) was enhanced upon excitation around 585 nm, but in this study we noticed that the corresponding RR band was also observable at 529 cm^{-1} upon excitation at 416 nm. The assignment was confirmed through observation of an isotopic frequency shift (−10 cm^{-1}) for CD_3OD. This RR band disappeared at Δt_d=20 ns. The Fe(II)-(2-MeIm) stretching band was identified at 203 cm^{-1}. This band was weak at Δt_d=20 ns but sufficiently intense at Δt_d=1 μs. These observations support previous proposal that the photoreduction intermediate is the four-coordinate ferrous complex.

II-D-3 Evidence for Direct Intermolecular Interactions as an Origin of the Hydration Shifts of the C-H Stretching Vibrations: 1,4-Dioxane/Water System

Keiji KAMOGAWA and Teizo KITAGAWA

[*Chem. Phys. Lett.* **179**, 271-276 (1991)]

Frequency shifts of the C-H stretching vibrations (ν_{CH}) of 1,4-dioxane (DX) and dimethylsulfoxide in aqueous solutions were observed as a function of concentration using a dual-beam difference Raman apparatus. A nonlinear positive increase of the shift was observed upon dilution for the ν_{CH} modes of DX, similar to the case of alcohol/water mixtures while negative and zero shifts were observed for its C-O and C-C stretching modes, respectively. The shift of the ν_{CH} mode is not the secondary effect arising from a change in hydrogen bonding at oxygen. The $\Delta\nu_{AA}$ versus x_A curve of the ν_{CH} mode exhibited a deep minimum around x_A=0.08, indicating the formation of molecular assemblies of DX with the C-H groups inside in the concentration region of $0.08 < x_A < 0.5$ and its collapse into molecular dispersion at $x_A < 0.08$. The transfer shift from H_2O to D_2O was significantly smaller for DX than for acetone and acetonitrile.

II-D-4 Attractive and Repulsive Solute Effects on the C-H Frequency Shifts on Hydration and a Spectroscopic Evaluation of the Energy for Hydrophobic Interaction

Keiji KAMOGAWA

Aqueous solute shifts ($\Delta\nu_{sol}$) of the C-H stretching vibrations of small amphiphiles were derived from the Raman frequency shifts upon mixing with water, thus permitting a spectroscopic evaluation of the hydrated state and the hydrophobic interaction energy of the C-H bonds. A plot of

$\Delta\nu_{sol}$ *vs* $R^{-6}\alpha$ (R: intermolecular distance, α: molecular polarizability) gave a straight line, as expected for the dispersion force between the oscillator and medium. From the intercept, ν_{sol} (the absolute shift due to the dispersion force in the liquid) was determined. The hydration shift ($\Delta\nu_h$) was expressed as the sum of $\Delta\nu_{sol}$ and an additional part, $\Delta\nu_{rea}$ (the shift ascribed to the rearrangement of the hydration sphere). Thus, the model corresponds to a two-step hydration process. The $\Delta\nu_{rea}$ exhibited a nonlinear dependence on α, which suggests an attractive interaction of the frameworks of the probe- and water molecules as the origin of the repulsion to the C-H vibration. The ν_{sol} was added to the probe-probe interaction factor ($\Delta\nu_{AA}$), previously reported for dilute solutions to obtain the absolute value (ν_{AA}). The spectroscopic energy for hydrophobic interaction, ΔG_{HI}, was evaluated with the expression, -RTln (ν_{AA}/ν_{sol}). Its magnitude was found to be ca. -4 kJmol^{-1} for the molecules studied here, and was highly correlated with the thermodynamically derived ΔG_{HI} values. The present ΔG_{HI} indicate restricted overlapping of the hydration shells upon hydrophobic association of the alkyl groups.

RESEARCH ACTIVITIES III
Department of Electronic Structure

III—A Photochemical Isomerization of Model Chemical Systems in Molecular Beams

The study of *cis-trans* isomerization in stilbenes and linear polyenes is vitally important for the understanding of photobiological processes, including energy transfer in photosynthesis, *cis-trans* photoisomerization in visual systems and photosynthetic bacteria, and the photochemistry of vitamin D. The complexity of the naturally occurring olefins inhibits both computational and experimental investigations into these molecules. The research emphasis thus has moved towards less complicated model systems which contain similar chromophores and have analogous photochemical behavior, but are simpler to investigate. We have made a systematic study of isomerization dynamics of several model stibenes and intermediate length polyenes in molecular beams. The ability to selectively excite a molecule to a specific quantum state with a well deffined energy in a molecular beam, is exploited to study isomerization dynamics of individual vibrational states. In solution, *cis*-stilbene isomerizes to *trans*-stilbene and dihydrophenanthrene (DHP) in ~1 ps. By modelling the spectroscopy and dynamics of several *cis*-stilbene analogs, we have determined an empirical potential energy surface for the photocyclization to DHP. For linear polyenes, we have measured the fluorescence excitation spectra and emission lifetimes of S_1 and S_2 states. We have found an energy activated nonradiative processes with a barrier of <200 cm^{-1} for trienes and ~2000 cm^{-1} for tetraenes, which we tentatively identify with *cis-trans* isomerization.

III-A-1 Modelling of Non-Radiative Decay of *cis*-Stilbene through Photocyclization to Dihydrophenanthrene

Hrvoje PETEK, Keitaro YOSHIHARA, Yoshihisa FUJIWARA *(Hiroshima Univ.)*, **Zhe LIN** *(West Virginia Univ.)*, **John H. PENN** *(West Virginia Univ.)*, **and John H. FREDERICK** *(Nevada Univ.)*

[*J. Phys. Chem.* **94**, 7539 (1991)]

The initial dynamics in the photoisomerization of *cis*-stilbene, especially the dynamics leading to photocyclization to dihydrophenathrene (DHP), is explored by studying the high resolution spectroscopy[1] and implied dynamics of a series of 1,2-diphenylcycloalkenes. In particular, the high resolution fluorescence excitation spectrum of 1,2-diphenylcyclobutene (DPC-4) reveals detailed information about the symmetric in-plane bend and symmetric phenyl ring twist motions which are crucial to photocyclization. The DPC-4 spectrum is analyzed theoretically and an empirical surface is constructed for the S_1 state which reproduces both line positions and relative intensities in the observed spectrum. An extrapolation of the DPC-4 potential surface is then made to construct S_1 state surfaces for 1,2-diphenylcyclopentene (DPC-5), 1,2-diphenylcyclohexene (DPC-6), and *cis*-stibene. As seen in Figure 1, these surfaces indicate that the initial dynamics of the molecule is to smaller bend angles and smaller phenyl twist angles upon excitation to the excited singlet state. For *cis*-stilbene and DPC-5 the surfaces show two minima corresponding to the stilbene and DHP structures, which are separated by 1-2 kcal/mol barriers. The calculated wavepacket propagation shows that the initial wavepacket on the S_1 surface reaches the saddlepoint for isomerization in ~200 fs.

Reference

1) H. Petek, K. Yoshihara, Y. Fujiwara, Z. Lin, J.H. Penn, and J.H. Frederick, *J. Phys. Chem.* **94**, 7539 (1990).

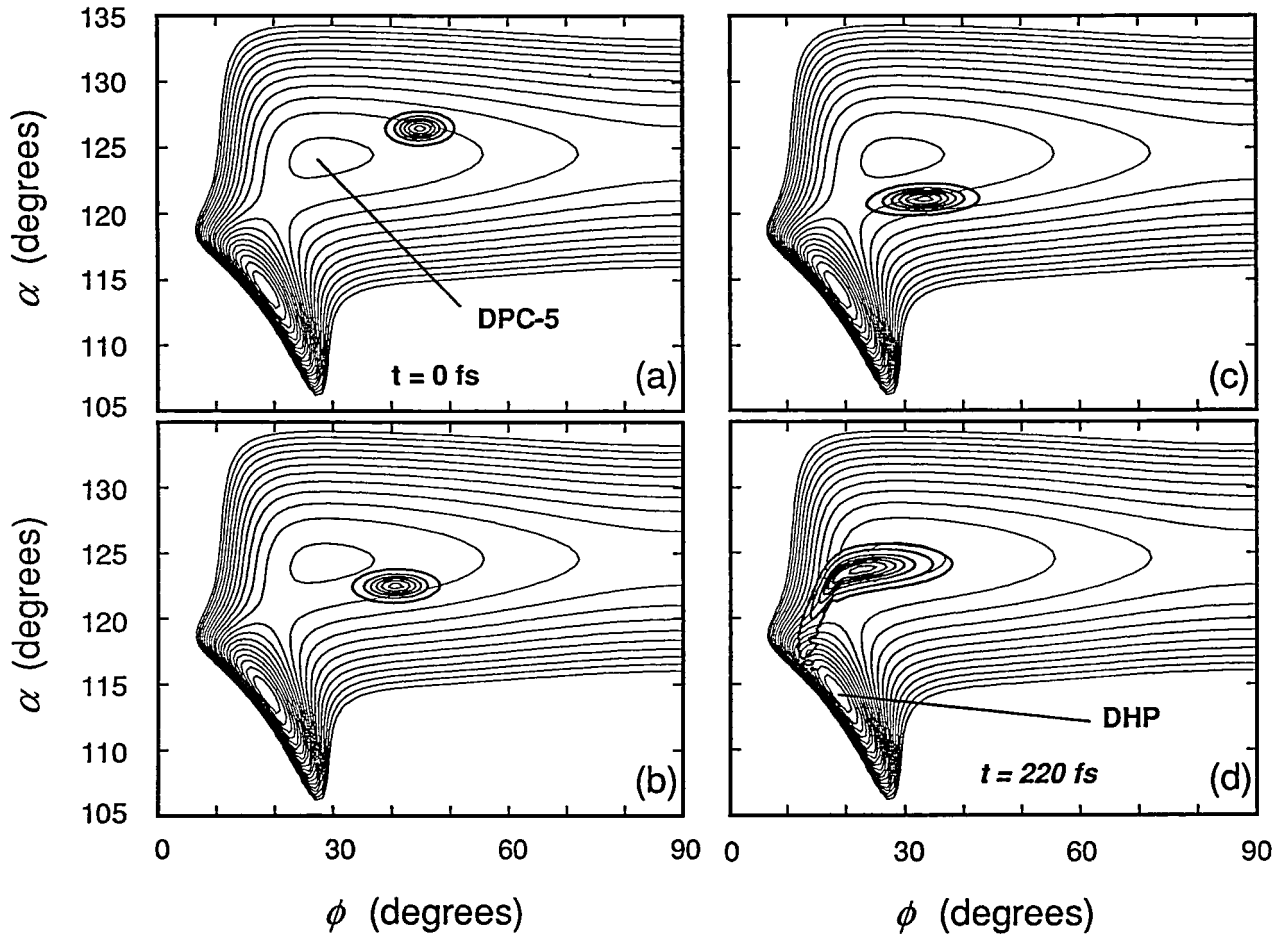

Figure 1. Snapshots from the early dynamics of the Franck-Condon wave packet on the DPC-5 empirical potential surface. The total time span of the dynamics shown is about 220 fsec. The wave packet originates at the position indicated in (a), then moves toward the lower left corner of the potential where the photocyclization product (DHP analog) is formed. Since the wave packet is moving parallel to the gap leading to DHP in this case, only a small portion "leaks" over into the DHP region of the potential (d).

III-A-2 Spectroscopic and Dynamical Study of Tetraenes in Supersonic Molecular Beams

Hrvoje PETEK, Andrew J. BELL, Keitaro YOSHIHARA, and Ronald L. CHRISTENSEN *(Bowdoin College)*

[*J. Chem. Phys.* **95**, 4739 (1991)]

Fluorescence excitation and emission spectra, and emission rates of *all-trans*-decatetraene and *all-trans*-nonatetraene have been obtained for isolated molecules in supersonic beams. The fluorescence excitation spectra and fluorescence decay rates of the S_1 states of the tetraenes are shown in Figure 1. This symmetry forbidden $^1A_g \leftarrow {}^1A_g$ transition is made possible by Herzberg-Teller mixing of the b_u vibronic symmetry states in S_1 with the nearby S_2 state. The b_u character can be derived either from inplane skeletal bending modes or from hindered methyl torsions. The analysis of the low frequency regions suggest that both b_u symmetry bending modes and torsions contribute to the complexity of the spectra. The methyl torsional structure shows that in the S_1 state the methyl torsional angle is unchanged from the ground state, however, the barrier to torsion drops from ~700 cm^{-1} to 40 cm^{-1}. At higher energies the most prominent features are due to the C - C single and double bond stretching vibrations, which are intense because of bond order inversion between S_0 and S_1 states. At the origin the fluorescence lifetimes are ~350 ns. There is a gradual decrease in the lifetime at higher energies due to increased mixing with the S_2 state. At ~2000 cm^{-1} excess energy a nonradiative decay channel can be deduced for both tetraenes from the sharp increase in the decay rate. The nonradiative decay of nonatetraene is significantly faster for nonatetraene than for decatetraene at the same excess energy, due to the lower density of states in nonatetraene. Tetraenes are promising models for understanding the structure and dynamics of longer, biologically important polyenes.

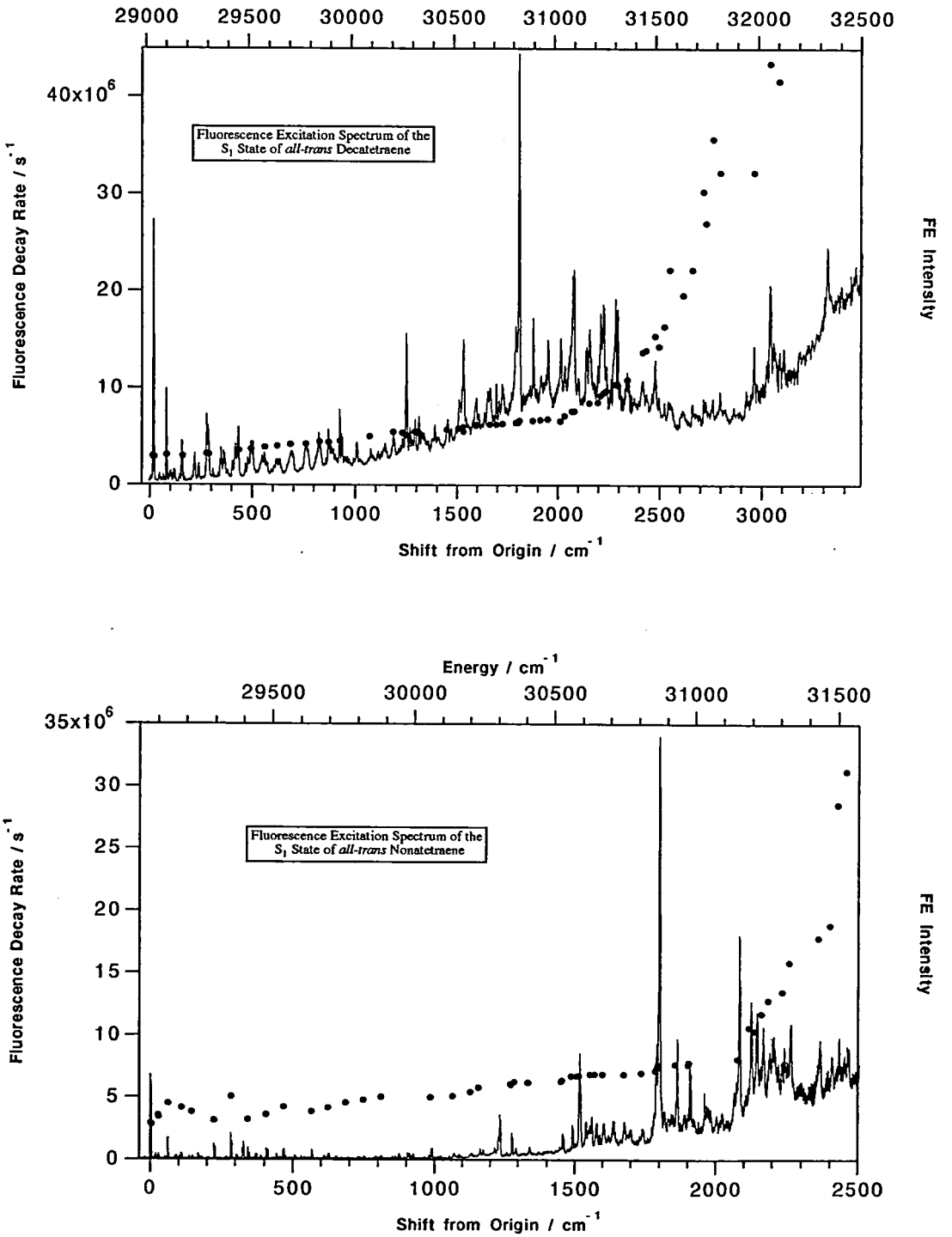

Figure 1. The $2^1A_g \leftarrow 1^1A_g$ ($S_1 \leftarrow S_0$) fluoresence excitation spectra of a) *all-trans*-decatetraene and b) *all-trans*-nonatetraene in a free jet expansion. The filed circles indicate the fluorescence decay rates of selected vibronic states.

III-A-3 Spectroscopic and Dynamical Study of Trienes in Supersonic Molecular Beams

Hrvoje PETEK, Andrew J. BELL, Ronald L. CHRISTENSEN *(Bowdoin College)*, **and Keitaro YOSHIHARA**

[*J. Chem. Phys.* (in press)]

For over 30 years there has been a consensus of opinion, based on both theoretical and experimental work, that linear polyenes with three or fewer conjugated double bonds do not emit from their lowest excited singlet state, S_1. Encouraged by the recent observation of fluorescence from the S_1 states of tetraenes,[1] and the measurement of the Resonance Enhanced Multi-Photon Ionization (REMPI) $S_1 \leftarrow S_0$ ($2^1A_g \leftarrow 1^1A_g$) spectra of several trienes by Buma *et al.*,[2] we have searched for fluorescence from several trienes under isolated conditions. We report the successful observation of fluorescence excitation $S_1 \leftarrow S_0$ spectra of the *cis*-isomers of hexatriene and octatriene. The fluorescence excitation spectrum and fluorescence decay rates of octatriene are presented in Figure 1. The complicated vibrational structure and intensity distribution is probably due to a significant change in the methyl torsional angle between the S_1 and S_0 states. Emission lifetimes and comparisons between the fluorescence excitation and REMPI spectra of trienes

indicate that in both hexatriene and octatriene there is a nonradiative process with an activation barrier of <200 cm^{-1}.

References

1) H. Petek, A.J. Bell, K. Yoshihara, and R.L. Christensen, *J. Chem. Phys.* **95**, 4739 (1991).
2) W.J. Buma, B.E. Kohler and K. Song, *J. Chem. Phys.*, **92**, 4622 (1990); *ibid* **94**, 6367 (1991); *ibid* **94**, 4691 (1991).

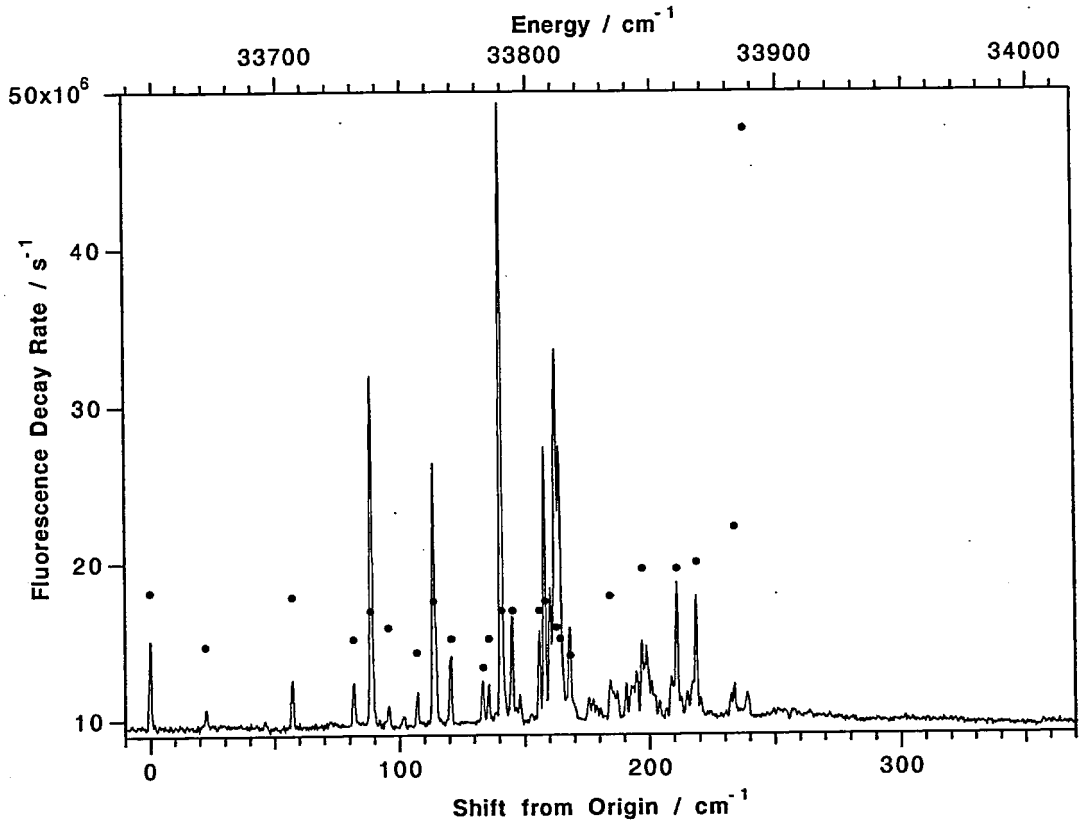

Figure 1. The fluorescence excitation spectrum and fluorescence decay rates of octatriene. The abscissa shows both absolute energy and energy shift from the origin, which is at 33648 cm^{-1}. The lifetimes of selected vibronic states are indicated by filled circles.

III—B Ultrafast Intermolecular Electron Transfer in the Electron Donating or Accepting Solvents

Studies on photo-induced intermolecular electron transfer reaction are usually carried out in solutions of electron donor and acceptor in non-reactive solvent, in which the rate of electron transfer is limited by the translational diffusion rate. To obtain direct information on the rate constant of fast intermolecular electron transfer, it is more favorable to perform the experiment in contact systems of electron donor and acceptor, in order to eliminate the limitation by translational diffusion. We have recently reported the ultrafast fluorescence quenching of excited dye molecule (nile blue A perchlorate) due to photo-induced electron transfer in neat anilne and N,N-dimethylaniline, acting as weakly-polar electron-donating solvents. The electron transfer rate constant, which reached up to 10^{13} s^{-1} is 10-100 times faster than the solvent longitudinal relaxation time. Strong contribution in weakly polar systems by ultrafast nuclear reorientation can provide ultrafast pathways for electron transfer.

In order to prove the photo-induced electron transfer, it is crucial to observe an ultrafast formation of ions. We have actually observed them in the above systems by subpicosecond transient absorption spectroscopy (III-B-1). One of the secondary processes of the initial electron transfer in these systems is sharing of positive holes by surrounding solvent molecules to form dimeric cation $^1(D_2^+...A^-)$, and further to n-meric forms, which is to say a "hole solvation process". This is observed by the picosecond and nanosecond photon counting method (III-B-1).

III-B-1 Ultrafast Fluorescence Quenching is Due to Intermolecular Electron Transfer Reaction: Subpicosecond Transient Absorption Study

Hideki KANDORI and Keitaro YOSHIHARA

Nile blue A has recently been found to display an ultrafast fluorescence decay in diffusionless, electron-donating solvent systems such as N,N-dimethylaniline (DMA) or aniline (AN), in which the shortest fluorescence decay reaches 10^{-13} s.[1] The reaction mechanism is studied in detail by transient absorption spectroscopy with an amplified subpicosecond pulse (600 nm, 25-100 μJ, 0.7 ps). As the result, it is concluded that the fluorescence quenching is due to an intermolecular electron transfer reaction by

detecting directly the absorptions of the products, neutralized nile blue (λ_{max}=470 nm) and solvent cations (λ_{max}=470 nm; DMA^+ and 405 nm; AN^+). In the system where a solvent molecule is electron donor itself and surrounding the acceptor molecule, the reverse electron transfer also occurs rapidly, Γ=4.0 ps in DMA and 2.7 ps in AN. The reaction mechanism and the rate constants are shown in Figure 1.

Reference

1) T. Kobayashi, Y. Takagi, H. Kandori, K. Kemnitz, and K. Yoshihara, *Chem. Phys. Lett.* **180**, 416, (1991).

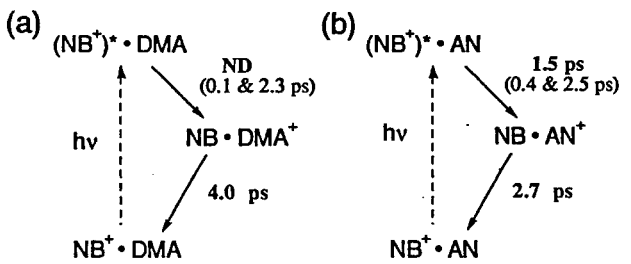

Figure 1. Schematic drawing of photochemical reactions of NB^+ in DMA (a) and AN (b). Nile Blue A is a salt formed with organic cation (described as NB^+) and perchlorate anion.

III-B-2 Electron Transfer in Diffusionless, Weakly Polar Systems: Temperature-dependent Fluorescence Decays and Time-Resolved Spectra

Klaus KEMNITZ, Abderrazzak DOUHAL, Yutaka NAGASAWA, and Keitaro YOSHIHARA

Wavelength- and temperature-dependent biexponential fluorescence decays are observed for a series of xanthene and oxazine dyes in electron-donating solvents with a sensitive picosecond-nanosecond single photon counting system. An excited-state 2-level system is thought to be responsible for the two-exponential decays, where the second emitting species is either the primarily formed contact ion-pair, $^1(D^+...A^-)$, or a consecutively formed triple complex, comprised of reduced dye and dimeric solvent cation, $^1(D_2^+...A^-)$. The lifetime of the first, (sub)picosecond component corelates with the electron affinity of the electron acceptor. The contribution of the slow, nanosecond component increases at long observation wavelengths. Figure 1a displays the time-resolved fluorescence spectra, of the system rhodamine 101 inner salt (Rh 101) in DMA, showing a redshift of about 0.1 eV, and compares it to the behaviour in 1-chloronaphthalene (Figure 1b), which serves as weakly polar reference system without electron transfer.

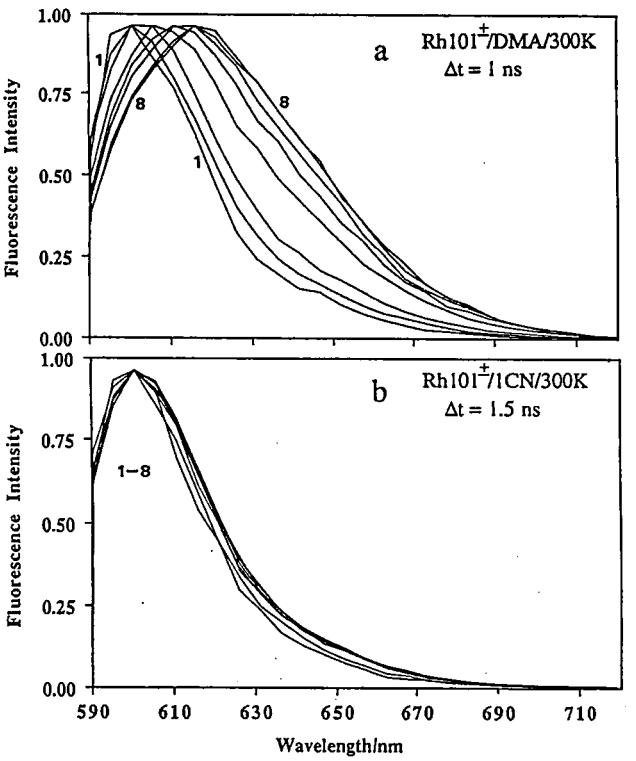

Figure 1. Time-resolved fluorescence spectra of Rh 101 in (a) dimethylaniline and (b) 1-chloronaphthalene. Each line 1,2,...8 gives a time delay of 1 ns.

III—C Photochemical Isomerization in Proteins

Photochemical isomerization in retinal containing proteins has been attracting great attentions among chemists, biophysicists and biologists. These retinal proteins can be classified into two types; one converts light energy to signals in animal vision, while the other converts light energy to membrane potential in bacterial ion pumping systems. Typical retinal proteins for the former is rhodopsin and for the latter is bacteriorhodopsin. In rhodopsin, light absorption yields isomerization of the retinal chromophore from 11-cis to all-trans form. Studies on photochemical and subsequent thermal reactions in 7-cis-rhodopsin have elucidated a specific interaction between the chromophore and protein moiety (III-C-1). Although a lot of spectroscopic studies were attempted, the photochemical isomerization mechanism in retinal proteins has not been well studied. One reason is that the excited state lifetimes of rhodopsin and bacteriorhodopsin are too short to be well studied, although the isomerization takes place in the excited state. Thus we choose a chloride pumping protein, halorhodopsin (hR), and study its primary process using subpicosecond transient absorption spectrocscopy. Because of longer lifetime of hR, excited state absorption spectrum is measured for the first time (III-C-2). Moreover, spectroscopic and kinetic studies of hR provide a new insight on cis-trans isomerization of the retinal chromophore in protein (III-C-3).

III-C-1 Photochemical Isomerization in Vision: Spectroscopic Study of 7-cis-Rhodopsin

Yoshinori SHICHIDA *(Kyoto Univ.)*, **Hideki KANDORI, Tetsui OKADA** *(Kyoto Univ.)*, **Toru YOSHIZAWA** *(Kyoto Univ.)*, **Nobuaki NAKASHIMA, and Keitaro YOSHIHARA**

[*Biochemistry* **30**, 5918-5926 (1991)]

The Photochemical and subsequent thermal reactions of

7-cis-rhodopsin prepared from cattle opsin and 7-cis-retinal are investigated by low-temperature spectrophotometry and laser photolysis, and compared with those of 11-cis-rhodopsin prepared from cattle opsin and 11-cis-retinal. Kinetic experiments of the photobleaching process of 7-cis-rhodopsin using picosecond and nansecond laser pulses reveal the formation of intermediates corresponding to the batho, lumi, meta I, and meta II intermediates from 11-cis-rhodopsin. The obtained results indicate that the difference in configuration of the original chromophore between 7-cis- and 11-cis-rhodopsin is a cause of different chromophore-opsin interactions in the batho and lumi stages, while in the meta I stage the difference has disappeared by the relaxation of the protein near the chromophores. It is probable that the interaction between the 9-methyl group of the chromophore and its neighboring protein changes during the lumi-meta I transition.

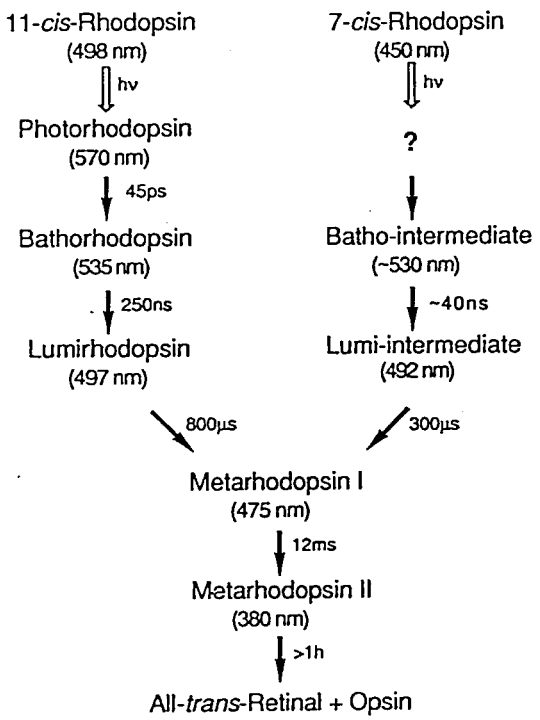

Figure 1. Photobleaching processes of 7-cis- and 11-cis-rhodopsins. The values in parentheses show absorption maxima. The decay time constants are shown on the right-hand side of the arrows.

III-C-2 Determination of Excited State Absorption Spectrum of Retinal Chromophore in Protein

Hideki KANDORI, Keitaro YOSHIHARA, Hiroaki TOMIOKA *(Riken)*, and Hiroyuki SASABE *(Riken)*

The excited-state absorption spectrum of retinal (protonated Schiff base) in protein is measured for a light-driven chloride ion pump, halorhodopsin (hR), by use of subpicosecond transient absorption spectroscopy. The excited state absorption spectrum, which appears immediately after excitation and decays with a time constant of 2.3 ps, is blue-shifted from the ground-state absorption spectrum. This is the first accurate determination of the excited state absorption spectrum of a retinal chromophore (Schiff base) in solution and in a protein. The spectrum of the excited state has a peak at 516 nm and a shoulder at about 460 nm. The origin of the spectral structure is interpreted to be, more likely, an overlap of two electronic transitions than a vibrational progression.

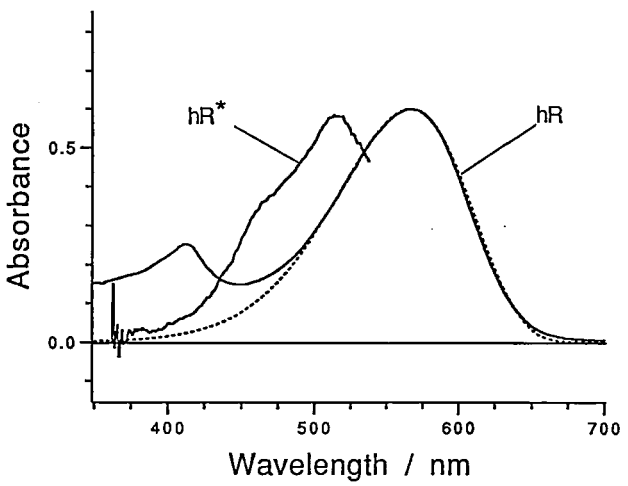

Figure 1. Ground (hR) and excited-state (hR*) absorption spectra of hR. Broken line indicates the log-normal fitting of hR to isolate the main absorption band of hR.

III-C-3 Photochemical Isomerization Mechanism in Protein Studied by Subpicosecond Transient Absorption Spectroscopy

Hideki KANDORI, Hiroaki TOMIOKA *(Riken)*, Hiroyuki SASABE *(Riken)*, and Keitaro YOSHIHARA

Primary photochemical events of the light-driven chloride-pump halorhodopsin (hR) are studied at room temperature by subpicosecond transient absorption measurements. On excitation of hR with a 600 nm, 0.6 ps pulse, excited state absorption and stimulated emission immediately appear in 420-530 nm and 650-770 nm wavelength regions, respectively, and both decay with a time constant of 2.3 ps. Accompanied with depopulation of hR*, primary ground state product, hR_K appears. The quantum yield of hR_K formation is directly determined to be 0.27. The time constant of the absorbance change at 645 nm that is mainly monitoring the rise time of hR_K is equal to 1.0 ps, which is faster than the excited state depopulation (2.3 ps). Thus it is impossible to understand the primary process of hR by the simple sequential kinetic model considering three states of hR*, hR_K and hR, which has been applied to the primary process of bacteriorhodopsin. The present results suggests that the excited state having a reaction channel to cis-trans isomerization is not located at the potential minimum of hR* and that the relaxation process in the excited state is a process in competition with ismerization.

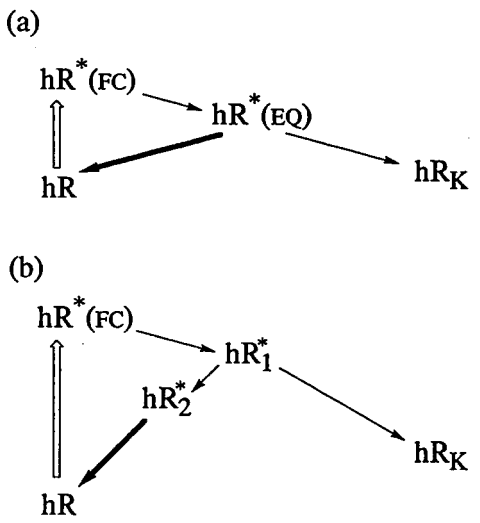

Figure 1. Primary photochemical schema in hR. Open, solid thin and thick arrows indicate photon absorption, internal conversion and both radiative and non-radiative processes, respectively. hR and hR_K have all-trans and 13-cis retinals as their chromophore, respectively. (a) In this scheme, excited hR molecule starts relaxation from the Franck-Condon state (hr*(FC)) to an excited equilibrium state (hr*(EQ)). Some hR molecules in the equilibrium state go to hR_K by internal conversion, while others come back to hR with or without emission. This simple scheme, which has been applied to the primary process of bacteriorhodospin cannot explain the experimental results of hR. (b) In this scheme, two excited states, hR_1^* and hR_2^*, are taken into account. Only hR_1^* has a channel to hR_K. hR_2^* decays to original hR with or without emission.

III—D Applications of Femtosecond Time-Resolved Coherent Raman Spectroscopy

Vibrational phase relaxation has attracted considerable attention in these several years. It has been demonstrated that the vibrational phase relaxation reflects liquid state structures and dynamics. Recent development in laser technology enables us to obtain coherent light pulses with duration of less than 100 fs. The time scale corresponds to a period of molecular vibration (100 fs=333 cm^{-1}, for example) and therefore this is an ultimate time scale for the study of vibrational relaxation. We have constructed a femtosecond laser system and a time-resolved coherent Raman measuring system. The overall time resolution is less than 100 fs. This system has been used to study vibrational relaxation of various molecules in liquids and solutions, and their environmental (solvent, biological systems, etc.) dependence.

III-D-1 Femtosecond Time-Resolved Cherent Anti-Stokes Raman Scattering from β-Carotene. Sub-picosecond Vibrational Relaxation in Various Solvents.

Hiromi OKAMOTO *(Univ. of Tokyo and IMS)* **and Keitaro YOSHIHARA**

[*Chem. Phys. Lett.* **177**, 568 (1991)]

Femtosecond time-resolved coherent anti-Stokes Raman scattering (CARS) has been observed for *all-trans* β-carotene in various solvents. A regular oscillating pattern (11 THz) owing to the beat between the two strong Raman transitions (~1520 cm^{-1} and ~1150 cm^{-1}) is observed when the frequency difference between the pump and Stokes radiation is set in-between the two strong Raman bands. The vibrational dephasing relaxation rate has been measured for the in-phase C=C stretching band (1520 cm^{-1}). The solvents used are cyclohexane, benzene, carbon tetrachloride, carbon disulfide, chloroform and acetone/cyclohexane mixture (~1:1 in volume). The relaxation rate is found to be T_2~0.6 ps and independent of solvent. The density of vibrational states is estimated to be ~10^{12} states/cm^{-1} in the double bond stretching region. The intramolecular relaxation rate may be so fast because of this very high density of states that the relaxation due to the intermolecular interaction have little effect on the observed signal decay.

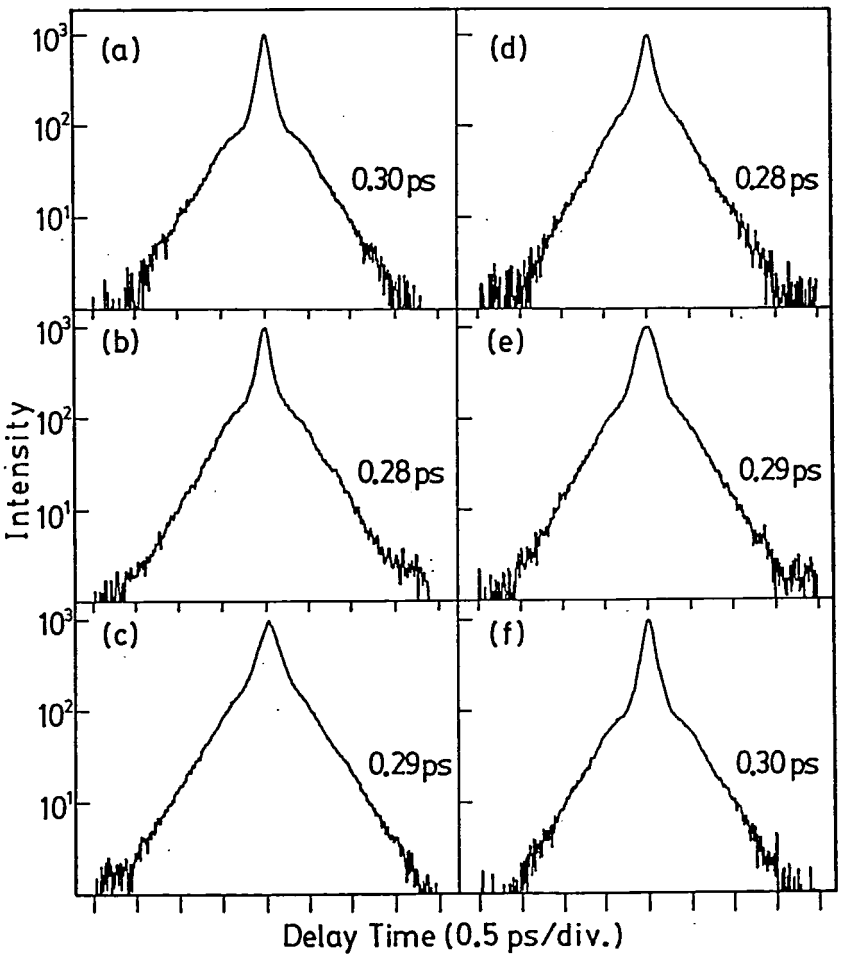

Figure 1. Time-resolved CARS for the in-phase C=C stretching (~1520 cm^{-1}) of β-carotene as a function of the decay time. The solvents are: (a) C_6H_{12}, (b) C_6H_6, (c) CCl_4, (d) CS_2, (d) CS_2, (e) $CHCl_3$ and (f) CH_3COCH_3/C_6H_{12} mixtute (~1:1).

III-D-2 Femtosecond Time-Resolved Coherent Anti-Stokes Raman Scattering from Carotenoids *in vivo* and *in vitro*: Comparison of Vibrational Relaxation Times (T_2) of the Inphase C=C Stretching Bands

Hiromi OKAMOTO *(Univ. of Tokyo and IMS)*, **Hidenori HAYASHI** *(Univ. of Tokyo and NIBB)*, **Keitaro YOSHIHARA, and Mitsuo TASUMI** *(Univ. of Tokyo)*

[*Chem. Phys. Lett.* **182**, 96 (1991)]

Femtosecond time-resolved coherent anti-Stokes Raman scattering has been observed for two carotenoids, rhodopin and spirilloxanthin, *in vivo* and *in vitro*. These two carotenoids have polar functional groups at the ends of the polyene chains. Intracytoplasmic membranes of a photosynthetic bateria *Chromatium vinosum* have been used as the *in vivo* sample where the carotenoids exist in the pigment-protein complexes. We have found that the vibrational dephasing relaxation rates in solvents (benzene, chloroform, acetone/chloroform mixture) are almost the same as those of β-carotene previously reported, even in a highly polar environment. This result suggests that the intermolecular interactions have only little effects *in vitro*. On the other hand, the relaxation rate *in vivo* has been found definitely faster than those *in vitro*. The carotenoids may be so tightly bound to the protein that the vibrational motion of the in-phase C=C stretching is coupled to that of the environmental system, causing its faster relaxation.

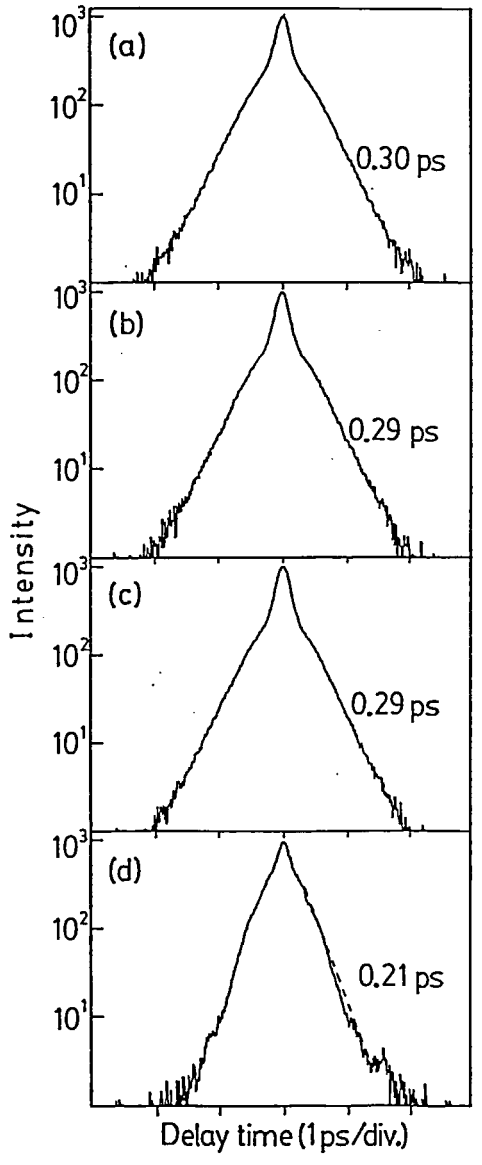

Figure 1. Time-resolved CARS for in-phase C=C stretching (~1520 cm^{-1}) of a 1:1 mixture of rhodopin and spirilloxanthin (a)~(c) and of chromatophores (d). The solvents are benzene in (a), chloroform in (b), and a acetone/chloroform mixture (~1:1 in volume) in (c). The dashed line in (d) was used to determine the decay time constant.

III-D-3 Femtosecond Time-Resolved Coherent Anti-Stokes Raman Scattering from Acetonitrile: Solvent Effects on the Vibrational Dephasing of the C≡N Stretching Band

Ryoji INABA *(Univ. of Tokyo and IMS)*, **Hiromi OKAMOTO** *(Univ. of Tokyo and IMS)*, **Keitaro YOSHIHARA, and Mitsuo TASUMI** *(Univ. of Tokyo)*

[*Chem. Phys. Lett.*, in press]

Femtosecond time-resolved coherent anti-Stokes Raman scattering (CARS) has been observed for the fundamental band of the C≡N stretching mode (2252 cm^{-1}) of acetonitrile. Under a properly chosen polarization condition, we can separate the contribution of vibrational dephasing from that of rotational diffusion. The CARS signal for the C≡N stretching shows a non-exponential decay. This signal behavior has been attributed to interference between fundamental and hot band transitions.

We have also examined solvent effect on the dephasing rate of the C≡N stretching of acetonitrile. It has been shown that the dephasing of the C≡N stretching becomes faster with increasing hydrogen-bonding ability of the solvent (proton donor) as shown in Figure 1. This result can be qualitatively explained as follows. The hydrogen bond formed between the acetonitrile molecule and a solvent molecule couples the C≡N stretching mode of acetonitrile with intramolecular vibrational modes of the solvent molecule and/or intermolecular modes. The relaxation of the C≡N stretching motion becomes rapid as the hydrogen bond increases in strength and the coupling becomes stronger.

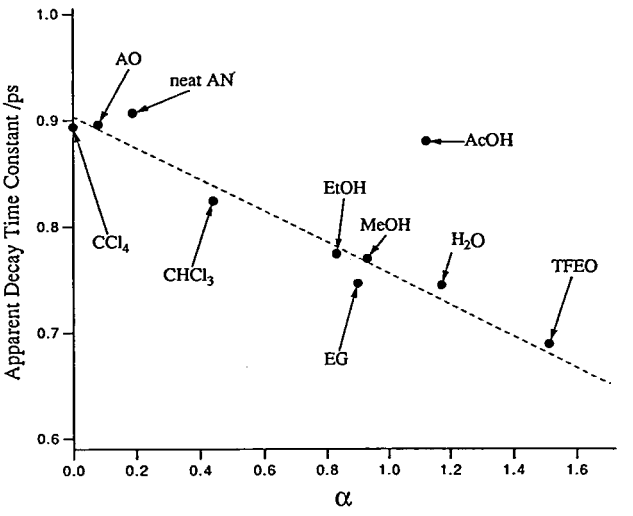

Figure 1. Relation between the apparent decay time constant and the hydrogen bonding ability of the solvent (α). The following abbreviations are used for the solvents: AO, acetone; AN, acetonitrile; EtOH, ethanol; MeOH, methanol; EG ethylene glycol; AcOH, acetic acid; TFEO, trifluoroethanol. The dashed line is a visual guide.

III—E Development of All Solid State Widely Tunable Laser Source Ultrashort Light Pulses for Spectroscopy

Recent advances in solid state laser technology such as feedback controlled mode-locking operation of flashlamp pumped lasers enable us to obtain long flat stable trains with short and energetic pulses which are suitable for synchronous pumping of picosecond and femtosecond lasers. Together with recent advances of material production, notably with newly developed nonlinear crystals KTP, beta-barium borate (BBO) and lithium triborate (LBO), they renewed interests in optical parametric oscillators (OPO), which provides a most attractive approach to produce coherent, widely tunable radiation. We have

studied different nonlinear elements such as GaAs, CdSe and InP for the use as passive negative feedback elements for near infrared solid state lasers and with a such pumping source we have developed widely tunable parametric oscillators using BBO and LBO crystals.

III-E-1 Self-Defocusing of Mode-Locked Nd:YAG Laser Radiation In GaAs, CdSe and InP

Vaclav KUBECEK *(Czech Tech. Univ. and IMS)*, **Shigeichi KUMAZAKI, Yoshihiro TAKAGI, Keitaro YOSHIHARA, and Giancarlo C. REALI** *(Pavia Univ.)*

[*Jpn. J. Appl. Phys.*, in press]

We studied the defocusing in GaAs, CdSe and InP of 25 ps pulse trains from a hybridly mode-locked flashlamp pumped Nd:YAG laser in order to investigate the possibility of their use as passive negative feedback element (NFE) in neodymium laser resonators. And our results were confirmed by our actual application.

Oscillograms of the pulse trains transmitted through the different semiconductors and an aperture are shown in Figure 1. It was found that CdSe has a saturated transmission of the same order of magnitude with GaAs, which is almost the only semiconductor used as passive NFE so far.[1,2] Using CdSe as NFE, single pulse duration of 5 ps and 14 ps were obtained from Nd:YAP and Nd:YAG respectively. And train duration were approximately 1000 ns in both cases. On the other hand a different behavior is evident in InP. InP has a far smaller saturated transmission compared with the other two semiconductors, and a large amount of energy (in any form) stored in the InP leads to some accumulation effect, as seen in the latter part of the transmitted train in figure 1d. And it was impossible to achieve negative feedback using InP in the Nd:YAG laser with our resonator configuration.

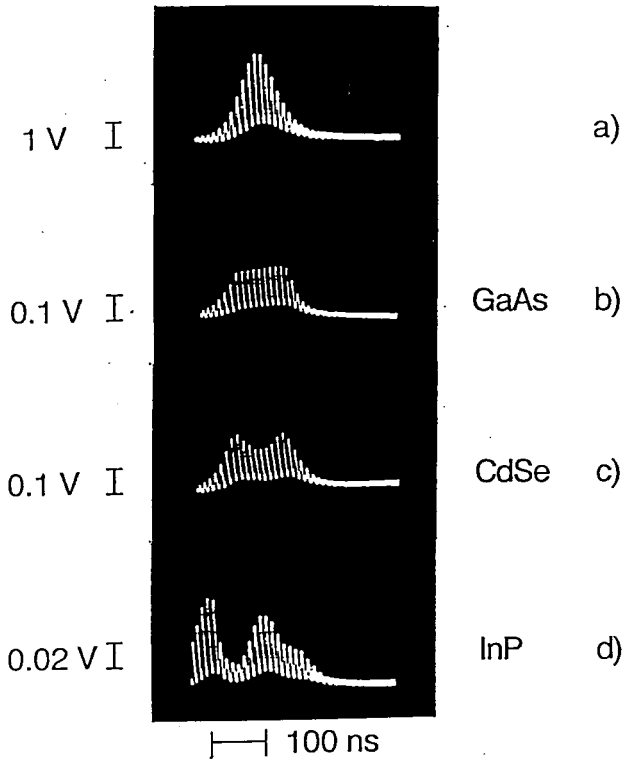

Figure 1. Oscillograms of the mode-locked pulse trains transmitted through an aperture only (a), and through different semiconductor wafers and apertures, (b)-(d). Thickness of the three semiconductors are 520 μnm, 400 μm and 500 μm for GaAs, CdSe and InP, respectively. All three wafers have the same normal-to-surface orientation <100> and are nominally undoped. Incident light intensity was 1 GW/cm^2.

References

1) A. Del Corno, G. Gabetta, G.C. Reali, V. Kubecek and J. Marek, *Opt. Lett.* **15**, 734 (1990).
2) A.V. Babushkin, N.S. Vorob'ev, A.M. Proknhorov and M.Ya. Shchelev, *Sov. J. Quantum Electron.* **19**, 1310 (1989).

III-E-2 Actively and Passively Mode-Locked Nd:YAP Laser with Negative Feedback using CdSe and GaAs

Vaclav KUBECEK *(Czech Tech. Univ. and IMS)*, **Shigeichi KUMAZAKI, Yoshihiro TAKAGI, Giancarlo C. REALI** *(Pavia Univ.)*, **and Keitaro YOSHIHARA**

[submitted to *Jpn. J. Appl. Phys.*]

The feedback controlled mode-locked operation of a flashlamp pumped Nd:YAP laser using a CdSe passive element is reported for the first time. Pulse trains with a duration of 1000 ns, pulse width of 5 ps and single pulse energy of 10 μJ were generated. The performance of CdSe and GaAs negative feedback elements (NFE) were compared.

Examples of generated pulse trains for different semiconductor NFE are shown in Figure 1. It must be pointed out that we observed different train durations for different NFE wafers even though they are nominally the same, as the two oscillograms for two GaAs wafers show. In most cases it was easier to get longer trains with CdSe than with GaAs.

Ideal passive negative feedback was realized with an optimum concentration of the saturable dye solution of 30% at 1.08 μm in all our cases. In the cases of CdSe and GaAs

I, after the first transient part of 100 ns to 200 ns, the duration and the amplitude of pulses in the train become constant. The pulse width (FWHM) in the flat part of the train is 5 ps, assuming single pulse shape to be a hyperbolic secant.

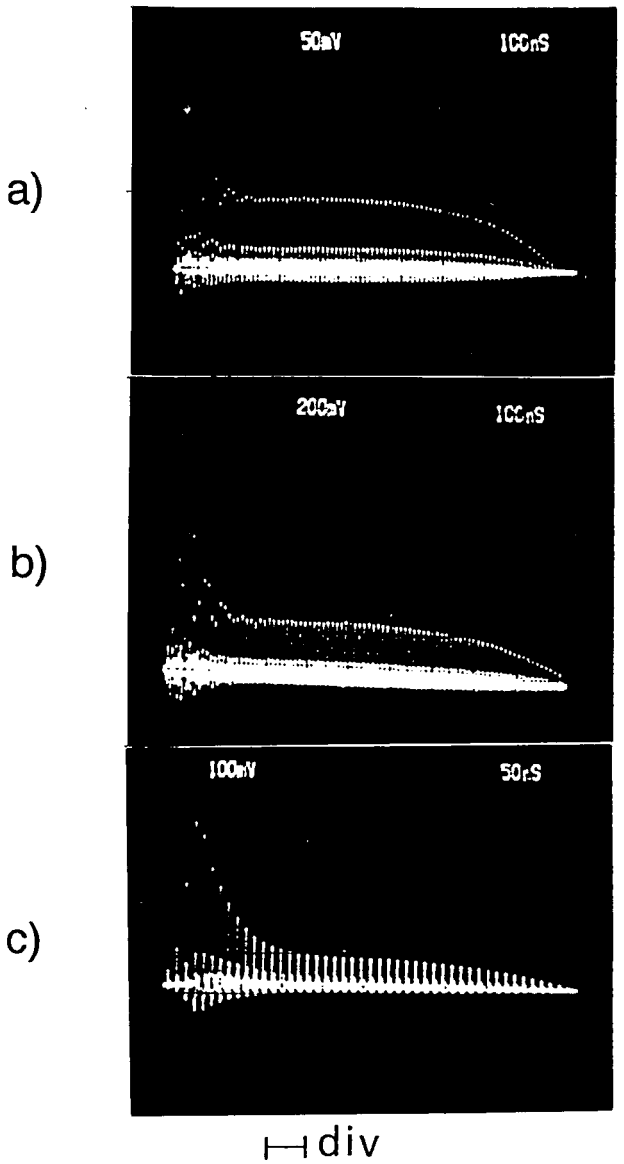

Figure 1. Pulse trains with different passive NFE. a) CdSe, b) GaAs I, c) GaAs II. The three wafers have the same thickness and normal-to-surface orientation: thickness 400 μm, the orientation <100>. All the three wafers are nominally undoped.

III-E-3 Barium Borate Optical Parametric Oscillator Synchronously Pumped by the Third Harmonic of a Mode-Locked Nd:YAG Laser with Passive Negative Feedback

Vaclav KUBECEK *(Czech Tech. Univ. and IMS)*, **Yoshihiro TAKAGI, Keitaro YOSHIHARA, and Giancarlo REALI** *(Pavia Univ.)*

We report here, for the first time, the results of operation of an Optical Parametric Oscillator (OPO) based on the use of a Beta-Barium Borate (BBO) cyrstal and synchronously pumped by the third harmonic of a Nd:YAG laser with passive negative feedback (PNFM). The experimental arrangement of the system is illustrated schematically in Figure 1. Pulse train from the PNFM Nd:YAG oscillator having energy of 1 mJ was amplified and third harmonic was generated with a 15% efficiency using two KDP type II crystals. The 0.35 μm beam with pulse duration of 8 ps was focussed into a type I, 5×7 mm and 7 mm long BBO crystal cut at θ=31°. Non-collinear pumping geometry was used. Single resonant oscillation of the signal wave between 0.4 and 0.65 μm (the available reflectivity of our mirrors) was achieved. This corresponds to an idler wave tunability between 2.8 and 0.76 μm. An idler conversion efficiency 10% was measured. The pump threshold for the OPO operation was of 150 μJ. Pulse duration measured, at the signal wavelength of λ_s=0.6 μm using a streak camera with resolution of 1.8 ps, was found to be 3.1 ps.

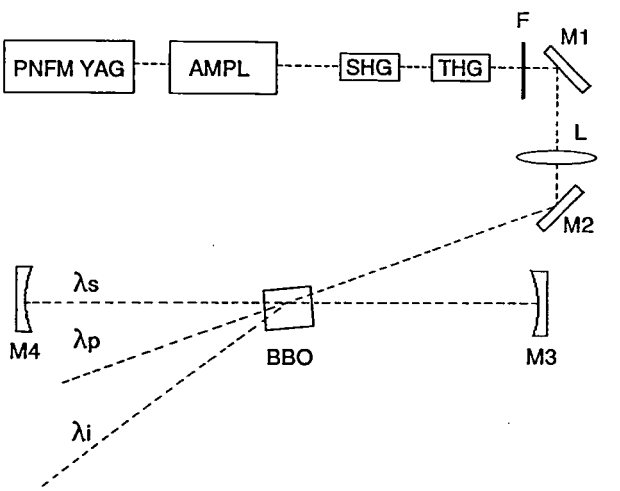

Figure 1. Schematic diagram of a singly resonant OPO with a PNFM Nd:YAG pump laser. AMPL, amplifier; SHG, second harmonic generation; THD, third harmonic generation; F, UV transmitting filter; L, spherical lens, f=1 m; M1, M2, flat mirrors; M3, M4, spherical mirrors, r=1 m; BBO, beta barium borate crystal.

III-E-4 Lithium Triborate Picosecond Optical Parametric Oscillator

Vaclav KUBECEK *(Czech Tech. Univ. and IMS)*, **Yoshihiro TAKAGI, Keitaro YOSHIHARA, and Giancarlo REALT** *(Pavia Univ.)*

[submitted to *Opt. Lett.*]

We report the first use of the lithium triborate crystal (LBO) for picosecond parametric generation. The arrangement of the system, is the same as for BBO optical parametric oscillator described in III-E-3. Only the BBO crystal was replaced by a 5×5 mm and 10.5 mm long LBO crystal cut for type I phase matching at θ=90° and φ=39°. Similar to BBO, when the pump 355 nm beam was focussed on the LBO crystal, a bright parametric luminiscence was observed, which did not propagate in the same direction as a pump beam but at a certain angle. This angle was 35 mrad in the present case, which was 2.5 times smaller than with BBO. The threshold pumping energy for parametric generation was 500 μJ, which is 3 times higher than that of a 7 mm long BBO crystal. At a pump energy 3 times above this

threshold the efficiency of the conversion of the UV pump into the idler IR wave at 900 nm was 10%. The pulse width at the signal wavelength of 575 nm was found to be 6 ps, with the pump pulse width being 9 ps. The tuning of the OPO was achieved by tilting the LBO crystal with respect to the axis of resonator. The measured tuning curve giving the dependence of the wavelength of the signal wave on the deviation of the LBO crystal axis from the resonator axis is shown in Figure 1. The shortest signal wavelength was 452 nm. The calculated idler wave tunability corresponding to this signal wave is from 731 nm to 1689 nm.

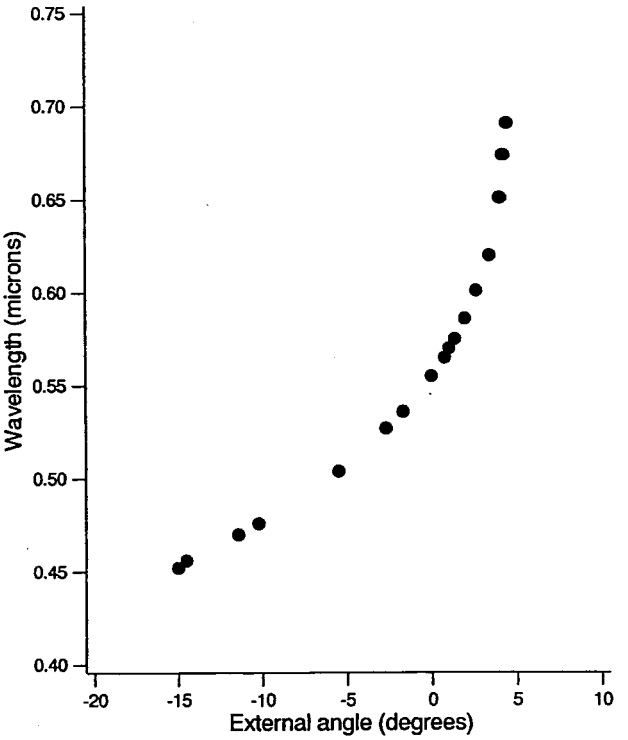

Figure 1. LBO OPO tuning curve-dependence of the parametric signal wave wavelength on the LBO crystal angular detuning from the resonator axis.

III—F Dynamic Behavior of Electronic Excited States

As it is described in the previous chapters, upon electronic excitation, numerous aromatic molecules undergo changes in their molecular structure. One of the drastic changes of vibrational and electronic spectra of molecule is caused by the photo-induced intramolecular proton-transfer. Excited state intramolecular proton transfer (ESIPT) reaction times shorter than 1 ps have been found in some compounds. In this chapter, we report some aspects of the dynamics of the ESIPT and back reaction in the ground state of a new molecule. The system has been studied by a subpicosecond transient absorption spectrometer.

III-F-1 Sub-picosecond Intramolecular Proton Transfer Reaction in Electronically Excited 2-(2'-Hydroxyphenyl)imidazo[1,2-a]pyridine

Abderrazzak DOUHAL, Hideki KANDORI, Fransisco AMAT *(CSIC, Madrid)*, **and Keitaro YOSHIHARA**

Dynamics of the excited state intramolecular proton-transfer (ESIPT) was studied in 2(2'-hydroxyphenyl)imidazo[1,2-a]pyridine (HPIP) in cyclohexane and dioxane using sub-picosecond transient absorption spectroscopy. The rate constant for the ESIPT in HPIP is greater than $(0.5\ ps)^{-1}$. Transient absorption spectrum of the excited tautomer of HPIP has its maximum at 400 nm and broad tail at 450~510 nm. The spectral difference between 3 and 200 ps delayed spectra (Fig. 1-a) suggests a cooling process (picosecond regime) of the vibrationally highly excited tautomer form. In dioxane, where the lifetime of the excited tautomer form of HPIP is 0.6 ns [1], transient absorption spectra do not show any contribution from the ground state tautomer form even in a 0.7 ns delayed absorption spectrum (Fig. 1-b). We suggest that the rapid reverse proton-transfer in the ground state tautomer is the main reason for the lack of its transient absorption.

Reference

1) A. Douhal, A.U. Acuna, F. Amat, Conference on Photochemistry, Sept. 1990, Kyoto.

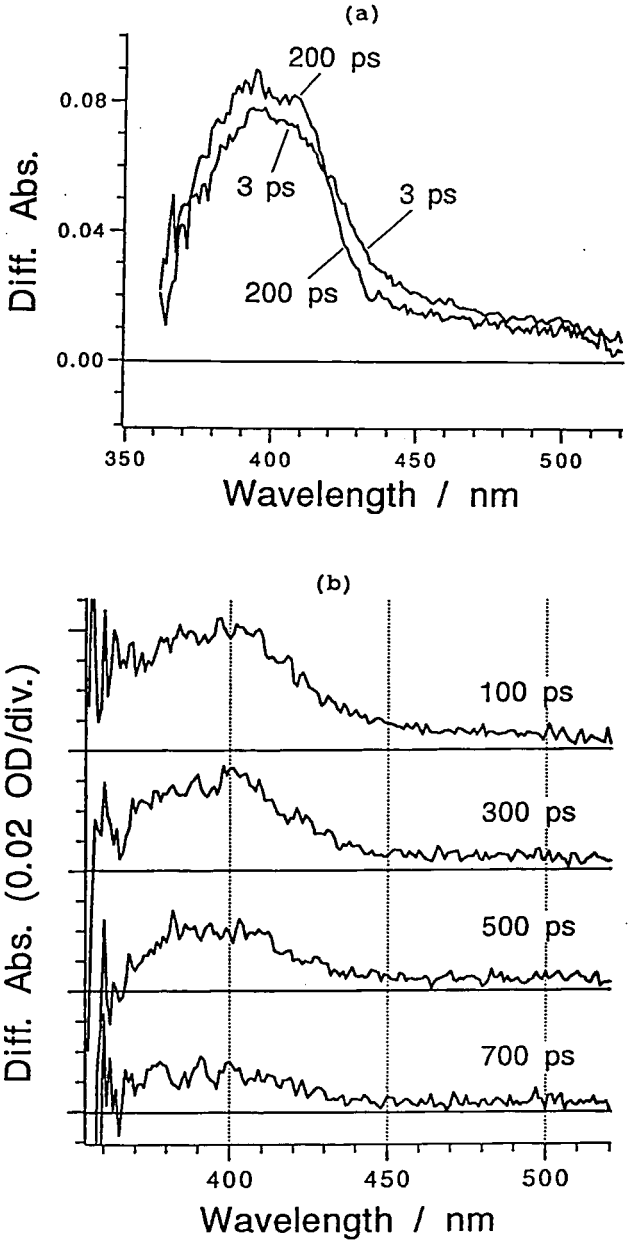

Figure 1. Picosecond time-resolved transient absorption spectra of HPIP in (a) cyclohexane and (b) dioxane.

III—G Photochemistry on Well-Defined Surfaces

While photochemistry in the gas phase is a mature field, photochemistry of adsorbed molecules on solid surfaces is still in its infancy. The irradiation of energetic photon on solid surfaces induces excitation of the electronic states of adsorbed molecules and/or surfaces, which promotes a variety of processes including photodesorption, photo dissociation of adsorbates, and photochemical reactions with coadsorbed molecules. In order to understand mechanisms of these processes, it is important to measure the wavelength dependence of cross sections, polarization effects, and the energy distributions of product species desorbed from surfaces. Recently we have just constructed an ultrahigh vacuum chamber to explore these processes. We are also now developing a laser system for sum frequency generation at surfaces, which has great potentialities to investigate dynamics of photochemical products on surfaces.

III-G-1 Construction of the UHV Apparatus for Studying Photo-Initiated Reactions on Well-Defined Solid Surfaces

Yoshiyasu MATSUMOTO and Kyoichi SAWABE

Molecules adsorbed on solid surfaces can be excited to electronic excited states by uv photon irradiation. The fate of the excited molecules depends on the strength of interactions between adsorbates and substrates. For example, molecules adsorbed on active metal surfaces suffer from rapid quenching, since they interact strongly with surface atoms. However, it has been recently known that even on

metal surfaces some molecules undergo dissociation and further initiate chemical reactions with coadsorbed molecules.

We have constructed a new apparatus for the observation of photo-initiated reactions on well-defined solid surfaces. The apparatus has two tiers: the upper tier is for observation and the lower tier for sample preparation. A schematic diagram of the upper tier of the apparatus is shown in Figure 1. The apparatus is equipped with a low energy electron diffraction (LEED) and Auger electron spectrometer (AES), a quadrupole mass spectrometer (QMS), an ion gun, a precision XYZ sample manipulator mounted on a differentially-pumped rotary platform, a samle holder, a gas doser, and inlet and outlet windows for laser beams. The main chamber is evacuated by a tandem turbomolecular pump and the housing of the QMS is differentially pumped by another tandem turbomolecular pump. The base pressure of the apparatus is kept below 2×10^{-10} Torr. The sample temperature can be cooled from 1300 to 80K in a few minutes. Impurities on the surface of samples can be removed by Ar ion sputtering and the impurity level is checked with AES. Surface order is determined with LEED. The quadrupole mass spectrometer is used for temperature-programmed desorption and time-of-flight measurements of neutral species desorbed from surfaces.

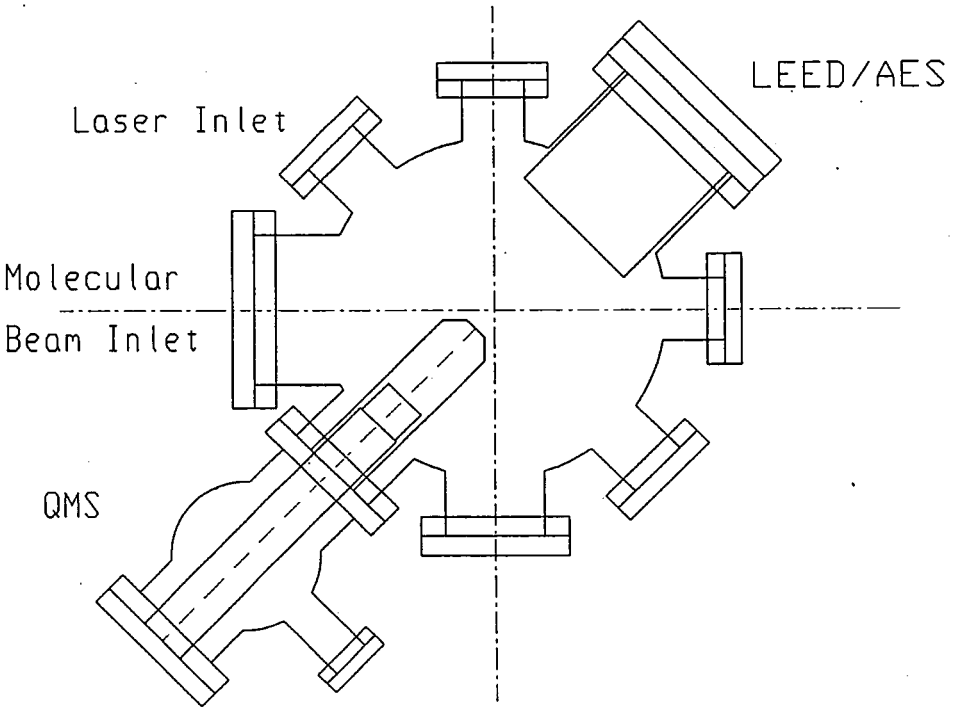

Figure 1. A schematic diagram of the upper tier of the UHV chamber.

III-G-2 Picosecond Sum Frequency Generation at Surfaces

Akihide WADA, Toshiya YOKOTA, Kazunari DOMEN, Chiaki HIROSE *(Tokyo Inst. Technology)*, **Yoshiyasu MATSUMOTO, Kyoichi SAWABE, Katsuhiko OKUYAMA, and Katsumi KIMURA**

Since infrared-visible sum frequency generation only occurs within a few angstroms of any interface which breaks the center of symmetry, this may be a sensitive spectroscopic technique to probe chemically interesting adsorbates on various surfaces and interfaces. Furthermore, this technique provides an inherently good time resolution, since the up-conversion takes place only in the overlapping time duration of laser pulses employed. Thus, this spectroscopy is an attractive technique to probe dynamics of adsorbed molecules. We are interested in rather longer wavelength region of infrared radiation (5 to 10 μm), where molecules which play an important role in surface science have vibrational transitions.

A tunable traveling-wave dye laser in the near infrared is pumped with a ps Nd:YAG laser consisting of a passive/active mode-locked oscillator, a single pulse selector, and a double-pass amplifier stage. The output of the near infrared laser and a part of the fixed pump beam are mixed in a $AgGaS_2$ crystal. Then, highly collimated idler pulse at the difference frequency is generated. The visible pulse of the second harmonic frequency of YAG laser and the infrared pulse of the mid-infrared frequency are overlapped at a specimen surface. The sum frequency signal in a collimated beam at an angle determined by k-vector matching at the surface is detected through band pass filters and a monochromator which rejected scattered 532 nm light. The application of this technique to Langmuire-Blodgett films and adsorbates on semiconductor and metal surfaces are underway.

III—H Dynamical Processes in Electronically-and/or Vibrationally Excited Molecules

Fundamental molecular aspects of chemical reactions and energy transfer processes in the electronically or vibrationally excited states have been studied. Particular interest has been directed to the dynamics of vibrationally-excited weakly-coupled complexes such as van der Waals and hydrogen-bonded complexes, and the "disproportionation" reaction caused by UV irradiation of the complexes. Dynamics of highly-excited vibrational states (local modes) and chemical reaction induced by their excitation have also been subjects of research. We have also studied the nonlinear self-organizing chemical processes which exhibit temporal chemical oscillation and spatial pattern formation. The photoinduction and photoinhibition of chemically oscillating systems have been studied. The dual-frequency oscillations and uncatalysed chemical oscillations have also been studied by spectroscopic means. See also papers in SPECIAL RESEARCH PROJECTS (3) Molecular Science of Promordial Chemical Evolution and Self-organization.

III-H-1 SEP-LIF Studies on Dynamics of Vibrationally Excited State of van der Waals Complexes: The Anisole · Ar Complex

Masao TAKAYANAGI and Ichiro HANAZAKI

We have applied the SEP-LIF (stimulated emission pumping-laser induced fluorescence) technique to observe directly the vibrational relaxation or vibrational predissociation of the anisole · Ar complex produced in supersonic free expansion. Figure 1 shows LIF spectra (a) without and (b) with the SEP excitation of the complex to the 782 cm^{-1} vibrational state. The frequency of the pump pulse for the SEP excitation was set at the 0-0 transition of the anisole · Ar complex (36347 cm^{-1}), while the dump frequency was set at 35565 cm^{-1}, which corresponds to the peak of a dip in the fluorescence dip spectrum. The delay between the SEP excitation and LIF measurement was 300 ns. The bands at 36386, 36347, and 36308 cm^{-1} are 0-0 bands of anisole monomer, anisole · Ar, and anisole · Ar_2, respectively. The latter two are accompanied by intermolecular vibronic bands on their higher frequency sides. Two broad bands were found to appear with the SEP excitation as marked with arrows in the figure. One of them around 36350-36365 cm^{-1} was observed as the increase of background under the vibronic progression of anisole · Ar. They are considered to be due to the species which are vibrationally relaxed or predissociated from the initially prepared vibrational state for the following reasons: (1) the bands are not observed with the application of either pump or dump pulse; (2) the bands are not observed with the slightly off-resonant dump pulse; (3) 0←1 type transition from the initially prepared vibrational state is not observed.

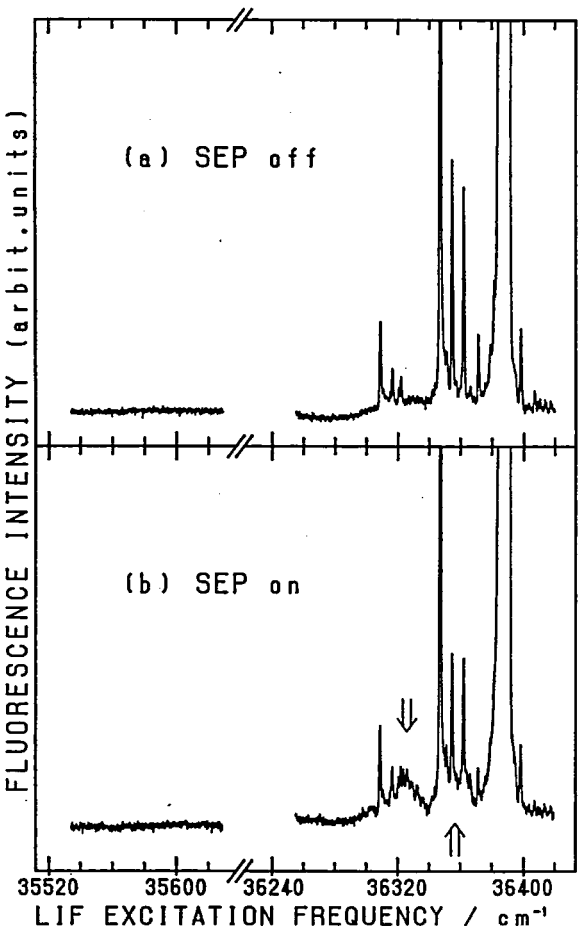

Figure 1. LIF spectra of anisole · Ar (a) without and (b) with SEP excitation to the 782 cm^{-1} vibrational state. Bands appearing by SEP are indicated by arrows.

III-H-2 SEP-LIF Spectra of Phenol in Molecular Beam

Masao TAKAYANAGI and Ichiro HANAZAKI

SEP-LIF spectra of phenol were measured. Phenol in a molecular beam was excited to one of the vibrational states, $6a_1$, $16a_2$ 12_1 and 1_1 (525, 813, 822 and 988 cm^{-1}, respectively) by SEP. After 300 ns delay, LIF spectrum was measured. Many new hot bands appeared upon the SEP excitation. In Figure 1, LIF spectrum and SEP-LIF spectra ($6a_1$ and $16a_2$ excitation) are shown. In the figure, only the positions and relative intensities of signals are shown. These spectra are drawn so that the final vibronic states are common in the abscissa; i.e. SEP-LIF spectra have been sifted

by the frequency of corresponding excited vibrational mode. LIF signal was observed without exception at the positions where the new bands were observed in the SEP-LIF spectra. This means that all new bands observed in the SEP-LIF spectra were due to the transition from the initially prepared vibrational state by SEP. Within the time scale of the delay between the SEP and LIF pulses, no vibrational relaxation occurs. The present result is in contrast with the result obtained for anisole. In the SEP-LIF spectra of anisole measured with the same experimental conditions as those in the present experiment, the bands due to the vibrationally relaxed species were observed.[1] The low frequency O-CH_3 torsional mode makes the state density of anisole higher and accelerates the vibrational relaxation.

Reference

1) M. Takayanagi, and I. Hanazaki, *Ann. Rev.* 70 (1990).

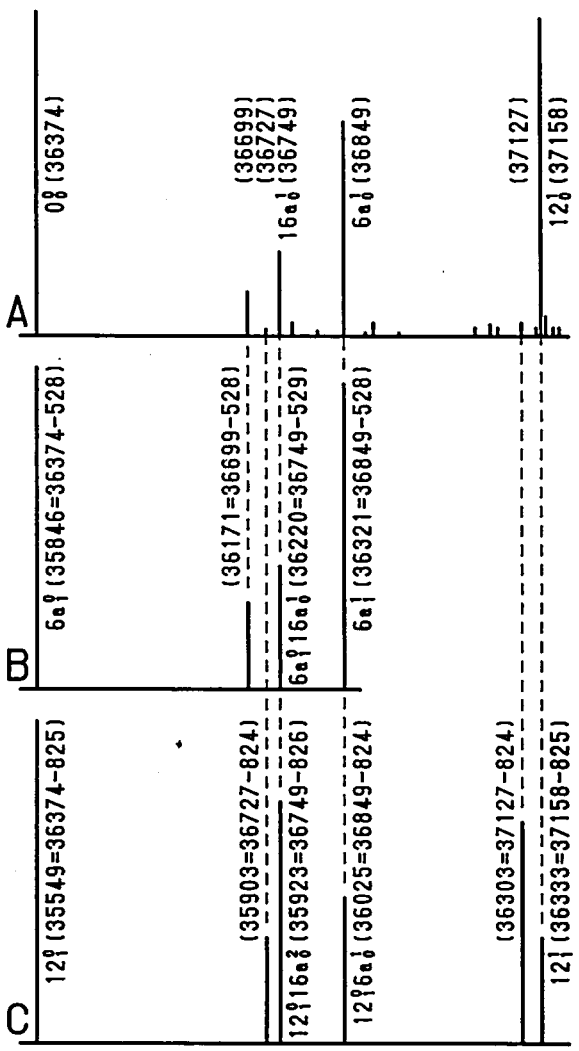

Figure 1. LIF spectra of phenol measured without SEP excitation (A) and with the SEP excitation to the (B) $6a_1$ and (C) 12_1 vibrational states.

III-H-3 Contribution of a Review "Photochemical Processes in Weakly-Bound Binary Complexes"

Masao TAKAYANAGI and Ichiro HANAZAKI

[*Chem. Rev.* in press]

Dynamics of the molecular complexes bound with weak intermolecular forces such as van der Waals forces and hydrogen-bonding has recently attracted considerable attention. The complexes give us an opportunity of investigating the "half reaction" or "half collision", which corresponds to the latter half of the bimolecular collisional process. We intended to review the current status on the photochemical reaction of weakly-bound binary complexes by trying to give a unified understanding of the phenomena and to survey possible future developments of the research field. Two types of reactions were reviewed: (1) The rearrangement reactions of the complexes initiated by photoexcitation of one of the constituent molecules to its dissociative excited state such as

$$HI \cdot N_2O + h\nu \rightarrow H \cdot N_2O + I \rightarrow OH + N_2 + I,$$

and (2) the rearrangement reactions initiated by the photoexcitation to the bound state of one of the constituents such as

$$Hg \cdot H_2 + h\nu \rightarrow Hg^* \cdot H_2 \rightarrow HgH + H.$$

III-H-4 Selective Preparation of Vibrationally Excited Vinoxy Radical ($CH_2CHO\cdot$) by Stimulated Emission Pumping (SEP)

Takumi KONO, Masao TAKAYANAGI, and Ichiro HANAZAKI

The stimulated emission pumping is an efficient and state-selective method for the preparation of vibrationally highly excited species. It is, therefore, interesting to study the unimolecular reaction dynamics of vibrationally excited states using this method. As a first step in this direction, the isomerization of vinoxy radical ($CH_2CHO\cdot \rightarrow CH_3CO\cdot$: the reaction barrier is expected to be small) was studied by measuring the SEP spectrum of the vinoxy radical.

The vinoxy radical in the electronic and vibrational ground state was prepared by the 193 nm photolysis of ethyl vinyl ether. It was excited to a single vibronic state in an electronically excited state ($\tilde{B}\,^2A''$) by tuning the pump laser. The SEP spectra were obtained by scanning the dump laser wavelength. (Figure 1) The SEP spectra are almost coincident with the fluorescence spectra, but the resolution of the SEP spectra is much higher. The dip intensity reaches nearly 40% of the total fluorescence, suggesting the existence of possible decay machanism such as the isomerization from the prepared state.

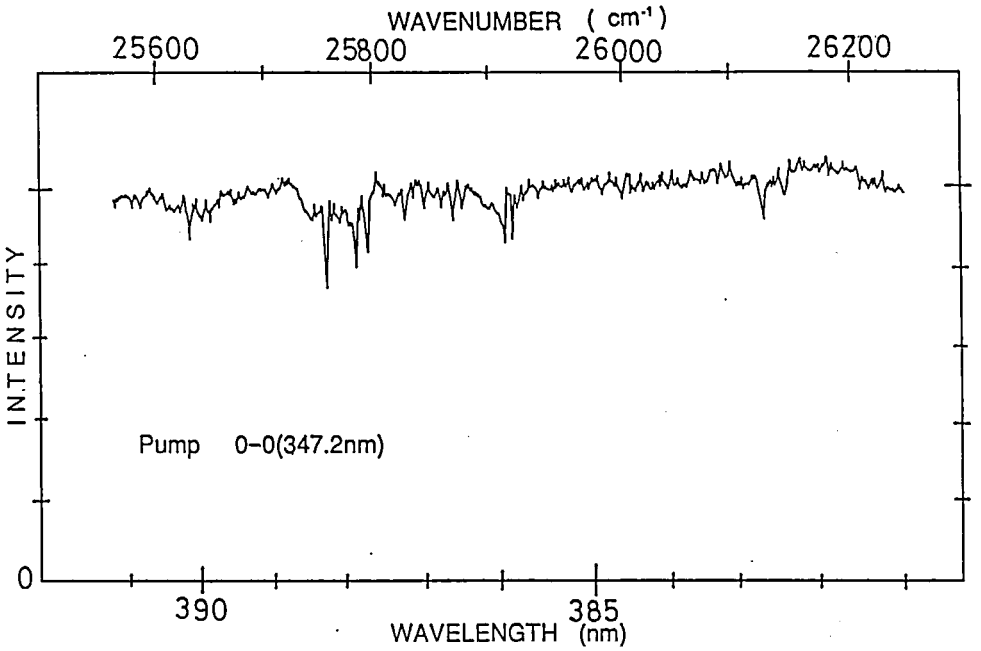

Figure 1. SEP spectrum of the vinoxy radical with pumping of the 0-0 band (347.2 nm, 28798 cm^{-1}) of $\tilde{B}\,^2A''$. Wavelength and wavenumber indicate dump laser wavelength and wavenumber, respectively.

III-H-5 Photodissociation of Ethyl Vinyl Ether at 193 nm: Rotational and Vibrational Energy Distributions of CH_2CHO · Fragment

Takumi KONO, Masao TAKAYANAGI, Teruhiko NISHIYA, and Ichiro HANAZAKI

Although the thermal decomposition of ethyl vinyl ether has been investigated extensively, there have been few studies on its photodissociation. We have recently confirmed the production of vinoxy radical (CH_2CHO ·) by the photodissociation of ethyl vinyl ether at 193 nm (ArF excimer laser) by measuring the nascent rotational and vibrational energy distributions of the radical in the laser-induced fluorescence (LIF) excitation spectra under collision-free condition. LIF excitation spectra (Figure 1) show that most vinoxy radicals are vibrationally in the ground state, whereas they are rotationally highly excited. The rotational high excitation of the vinoxy radical is not sufficient to account for the excess energy of the reaction ($CH_3CH_2OCHCH_2$+hν (193 nm)→CH_3CH_2 · +CH_2CHO · +93 kcal/mol). Most of the released energy seems to go to the internal degrees of freedom of CH_3CH_2 · or to the relative translational energy.

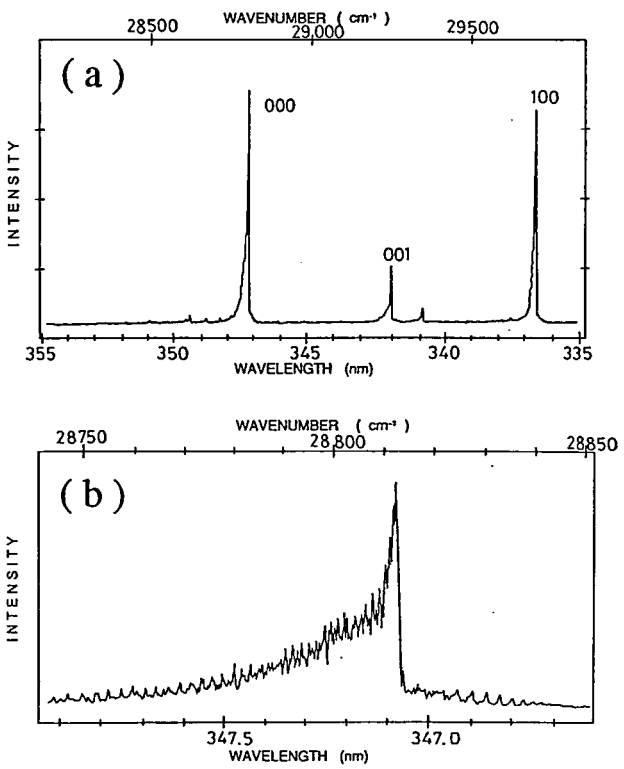

Figure 1. LIF excitation spectrum of vinoxy radical prepared by the photodissociation of ethyl vinyl ether (a), and the 0-0 band taken with high resolution (b).

III-H-6 Reaction Dynamics of the 248 nm Photolysis of HI · N_2O.

Kazuhiro HONDA, Masao TAKAYANAGI, Teruhiko NISHIYA, and Ichiro HANAZAKI

Photochemical reaction of weakly-bound complex HI · N_2O has been studied in a supersonic jet, with 248 nm irradiation. HI · N_2O is generated by the supersonic expansion of helium containing HI and N_2O. The OH radical

produced by the photolysis is monitored by the laser induced fluorescence in the $\tilde{A}$-$\tilde{X}$ transition ((0-0)band). Figure 1 shows the Boltzmann plot for the rotational distribution in the F_1A' manifolds of OH obtained from the R_{11} transitions. The rotational distribution is three Boltzmann distributions characterized by rotational temperatures of 500, 1300 and 4900 K. This distribution is hotter than those obtained in the photodissociation at 266 nm. Photodissociation at 248 nm yields I atoms in two spin-orbit states ($^2P_{3/2}$ and $^2p_{1/2}$), corresponding to the translational energies of H atom of about 43 kcal/mol and 23 kcal/mol, repectively, which may be compared with 36 kcal/mol and 14 kcal/mol, respectively, at the 266 nm photodissociation. It can composed of therefore be concluded that 40% of the additional excess energy given by varying the photon energy from 266 nm to 248 nm is distributed in the rotational degrees of freedom of OH.

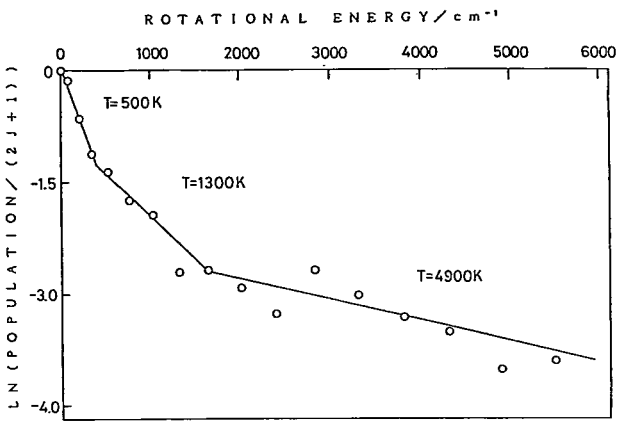

Figure 1. Boltzmann plot for the R_{11}-branch rotational distribution of OH in the v"=0 state produced by the 248 nm photolysis of HI · N_2O. Stagnation pressure=2.5 atm. HI:N_2O:He=2.6:4.4:93.

III-H-7 Primary Absorber of Light-Induced Bifurcation of Nonlinear Chemical Reaction

Yoshihito MORI, Prem Kumar SRIVASTAVA, and Ichiro HANAZAKI

We have studied the primary process in the light-induced bifurcation from monostable to oscillatory states in a reaction system of hexacyanoferrate(II), hydrogen peroxide and sulfuric acid. When the reactants are fed to a CSTR (continuous flow-stirred tank reactor), the pH value of the reaction mixture is constant in dark. Under irradiation by monochromatic light (resolution ~10 nm) with intensity above the critical value, pH oscillates periodically. We measured the critical intensity as a function of wavelength and the wavelength-dependence of the relative efficiency was calculated as shown in the figure. Comparing it with absorption spectra, peaks at 420 nm and 290 nm, and a shoulder at 320 nm in the relative efficiency coincide with peaks at 420 nm and 300 nm, and a shoulder at 320 nm, respectively, of the absorption spectrum of hexacyanoferrate(III). This coincidence suggests that the primary absorber in the light-induced bifurcation is hexacyanoferrate(III). In a separate dark experiment, we have confirmed that an increase of temperature by 2°C induces bifurcation. Therefore we have controlled the temperature of the reaction mixture by a water jacket so that the increase of temperature due to irradiation is supressed to ~0.1°C.

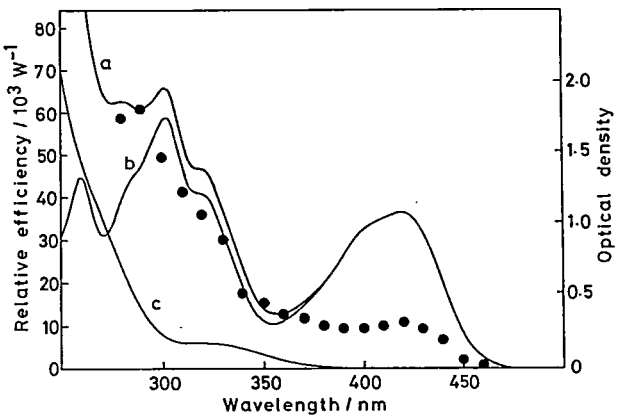

Figure 1. Relative efficiency and absorption spectra relative efficiency (closed circles) and absorption spectra of (a) the reaction mixture, (b) hexacyanoferrate(III) solution and (c) hexacyanoferrate(II) solution, respectively.

III-H-8 Wavelength-Dependent Photoinhibition in Ruthenium-Catalysed Belousov-Zhabotinskii Oscillator

Prem Kumar SRIVASTAVA, Yoshihito MORI, and Ichiro HANAZAKI

Light perturbation of oscillatory chemical reactions has been a subject of scientific interest for understanding the role of photosensory intermediates in oscillatory mechanism. Srivastava et al. have recently investigated the wavelength dependence of photoinhibition in uncatalysed bromate driven oscillators [1]. This study suggests that light absorption plays an important role in inhibiting oscillation. This mechanism has been further verified on the ruthenium-catalysed B-Z oscillator. This has been studied in a continuously stirred tank reactor where the oscillation takes place between in two well-defined states with a well-defined period. On irradiation of the oscillatory solution at moderate intensity the amplitude of oscillation has been found to decrease, while at higher intensity oscillation gets completely inhibited and the system tends to stay at the reduced state. We measured the critical intensity for the inhibition of oscillation as a function of wavelength. The efficiency of inhibition has been calculated and plotted as a function of wavelength as shown in Fig. 1 (a) together with the absorption spectrum of the oscillatory solution (b) and the $Ru(bpy)_3^{2+}$ solution (c). The efficiency spectrum (a) has a peak at 455 nm which coincides with the $Ru(bpy)_3^{2+}$ absorption band. From this study it is proposed that $Ru(bpy)_3^{2+}$ is the primary absorber in the photo-inhibition phenomenon in this system.

Reference

1) P.K. Srivastava et al. *Chem. Phys. Letters* **177**, 213 (1991).

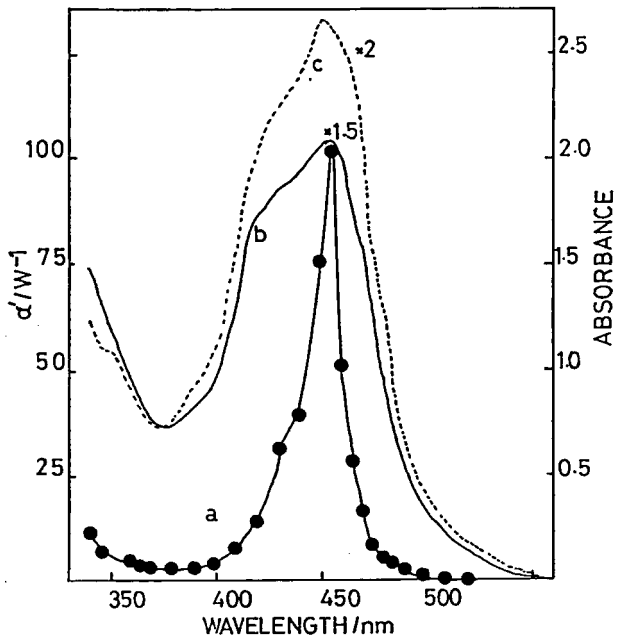

Figure 1. (a) Wavelength-dependent relative efficiency α' as defined in Ref. 1. Initial concentrations are: [malonic acid]$_0$=0.025M, $[BrO_3^-]_0$=0.025M, $[Ru(bpy)_3^{2+}]_0$=0.00025M, $[H_2SO_4]_0$=1.5M, k_o=0.0373 min^{-1} and temperature = 25°C. (b) Absorption spectrum of the oscillatory solution. Initial conditions are the same as in (a). (c) Absorption spectrum of $Ru(bpy)_3^{2+}$ (0.00025M) in the H_2SO_4 (1.5M) solution.

III—I Molecular Association and Cluster Formation in Aqueous Environments Studied by Mass-Spectrometry of Liquid Fragments

Mass spectrometry of molecular clusters isolated as fragments of liquid by adiabatic expansion of liquid droplets was extended for the study of high mass region where hydrate clusters with more than 50 water molecules are observable with nearly unit mass resolution. By comparing various data of bulk solutions with the previous and new mass spectrometric observation of liquid fragments, we have been convinced that the mass spectrometry provides even quantitative information on the association-dissociation processes in aqueous solutions.

III-I-1 Correlation of the Stability Constants of Monomer Hydrates (κ_1) with the Free Energy Changes of Hydration obtained for Bulk Solutions

Nobuyuki NISHI and Kazunori YAMAMOTO

The cluster intensity ratios, $[H^+A_m(H_2O)_{n-1}]/[H^+A_{m-1}(H_2O)_n]$, obtained from the mass spectra of the hydrate clusters generated by the adiabatic expansion of "superheated" liquid droplets in vacuum increased linearly with increasing hydration number (n) in most cases so far studied. This is consistent with a stochastic point of view, although the slope of the plots largely deviate from a simple stochastic (random mixing model). The value of this slope (a) provides a stability constant (κ_m) of an m-mer hydrate: κ_m=a([H_2O]/[A])m, where [H_2O]/[A] is the ratio of free water molecules to free solute molecules. The κ_m is also related to the equilibrium constant K_m^n of the association-dissociation equilibrium: $A_{m-1}(H_2O)_n+A=A_m(H_2O)_{n-1}+H_2O$. This reaction takes place in the final liquid state of the "superheated" droplets just before the expansion. For m=1, we obtained the stability constants of monomer hydrates of various alkyl alcohols and alkyl carboxylic acids. Butler reported the free energies, heats, and entropies of hydration of various alcohols.[1] Figure 1 shows the correlation of the logarithms of the stability constants of monomer hydrates (κ_1) with the free energy changes of hydration at 55°C, exhibiting a linear relation of these two quantities obtained from the completely different methods. This result is reasonable in the light of the relation of the free energy change and the equilibrium constant: $\Delta G=-RT \ln K$, and demonstrates that the increase of the "stability" constants originates from not only the "enthalpy" change but also the "entropy" change in the aqueous solutions.

References

1) J.A.V. Butler, Trans. Faraday Soc. **33**, 229 (1937).

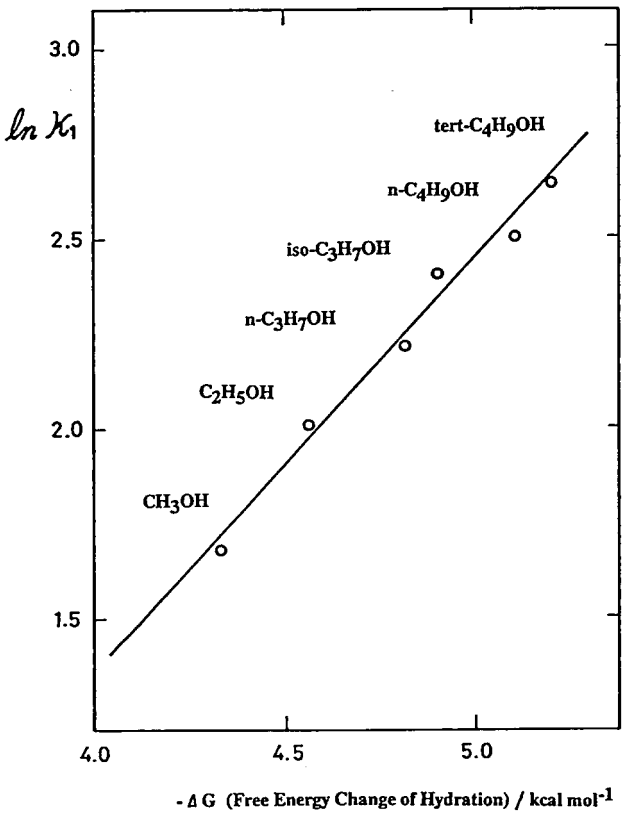

Figure 1. Logarithms of stability constants of monomer hydrates ($\ln \kappa_1$) vs. free energy changes of hydration by Butler[1] for methylalcohol, ethylalcohol, *n*-propylalcohol, *iso*-propylalcohl, *n*-butylalcohol, and *t*-butylalcohol.

III-I-2 Interaction of Hydrophobic Molecules with Water in Acetonitrile-Water Mixtures

Akihiko WAKISAKA *(NRIPR*)*, **Nobuyuki NISHI, Yukio SHIMIZU** *(NRIPR)*, **Hirochika SAKURAGI** *(Univ. Tsukuba)*, **and Katsumi TOKUMARU** *(Univ. Tsukuba) (*NRIPR: National Research Institute for Polution and Resources)*

In acetonitrile-water mixtures, dynamical processes of hydrophobic substrates, such as deprotonation of excited-state 2-naphthol and hydrolysis of t-butyl chloride, hardly take place at water mole fractions (X_w) less than 0.8. In contrast, such reaction rates increase markedly with increasing X_w in $X_w>0.8$. These results are correlated with the properties, which reflect the solvent clustering conditions, such as partial vapor pressures and IR absorption of acetonitrile-water mixtures. IR absorption of water molecules due to the antisymmetric O-H stretching vibration showed a step-wise change of the absorption peak position suggesting the presence of four different solvent structures in the regions of $0<X_w<0.2$, $0.2<X_w<0.5$, $0.5<X_w<0.8$, $0.8<X_w<1.0$. Mass spectrometric analyses of liquid fragments of acetonitrile-water mixtures and the solutions with phenol, benzylalcohol, and 2-n-butoxyethanol showed clustering conditions characteristic of the water mole fractions in the mixtures. In $0.8<X_w<1.0$, the hydrate clusters of the solutes increased very quickly with increasing X_w. In $0.2<X_w<0.8$, the signals of the hydrate clusters were very weak, while the acetonitrile hydrates increased with decreasing X_w. The observed mass spectral change with varying X_w is discussed in relation to the structure of acetonitrile-water solutions and its effect on the dynamical processes of hydrophobic substrates.

III—J Excited State Dynamics and Electronic Structure of Molecular Clusters

Cluster specific excited state dynamics are explored with the aid of two-color Resonance Enhanced Two-photon Ionization method and size selection by time-of-flight technique. Molecular clusters sometimes show disproportionation reactions in the excited states of the ions. Observation of photoevapolation of molecules from size-selected cluster ions as functions of excitation wavelength provided us with electronic spectra of the cluster ions.

III-J-1 Photodepletion Spectroscopy of Benzene Cluster Ions: $(C_6H_6)_2^+$ and $(C_6H_6)_3^+$

Kazuhiko OHASHI and Nobuyuki NISHI *(IMS and Kyushu Univ.)*

Photodissociation of size-selected benzene cluster ions was studied in the 750-970 nm wavelength range. Photodepletion spectra, i.e., depletion of parent ions as a function of dissociation wavelength, of $(C_6H_6)_2^+$ and $(C_6H_6)_3^+$ were obtained.

The experiment was carried out using a reflectron-type time-of-flight mass spectrometer. Parent ions were produced by multiphoton ionization of neutral benzene clusters. The prepared ions were size-selected and excited by a dissociation laser. Depletion of the parent ions was monitored instead of appearance of fragments because $(C_6H_6)_3^+$ has two dissociation channels.

Figure 1 shows the photodepletion spectra of $(C_6H_6)_2^+$ and $(C_6H_6)_3^+$. The spectrum for $(C_6H_6)_2^+$ shows a broad and featureless band with a maximum at $\approx$920 nm. Although low-energy wing of the band was not measured, a fwhm of $\approx$2100 cm^{-1} could be estimated. This band has been assigned to a charge resonance (CR) band which arises from the transition between the bound ground state and its sister repulsive excited state of $(C_6H_6)_2^+$. The charge resonance energy is determined to be $\approx$5400 cm^{-1} from the position of the absorption maximum. The corresponding band for $(C_6H_6)_3^+$ seems to peak at longer wavelength than 970 nm, indicating a red-shift of at least 500 cm^{-1} relative to $(C_6H_6)_2^+$. Assuming that $(C_6H_6)_3^+$ has a triple sandwich structure and the charge is delocalized over three molecules, then a calculation shows that CR band of $(C_6H_6)_3^+$ should be split into two (intense and weak) bands and the intense one should be shifted to the red of the CR band of $(C_6H_6)_2^+$.

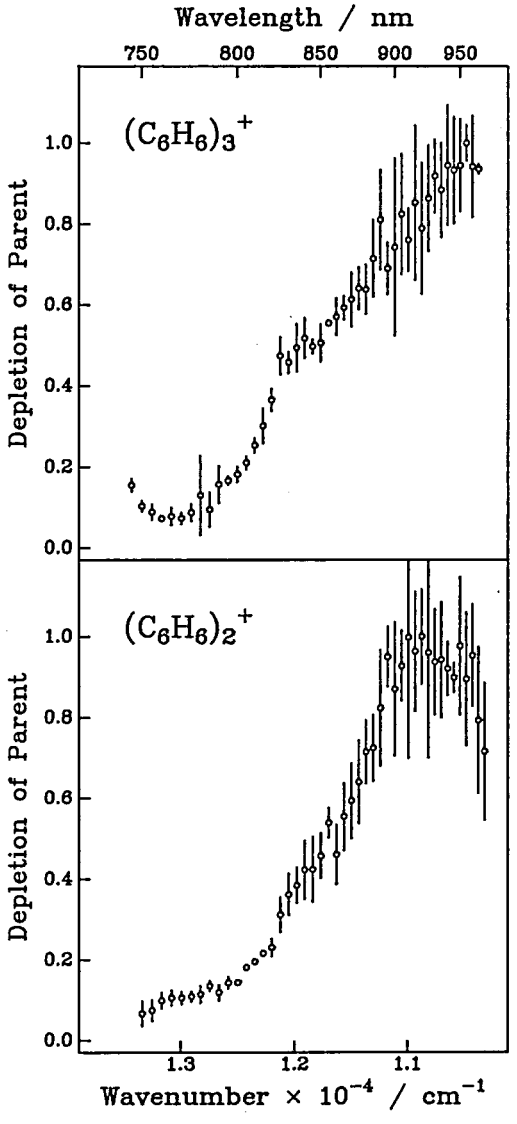

Figure 1. Photodepletion spectra of $(C_6H_6)_2^+$ and $(C_6H_6)_3^+$. The observed depletion is normalized by the power of the dissociation laser. Error bars show one standard deviation determined from 4-6 different measurements.

III-J-2 Photodissociation Dynamics of $(C_6H_6)_2^+$

Kazuhiko OHASHI and Nobuyuki NISHI *(IMS and Kyushu Univ.)*

Photodissociation of $(C_6H_6)_2^+$ was studied with photon energies between 1.29 and 2.81 ev. The average relative translational energy, $<\varepsilon_t>$, and the angular distributions of the photofragments ($C_6H_6^+$ and C_6H_6) were measured as a function of photon energy.

Mass-selected ion beams of $(C_6H_6)_2^+$ were photodissociated by a pulsed laser in the field-free region of a time-of-flight mass spectrometer with a crossed beam configuration. Determination of $<\varepsilon_t>$ was performed based on an analysis of peak shapes in the mass spectra.

Plots of $<\varepsilon_t>$ against the available energy ($h\nu$ - ε_0) are shown in Figure 1. As a result of the transition to a bound upper state in the local excitation (LE),[1] only a small fraction ($\approx$3%) of the available energy is partitioned into the translation. This energy disposal is consistent with a statistical phase space theory. A probable photodissociation mechanism is vibrational predissociation after internal conversion to vibrationally excited levels of the ground state of $(C_6H_6)_2^+$. Charge resonance (CR) absorption excites $(C_6H_6)_2^+$ to a repulsive upper state.[1] This transition is expected to result in the partitioning of a large fraction of the available energy into translational energy. However, the observed values for $<\varepsilon_t>$ are at most 10% of the available energy, even though they are larger than the calculated values by the phase space theory. We can expect that $\approx$90% of the available energy is transferred into vibrational energy of the fragments during the dissociation. This indicates that the CR band excitation prepared $(C_6H_6)_2^+$ in the highly vibrationally excited levels of the repulsive state.

Reference

1) K. Ohashi and N. Nishi, *J. Chem. Phys.*, in press.

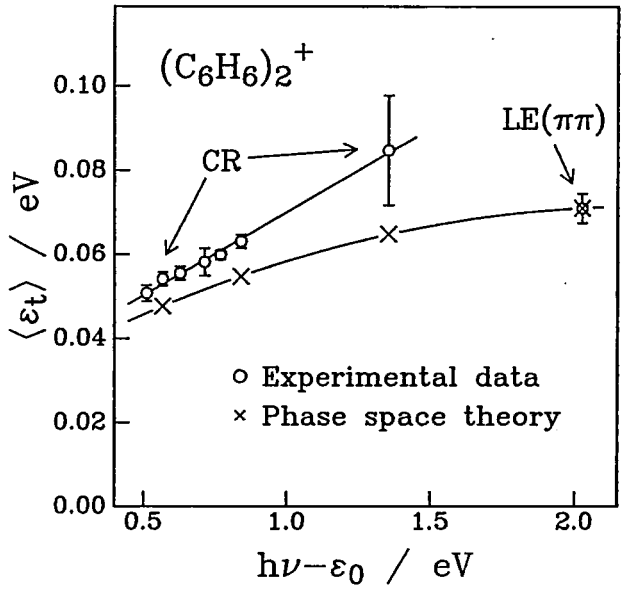

Figure 1. Plot of the average relative translational energies (O) against the available energies at the charge resonance (CR) band and the local excitation (LE) band. ε_0 is the binding energy of $(C_6H_6)_2^+$. Results of the phase space calculation (×) are also shown.

III-J-3 Photodissociation Dynamics of $(C_6H_6)_3^+$

Kazuhiko OHASHI and Nobuyuki NISHI *(IMS and Kyushu Univ.)*

Time-of-flight (TOF) spectra of both ionic and neutral fragments produced in the photodissociation of $(C_6H_6)_3^+$ were observed. The average translational energy of the fragments was compared with that calculated on the basis of a statistical theory in order to evaluate dissociation mechanisms.

Mass-selected $(C_6H_6)_3^+$ was photodissociated by a pulsed laser in the field-free region of a TOF mass spectrometer with a crossed beam configuration. The applied photon energy of 2.81 eV corresponds to the ($\pi\pi$) local excitation (LE) of $(C_6H_6)_3^+$.[1] TOF spectra of $C_6H_6^+$ and neutral fragments are shown in Figure 1. Only $C_6H_6^+$ was observed as a photofragment ion from $(C_6H_6)_3^+$. Although no mass analysis of neutral fragments was made, production of $(C_6H_6)_2^+$ is unlikely because of a small binding energy of $(C_6H_6)_2^+$. Two possible dissociation pathways to the formation of three fragments ($C_6H_6^+$ and $2C_6H_6$) are the simulta-

neous dissociation:

$$(C_6H_6)_3^+ \rightarrow C_6H_6^+ + C_6H_6 + C_6H_6, \quad (1)$$

and the sequential (two-step) dissociation:

$$(C_6H_6)_3^+ \rightarrow (C_6H_6)_2^+ + C_6H_6, \quad (2a)$$

$$(C_6H_6)_2^+ \rightarrow C_6H_6^+ + C_6H_6. \quad (2b)$$

Different energy partitionings in the fragments are expected for the two mechanisms. By analogy with $(C_6H_6)_2^+$, the photodissociation at the LE band is expected to occur via a statistical vibrational predissociation. Calculations based on a statistical model were performed to predict the translational energies of the fragments in the two mechanisms. The result for the sequential mechanism is in better agreement with the experimental data.

Reference

1) K. Ohashi and N. Nishi, *J. Chem. Phys.*, in press.

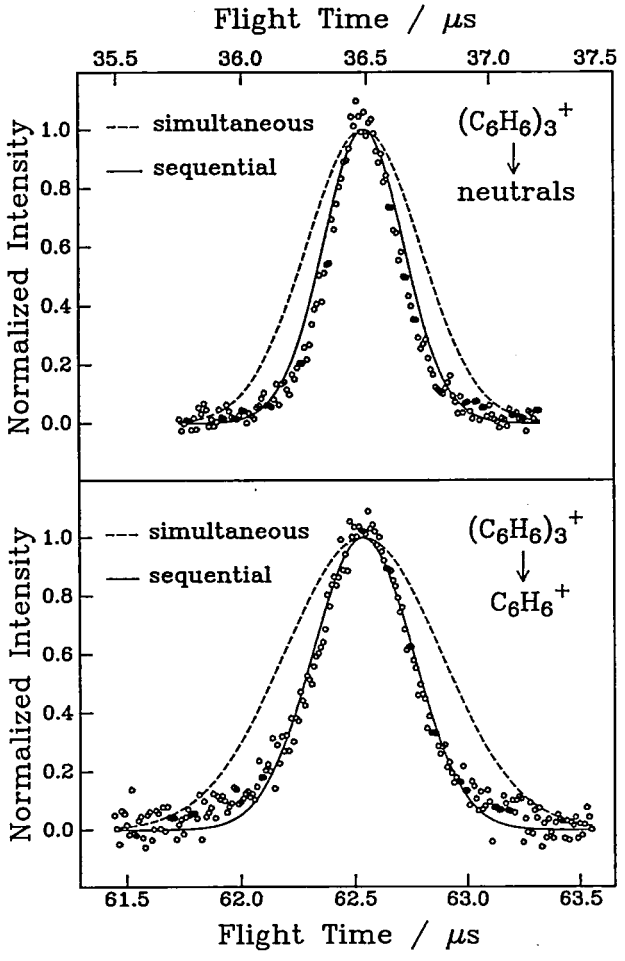

Figure 1. TOF spectra of ionic fragment $C_6H_6^+$ (lower panel) and neutral fragments (upper panel) produced in the photodissociation of $(C_6H_6)_3^+$ with $h\nu$=23.81 eV. Experimental points (O) are compared with the results of a calculation based on the simultaneous mechanism (---) and the sequential mechanism (—).

III-J-4 Chemical Reactivity Promoted by Optical Excitation Transfer in Mixed Clusters

Anthony J. STACE, Kazuhiko OHASHI, Pascal LABLANQUIE, and Nobuyuki NISHI

Chemical reactivity in mixed clusters can, to some degree, be controlled by the nature of a single component, i.e. in clusters of the type Y_nX, the range of excited neutral and ionic states in Y determines how much excess energy is available to X^+ for the purpose of promoting chemical reactions. We provide evidence of such a process in mixed benzene-bromomethyl benzene (benzyl bromide, $C_6H_5CH_2Br$) clusters. Laser excitation of the benzene component is seen to promote a very specific fragmentation process which we believe to proceed via formation of the bromomethyl benzene ion. Mass spectra were recorded with an ionization laser wavelength of 210 nm following the adiabatic expansion of mixtures of bromomethyl benzene, benzene, and argon with various ratios. For the gas mixture with sufficient benzene, a number of ions including $C_6H_6^+$(m/e=78), $(C_6H_6)_2^+$(m/e=156), and $C_{13}H_{12}^+$(m/e=168) appeared in addition to the ion at m/e=91 (a fragment of bromomethyl benzene ion). The ion at m/e=168 has no analogue in the mass spectra of either pure benzene cluster ions or $C_6H_5CH_2Br^+$ and clearly this is associated with the interaction of bromomethyl benzene with a larger $(C_6H_6)_n$ component. In identifying the origin of this species, $C_{13}H_{12}^+$, we suggest that the ion could adopt either of the two forms: (a) $C_6H_5 \cdot C_7H_7^+$ or (b) $C_6H_5CH_2C_6H_5^+$ and, therefore, corresponds to the loss of HBr (or H+Br) from the mixed clusters. Surplus monomer units would then be lost through evaporation.

III—K Photodissociation Dynamics Studied by Photofragment Time-of-Flight Spectroscopy

III-K-1 Photodissociation Dynamics of the $C_7H_7^+$ Ion

Pascal LABLANQUIE, Kazuhiko OHASHI, and Nobuyuki NISHI *(IMS & Kyushu Univ.)*

The $C_7H_7^+$ ion is an abundant component in the mass spectrum of a variety of hydrocarbons; its interest relies in its possible cyclic structure (tropylium). We created $C_7H_7^+$ through resonant 3 photon (1+2) absorption in chlorotoluene (at 275.55 nm, resonant with the vibrationless S_1 state), and photodissociated it with a second laser in the 500—270 nm range. A reflectron mass spectrum was used to isolate the photodissociation products. Figure 1 shows the observed fragmentation pattern: 1 photon absorption induces C_2H_2 loss while 2 photon absorption yields $C_5H_5^+$ (fast dissociation), $C_5H_3^+$, $C_4H_3^+$, $C_3H_5^+$ and $C_3H_3^+$. Special attention was given to characterize the $C_7H_7^+ + h\nu \rightarrow C_5H_5^+ + C_2H_2$ reaction:
1) the cross section for this process is found to show a structureless, smooth increase with the photon energy. 2) the kinetic energy released during the dissociation (150 meV) is found to be the same at 340 or 460 nm. 3) In flight dissociation observed above 340 nm (see Figure 1) enables us to measure the rate constant of the reaction as a function of the dissociating wavelength. Comparison with the same measurement performed with the deuterated analog $C_7D_7^+$ and modelling with the RRKM theory gives information on the transition state of the reaction.

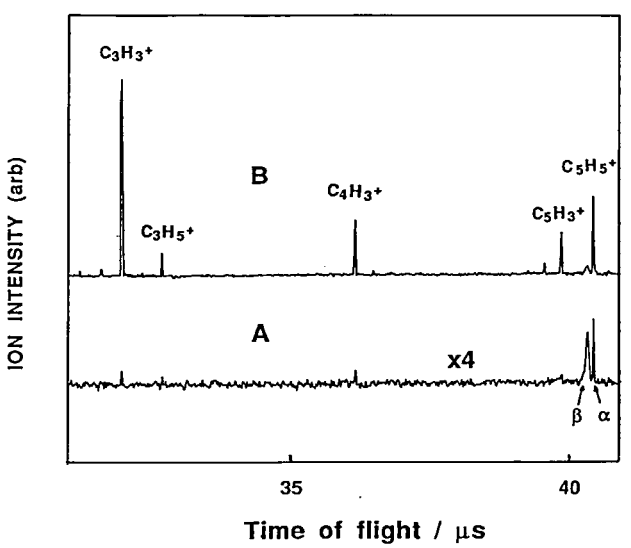

Figure 1. Mass spectrum of the fragments resulting from the photodissociation of $C_7H_7^+$ at 460 nm. In B), the power of the dissociating laser was increased by a factor 9, thus revealing the multiphoton dissociation prcesses. The $C_5H_5^+$ peaks shows 2 components corresponding to dissociations occurring in the acceleration (component α) or the drift zone (comoponent β) of the apparatus.

III-K-2 Laser Photodissociation of Organometallic Compounds on a Cryosubstrate

Masahiro KAWASAKI *(Hokkaido Univ.)* **and Nobuyuki NISHI**

Photodissociation dynamics of organometalic compounds (tetramethyltin, trimethylgallium, trimethylindium, and dimethylzinc) adsorbed on a quartz substrate at 100K has been studied by time-of-flight mass spectrometry with detecting mainly CH_3 photofragments. Shapes of the time-of-flight spectra depend on fluence of dissociation laser at 193 nm and thickness of multilayers of organometallic compounds. For thick layer deposition, gas phase dissociation occurs because of vaporization of solid compounds by absorbing laser photons. For thin layer deposition, relaxation processes take place so quickly that product time-of-flight profiles were characterized by a Maxwell-Boltzmann distributions.

III—L External Magnetic Field Effects on Chemical Reactions

III-L-1 Excimer Formation of Pyrene as a Probe to Investigate the Recombination of Geminate Pairs (III): The Effect of Charge Hopping Process on Fluorescence and ODESR Spectra in X-Irradiated Ethylene Propylene Rubber Doped with Pyrene

Masaharu OKAZAKI *(Gov. Ind. Res. Inst., Nagoya and IMS)*, **Kazumi TORIYAMA** *(GIRIN)*, **Yutaka TAI** *(GIRIN)*, **and Keichi NUNOME** *(GIRIN)*

[*Appl. Magn. Reson.* **1**, 213 (1990)]

The fluorescence detected ESR(ODESR) spectrum and X-induced and UV-excited fluorescence spectra were successfully obtained for ethylene propylene rubber (EP-rubber) doped with pyrene under various conditions. From the analysis of the ODESR intensity and its linewidth, it was found that charge hopping between the solute pyrene is the main mechanism for geminate recombination at the pyrene content larger than 0.3 wt%. At elevated temperatures, the excimer fluorescence relative to the monomer fluorescence induced by X-ray excitation is considerably stronger than that by UV-excitation, especially at high concentrations. On the other hand, at lower temperatures below ca. 280K this difference could not be observed even at high concentration of 3 wt%. These observations indicate that the formation of dimer cation, from which the excimer fluorescence is efficiently emitted, is accelerated by the hopping of cation-radical center to the clustering pyrenes at high temperatures and high concentrations. While, only the electron hopping takes place at low temperatures, thus whether a charge recombination results in excimer formation or not is determined by the cationic trapping site, i.e. if several pyrenes are clustering there, excimer may be formed regardless of the excitation source. Although rapid translational motion is restricted in EP-rubber, the effective formation of excimer or dimer cation at high temperatures indicates that rotational diffusion and small distance translational diffusion are allowed within the fluorescence lifetime at those temperatures.

III-L-2 Hyperfine vs. Relaxation Mechanism of the Magnetic Field Effect on Recombination Fluorescence of Geminate Pairs

Masaharu OKAZAKI *(Gov. Ind. Res. Inst., Nagoya and IMS)*, **Yutaka TAI** *(GIRIN)*, **Keichi NUNOME** *(GIRIN)*, **Kazumi TORIYAMA** *(GIRIN)*, **and Saburo NAGAKURA** *(Grad. Univ. for Adv. Studies)*

[Submitted to *Chem. Phys.*]

Magnetic field effects on the recombination luminescence of delayed geminate pairs in several X-irradiated systems were observed. In decane solution of pyrene, the magnetic field effect was sharp, i.e. it saturates at a relatively low magnetic field. In squalane solution, on the other hand, the magnetic field effect is dull, and the fluorescence continues to increase even at 300 mT. In the case of pyrene doped ethylene propylene rubber (EP-rubber), the magnetic field effect becomes sharp again though the viscosity of the medium is much higher than squalane. In the presence of a quencher, the magnetic field effect for squalane solution becomes sharp, and is similar to that for decane solution without quencher. These observations were analyzed with referring both the calculation for a simple model system and the amplitude of fluorescence detected ESR(ODESR) observed for the same systems. It has been shown that time profile of the (delayed) geminate recombination can be obtained through the analysis.

III-L-3 Magnetic Field Effects on the Lifetime of Perturbed Rotational Levels of CN in the Electronically Exicted States

Kaoru SUZUKI and Saburo NAGAKURA *(Grad. Univ. for Adv. Studies)*

The CN radical is one of the classic examples whose "violet" ($B^2\Sigma^+$-$X^2\Sigma^+$) emission exhibits a typical magnetic-field dependence. This is known to be due to a perturbation between the $A^2\Pi_i$ and $B^2\Sigma^+$ states, and the external magnetic field "mixes" there two states. To date, steady-state emission intensities of the perturbed lines have been measured against the magnetic field, and a model has been proposed to give an explanation of the observed magnetic-field effects. The aim of the present study is to measure the magnetic-field dependent *time profile* of the emission intensities of the perturbed levels accurately to obtain complementary information on the magnetic-field effects of the CN radical. The CN radicals were produced in the "active" nitrogen flame of CH_2Cl_2. The CN $B^2\Sigma^+$ state was then produced by laser excitation (Lambda Physik FL2002). A typical example of the decay of an excited rotational level is shown in Figure 1. In principle, a perturbed level should show a single exponential decay. The observed decay curve contains, however, fast and slow components. This is due to a poor resolution of the spectral lines at present; spin components are not resolved and the emission lines of the vibrationally excited state overlaps. The observed fast and slow components correspond to the decay of the unperturbed and perturbed levels, respectively. It is clearly seen in Figure 1 that it is the slow component which shows a magnetic-field dependence, indicating that the degree of mixing of the $A^2\Pi_i$ state with the $B^2\Sigma^+$ state is sensitive to the magnetic field. The detailed quantitative analysis, including the collisional rotational transfer due to a moderate ambient pressure, is in progress.

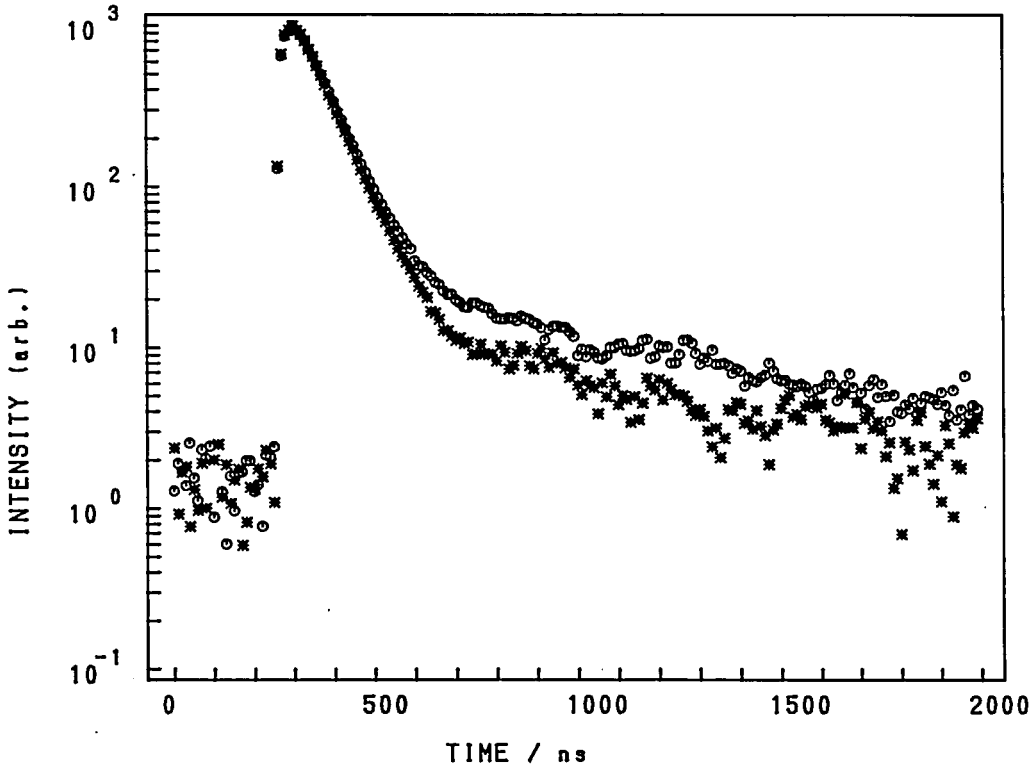

Figure 1. Decay curves of the R(6) perturbed line of the CN $B^2\Sigma^+$-$X^2\Sigma^+$ transition with the without magnetic field at an ambient pressure of 1.8 Torr: 8.3 kG (O) and 0 G (*).

RESEARCH ACTIVITIES IV
Department of Molecular Assemblies

IV—A Solid State Properties of Metallophthalocyanine Salts

Some metallophthalocyanine molecules contain unpaired *d*-electrons besides the conjugated π-electron system. Owing to this characteristic nature, the itinerant π-electrons and localized magnetic moment of the *d*-electrons coexist in solid metallophthalocyanine salts. The magnetic interaction between itinerant π-electrons and localized magnetic moments is a new aspect in the field of organic metals. For the basic understanding of these materials and to search for a new phenomenon, where a magnetic interaction takes an important role, we prepare and characterize solid metallophthalocyanine salts and related compounds. In this project we are also interested in the exciton-coupled materials in which itinerant π-electrons might couples with *d*-electrons.

IV-A-1 *d*-π Interaction in Conducting Phthalocyaninatocobalt Hexafluoroarsenate, $CoPc(AsF_6)_{0.5}$

Kyuya YAKUSHI, Hideo YAMAKADO, Takashi IDA, and Akito UGAWA

[*Solid State Commun.* **78**, 919 (1991)]

The spectroscopic study of semiconductive $CoPc(AsF_6)_{0.5}$ evidence the ligand-centered oxidation. The possible origin of the semiconductive band gap is related to the magnetic interaction between the itinerant π-electrons on the ligand channel and the unpaired *d*-electrons interacting antiferromagnetically within the Co^{2+} channel.

IV-A-2 Polarized Reflectance Spectra of the Single Crystals of Phthalocyanine Radicals, $NiPc(AsF_6)_{0.5}$, $H_2Pc(AsF_6)_{0.5}$, and LiPc

Kyuya YAKUSHI, Takashi IDA, Akito UGAWA, Hideo YAMAKADO, Hideshi ISHII*, and Haruo KURODA*
*(*Univ. of Tokyo)*

[*J. Phys. Chem.* **95**, 7636 (1991)]

Polarized reflectance spectra in the range 1000—25000 cm^{-1} are given for the single crystals of electrochemically prepared phthalocyanine radicals, $NiPc(AsF_6)_{0.5}$, $H_2Pc(AsF_6)_{0.5}$, and LiPc. Solid spectra are interpreted with the aid of the solution spectra of $LuPc_2$ and $LuPc_2^+$. The assignment of the intramolecular transition of $NiPc(AsF_6)_{0.5}$ provides the clue to judge the oxidized part (ligand or metal) of the MPc molecule. This assignment is consistent with the change of the degree of oxidation among the three solid phthalocyanine radicals. The intermolecular transfer integrals of these materials are estimated by analyzing the charge-transfer absorption band.

IV—B Optical and Electrical Properties of Organic Metals

The study of organic metals has rapidly developed since the finding of the molecule which can expand the dimensionality of intermolecular charge-transfer interaction in solid state. This expansion of dimensionality is materiarized in the salts of BEDT-TTF or C_{60}, *etc.* In this project we treat one-, two-, and three-dimensional organic metals and superconductors to investigate what is most important for stabilizing a metallic state and for designing new superconducting materials.

IV-B-1 Metallic Behavior Stable against Peierls Instability in the One-Dimensional Organic Conductor Tetraselenotetracene-Bis(1,2,5-thiadiazolo)tetracyanoquinodimethane (TSeT)(BTDA-TCNQ)

Akito UGAWA, Kentaro IWASAKI, Atsushi KAWAMOTO, Kyuya YAKUSHI, Yoshiro YAMASHITA, and Takanori SUZUKI *(Tohoku Univ.)*

[*Phys. Rev.* **B43**, 14718 (1991)]

Tetraselenotetracene (TSeT) forms a charge-transfer complex with bis(1,2,5-thiadiazolo)tetracyanoquinodimethane (BTDA-TCNQ), the complex showing a metallic behavior down to 1.5 K without undergoing a Peierls transition. The structure consists of segregated columns of TSeT and BTDA-TCNQ molecules, among which there also exist short intermolecular contacts. The polarized reflectance spectra indicate that the material is a one-dimensional metal in contrast to the structural features. The electronic structure is characterized by a one-dimensional conduction band lying on the two-dimensional lattice, which prevents the system from undergoing a Peierls distortion.

IV-B-2 Evolution of Superconductivity of K_xC_{60} upon K-doping: Microwave Low-Field Signal and ESR Study

Anvar. A. ZAKHIDOV, Akito UGAWA, Kenichi IMAEDA, Kyuya YAKUSHI, Hiroo INOKUCHI, Koichi KIKUCHI*, Isao IKEMOTO*, Shinzo SUZUKI*, and Yohji ACHIBA* *(*Tokyo Metropolitan Univ.)*

[*Solid State Commun.* **79**, 939 (1991)]

By means of low magnetic-field microwave absorption (Low-Field Signal) and conventional ESR, we have studied the evolution of superconductivity in bulk K_xC_{60} dependent on the variation of K-doping temperature and time. The first LFS as an occurrence of superconoductivity is observed in a doping time as short as t_d=0.5 h with a discrete T_c~19 K, and the volume of the superconducting phase increases on further dopings. The sample in a superconducting state exhibits strong ESR absorptions, which indicates a

non-superconducting metallic phase coexisting with a superconducting phase in an inhomogeneously doped K_xC_{60}. These phases are closely correlated to each other, and disappear at the same time by overdoping.

IV-B-3 Microwave Low-Field Signal and ESR in $K_x(C_{60})_{1-y}(C_{70})_y$ and K_xC_{70}

Anvar A. ZAKHIDOV, Kenichi IMADEA, Akito UGAWA, Kyuyu YAKUSHI, Hiroo INOKUCHI, Z. IQBAL*, Ray H. BAUGHMAN*, B.L. RAMAKRISHNA, and Yohji ACHIBA***** *(*Allied signal, **Arizona State Univ., *** Tokyo Metropolitan Univ.)*

[*Physica C*, to be published in M²S-HTSC-III Proceedings, Kanazawa]

Superconductivity (SC) in K-doped molecular alloys of C_{60} and C_{70} are studied by means of nonresonant microwave low-field signal (LFS) and conventional ESR. A LFS-search for SC is performed in K_xC_{70} as well. The critical temperature of $K_x(C_{60}/C_{70})$ determined at the onset of hysteretic LFS, systematically decreases to T_c=16 K (at about 10% C_{70}), and T_c=10 K (at about 25% C_{70}) from T_c=19 K of pure K_xC_{60}, suggesting the decrease of electron-phonon coupling. SC is not detected in K_xC_{70}, above 5 K.

IV-B-4 Structure and Superconductivity of Single Crystalline C_{60}

Koichi KIKUCHI*, Shinzo SUZUKI*, Kazuya SAITO*, Haruo SHIROMARU*, Isao IKEMOTO*, Yohji ACHIBA*, Anvar. A. ZAKHIDOV, Akito UGAWA, Kenichi IMAEDA, Hiroo INOKUCHI, and Kyuya YAKUSHI *(*Tokyo Metropolitan Univ.)*

[*Physica C*, to be published in M²S-HTSC-III Proceedings, Kanazawa]

We have succeeded in synthesis of C_{60} single crystals with orthorhombic lattice structure contrary to the known cubic form. The structure of the orthorhombic form was confirmed by a fourcircle X-ray diffractometer. The intense microwave absorption signal in low magnetic field on the K-doped C_{60} single crystals was detected with the onset at T_c=17.7 K.

IV-B-5 Optical and Electrical Properties of the Superconducting K_xC_{60} Single Crystal

Akiko UGAWA, Hideo YAMAKADO, Koichi KIKUCHI*, Shinzo SUZUKI*, Kazuya SAITO*, Yohji ACHIBA*, and Isao IKEMOTO* *(*Tokyo Metropolitan Univ.)*

[Submitted to *Phys. Rev. Lett.*]

We have observed superconductivity in the potassium-doped C_{60} single crystal by the electrical resistivity measurements. The onset of a superconducting transition occurs at 19.4 K, which is the same as the value reported for polycrystalline samples. The reflectance spectra of K_xC_{60} indicate that the intermolecular interaction between neighboring fullerences is considerably weaker and/or the carrier density is significantly lower than other organic superconductors.

IV-B-6 Reflectance Spectra of Some Two-Dimensional Organic Metals Based on BEDT-TTF and $[Ni(dmit)_2]$

M. TAMURA*, R. MASUDA*, T. NAITO*, H. TAJIMA*, H. KURODA*, A. KOBAYASHI*, K. YAKUSHI, R. KATO, H. KOBAYASHI**, M. TOKUMOTO***, N. KINOSHITA***, and H. ANZAI***** *(*Univ. of Tokyo, **Toho Univ., ***ETL)*

[*Synth. Met.* **41-43**, 2499 (1991)]

In order to probe the conduction band structure and the inter-molecular interactions, we have investigated the polarized infrared reflectance spectra of single crystals of θ- and κ-$(BEDT\text{-}TTF)_2I_3$, $(BEDT\text{-}TTF)_2KHg(SCN)_4$, $Me_4N[Ni(dmit)_2]_2$ and α-$(Et_2Me_2N)[Ni(dmit)_2]_2$. From the low temperature spectra, the Drude parameters are estimated by a Drude-Lorentz curve-fitting. Analyses of the plasma frequencies based on tight-binding band model afford the estimation of transfer integrals of these salts. The shape of Fermi surface and the conduction band structure are deduced by using these parameters.

IV-B-7 Low-Field Microwave Absorption in Organic Superconductor κ-$(ET)_2[Cu(NCS)_2]$

Anvar A. ZAKHIDOV, Akito UGAWA, Kyuya YAKUSHI, Kenichi IMADEA, Hiroo INOKUCHI, I.I. KHAIRULLIN*, and P.K. KHABIBULLAEV* *(*Uzbek SSR Academy of Science)*

[*Physica C*, to be published in M²S-HTSC-III Proceedings, Kanazawa]

Low-magnetic field spectra (LFS) of microwave absorption in κ-$(ET)_2[Cu(NCS)_2]$ single crystal is found to be highly anisotropic. For the magnetic field parallel to conducting planes ($H \| bc$) the LFS maximum is shifted to high H_M=400 G while its intensity and hysteresis width are strongly enhanced compared with LFS at $H \perp bc$. This indicates that the fluxons easily penetrate between 2-D conduction layers coupled by Josephson junctions. Temperature behavior of LFS is also anisotropic. For $H \| bc$ hysteretic LFS shows the onset at T~10 K, but for $H \perp bc$ it disappears abruptly at T~8.5 K though noisy LFS without hysteresis can be found at temperatures above T_c.

IV-B-8 The Fermi Surfaces in the κ-Type BEDT-TTF Based Organic Superconductors

K. OSHIMA*, K. ARAKI*, H. YAMAZAKI*, K. KATO, Y. MARUYAMA, K. YAKUSHI, T. MORI, H. INOKUCHI, H. MORI, and S. TANAKA**** *(*Okayama University, **ISTEC)*

[*Physica C*, to be published in M²S-HTSC-III Proceedings, Kanazawa]

The Fermi surfaces in the κ-type organic superconductors have been studied using Shubunikov de Haas (SdH) and de Haas van Alphen (dHvA) effect. The systematic change in the superconducting transition temperature among the κ-phase superconductors are discussed in relation to the contribution of anion layers to the transport

properties. The dHvA effect in κ-(BEDT-TTF)$_2$Ag(CN)$_2$H$_2$O show an similar but characteristic quantum oscillation compared with that of κ-(BEDT-TTF)$_2$Cu(NCS)$_2$. We could obtain no oscillation in κ-(BEDT-TTF)$_2$Cu[(NCN)$_2$]Br which has the highest Tc so far observed at ambient pressure.

IV-B-9 Reflectance Spectra of κ-(BEDT-TTF)$_2$I$_3$: Electronic Structure of Dimeric BEDT-TTF Salts

Masafumi TAMURA*, Hiroyuki TAJIMA*, Kyuya YAKUSHI, Haruo KURODA*, Akiko KOBAYASHI*, Reizo KATO, and Hayao KOBAYASHI**** *(*Univ. of Tokyo, **Toho Univ.)*

[Submitted to *J. Phys. Soc. Jpn.*]

Polarized reflectance spectra of a single crystal of κ-(BEDT-TTF)$_2$I$_3$ were measured at 295 K and 15 K over the spectral range from 500 cm^{-1} to 25000 cm^{-1}. The infrared property was two-dimensional. Non-Drude mid-infrared features were observed in spite of the metallic DC conductivity. A comparison with β- and θ-(BEDT-TTF)$_2$I$_3$ shows that this behavior has a close connection with the dimeric structure of κ-salts. We analyzed the observed line shape by the curve-fitting analysis, and obtained optical effective masses. On the basis of the perturbation theory, an effective tight-binding band model for κ-salt was derived. We estimated the transfer integrals using this model.

IV—C High-Pressure Study on Charge-Transfer Complexes

We have studied the pressure dependence of the charge-transfer band of mixed-stacked charge-transfer complexes. This type of organic solid sometimes shows a neutral-ionic phase transition at high pressure, and might become metallic under an extremely high pressure. The aim of this project is to determine the pressure dependence of the fundamental microscopic parameters for predicting a new state at high pressure.

IV-C-1 Pressure Dependence of the Polarized Reflectance Spectrum of a Solid Charge-Transfer Complex, Perylene-Hexacyanobutadiene (HCBD)

Takashi IDA, Kyuya YAKUSHI, Haruo KURODA*, Hideki YAMOCHI, and Gunzi SAITO**** *(*Univ. of Tokyo, **Kyoto Univ.)*

[*Chem. Phys.*, in press]

The polarized reflectance spectrum of the perylene-HCBD complex has been measured at high pressures up to 26 kbar. Extraordinary intensity of the charge-transfer band is observed at high pressures, which cannot be reproduced by a conventional analytical model such as a dimer or trimer model. It is shown that this intensity can be naturally explained by applying the results of diagrammatic valence-bond calculations for an infinite-chain model, which has been reported by Painelli et al. The degree of charge transfer ρ, the transfer integral t, and the site-energy difference from the donor to acceptor Δ at each pressure are estimated, and the pressure dependence of t and Δ is found to be $dlnt/dP$=+2.9% kbar^{-1} and $d\Delta/dP$=—9.6meV kbar^{-1}, respectively.

IV—D Construction of Microspectrophotometer

We are constructing microspectrophotometric systems to measure the optical reflectivity of a small single crystal in the wide spectral range from ultraviolet region to far-infrared region.

IV-D-1 Design of an Instrument for Far-Infrared Microspectroscopy using a Synchrotron Radiation (SR) Source

Akito UGAWA, Hideshi ISHII, Kyuya YAKUSHI, Hiroshi OKAMOTO, Tadaoki MITANI, Makoto WATANABE, Kusuo SAKAI, Koichi SUZUI, and Shinji KATO

[*Rev. Sci. Instrum.*, in press]

A design of a microspectro-photomeric system using a synchrotron radiation (SR) source is described. The system covers a wide spectral range of 50—13000 cm^{-1}, being under construction at the UVSOR BL6B beam-line in the Institute for Molecular Science. Preliminary experiments in the mid-infrared region (500—5000 cm^{-1}) have qualitatively confirmed the theoretical calculation that the synchrotron radiation is more intense than a blackbody (T=1200 K) when a microspectrophotomeric technique is applied, which is due to the natural collimation and high brilliance of SR source. The SR as an infrared source exhibits its advantage on measuring the spectra of small single crystals especially in the far-infrared region.

IV-D-2 Improvement of Microspectrophotometer

Atsushi KAWAMOTO, Hideshi ISHII*, Kentaro IWASAKI, and Kyuya YAKUSHI *(*Univ. of Tokyo)*

We have constructed a microspectrophotometer for the use of 2150 cm^{-1} to 35000 cm^{-1}. To improve the efficiency of the available light, we changed the mirror configuration for collecting the light, the transfer optics from the monochromator to the microscope, the mirror system to focus the light from the microscope to the detector element, and the position of polarizers. We improved the interface circuits for the automatic change of the mirrors, polarizers, and electric signals from detectors. All of these optics was newly designed and reconstructed. We improved the efficiency by an order of magnitude as compared with the old system.

IV—E Synthesis and Electrical Properties of Organic Conductors

In order to obtain the knowledge required for the further development in the field of organic conductors, charge-transfer complexes and radical salts of OCNAQ and phthalocyanines have been prepared and their structural and electrical properties have been studed.

IV-E-1 Approaches to Controlling the Dimensionality in Molecular Conductors. Axially Substituted Phthalocyanines and Twin-Type Molecules

Tamotsu INABE, Yusei MARUYAMA, and Tsutomu MITSUHASHI *(The Univ. of Tokyo)*

[*Synth. Met.* **41-43**, 2629 (1991)]

Two kinds of novel approaches to increasing the dimensionality in molecular conductors are presented. The first approach is based on the slipped stacking of planar molecules due to the steric interaction of axial substituents. The second approach is based on the interleaved stacking of twin-type molecules, which are composed of two units of a donor or an acceptor. As examples, two kinds of radical salts of an axially substituted phthalocyanine, and the TTF complex of OCNAQ, a twin-TCNO-type acceptor, are presented.

IV—F Synthesis and Characterization of Proton-Transfer/ Charge-Transfer System

Hydrogen-bonded systems, in which the proton transfer is coupled with the π-electron configurational change, are the subject of this study. If the interaction between the molecules is sufficiently strong in the crystalline state, the proton motion is expected to modulate the electronic properties of the crystal. In order to examine such a possibility, a number of compounds which have a common framework of salicylideneaniline have been synthesized as the intramolecular proton transfer system. In order to extend the system to the intermolecular cases, charge transfer complexes of aromatic amines have also been prepared and subjected to structural, electrical, magnetic, and optical studies.

IV-F-1 Structure and Optical Properties of Thermochromic Schiff Bases. Charge Transfer Interaction and Proton Transfer in the *N*-(Tetrachlorosalicylidene)aniline and *N*-Tetrachlorosalicylidene-1-pyrenylamine Crystals

Tamotsu INABE, Isabelle GAUTIER-LUNEAU, Naomi HOSHINO *(Hokkaido Univ.)*, **Kaoru OKANIWA, Hiroshi OKAMOTO, Tadaoki MITANI, Umpei NAGASHIMA, and Yusei MARUYAMA**

[*Bull. Chem. Soc. Jpn.* **64**, 801 (1991)]

Two kinds of *N*-salicylideneaniline derivatives, *N*-tetrachlorosalicylideneaniline (CL4SA) and *N*-tetrachlorosalicylidene-1-pyrenylamine (CL4SPY), have been prepared and subjected to structural and optical studies in the crystalline state. A thermochromic-type behavior of the former crystal has been observed as a shift of the absorption edge, while that of the latter crystal is much less pronounced. Fairly short O-H···N hydrogen bonds are found in both compounds from the crystallographic studies, which may be mainly due to a steric effect of chlorine substituents. The difference in the proton transfer behavior of CL4SA and CL4SPY should presumably be caused by an intermolecular charge transfer interaction in the latter crystal.

IV-F-2 Proton Transfer in *N*-Salicylideneanilines. As Approach to Controlling the Charge Transport in Molecular Materials

Tamotsu INABE

[*New J. Chem.* **15**, 129 (1991)]

The structural and optical studies on the proton transfer in various derivatives of *N*-salicylideneaniline, including their charge transfer complexes, are presented. From X-ray analyses of the OH···N hydrogen-bond structure it has been confirmed that the proton transfer is controllable by chemical modification of the molecule or by adjustment of the intermolecular interactions. On the basis of these experimental results, a novel type of molecular electronic devices is proposed.

IV-F-3 Charge Transfer Complexes of Salicylideneaniline Derivatives

Tamotsu INABE, Naomi HOSHINO *(Hokkaido Univ.)*, **Isabelle GAUTIER-LUNEAU, Hiroshi OKAMOTO, Kaoru OKANIWA, Tadaoki MITANI, Yusei MARUYAMA, and Sadamu TAKEDA** *(Osaka Univ.)*

Since some of the salicylideneaniline derivatives have been found to have rather low ionization potential, they have been employed as a donor component of charge transfer complexes. There is a clear relationship between the charge transfer energy and the equilibrium position of the proton in the O-H···N hydrogen bond. The NH and OH forms are obtained when the charge transfer energy is high, while the intermediate form is observed when the energy is low. In the latter case, the coupling between the proton motion and conduction electrons is expected to lead a novel type of electrical properties.

IV-F-4 Charge Transfer Complexes with Intermolecular Hydrogen-Bonds

Tamotsu INABE, Hironori OGATA, Kaoru OKANIWA, Hiroshi OKAMOTO, Tadaoki MITANI, and Yusei MARUYAMA

In order to examine the possibility of coupling between the proton motion and conduction electrons in the intermolecular hydrogen-bond systems, charge transfer complexes of aromatic amines have been prepared and subjected to structural, electrical, magnetic, and optical studies. The donors employed so far are 1,6-pyrenediamine, 3,3′,5,5′-tetramethylbenzidine, and 3,3′-dimethylbenzidine, and the acceptors are derivatives of *p*-benzoquinone and derivatives of TCNQ. All complexes structurally studied have a hydrogen-bond network in the lattice. Depending on the donor-acceptor combination, and on the crystal morphology, the complexes show a variety of charge transport behaviors. A systematic study of these complexes, including solid-state NMR, is now under way.

IV—G Ultra-Thin Organic Film Systems Prepared by Molecular Beam Epitaxy (MBE) Technique

As a strategy for the development of new types of organic materials, we have undertaken the fabrication of ultra-thin organic multi-layer systems with the use of an "MBE" technique. We are expecting new types of charge transfer compounds and/or intercalation compounds (hybrid compounds), and also the realization of novel 2-dimensional materials in such systems. We have prepared ultra-thin well-oriented phthalocyanine films on alkali halide single crystal substrates.

IV-G-1 Epitaxial Growth of Chloroaluminum and Vanadyl Phthalocyanine Films on Alkali Halide Single Crystals by the Molecular-Beam-Epitaxy Technique

Hajime HOSHI and Yusei MARUYAMA

[*J. Appl. Phys.* **69**, 3046 (1991)]

Epitaxial chloroaluminum and vanadyl phthalocyanine (AlPcCl and VOPc) films have been prepared on alkali halide (100) surfaces by the molecular-beam-epitaxy technique. Their structures have been studied by scanning electron microscopy and transmission electron microscopy. The films consist of densely packed crystallites and seem to be continuous. The predominant phase of AlPcCl/NaCl is newly found bidirectionally oriented tetragonal, NaCl(100)($\sqrt{13}\times\sqrt{13}$)*R* 11°-AiPcCl. The phase of AlPcCl/KCl and AlPcCl/KBr is bidirectionally oriented tetragonal, KCl(100)($\sqrt{10}\times\sqrt{10}$)*R* 27°-AlPcCl and KBr(100)($\sqrt{10}\times\sqrt{10}$)*R* 27°-AlPcCl, respectively. The predominant phase of AlPcCl/KI is unidirectionally oriented tetragonal, KI(100)(3×3)*R* 45°-AlPcCl. The phase of VOPc/KCl is bidirectionally oriented tetragonal, KCl(100)($\sqrt{10}\times\sqrt{10}$)*R* 27°-VOPc, while that of VOPc/KBr is unidirectionally oriented tetragonal, KBr(100)(3×3)*R* 45°-VOPc. The preferential epitaxial latice orientation is discussed based on the degree of lattice matching between phthalocyanine and substrates.

IV-G-2 Second and Third Harmonic Generations in Ultrathin Phthalocyanine Films Prepared by the Molecular Beam Epitaxy Technique

Hajime HOSHI, Naoki NAKAMURA *(Toyota Motor Corp. and IMS)*, **and Yusei MARUYAMA**

[Submitted to *J. Appl. Phys.*]

Second and third harmonic generations in ultrathin (200 Å) films of fluoro-bridged aluminum phthalocyanine polymer have been observed in the geometry of Maker fringe experiment using Nd:YAG laser fundamental light. Two types of films, single-crystalline and polycrystalline films, with different orientations grown by the molecular-beam epitaxy technique have been used. Observed dependence of the generated second and third harmonic intensities on the polarization of light and the angle of incidence is discussed based on the symmetry of the film structures. Enhancement of the harmonic intensities is realized in the single-crystalline film.

IV—H Novel Molecular System C_{60}: Fullerites and Fullerides

After the discovery of superconductivity in potassium doped C_{60} films, much attention has been attracted to the versatility of solid state C_{60} (Fullerite). In this research project, the micro-structural and optical properties of fullerite films prepared by the MBE technique, and the electrical properties of the doped films and single crystals are studied.

IV-H-1 Visible, UV, and VUV Absorpiton Spectra of C_{60} Thin Films Grown by the Molecular-Beam Epitaxy (MBE) Technique

Yohji ACHIBA *(Tokyo Metropol. Univ.)*, **Takashi NAKAGAWA** *(Tokyo Metropol. Univ.)*, **Shinzo SUZUKI** *(Tokyo Metropol. Univ.)*, **Haruo SHIROMARU** *(Tokyo Metropol. Univ.)*, **Kotaro YAMAUCHI** *(Tokyo Metropol. Univ.)*, **Kozaburo NISHIYAMA** *(Tokyo Metropol. Univ.)*, **Masatsune KAINOSHO** *(Tokyo Metropol. Univ.)*, **Hajime HOSHI, Yusei MARUYAMA, and Tadaoki MITANI**

[*Chem. Lett.* **1991**, 1225]

On single-crystal alkali halide substrates, the C_{60} film prepared by the MBE technique shows a new band in visible wavelength region. The absorption spectrum of the C_{60} film has been extended to vacuum UV region, and several new bands and/or humps were found for the first time.

IV-H-2 Optical Second- and Third-Harmonic Generations in C_{60} Film

Hajime HOSHI, Naoki NAKAMURA *(Toyota Motor Corp. and IMS)*, **Yusei MARUYAMA, Takashi NAKAGAWA** *(Tokyo Metropol. Univ.)*, **Shinzo SUZUKI** *(Tokyo Metropol. Univ.)*, **Haruo SHIROMARU** *(Tokyo Metropol. Univ.)*, **and Yohji ACHIBA** *(Tokyo Metropol. Univ.)*

[*Jpn. J. Appl. Phys.* **30**, L1397 (1991)]

Optical second- and third-harmonic generations in C_{60} film have been studied using an Nd:YAG laser as the fundamental light source. Observed dependences of the generated second- and third-harmonic intensities on the polarization of light and on the angle of incidence are discussed based on the symmetry of the film structure. The relatively large third-order nonlinear response of $|\chi^{(3)}(-3\omega;\ \omega,\ \omega,\ \omega)|=2\times10^{-10}$ esu is obtained.

IV-H-3 STM Image of C_{60} Monomolecular Films on an HOPG

Yoshihisa MORI, Hajime HOSHI, Yusei MARUYAMA, Yohji ACHIBA *(Tokyo Metropol. Univ.)*, **Shinzo SUZUKI** *(Tokyo Metropol. Univ.)*, **and Haruo SHIROMARU** *(Tokyo Metropol. Univ.)*

Unidirectionally oriented one-dimensional arrays of C_{60} molecules are clearly observed in the STM images of submonomolecular films prepared by the MBE technique. This fact is suggesting the epitaxial growth of the C_{60} film on graphite (HOPG) due to fairly strong interaction between them. A possible model for epitaxial accommodation is discussed.

IV-H-4 Electrical Properties of Alkali-Metal Doped C_{60} Films and Single Crystals

Yusei MARUYAMA, Tamotsu INABE, Hironori OGATA, Hajime HOSHI, Yohji ACHIBA *(Tokyo Metropol. Univ.)*, **Shinzo SUZUKI** *(Tokyo Metropol. Univ.)*, **Koichi KIKUCHI** *(Tokyo Metropol. Univ.)*, **and Isao IKEMOTO** *(Tokyo Metropol. Univ.)*

The processes of alkali-metal doping into C_{60} films or single crystals have been studied by monitoring the resistivity in situ. The K-doped films and single crystals, of which doping level has been optimized by this method, have been found to show the superconducting transition. The Rb- and Cs-doping have also made the materials highly conducting. Preparation of the materials which have the optimum doping levels and the measurements of the temperature dependence of the resistivities are now under way.

IV—I Black Phosphorus

Black phosphorus is a layered structure semiconductor. We have prepared iodine intercalated compounds of black phosphorus and revealed their metallic character. Recently, inclusion or doping of silicon or germanium to black phosphorus has been undertaken.

IV-I-1 Electrical Conductivity of Black Phosphorus-Germanium Compound

Yusei MARUYAMA, Tamotsu INABE, Lin HE *General Institute for Colored Metal, Beijing, and IMS)*, **and Kokichi OSHIMA** *(Okayama Univ.)*

[*Synth. Met.* **41-43**, 4067 (1991)]

Single crystals of a new material, black phosphorus doped with germanium, have been prepared by a bismuth-flux method. Germanium atoms are incorporated into the black phosphorus in 2 to 4 atomic percent. The resistivity is reduced by two to three orders ($\rho = 6\times10^{-3}$ Ωcm) compared with the pure black phosphorus, and its temperature dependence is metallic at low temperatures. There is no magnetoresistance up to 12 T at 0.6 K in striking contrast to the pure black phosphorus which shows negative magnetoresistance in this region. The crystal lattice constants decrease with germanium doping, especially in the interlayer direction. These facts indicate the enhanced 3-dimensionality with germanium doping.

IV-J Preparation and Characterization of Copper Oxide High T_c Superconductor Films

After the discovery of novel high T_c superconductors, a lot of works including the film preparation have been carried out. We have carried out to fabricate thin films of such superconductors by a sputtering method and an electron-beam evaporation technique with the purpose of searching for new composition, structures, and elements in high T_c superconductors.

IV-J-1 La-Sr-Cu-O Superconducting Thin Films Preparation by MBE with Multi Electron-Beam Gun Sources

Toshifumi TERUI, Tamotsu INABE, and Yusei MARUYAMA

The objective of this project is to fabricate La-Sr-Cu-O superconducting films with artificially controlled layer-by-layer deposition technique. In a high vacuum vessel three electron-beam guns are equipped and controlled by a computer independently.

IV—K STM/STS Study on Electronic Structures of Some Superconductors

Scanning tunneling microscopy (STM) and spectroscopy (STS) are very useful and direct methods to study the electronic structures of electrical conductors. We are focusing to investigate site-selective superconducting gap structures of organic or copper oxide superconductors. The system for room temperature STM/STS has been set up, and a low temperature system is now under construction.

IV-K-1 Electronic Structure of (BEDT-TTF)$_2X$ Salts Studied by Scanning Tunneling Spectroscopy

Yoshihisa MORI, Yusei MARUYAMA, Hatsumi MORI *(ISTEC),* **and Gunzi SAITO** *(Kyoto Univ.)*

[*Jpan. J. Appl. Phys.* **30**, L358 (1991)]

Two-dimensional arrangements of molecular images by Scanning Tunneling Microscopy are observed for some (BEDT-TTF)$_2X$ salt crystals, and moreover Scanning Tunneling Spectroscopy has clearly revealed the two-dimensional electronic structure of such crystals.

IV—L Photoelectron Spectroscopy of Organic Solids in Vacuum Ultraviolet Region

The work of ultraviolet photoelectron spectroscopy (UPS) combined with synchrotron radiation light source (UVSOR)-(UVSOR-UPS)- of organic solids and graphite compounds has been proceeded to find their quantitative electronic structures.

IV-L-1 UPS of New Type Polyacetylene

Koji KAMIYA*, Hiroo INOKUCHI, Masato OKU*, Shinji HASEGAWA, Chizuko TANAKA*, Jiro TANAKA*, and Kazuhiko SEKI* *(*Nagoya Univ.)*

[*Synth. Met.* **41-43**, 155 (1991)]

We measured the ultraviolet photoemission spectra of new type polyacetylene(N-PA) synthesized by methods of Naarmann or Tsukamoto. The spectra are measured with photon of 40 eV energy by incident angle of 50° at UVSOR of IMS.

The spectra are measured for both neat (cis content is 90%) and trans films, the latter is obtained by thermal isomerization of neat film. The observed spectra are compared with the calculated energy levels of model compounds.

The change of spectra with doping by perchlorate ion are illustrated in Figure 1, where the dopant level is monitored by the conductivity measurement. In the series of spectra, several stages of structural changes are found. The spectral feature of cis-PA is retained at the initial stage ((a) and (b) in Figure 1.). The intensity of the top band is decreased even at conductivity of 1600 S/cm ((c) and (d)). The spectra changed to new form by further doping to the conductivity of 8100 S/cm. Finally a Fermi level is clearly observed for the film of the conductivity of 11000 S/cm (f), where the concentration of the perchlorate ion is about 8%.

Appearance of DOS near the Fermi level is shown in Figure 2 by expanded scale for each curves of Figure 1. Here E_F is the Fermi edge measured for gold. The curve Figure 2 (f) definitely shown that a genuine metallic state is formed in the high conductive N-PA.

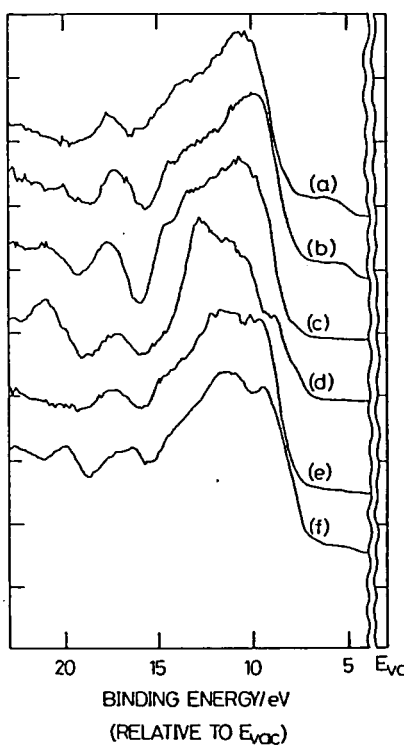

Figure 1. Change of UPS by perchlorate doping. (a) cis-PA (b) σ =1.4 S/cm (c) σ =170 S/cm (d) σ =1600 S/cm (e) σ =8100 S/cm (f) σ =11000 S/cm (8%).

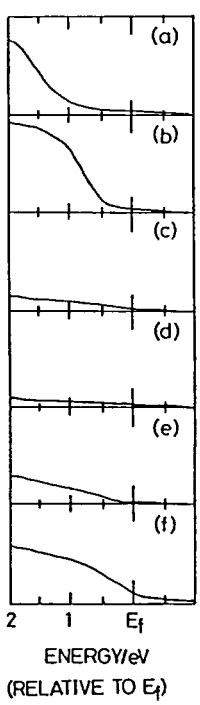

Figure 2. UPS of Figure 1 by extended scale near E_F. Here E_F indicates the Fermi edge for a metal.

IV-L-2 Nature of the Temperature Dependence of Conduction Bands in Polyethylene

Nobuo UENO*, Kazuhiko SEKI, Kazuyuki SUGITA*, and Hiroo INOKUCHI** *(*Chiba Univ., **Nagoya Univ.)*

[*Phys. Rev.* **B43**, 2384 (1991)]

The secondary-electron-emission (SEE) spectra of thin films of four types of polyethylene with different crystallinities were measured as a function of temperature. Further, the spectral changes due to melting of the films were measured. The temperature dependence of the spectra showed pronounced difference from that of n-$C_{44}H_{90}$, a model compound of crystalline parts of polyethylene. Polyethylene showed a large temperature dependence of the conduction bands even far below the melting point, while n-$C_{44}H_{90}$ underwent a sharp change at the melting point due to the phase transition. Comparison between the temperature dependences of the SEE spectra and those of X-ray diffraction patterns reveals that the large temperature dependence of the conduction bands of polyethylene is the result of the two-phase structure, a coexistence of crystalline parts and amorphous parts. Present results point out that the electronic stats of polymeric solids with two-phase structures depend strongly on temperature, which should be taken into account in analyzing the temperature dependences of their carrier-transport properties.

IV-L-3 Angle-resolved Photoemission Study of Nonsuperconductive $Bi_2Sr_2Ca_{0.4}Y_{0.6}Cu_2O_8$

Takashi TAKAHASHI*, Hiroyoshi MATSUYAMA*, Hiroshi KATAYAMA-YOSHIDA*, Kazuhiko SEKI, Koji KAMIYA, and Hiroo INOKUCHI** *(*Tohoku University, **Nagoya University)*

[*Physica* **C170**, 416 (1990)]

A comparative angle-resolved photoemission measurement has been performed on nonsuperconductive $Bi_2Sr_2Ca_{0.4}Y_{0.6}Cu_2O_8$ and superconductive $Bi_2Sr_2CaCu_2O_8$ to study the nature and the origin of the electronic states near the Fermi level. It was found that the hole-doping does not cause a rigid shift of the density of states relative to the Fermi level but creates new electronic states in the vicinity of the Fermi level.

IV-L-4 Angle-resolved Photoemission Study of $Bi_2Sr_2Ca_{1-x}Y_xCu_2O_8$ (x=0.0, 0.2, 0.4, 0.6) Single Crystals

Toshiaki KUSUNOKI*, Takashi TAKAHASHI*, Shigeru SATO*, Hiroshi KATAYAMA-YOSHIDA* Koji KAMIYA, and Hiroo INOKUCHI *(*Tohoku University)*

[*Physica C*, to be published in M^{2}S-HTSC-III Proceedings, Kanazawa]

Angle-resolved photoemission measurements were performed on a series of $Bi_2Sr_2Ca_{1-x}Y_xCu_2O_8$ (x=0.0, 0.2, 0.4, and 0.6) single crystals. It was found that the hole-doping in an insulator (x=0.6) produces new electronic states in the charge-transfer gap and the density of new states gradually increases with the hole-concentration. In the "overdoped" region (x=0.0 and 0.2), where the superconductivity is suppressed by the excess carriers, a slight rigid shift of the bands crossing the Fermi level was observed. This suggests that a band picture may be recovered once the Fermi-liquid-like states are formed at the Fermi level.

IV-L-5 Photoemission Study of C_{60} and Its Alkali-Metal Compounds

Takashi TAKAHASHI[1], Takashi MORIKAWA[1], Shigeru SATO[1], Hiroshi KATAYAMA-YOSHIDA[1], Akira YUYAMA[2], Kazuhiko SEKI[2], Hitoshi FUJIMOTO[3], Shojun HINO[4], Shinji HASEGAWA, Koji KAMIYA, Hiroo INOKUCHI, Koichi KIKUCHI[5], Sinzo SUZUKI[5], Isao IKEMOTO[5], and Yohji ACHIBA[5] *([1]Tohoku University, [2]Nagoya University, [3]Kumamoto University, [4]Chiba University, [5]Tokyo Metropolitan University)*

[*Physica C*, to be published in M^{2}S-HTSC-III Proceedings, Kanazawa]

We report photoemission study of solid C_{60} and its alkali (K and Rb)-metal compounds. Photoemission spectra were measured during continuous deposition of alkali (K or Rb) metal on an evaporated C_{60} film. We studied the correlation between the photoemission spectra of the film and its electrical property by monitoring the resistivity of a film placed just next to the photoemission sample. The valence-band photoemission spectrum of C_{60} shows a rich structure reflecting its molecular property. Upon alkali-metal doping, the photoemission spectrum exhibits a unique change which is not explained in terms of a simple rigid band-filling. The valence band is shifted as a whole at first toward the high-binding-energy direction by 0.2—0.3 eV and the resistivity of the film gradually decreases. Further doping produces broad electronic states spreading from E_F to the HOMO (Highest Occupied Molecular Orbital) band with a clear Fermi-edge. While the density of electronic states at E_F increases with the further alkali-metal doping, the HOMO band again moves back to E_F. When the resistivity of the film reaches the minimum, the density of states at E_F becomes the maximum and the HOMO band approaches closest to E_F. Further deposition of K or Rb causes an increase of the resistivity of the film. Although this further deposition increases the intensity of the "new band" near E_F, it brings about a rigid shift of the bands toward the high-binding-energy direction. This results in decrease of the density of states at E_F and finally the states at E_F completely disappears, showing that the film becomes insulator (K_6C_{60} or Rb_6C_{60}).

IV—M Electrical Conduction and its Related Properties of Organic Solids

As new type single component organic semiconductor, the electronic properties of bis[1,2,5]thiadiazolo-p-quinobis(1,3-dithiole) (BTQBT) and its related compound has been observed.

IV-M-1 On Charge Carrier Photogeneration Mechanisms in Organic Molecular Crystals

Edgar A. SILINSH* and Hiroo INOKUCHI *(*Inst. Physics and Energetics, Latvian Acad. Sci.)*

[*Chem. Phys.* **149**, 373 (1991)]

Photoconductivity spectra characteristics in polyacene crystals are reported which may be interpreted in terms of two possible autoionization mechanism. It is shown that the step-like character of the spectral dependence of the photogeneration activation energy E_a^{ph} ($h\nu$) allows the determination of the dominant autoionization mechanism in a given spectral range, while the structure of the intrinsic photoconductivity quantum efficence $\eta(h\nu)$ curves indicates the energy values at which the excitation from lower-lying valence levels begin to switch on. The relaxation kinetics of both competitive autoionization channels are discussed.

IV-M-2 Crystal Structures and Electrical Conductivities of TXC_n-TTF (X=Sulfur, Selenium, Tellurium; n=2,3) · TCNQ Charge-Transfer Complexes

Kenichi IMAEDA, Takehiko MORI, Chikako NAKANO, Hiroo INOKUCHI, Naoko IWASAWA*, and Gunzi SAITO* *(*Univ. of Tokyo)*

[*Bull. Chem. Soc. Jpn.* **64**, 2159 (1991)]

The crystal structures and the electrical conductivities have been studied for tetrakis(alkylchalcogeno)tetrathiafulvalene (TXC_n-TTF (X=sulfur, selenium, tellurium; n=2,3)) complexes with tetracyanoquinodimethane (TCNQ). All the complexes with a composition of 1:1 had the same crystal system (triclinic) and the same space group ($P\bar{1}$). The donor and acceptor molecules were alternately stacked in their crystals. ($TSeC_2$-TTF)TCNQ was obtained as plate and needle crystals. The molecular structure of $TSeC_2$-TTF and the overlapping mode between $TSeC_2$-TTF and TCNQ molecules of the two complexes were subtly different. All the complexes were semiconductors because of their mixed-stack structures. ($TTeC_2$-TTF)TCNQ showed the lowest resistivity (5 Ωcm at room temperature). Its good conductivity was brought about by the effective degree of charge-transfer and the favorable overlap between $TTeC_2$-TTF and TCNQ molecules. An overall discussion on the structural and physical properties of a series of TCNQ complexes with TXC_n-TTF (X=sulfur, selenium, tellurium; n=1,2,3) is presented.

IV-M-3 Hall Effect Observation in New Organic Semiconductor Bis[1,2,5]thiadiazolo-*p*-quinobis(1,3-dithiole) (BTQBT)

Kenichi IMAEDA, Yoshiro YAMASHITA, Yongfang LI, Takehiko MORI, Hiroo INOKUCHI, and Mizuka SANO *(International Christian Univ.)*

[*J. Mater. Chem.*, in press]

Single crystals of bis[1,2,5]thiadiazolo-*p*-quinobis(1,3-dithiole) (BTQBT) were grown by the methods of recrystallization from a nitrobenzene solution and sublimation in nitrogen atmosphere. The electrical resistivities are 1.2×10^3 Ωcm and 2.7×10^5 Ωcm at room temperature for a crystal grown by recrystallization and that obtained by sublimation, respectively. These values are noticeably low for the value of a single-component organic crystal. In addition, the BTQBT crystals have a small anisotropy in resistivity ($\rho_\perp/\rho_\parallel$~2), which is ascribed to strong intermolecular interactions inherent in the crystal structure. They show a Hall effect which is an unusual observation in organic semiconductors. The sign of carriers was determined to be positive and the Hall mobility was found to be ca. 4 $cm^2V^{-1}s^{-1}$ at room temperature. (See page 117.)

IV-M-4 Thermal Properties of Tetrakis(Alkyltelluro)Tetrathiafulvalene ($TTeC_n$-TTF)

Jeremiasz K. JESZKA*, Toshiaki ENOKI, Zurong SHI, Kenichi IMAEDA, Hiroo INOKUCHI, Naoko IWASAWA, Hideki YAMOCHI**, and Gunzi SAITO**** *(*Center of Mol. and Macromol. Sci., Polish Acad. Sci., **ISSP)*

[*Mol. Cryst. Liq. Cryst.* **196**, 167 (1991)]

Thermal properties of $TTeC_n$-TTF are investigated using DSC technique. It is shown that combining tellurim substituted TTF skeleton with the alkylchains of different length we obtained a variety of thermal properties due to a competition between alkyl chains and the TTF moiety. This competition leads to a polymorphism and to an irregular dependence of the melting point as well as enthalpy and entropy of melting, on the alkyl chain length between the carbon number n=4 and 7. For the copounds with long alkyl chains (n>6) the analysis of thermodynamic properties confirms the existence of the molecular fastener effect, i.e. fastening of the TTF skeletons and decreasing of the distances between them in the crystal structure by crystallization of the long alkyl chains.

IV-M-5 Phase Transion of Tetrakis(octylthio)tetrathiafulvalene(TTC_8-TTF) and Crystal Structure Analysis

Chikako NAKANO*, Kenichi IMAEDA, Takehiko MORI, Yusei MARUYAMA, Hiroo INOKUCHI, Naoko IWASAWA, and Gunzi SAITO***** *(*Toyota Physical and Chemical Research Inst., and IMS, **ISSP, ***Kyoto Univ.)*

[*J. Mater. Chem.* **1**, 37 (1991)]

Tetrakis(octylthio)tetrathiafulvalene(TTC_8-TTF) crystallizes into two different phases (Form I and Form II). Form I undergoes a slightly endothermic, phase transition at ca. 33°C with a steep increase in the resistivity and a decrease in the drift mobility. Powder X-ray diffraction confirms that this transion is the result of a structural transition from Form I to Form II. The microscopic origin of the phase transition is ascribed to a subtle repulsive motion in the nearest-neighboring π-electron moieties of TTC_8-TTF molecules within a segregated column.

IV-M-6 Structural Study of the Two Phases of Tetrakis(methylseleno)tetrathiafulvalene ($TSeC_1$-TTF)

Chikako NAKANO*, Ping WANG, Takehiko MORI, Yusei MARUYAMA, Hiroo INOKUCHI, Hideki YAMOCHI, and Gunzi SAITO**** *(*Toyota Physical and Chemical Research Inst., and IMS, **Kyoto Univ.)*

[*Bull. Chem. Soc. Jpn.*, in press]

The crystal structure of the low-melting point phase (L-phase) of a single component organic semiconductor, $TSeC_1$-TTF, is determined and compared with that of the high-melting point phase (H-phase). The intracolumnar overlap mode and the calculated intermolecular overlap integrals are slightly larger in the L-phase, to which is ascribed the low resistivity of the L-phase. The L-phase, however, does not have two-dimensional networks of intercolumnar Se···Se contacts, which exist in the H-phase. This may be associated with the difference of the melting points.

IV-M-7 Crystal Structures of TXC_8-TTF(X=Se,Te)

Chikako NAKANO*, Ping WANG, Kenichi IMAEDA, Yusei MARUYAMA, Hiroo INOKUCHI, Hideki YAMOCHI, and Gunzi SAITO**** *(*Toyota Physical and Chemical Research Inst., and IMS, **Kyoto Univ.)*

[Submitted to *Bull. Chem. Soc. Jpn.*]

The crystal structures of $TSeC_8$-TTF and $TTeC_8$-TTF are determined by X-ray analysis. The molecules in both compounds have chair-like forms and take columnar structures. The distance between the least square planes of the central skeleton along the stacking axis in the $TSeC_8$-TTF crystal is nearly equal to that of the $TTeC_8$-TTF crystal. This result is consistent with the fact that the electrical resistivities for both single crystals are in the same order.

IV-M-8 Crystal Structures and Molecular Packing of TTC_8-TTF(n=3,4,6,7,9,11).

Chikako NAKANO*, Takehiko MORI, Kenichi IMAEDA, Yusei MARUYAMA, Hiroo INOKUCHI, Naoko IWASAWA, and Gunzi SAITO***** *(*Toyota Physical and Chemical Research Inst., and IMIS, **ISSP, ***Kyoto Univ.)*

[Submitted to *Bull. Chem. Soc. Jpn.*]

The crystal structures of TTC_n-TTF were determined by X-ray structure analysis. The TTC_3-TTF molecule has a boat-like shape like TTC_1-TTF and TTC_2-TTF. The structure of TTC_n-TTF drastically changes between n=3 and 4. TTC_4-TTF and TTC_6-TTF molecules have chair-like shapes like TTC_5-TTF and columnar structures. These alkyl chains elongate nearly perpendicular to the central skeleton (Form III). The structures of TTC_n-TTF with long alkyl chain ($7 \leqq n \leqq 11$) can be divided into two different groups (Form I and Form II), according to the packing manner of the alkyl chains. The TTC_7-TTF crystals have only Form II structures (the triclinic phase and the monoclinic phase). TTC_9-TTF crystallizes in the two different forms: Form I (the triclinic phase) and Form II (the monoclinic phase). The TTC_{11}-TTF crystal takes only Form I structure. Although the molecules in both forms have chair-like shapes (the alkyl chains are largely bent to the C_6S_8 skeleton), the chains in the Form I crystals are arranged parallel to each other to make more strongly fastened packing than those in the Form II crystals. These results are associated with the change of the electrical resistivities and activation energies of TTC_n-TTF crystals.

IV—N Organic Metals

In an attempt to develop new organic superconductors and to explore the related phenomena, new organic conductors have been prepared and their structural and physical properties have been investigated. A new organic superconductor $(BEDT\text{-}TTF)_4Pt(CN)_4H_2O$ has been found, and its structural and physical properties have been investigated.

IV-N-1 Synthesis, Structure and Electrical Properties of $Ag_{1.2}$(2,5-dimethylthio-*N,N*-dicyanoquinonediimine)

Takehiko MORI and Hiroo INOKUCHI

[*Chem. Lett.* **1990**, 2077]

Several new DCNQI's (*N,N*-dicyanoquinonediimines) with methilthio groups are synthesized. One of their silver salts, the title compound, is metal down to 188 K. In this salt, a part of Ag atoms are coordinated by the S and the inner N atoms.

IV-N-2 Band Structure and Fermi Surface of Organic Conductors

Takehiko MORI and Hiroo INOKUCHI

[*Synth. Met.* **42**, 2447 (1991)]

The density of states $N(E_F)$ of isostructural organic conductors $(BEDT\text{-}TTF)_2MHg(SCN)_4$ (M = K, Rb, and NH_4) is investigated by means of band calculation, the measurements of thermoelectric power, magnetic susceptibility, and low-temperature electronic specific heat. Though the change of the unit cell volume is as small as 0.6%, $N(E_F)$ estimated from the band calculation changes by 8%. The change of experimentally observed $N(E_F)$ is further enhanced to 70%, due probably to the electron-electron interaction. The correlation of $N(E_F)$ and the superconducting transition temperature T_c is discussed.

IV-N-3 Superconductivity in $(BEDT\text{-}TTF)_4Pt(CN)_4H_2O$

Hatsumi MORI*, Izumi HIRABAYASHI*, Shoji TANAKA*, Takehiko MORI, Yusei MARUYAMA, and Hiroo INOKUCHI *(*ISTEC)*

[*Synth. Met.*, in press]

New organic conductors $(BEDT\text{-}TTF)_4M(CN)_4H_2O$ (M=Pt and Ni) show broad metal-insulator transitions around 100 K, but the increase of resistivity at low temperature is very small ($R(1.5K)/R(rt)<10$). By suppressing

the transition, superconductivity in the Pt salt is observed at 2 K under 6.5 kbar. The crystal structure and electrical resistivities of the Pt and Ni salts are reported.

IV—O Electron Transport in Cytochromes

IV-O-1 pH and Temperature Effects on the Absorption Spectra of *Pseudomonas aeruginosa* Cytochrome *c*-551 Solution

Yongfang LI, Kenichi IMAEDA, and Hiroo INOKUCHI

The temperature dependence of the absorption spectra of aqueous solutions of ferricytochrome *c*-551 from *Pseudomonas aeruginosa* was investigated in the temperature range 20—80 °C at different pH values. The spectral change by the temperature strongly depended on the pH of the solution. For the neutral or acidic solution, the absorbance at 695 nm decreased and that at 620 nm increased with increasing temperature. This spectral change was suggested to be the transition from low-spin state to high-spin state. For the alkaline solution, the 551 nm and 521 nm bands which are characteristic of ferrocytochrome *c*-551, newly appeared and became stronger and stronger when the temperature was increased. This spectral change based on the oxidation-state change was speculated to result from the chemical bond-cleavage between heme ion and methionine sulfur followed by combination of OH^- ion with heme iron. The pH-temperature phase diagram for 695 nm and 620 nm bands is presented.

IV—P Physics and Chemistry of Graphite and its Intercalation Compounds

IV-P-1 Three-dimensional Positron-electron Momentum Distribution Single-crystal Graphite

Ikuzo KANAZAWA*, Shoichiro TANIGAWA, Ryoichi SUZUKI**, Mizuka SANO***, and Hiroo INOKUCHI** *(*Tokyo Gakugei Univ., **Univ. of Tsukuba, ***Kumamoto Univ.)*

[*Phys. Rev.* **B42**, 583 (1990)]

Three-dimensional positron-electron momentum distribution in single-crystal graphite is determined from the reconstruction of the measured two-dimensional angular corelation of positron annihilation. The Lock-Crisp-West rate obtained through periodic superposition of the experimentally determined momentum density is compared with theoretical rate calculated on the basis of linear combination of atomic orbitals X_α by Saito et al. (Synth. Met. *23*, 217 (1988)).

RESEARCH ACTIVITIES V
Department of Applied Molecular Science

V—A New Multi-Stage Redox Systems

Interdisciplinary cooperation between synthetic chemistry, physical chemistry, and solid state physics has opened a new field of science which can explore molecular materials having interesting electrical, magnetic, and optical properties in the solid state. In general, molecular level correlations of physical properties between molecules and the solid state are essential to construct new molecular materials. Such a consideration into highly electrically conducting behaviors reveals the importance of conjugated electronic systems having multi-stage redox nature, which can transfer electrons smoothly by multi-stage manners. We have designed and synthesized two classes of new multi-stage redox systems, such as peri-condensed Weitz type donors and amphoteric multi-stage redox systems. The peri-condensed Weitz type redox systems are designed by replacing two of the sp^2 carbon atoms in a polycyclic arene by two sulfur atoms. Such heterocycles have produced new organic molecular metals which contain non-TTF and non-TCNQ type components. The amphoteric multi-stage redox systems are designed so as to decrease the difference between the oxidation and the reduction potentials of a molecule. We have already reported the synthsis and properties of conjugated hydrocarbons with the highest amphotericity. Design and synthesis of new types of multi-stage redox systems, and investigations of their physical and solid state properties are actively continued.

V-A-1 Synthesis and Properties of 1,6-Diselenapyrene (DSPY)

Takeshi OHMAE, Yasushi MORITA, Jiro TOYODA, Kazuhiro NAKASUJI, Shotaro MATSUDA,[a] and Fumio TODA[a] *([a]Ehime Univ.)*

Peri-condensed Weitz-type donors, such as dithiaperylene (DTPR) and dithiapyrene (DTPY) containing sulfur atoms in the conjugated systems, have produced a variety of organic conductors ranging from semiconductors to molecular metals. We reported the synthesis of one of the isomers of DTPY, 1,6-DTPY, and three isomers of DTPR, 3,10-, 1,7-DTPR, and 3,9-DTPR. One of the known procedure increasing the dimensionality of electronic structure for charge transfer complexes is the replacement of sulfur atoms into selenium atoms. In this study, a selenium analogue of 1,6-DTPY, 1,6-diselenapyrene (1,6-DSPY), was prepared. The synthetic route is almost same as that of 1,6-DTPY. The oxidation potentials are 0.37 and 0.84 eV vs. SCE, therefore, the new donor also shows the two stage redox nature with relatively strong donor property.

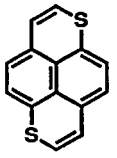

DTPY

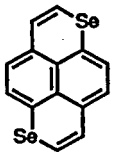

DSPY

V-A-2 The Crystal Structure and Physical Properties of the 3:2 Charge Transfer Complex of Bis(ethylenedithio)dithiapyrene (ETDTPY) and Dibenzobarrelenotetracyanoquinodimethane (DBBTCNQ)

Jiro TOYODA, Kazuhiro NAKASUJI, Tomoyuki KOTANI,[a] Ichiro MURATA,[a] Atsushi KAWAMOTO,[b] and Jiro TANAKA[b] *([a]Osaka Univ., [b]Nagoya Univ.)*

[*Chem. Lett.*, 1237 (1991)]

The V-shape correlation between $h\nu_{CT}$ and $\Delta E^{o,r}$ of the charge transfer complexes is convenient to judge the gross features of the solid state properties. Using this correlation, we found the 3:2 charge transfer complex of bis(ethylenedithio)dithiapyrene (ETDTPY) and dibenzobarrelenotetracyanoquinodimethane (DBBTCNQ) which showed an unique crystal structure. The peri-condensed Weitz-type donor, ETDTPY, is designed so as to increase the number of chalcogen sites responsible for interstack interactions in the solid state, like bis(ethylenedithio)tetrathiafulvalene (BEDT-TTF). The single crystals of the CT complex, $(ETDTPY)_3(DBBTCNQ)_2$, were prepared as black needles by slow evaporation by standing of a solution of the donor and the acceptor. The donor molecules form the trimeric stacks to avoid the steric repulsion between the nonplanar and bulky ethylenedithio moieties. The acceptor molecules form the dimeric stacks. The trimeric and the dimeric stacks pack alternately along the [110] direction. Therefore, this complex is characterized as the columnar structure of the alternating trimeric stack of the donor and dimeric stack of the acceptor.

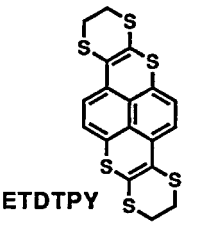

ETDTPY

DBBTCNQ

V-A-3 Crystal Structure of an Alternated Stacking Charge Transfer Complex of 2,7-Bis(methylthio)-1,6-dithiapyrene (MTDTPY) with Tetracyanoquinonaphthodimethane (TNAP)

Jiro TOYODA, Atsushi KAWAMOTO,[a] Jiro TANAKA,[a] and Kazuhiro NAKASUJI *([a]Nagoya Univ.)*

Recently, we have reported that 2,7-bis(methylthio)-1,6-dithiapyrene (MTDTPY) produces the metallic conducting charge transfer (CT) complexes with tetracyanoquinodimethane (TCNQ), chloranil, and bromanil. An extended

conjugated type acceptor of TCNQ, tetracyanonaphthoquinodimethane (TNAP), is known to have stronger acceptor ability than TCNQ. Although our efforts to prepare metallic CT complexes with TNAP have not been established so far, an alternated stacking mode of complex, MTDTPY-TNAP, was obtained as black needles. No special shorter intermolecular heteroatom contacts were found. The ionicity of the complex was determined as non-ionic by known procedures using IR and solid state electronic spectra.

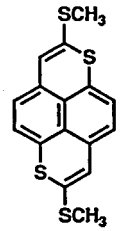

2,7-MTDTPY

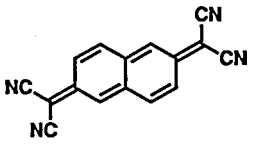

TNAP

V-A-4 Adoption of β-Structure Packing Type with Linear Ribbon Mode in Condensed Sulfur-Heterocycles

Jiro TOYODA, Atsushi KAWAMOTO,[a] Jiro TANAKA,[a] and Kazuhiro NAKASUJI *([a]Nagoya Univ.)*

Importance of crystal engineering has increased because of need in design of new molecular materials having interesting chemical reactivities and physical properties in the solid state. Recently, the crystal structures of the condensed aromatic hydrocarbons are classified into four packing types and the prediction of packing type is proposed on the basis of the structural formula. As an essential expansion of such a prediction method, we studied the crystal structure of 3,9-dithiaperylene and found the adoption of β-structure packing type with linear ribbon mode for the basic condensed sulfur-heterocycles. This is a first typical example of steering the packing type of the condensed aromatic hydrocarbons to the β-structure by exchange sp^2 carbon atoms into sulfur atoms.

V-A-5 Synthesis of a Highly Amphoteric *s*-Indaceno[1,2,3-*cd*:5,6,7-*c*′d′]diphenalene: Switching between Diatropism and Paratropism Due to Changes in Oxidation Level

Ichiro MURATA,[a] Shigeru, SASAKI,[a] Kay-Uwe KLABUNDE,[a] Jiro TOYODA, and Kazuhiro NAKAUSJI *([a]Osaka Univ.)*

[Angew. Chem. Int. Ed. Engl., 30, 172 (1991)]

We can use the phenalenyl group as a crucial unit for the construction of highly amphoteric hydrocarbons such as pentaleno[1,2,3-*cd*;4,5,6-*c*′d′]diphenalene. In addition to such an example, *s*-Indaceno[1,2,3-*cd*:5,6,7-*c*′d′]diphenalene (IDPL, **1**) is also expected to be a highly amphoteric hydrocarbon, since the neutral state of **1** will be destabilized by unfavorable electronic contribution of a nonaromatic *s*-indacene system and the redox states $\mathbf{1}^{2+}$, $\mathbf{1}^{\cdot+}$, $\mathbf{1}^{\cdot-}$, and $\mathbf{1}^{2-}$ will be substantially stabilized by the formation not only of two terminal phenalenyl segments but also of a central benzene structure with loss of the s-indacene conjugation. We have synthesized the diisopropyl derivative of **1**, *i*-Pr_2IDPL (**2**), by choosing dibromoacenaphthyleno[1,2-*k*]fluoranthene as a key intermediate which was converted in a straightforward fashion into the final skeleton. Investigation of the electrochemical behavior of **2** by cyclic voltammetry revealed two reduction waves (−0.48, −1.07 V) and two irreversible oxidation waves (0.62, 0.84 V). The value of E^{sum}, a experimental measure for the amphotricity of a molecule, for **2** is 1.10 V which shows a highly amphoteric nature. The dication and the dianion of **2** were generated and studied by ^{1}H-NMR. The most striking feature found is that although $\mathbf{1}^{2-}$ exhibited the operation and dominance of a diamagnetic ring current, $\mathbf{1}^{2+}$ exhibited paratropism despite having 4n+2 π electrons.

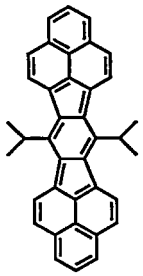
^{i}Pr$_2$-IDPL
2

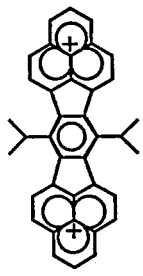
2^{2+}

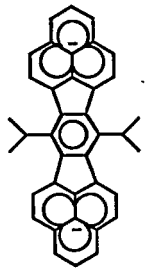
2^{2-}

V—B New Conjugated Electronic Systems

Design and synthesis of new conjugated electronic systems have been performed as general interests to explore new molecular materials which might have interesting chemical reactivites and physical properties. In this research project, new electronic systems having not only closed shell electronic systems but also open shell electronic systems are searched for. Chemical modifications for known electronic systems are also important. An example is as follows. The stable conjugated neutral radicals have been attracted much attention to explore new materials having potentially interesting solid state properties, for example single component conductors, and magnetically interesting materials. We have utilized odd alternant hydrocarbon, phenalenyl, as the basic skeleton for neutral radicals, and modified the phenalenyl skeleton by introducing donor and acceptor substituents to suppress the thermodynamic and kinetic instability. Such modification is one of the typical procedure in physical organic chemistry to stabilized unstable electronic systems.

V-B-1 Generation and Characterization of Phenalenyl Radicals Having Donor and Acceptor Substituents by Electrochemical Oxidation

Kazuhiro NAKASUJI, Masakazu YAMAGUCHI,[a] Ichiro MURATA,[a] and Hiroaki OHYA-NISHIGUCHI[b] *([a]Osaka Univ., [b]Kyoto Univ.)*

Three redox states of an odd alternant hydrocarbon, phenalenyl cation, radical, and anion, have attracted much attention to explore new molecular materials. As basic study of the stable conjugated neutral radicals, we have generated the phenalenyl radicals having the donor and the acceptor substituents. Methoxy or methylthio groups as the donor and cyano group as the acceptor are introduced at the electronically active α-positions of phenalenyl. The radicals species were generated by electrochemical oxidation of the corresponding phenalene derivatives in a CH_2Cl_2 solution containing n-Bu_4NBF_4 as supporting electrolyte at 3.10V. The radical species were characterized by ESR spectra which were well reproduced by computer simulations.

V-B-2 Synthesis and Crystal Structure of 2-*t*-Butyl-1,3-diazaphenalene

Yasushi MORITA, Jiro TOYODA, and Kazuhiro NAKASUJI

Diazaphenalenes are tricyclic conjugated molecules with two sp^2 nitrogen atoms which might be used as potentially interesting skeleton for new radical species. As an preliminary investigation, we prepared 2-*t*-butyl derivative of 1,3-diazaphenalene in order to study the general characteristics of the crystal structures for diazaphenalenes. Crystal structure data: $C_{15}H_{16}N_2$, monoclinic, $P2_1/n$, a = 4.2812(5), b = 12.9424(7), c = 14.4490(9) Å, β = 109.242(4) °, Z = 8, R = 8.36%.

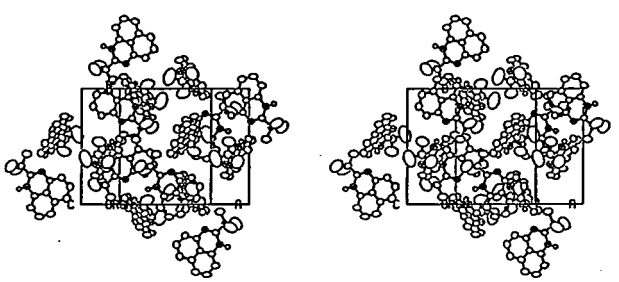

V-B-3 (Thiepine)iron Tricarbonyl: Stabilization of Thermally Labile Parent Thiepine by Transition-Metal Complexation

Keitaro NISHINO,[a] Masanobu TAKAGI,[a] Teruhisa KAWATA,[a] Ichiro MURATA,[b] Junji INANAGA, and Kazuhiro NAKAUSJI *([a]Osaka Kyoiku Univ., [b]Osaka Univ.)*

[J. Am. Chem. Soc., **113,** *5059 (1991)]*

Despite the successful synthesis of several monocyclic thiepine derivatives stabilized by bulky groups at both the 2- and 7-positions, the parent thiepine (**1**) has eluded synthesis. This is mainly due to the pronounced thermal instability of **1**. Ready loss of sulfur from **1** presumably occurs by valence isomerization of **1** to the corresponding thianorcaradiene followed by irreversible cheletropic loss of sulfur. On the other hand, the ability of transition metals to stabilize labile species by complexation has allowed isolation of kinetically unstable conjugated molecules such as cyclobutadiene, pentalene, and norcaradiene. In this study, the first synthesis and characterization of thiepine-iron tricarbonyl are described. Reaction of thiepine 1,1-dioxide with $Fe_2(CO)_9$ afforded thiepine 1,1-dioxide-iron tricarbonyl in 99% yield. Treatment of this complex with *p*-toluenediazonium tetrafluoroborate led to the corresponding tolyloxysulfonium tetrafluoroborate as a mixture of stereoisomers. Samarium diiodide-THF reduction of this mixture produced thiepine-iron tricarbonyl as a stable yellow needles in 38% yield. The structure of this complex was fully confirmed by ^1H and ^{13}C NMR, MS, IR, and UV spectroscopies. These results demonstrate that thermally labile thiepine is highly stabilized as a ligand in complex.

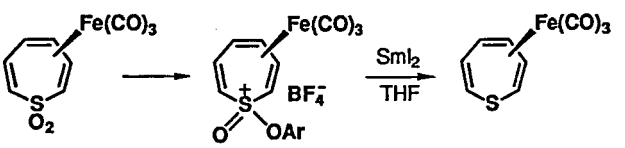

V—C New Cooperative Proton-Electron Transfer (PET) Systems

From synthetic chemistry viewpoints, we have started to explore a new type of molecular materials having interesting chemical reactivities and physical properties, while searching for a new concept or a general strategy with interdisciplinary cooperations. Our particular attention in this research project is concentrated on the molecular materials which can exhibit the cooprative interactions between hydrogen bonding and charge transfer in the solid state. A typical example is a phase transition found for benzoquinhydrone which can be regarded as a cooperative proton-electron transfer (PET) phenomenon from a stepwise molecular level consideration. The final PET state is characterized as molecular assemblies of hydrogen-bonded neutral radicals. Thus, an important strategy toward new materials is derived from such a characterization: the exploration of the stable neutral radicals having hydrogen bonding networks. We are now improving the molecular level concept, designing, and synthesizing new molecular materials.

V-C-1 Exploration of New Cooperative Proton-Electron Transfer (PET) Systems: First Example of Extended Conjugated Quinhydrones, 1,5-Dihalo-2,6-Naphthoquinhydrones

Kazuhiro NAKASUJI, Kenichi SUGIURA, Toshikazu KITAGAWA, Jiro TOYODA, Hiroshi OKAMOTO, Kaoru OKANIWA, Tadaoki MITANI, Hiroshi YAMAMOTO,[a] Ichiro MURATA,[a] Atsushi KAWAMOTO,[b] and Jiro TANAKA[b] *([a]Osaka Univ., [b]Nagoya Univ.)*

[*J. Am. Chem. Soc.*, **113**, 1862 (1991)]

The final phase transition state of cooperative proton-electron transfer (PET) phenomena can be characterized as a molecular assembly of *H-bonded neutral radicals.* From a stepwise consideration, two reasonable molecular design strategies to construct new cooperative PET systems are revealed; (a) the exploration of a quinone-hydroquinone pair with a smaller intermolecular CT gap and (b) the stabilization of the PET state by introducing donor and acceptor substituents. In this study, the synthesis and physical properties of the four new quinhydrones with extended conjugated electronic systems were reported. Smaller energies of the CT gaps are observed for the quinhydrones compared with that of BQH (2.34 eV). These are the first examples of *the extended conjugated quinhydrones* whose characteristic features are clarified. These quinhydrones showed pressure-response spectral characteristics (Figure 1). In addition, electronic absorption spectra in the CT transition energy regions also showed decreasing energies with increasing pressure. A closer insight into the concept and design strategy might lead to a new aspect of molecular assemblies with unique solid-state properties originated in the PET radicals.

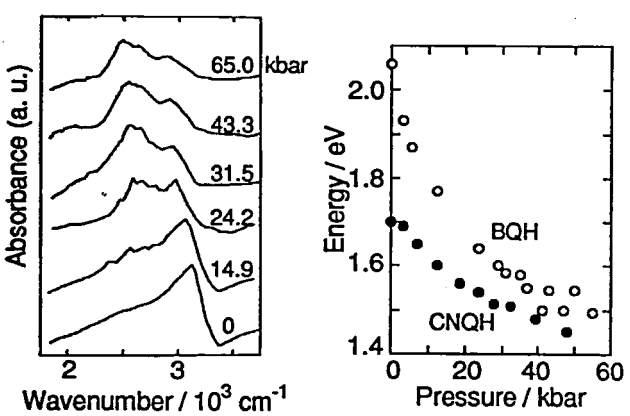

Figure 1.

V-C-2 Cooperative Proton-Electron Transfer System Containing 1,5-Bis(4-hydroxyphenylthio)naphthalene as Donor Component

Kenichi SUGIURA, Jiro TOYODA, Kaoru OKANIWA, Hiroshi OKAMOTO, Tadaoki MITANI, and Kazuhiro NAKASUJI

In order to expand the range of cooperative PET systems, the search for new donors with a proton donating character is still continued. In this study, a new donor, 1,5-bis(4-hydroxyphenylthio)naphthalene, was designed and synthesized. A charge transfer complex of the donor with chloranil was obtained as a large-size of single crystals of black cubics. X-ray crystal structure analysis was performed. Crystal structure data: $C_{28}H_{16}C_{14}S_2H_2O$, triclinic, $P\bar{1}$, a=11.224(2), b=17.366(4), c=7.1437(7)Å, α=83.52(1), β=96.97(2), γ=102.86(2)°, Z=2, R=5.2%.

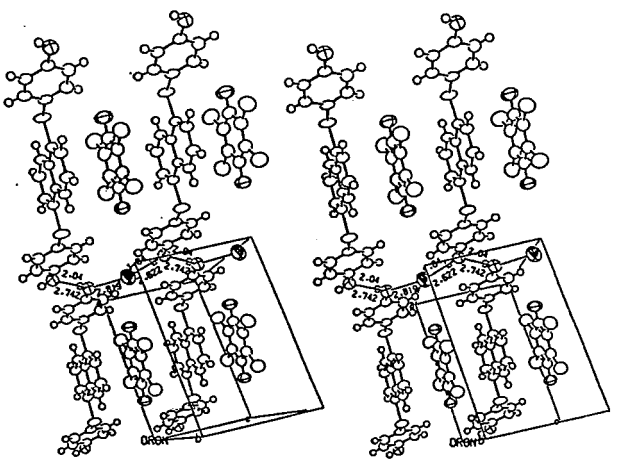

V—D Transition Metal Oxide Clusters

Finding method to control the arrangement of mixed valence or mixed metal centers in particular three-dimensional frameworks would greatly aid in the design of cluster compounds with desired chemical and physical properties. In recent years, we have directed our efforts primarily toward the synthesis of integrated cubane-type clusters as potential models for inorganic solid surfaces to understand the chemistry on them and have been reporting novel organometallic oxide clusters which contain soft as well as hard multimetal centers.

V-D-1 Trishomocubane-Type Methoxide Cluster as a Novel Mediator in the Extension of Cube Size in Organometallic Oxide Cluster: Synthesis and Structures of $[(RhCp^*)_2Mo_3O_9(OMe)_4]\cdot MeOH$ and a Linear Quadruple Cubane-Type Cluster $[(RhCp^*)_4Mo_6O_{22}]\cdot 4CH_2Cl_2$ ($Cp^*=\eta^5$-C_5Me_5)

Youngkyu DO *(KAIST and IMS)*, **Xiao-Zeng YOU** *(Nanjing University and IMS)*, **Cuiju ZHANG** *(ICAS and IMS)*, **Yoshiki OZAWA, and Kiyoshi ISOBE**

[*J. Am. Chem. Soc.*, **113**, 5892 (1991)]

The explotation of the reaction of the triple cubane-type cluster **1** with MeOH was undertaken to understand the heterogeneous $MeOH/MoO_3$ catalytic system. We found novel conversion, outlined in the scheme, of cluster **1** to a trishomocubane-type cluster $[(RhCp^*)_2Mo_3O_9(OMe)_4]$ (**2**) then to a linear quadruple cubane-type cluster $[(RhCp^*)_2Mo_6O_{22}]$ (**3**).

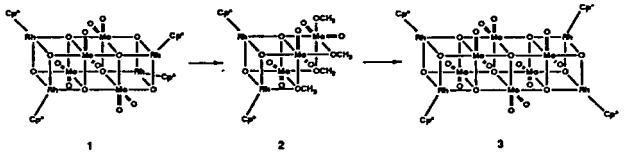

The molecular structures of clusters **2** and **3** were established by single crystal X-ray analyses and characterized by IR and NMR (^1H, and ^{13}C) spectroscopy.

V-D-2 Synthesis, Structure, and Properties of Vanadium Oxide Cluster with Supported β-Methallyl Rhodium(III) Complex

Haruo AKASHI, Atsushi YAGASAKI, Yoshiki OZAWA, and Kiyoshi ISOBE

The chemistry of oxide-bound η^3-allylrhodium complexes has developed the many interesting and important catalytic reactions in hydrocarbon transformations. Although theoretical studies employing tight-binding calculations have been carried out to elucidate the interaction of η^3-allylrhodium fragment with metal oxide, still in the many stages in the catalytic cycle, the nature of the rhodium-oxygen bonding is ambiguous: for instance, we do not know if more than one oxygen atom interacts with the rhodium center at any stage. We approach the subjects by using model clusters mimicking the oxide surfaces attached with the η^3-allylrhodium groups

Reaction of $[(\eta^3\text{-}C_4H_7)_2Rh(CH_3CN)_2]PF_6$ (η^3-C_4H_7 = β-methallyl) with $[(n\text{-}C_4H_9)_4N](VO_3)$ gives a new cluster $[(n\text{-}C_4H_9)_4N]_2[\{(\eta^3\text{-}C_4H_7)_2Rh\}_2(V_4O_{12})]$ **1** (Figure 1). The cluster consists of the vanadium oxide group and two η^3-allylrhodium groups which show dynamic behaviors in CH_2Cl_2.

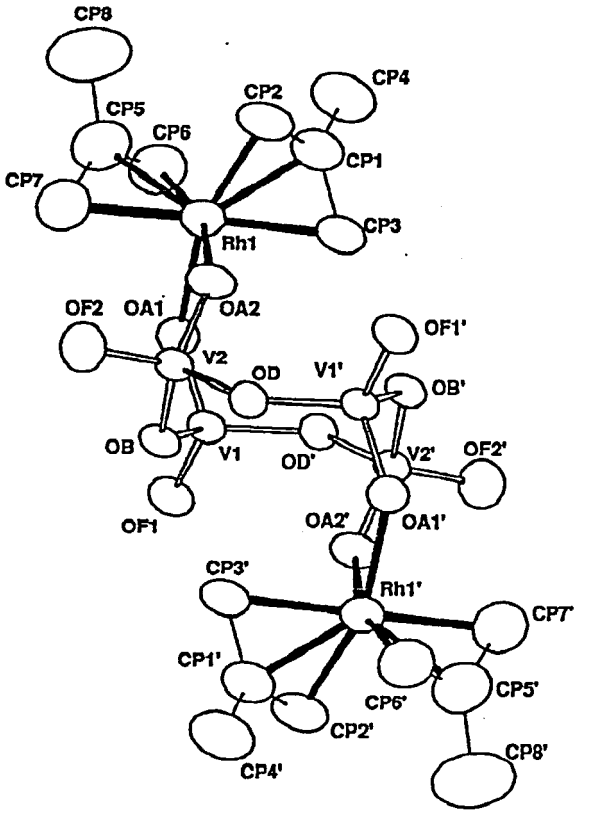

Figure 1. Perspective view of $[\{(\eta^3\text{-}C_4H_7)_2Rh\}_2(V_4O_{12})]^{2-}$ with selected interatomic distances (Å) and angles (°): mean V-O_A 1.668, V-O_B 1.805, V-O_D 1.799, V-O_F 1.617, Rh-O_A 2.169; Rh-C_{P1} 2.15(2), Rh-C_{P2} 2.09(2), Rh-C_{P3} 2.23(2); mean O_B-V-O_D 110.7; V-O_B-V 121.0, V-O_D-V 134.4, V-O_{A1}-Rh 124.4(3), V-O_{A2}-Rh 140.2(4), O_{A1}-Rh-O_{A2} 87.8(3). (Prime denotes a transformation of X,Y,Z.)

V-D-3 Synthesis and Structure of Vanadium Oxide Cluster with Supported Diene Rhodium(III) Complex

Haruo AKASHI, Atsushi YAGASAKI, Yoshiki OZAWA, and Kiyoshi ISOBE

Reactivities of $[(n\text{-}C_4H_9)_4N]_2[\{(\eta^3\text{-}C_4H_7)_2Rh\}_2(V_4O_{12})]$ **1** towards the reagents such as CO, H_2, olefins, and tertiary phosphines are of interest in connection with the elemental reactions in the catalytic cycle of hydrocarbon transformations on the tailored catalysts.[1] The reaction of **1** with CO gas or $P(OEt)_3$ in tetrahydrofuran gave the diene cluster, $[(n\text{-}C_4H_9)_4N]_2[(C_8H_{14})_2Rh_2(V_4O_{12})]$ **2** in 23% yield through the reductive coupling of the η^3-allyl ligands with changing the oxidation state of the rhodium atoms from +3 to +1. $\mathbf{2}\cdot CH_2Cl_2$ has been characterized by single crystal X-ray diffraction. The structure of its anion is shown in Figure 1. Each rhodium is surrounded by two terminal oxygens and two C=C double bonds to form a planner structure and the V_4O_4 ring has a twist-chair type conformation.

The clusters described here provide a model for the oxide-bound organorhodium complexes to understand the nature of the rhodium-oxygen bonding and the active site in them. The mechanism of formation of **2** remains to be established and currently, we are trying to isolate the intermediates of the reaction of **1** with CO or $P(OEt)_3$.

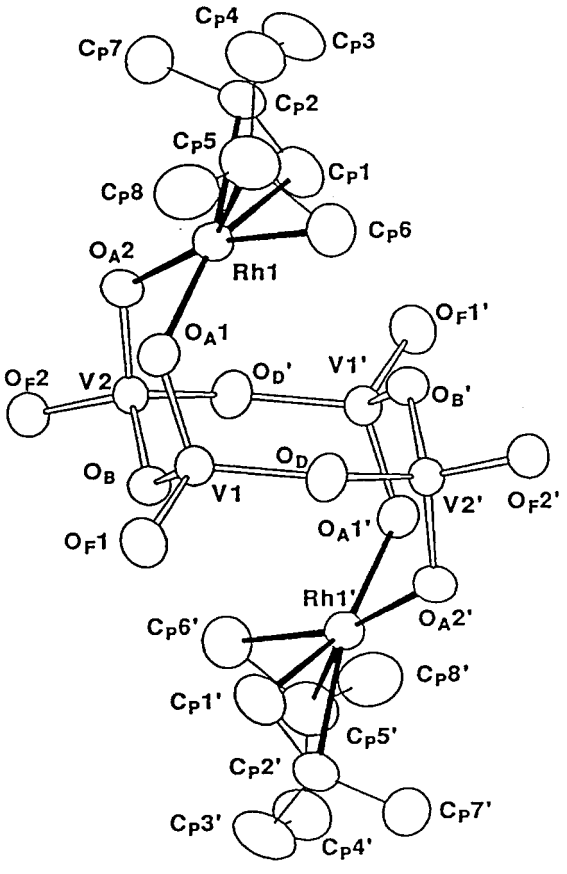

Figure 1. Perspective view of $[(C_8H_{14})_2Rh_2(V_4O_{12})]^{2-}$ with selected interatomic distances (Å) and angles (°): mean V-O_A 1.679, V-O_B 1.800, V-O_D 1.792, V-O_F 1.620, Rh-O_A 2.055; Rh-C_{P1} 2.14(2), Rh-C_{P2} 2.09(2), Rh-C_{P3} 2.23(2); mean O_B-V-O_D 110.7; V-O_B-V 126.1, V-O_D-V 138.5, V-O_{A1}-Rh 117.1. (Prime denotes a transformation of X,Y,Z.)

V—E Transition Metal Sulfide Compounds

Complexes containing H_2S, SH^-, S^{2-}, and S_2^{n-} (n =1 and 2) ligands have now become of considerable interest because of the novelty of these complexes, their potential for serving as models for biological systems and as industrial hydrotreating catalysts, and important intermediates of mineralogical processes. Responsible for the key function of the M-S bond in chemical processes is the "softness" and high polarisability of S atom, which can act as an electron sink and cause delocalized electronic states. We have continued to study the functionality of the M-S bond.

V-E-1 Rhodium μ-Methylene Complex with bridged SH Ligand

Amelio VAZQUEZ DE MIGUEL *(University of Alcala of Henares and IMS)*, **Yoshiki OZAWA, and Kiyoshi ISOBE**

In a pathway of the hydrodesulphurization complete decomposition occurs and results in surface sulphur, carbon, and hydrocarbon fragments which contain carbyne, carbene, and other hydrocarbyl species. In order to understand such surface by using model compounds containing the sulphur and carbene ligands we start to synthesize μ-methylene rhodium complexes with sulphur ligands. Here we report the first stable μ-methylene rhodium complexes with a bridged SH ligand, $[Rh_2Cp^*_2(\mu\text{-}CH_2)_2(\mu\text{-}SH)]BPh_4$ (**1**).

Complex **1** has been isolated from the reaction of trans-$[Rh_2Cp^*_2(\mu\text{-}CH_2)_2Cl_2]$ with H_2S in CH_3OH and readily converted to trans-$[Rh_2Cp^*_2(\mu\text{-}CH_2)_2(SH)_2]$ **2** in the presence of NEt_3 and H_2S; **1** has been characterized cystallographically (Figure 1).

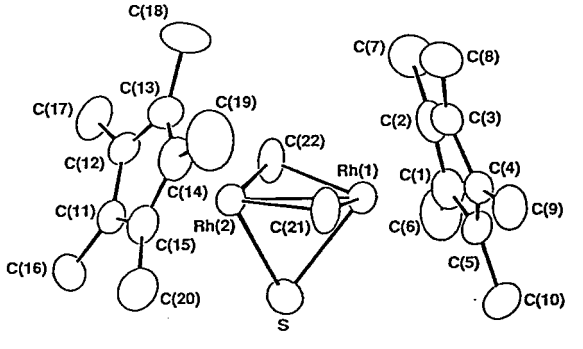

Figure 1. ORTEP diagram of $[Rh_2Cp^*_2(\mu\text{-}CH_2)_2(\mu\text{-}SH)]^+$ in **1** with the atom-numbering scheme. Selected bond lengths (Å) and angles (°): Rh(1)-Rh(2) 2.554(1), Rh(1)-S 2.407(4), Rh(2)-S 2.394(4), Rh(1)-C(21) 2.06(1), Rh(1)-C(22) 2.04(1), Rh(2)-C(21) 2.03(1), Rh(2)-C(22) 2.06(1), Rh(1)-S-Rh(2) 64.3(1), Rh(1)-C(21)-Rh(2) 77.1(3), Rh(1)-C(22)-Rh(2) 77.1(4), C(21)-Rh(1)-C(22) 100.6(4), C(21)-Rh(2)-C(22) 101.1(4).

V-E-2 Novel Tetranuclear μ-Methylene Rhodium Complex with Doubly bridged S_2 Ligand: $[(Rh_2Cp^*_2(\mu\text{-}CH_2)_2(\mu\text{-}S_2)_2](BF_4)_2$

Amelio VAZQUEZ DE MIGUEL *(University of Alcala of*

Henares and IMS), **Yoshiki OZAWA, and Kiyoshi ISOBE**

Oxidation of the MSH functionality have been little studied although the oxidation of organic thiols RSH is well-known. Recently we have isolated $[Rh_2Cp^*_2(\mu\text{-}CH_2)_2(\mu\text{-}SH)]BF_4$ from the reaction of trans-$[Rh_2Cp^*_2(\mu\text{-}CH_2)_2Cl_2]$ with H_2S in CH_3OH. The μ-SH complex reacts with O_2 in the presence of excess H_2S to give a doubly bridged disulfide complex $[\{Rh_2Cp^*_2(\mu\text{-}CH_2)_2\}_2(\mu\text{-}S_2)_2](BF_4)_2$ (**1**) in 81.3% yield according to equation 1.

$$2[Rh_2Cp^*_2(\mu\text{-}CH_2)_2(\mu\text{-}SH)]BF_4 + 2H_2S + 3/2O_2 \rightarrow [\{Rh_2Cp^*_2(\mu\text{-}CH_2)_2\}_2(\mu\text{-}S_2)_2](BF_4)_2 + 3H_2O$$

The formation of **1** is quite slow ($t_{1/2}$=ca. 15h at 22°C, the concentration of trans-$[Rh_2Cp^*_2(\mu\text{-}CH_2)_2Cl_2]$) and involves a net 6e oxidation to produce one molecule of **1**. **1** has been characterized crystallographically (Figure 1).

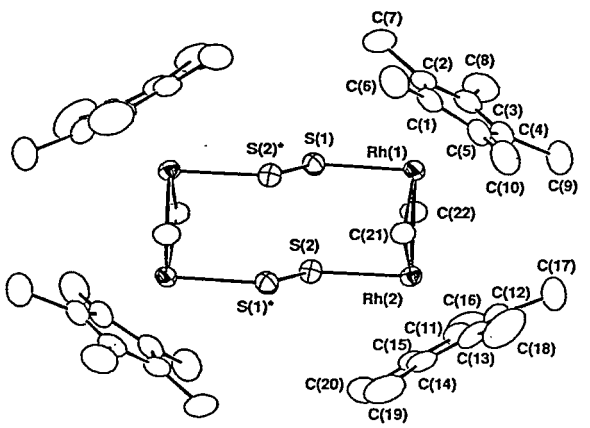

Figure 1. ORTEP diagram of $[\{Rh_2Cp^*_2(\mu\text{-}CH_2)_2\}_2(\mu\text{-}S_2)_2]^{2+}$ in **1** with the atom-numbering scheme. Selected bond lengths (Å) and angles (°): Rh(1)-Rh(2) 2.6608(5), Rh(1)-S(1) 2.350(1), Rh(2)-S(2) 2.345(1), Rh(1)-C(21) 2.033(4), Rh(2)-C(22) 2.060(5), S(1)-S(2)* 1.980(2) Rh(2)-Rh(1)-S(1) 90.88(3), Rh(1)-S(1)-S(2) 112.23(6), Rh(1)-C(21)-Rh(2) 81.6(2).

V-E-3 Synthesis and Properties of Trinuclear Transition Metal Sulfide Cluster $[RhCp^*P(OEt)_3MS_4CuCl]$ (M=Mo,W)

Yoshiki OZAWA, Yoshihito HAYASHI, and Kiyoshi ISOBE

Condensed metal sulfide clusters containing high-valent Mo or W atoms have been quite different character from that for low-valent (+2-+4) metal atoms. In these clusters thiomolybdate or tungstate keep MS_4 tetrahedral coordination forms, and provide no d-electrons for metal-metal bondings with neighboring metal atoms. The title compounds were obtained from the reaction of $[RhCp^*P(OEt)_3MS_4]$ with CuCl. Crystal data for $[RhCp^*P(OEt)_3WS_4CuCl]$: monoclinic $P2_1$, a=10.281 (2), b=11.967 (1), c=10.785 (1)Å, β=94.73(1)°, V=1322 (2) Å^3, Z=2. The molecular structure consists of Rh–M–Cu linear transition metal sequence. Cyclic voltammogram for these clusters show three distinct one-electron reduction steps (for Rh–W–Cu: −0.85, −1.12, −1.56 V vs Ag/AgCl). The first electron transter in the reduction process occurs on the Cu atom. The following two reduction potentials are attributed to the Rh(III)/Rh(II) and Rh(II)/Rh(I). The MS_4 moiety binds two different transition metal atoms with little influence for their electrochemical properties.

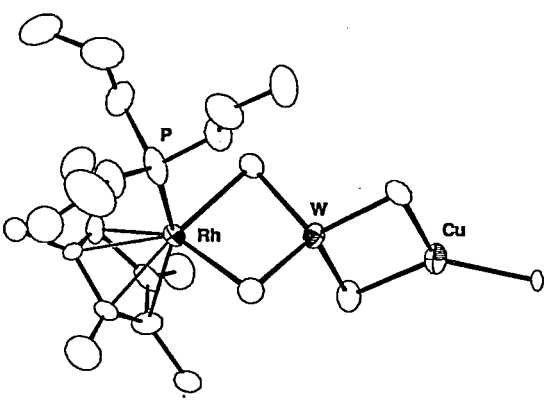

Figure 1. Molecular Structure of $[RhCp^*P(OEt)_3WS_4CuCl]$. Selected bond distances (Å) and angles (°) are: Rh–W 2.900 (2), W–Cu 2.638 (2), Rh–S 2.432 (6), 2.354 (6), Cu–S 2.229 (5), 2.251 (5), W–S (bound to Rh atom) 2.174 (5), 2.272 (5), W–S (bound to Cu atom) 2.208 (5), 2.200 (4), Cu–Cl 2.228 (4), Rh–W–Cu 166.07 (6), W–S–Rh 77.8 (2), 77.6 (2), W–S–Cu 73.0 (2), 72.7 (1).

V—F Control of the Intra- and Intermolecular Magnetic Interaction

A great deal of effort has been devoted to building a molecular based ferromagnet. In order to prepare a complex which exhibits the magnetic ordering at higher temperature, the three dimensional magnetic interaction must be made as strong as possible. Control of the magnetic interaction in multinuclear and low dimensional metal complexes promise to be the basic technology for building the molecular based ferromagnet.

V-F-1 Control of the Intramolecular Magnetic Interaction by the Spin Polarization of d_π-Electrons: Ferromagnetic Interaction between Iron Centers through an Organic Bridging Ligand

Hiroki OSHIO

[*J. Chem. Soc. Chem. Comm.*, 240 (1991)]

Some strategies to have a ferromagnetic interaction in organic multi-radical compounds have been proposed,[1] and a spin polarization mechanism, that is a topological symmetry of the π electrons network, was used to design high-spin organic molecules which have carbenes as paramagnetic centers.[2] Is it possible to apply the concept of the spin polarization of d_π-spins to designing the multinuclear metal complexes which have ferromagnetic interaction through an organic bridging ligand? In this report, the magnetic properties of dinuclear iron(III) complexes $[Fe_2(bpmar)(H_2O)_4](NO_3)_4 \cdot 3H_2O$, in which the bridging ligand was designed by taking into account the spin polarization of the d_π spins to ligand p_π electrons, is presented.

Reaction of ferric nitrate enneahydrate with H_2bpmar (Fig. 1), which was obtained by a condensation reaction of 2-methylresorcinol with N,N-bis(2-pyridylmethyl)amine and formalin in methanol, gave dark blue micro crystalline. Cryogenic magnetic susceptibilities were measured down to 2.0 K. $\chi_m T$ vs Temperature plot (Fig. 2) shows gradual increase starting from 75 K as the temperture decreased and reached to the maximum $\chi_m T$ value (11.356 emu mol^{-1} K) at 10.8 K. This magnetic behavior does indicate the existence of the ferromagnetic interaction between the two metal centers. A least squares calculation to the Van Vleck equation for the S=5/2 dinuclear system gave best fit parameters to be $J = +0.62(3)$ cm^{-1} and g=1.956(4). The propagation of the ferromagnetic intraction can be explained by the spin polarization of the d_π-spins to p_π-electrons on the organic ligand (Fig. 3). It should be concluded that the ferromagnetic interaction in multinuclear metal complexes can be obtained if the bridging ligand is designed by considering the topological symmetry of the d_π-electrons to the ligand p_π-electrons network.

References

1) H.M. MacConnel, *J. Chem. Phys.* **31**, 299 (1963), N. Mataga, *Theor. Chim. Acta*, **10**, 372 (1968), A.A. Ovchinnikov, *Theor. Chim. Acta*, **47**, 297 (1978), K. Itoh, *Pure Appl. Chem.* **50**, 1251 (1978), and R. Breslow, B. Juan, R.Q. Kluttz, and C.Z. Xia, *Tetrahedron*, **38**, 863 (1982).
2) K. Itoh, *Chem. Phys. Lett.* **1**, 235 (1967) and T. Sugawara, S. Bandow, K. Kimura, H. Iwamura, and K. Itoh, *J. Am. Chem. Soc.*, **108**, 368 (1986).

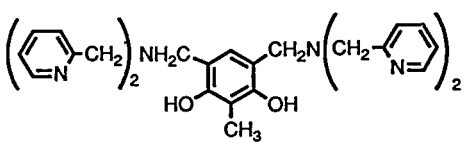

Figure 1. Structure of H_2bpmar

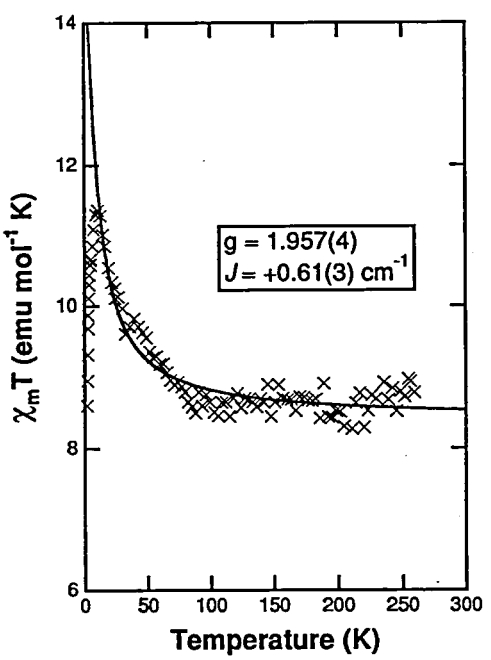

Figure 2. Plot of $\chi_m T$-T for $[Fe_2(bpmar)(H_2O)](NO_3)_4$ $3H_2O$. The solid line was generated from best fit calculation using the Van Vleck equation for the S=5/2 dimer.

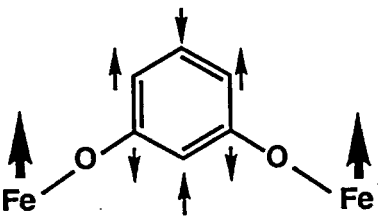

Figure 3. Spin polarization scheme

V-F-2 Design of a Homonuclear Ferromagnetic Chain: Structures and Magnetic Properties of Oxalato Bridged Copper(II) Complexes with One Dimensional Structure

Hiroki OSHIO and Umpei NAGASHIMA

An orthogonality of the magnetic orbitals results in the stabilization of a high spin state, that is, a propagation of a ferromagnetic interaction between magnetic centers. Oxalato bridged one-dimensional copper(II) complexes (Fig. 1), $[Cu(en)_2][Cu(ox)_2]$ (**1**) and $[Cu(bpy)(ox)] \cdot 2H_2O$ (**2**), were designed for an each magnetic orbital on adjacent units to be orthogonal, which might result in a ferromagnetic intrachain interaction. In the complex (**1**), oxalato anions are tri-dentate ligands, and the terminal oxygen atoms of the $[Cu(ox)_2]^{2-}$ unit birdge the adjacent $[Cu(en)_2]^{2+}$ unit from the axial (d_z2 orbital) position of the cation. The ground states of the cations and anion units are d_{x2-y2}. Magnetic susceptibility data (Fig. 2) have revealed that the complex (**1**) is an antiferromagnetic S=1/2 Heisenberg chain, and exchange couplingconstant (J) and g values were estimated to be 2.1(1) cm^{-1} and 2.118(2), respectively, based on an antiferromagnetic Heisenberg linear chain model. In the complex (**2**), the oxalato anions are centrosymmetric and act as a quadri-dentate bridging ligand, where the oxygen atoms coordinate to each copper atom both from the equatorial (d_{x2-y2} orbital) and axial (d_{z2} orbital) positons. Magnetic susceptibility data (Fig. 2) have shown that the complex (**2**) is the ferromagnetic S=1/2 Heisenberg chain, and exchange coupling constant and g values were estimated to be 1.22(4) cm^{-1} and 2.185(6), respectively, by using a ferromagnetic Heisenberg linear chain model. Magnetization experiments of the complex (**2**) have revealed that a spin multiplicity (S) is greater than 3/2 at 2 K. This ferromagnetic behavior can be readily understood by considering the fact that the spin density on the copper atom is spread over the oxalato groups, as confirmed by the all-electron ab initio unrestricted Hatree-Fock calculation for $[Cu(ox)_2]^{2-}$. The spin on the terminal oxygen atom, which coordinates to the adjacent copper atoms from its d_{z2} direction, induces spin on that d_{z2} orbital. The orthogonality of the primary spin orbital (d_{x2-y2}) and induced spin orbitals (d_{z2}) causes the ferromagnetic interaction. The extended Hückel molecular orbital calculation for $[Cu_2((NH_3)_8(ox)]^{2+}$, which has a similar coordination geometry to complex (**2**), has shown that the HOMO and LUMO are effectively degenerate (separated by only 0.02 eV), and this calculation is in good agreement with the experimental result. Crystal Data: $[Cu(en)_2][Cu(ox)_2]$, monoclinic, space group $C2/c$, a=14.884(2)Å, b=12.770(2)Å, c=7.147(1)Å, β=94.83(2)°, V=1353.6(4)Å^3, Z=4,

R=0.026 (R_w=0.035) for 1938 data with $|F_0|>3\sigma(F_0)$. [Cu(bpy)(ox)]·$2H_2O$, triclinic, space group $P\bar{1}$, a=9.110(1)Å, b=9.675(1)Å, c=8.922(1)Å, α=97.54(1)°, β=105.80(1)°, γ=110.26(1)°, V=687.4(2)Å^3, Z=2, R=0.037 (R_w=0.052) for 4161 data with $|F_0|>3\sigma(F_0)$.

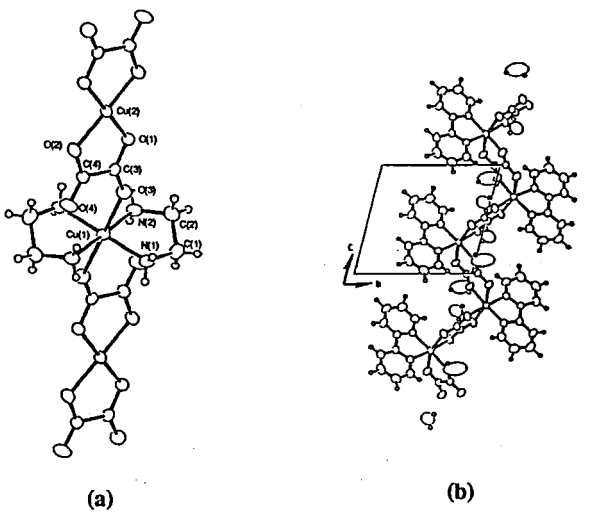

Figure 1. Chain structures of (a) $\{[Cu(en)_2][Cu(ox)_2]\}_n$ and (b) $\{[Cu(bpy)(ox)]2H_2O\}_n$

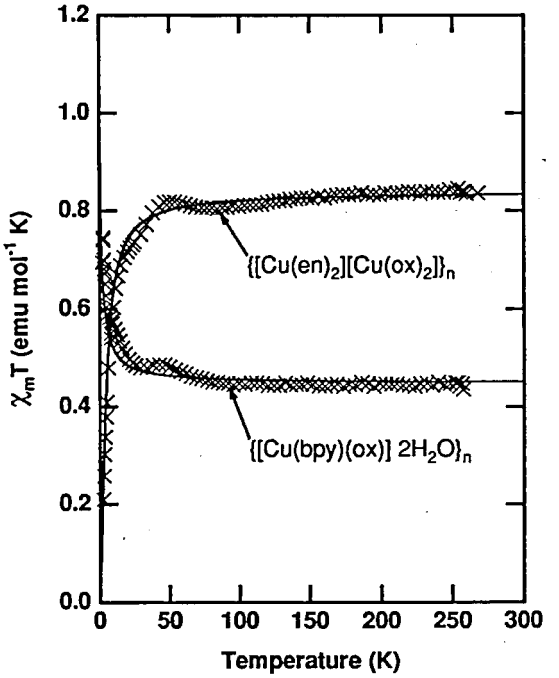

Figure 2. χ_mT-T plots of the complexes $\{[Cu(en)_2][Cu(ox)_2]\}_n$ and $\{[Cu(bpy)(ox)]2H_2O\}_n$

V—G Thermodynamic Stabilities of Gaseous Ions

Thermochemical data such as acidity and basicity of organic molecules in the gas phase provide the most precious basis for investigation of an essential relationship between structure and chemical reactivity. In this project, thermodynamic stabilities of various ionic species which are considered to be intermediates of organic reactions in solution have been determiend by measuring equilibrium constants of H^+, Me_3Si^+, and electron transfer reactions using a pulsed ion cyclotron resonance (ICR) spectrometer. Effects of molecular structure on the stability of ions have been studied in detail. Furthermore, substituent effects for stabilities of gaseous ions have been compared with those for reactions in solution of relevant substrates to establish the basic concept for relating the transition states to intermediate ions.

V-G-1 Substituent Effect on the Stability of l-t-Butyl-l-phenylethyl Cation

Masaaki MISHIMA, Kazuhide NAKATA, Hideyuki NOMURA,* Mizue FUJIO,* and Yuho TSUNO *(*Kyushu Univ.)*

Relative stabilities l-t-butyl-l-phenylethyl cations were determined based on the measurement of gas phase basicities of the corresponding olefins. Unsubstituted l-t-butyl-l-phenylethyl cations is found to be 1.1 kcal mol^{-1} less stable than α-cumyl cation. The substituent effect on the stability of this carbocation has been analyzed by the LArSR correlation, providing a ρ value of −12.5 and an r value of 0.86.

$$\delta\Delta G^\circ = \rho\,(\sigma^\circ + r\,\Delta\bar{\sigma}_R^+)$$

where the r value is a measure of π-interaction between the aryl π-system and reaction site. This ρ value is identical to those observed for ordinary benzylic cation such as α-cumyl cation and l-phenylethyl cation systems, while the r value is somewhat smaller than that of α-cumyl cation. The reduced r value may be attributed to steric loss of through-conjugative interaction of the benzene ring with the cation center. Most importantly, the r value of 0.86 is in complete agreement with that for the solvolysis of the corresponding substrates, l-t-butyl-l-arylethyl chlorides.

V-G-2 Me_3Si^+ Basicities of Acetophenones in the Gas Phase

Masaaki MISHIMA, Chul-Hyun KANG, and Yuho TSUNO

Ion-molecule reaction of Me_3Si^+ generated by electron impact ionization of tetramethylsilane with various ketones has been studied using an ion cyclotron resonance spectrometer. It was found that stable adduct ions Me_3SiB^+ (B: ketones) were formed in association reaction when the pressure of tetramethylsilane was relatively high, 3 to 10×10^{-6} torr, and that the binding of Me_3Si^+ to the bases was reversible. This suggests that it is possible to measure relative basicity toward Me_3Si^+ under ICR conditions. By this way we have determined Me_3Si^+ basicities of a series of acetophenones. The substituent effect has been analyzed in terms of the LArSR Eq., giving a ρ value of −12 and an r value of 0.7. A ρ value of −12 is in complete agreement with that for H^+ basicities. This means that the degree of charge transfer toward Me_3Si^+ is similar to that toward H^+. On the other hand, an r value of 0.7 is smaller than that for H^+ basicities, indicating clearly that π-delocalization of the

positive charge into aryl π-system is reduced in the Me_3Si adduct ion compared with in the protonated ion. The reduced r value suggests greater electron donating ability of $OSiMe_3$ group than OH group, being consistent with the fact that Si is electropositive relative to H.

V-G-3 Basicities of Styrenes toward Trimethylsilyl Cation. β-Effect of Me_3Si Group on the Stability of Carbenium Ions

Masaaki MISHIMA, Chul-Hyun KANG, and Yuho TSUNO

Gas phase basicities of styrenes toward Me_3Si^+ have been studied on the basis of free energy changes of Me_3Si^+ transfer equilibrium in order to explore "Si-effect" on the stability of the carbenium ion at β position. Effects of ring-substituent on the stability of Me_3Si adduct ion has been found to be significantly small compared with the corresponding protonated ion (l-phenylethyl cation). Furthermore, resonance effect of para π-donor substituent is also reduced significantly. Both facts suggest that Me_3Si adduct ion is a Si-bridged ion rather than a open cation. Quantitative analysis of the substituent effect is in progress.

V—H Structure-Reactivity Relationship and Reaction Mechanism

The substituent effect in the systems where the direct π-interaction between the aryl and carbocationic center is possible, can be generally described by the LArSR equation.

$$\log k/k_o = \rho(\sigma^o + r\Delta\bar{\sigma}_R^+)$$

The real significance of the substituent effect in organic chemistry is that the correlation results are related with reaction mechanisms. It is therefore of importance to establish an essential relation between the LArSR correlation results and the structure of transition state. From this point of view, the substituent effects and reaction mechanisms have been studied in detail for various systems.

V-H-1 Evidence for a Clear S_N1-S_N2 Mechanistic Changeover for Nucleophlic Displacement Reaction

Mizue FUJIO,* Ken-ichi YATSUGI,* Yutaka TSUJI,* Sung-Hong KIM, Masaaki MISHIMA, and Yuho TSUNO *(*Kyushu Univ.)*

The Menschtukin-type reaction of benzyl tosylates with N,N-dimethylanilines has been studied in MeCN at 35°C. Activated benzyl tosylates such as p-SMe and p-MeO-m-Br substituted ones react with dimethylanilines by unimolecular and bimolecular process. These processes are quite distinct and afford no evidence for a mechanism intermediate between S_N1 and S_N2. The kinetic dependence are expected for the simultaneous occurrence of S_N1 and S_N2 reactions, as in equation (1). These results do not support the Sneen unified ion-pair mechanism theory of nucleophilic substitution.

$$k_{obs} = K_1 + k_2[N] \quad (1)$$

V-H-2 Substituent Effects on the Solvolysis of o-Methyl- and o,o'-Dimethyl-α-t-Butylbenzyl Tosylates

Mizue FUJIO,* Yutaka TSUJI,* Toshiaki OTSU, and Yuho TSUNO *(*Kyushu Univ.)*

[*Tetrahedron Lett.*, **32**, 1805 (1991)]

Substituent effect in the solvolysis of o-methyl- and 2,6-dimethyl-α-t-butylbenzyl tosylates was analyzed compared with that of the parent α-t-butylbenzyl tosylates. No significant steric loss of resonance was observed by introducing o-Me groups, indicating that the stabilization by the extended π-delocalization should be the most predominant driving force to promote ionization in the ordinary benzylic solvolysis.

V-H-3 The Unexalted Resonance Scale of Substituent Effect in the Benzylic Solvolysis

Mizue FUJIO,* Kazuaki NAKASHIMA,*, Eiko TOKUNAGA,* Yutaka TSUJI,* and Yuho TSUNO *(*Kyushu Univ.)*

[*Tetrahedron Lett.*, in press]

The solvolysis rates of 4-methylbenzobicyclo[2,2,2] octen-l-yl triflates (*1*) where no through-conjugative aryl-cation center interaction is possible were determined by the conductivity method. The solvolysis rate of this system is extremely slow to require a strong leaving group triflate, to realize measurable rates, and the rate change with ring substituents appears rather significantly small compared with that in the ordinary simple benzylic solvolysis. The substituent effect can be described in terms of resonance-unexalted σ^o parameters of the aryl substituents, giving ρ=—2.18. The r value in this system must be evidently zero, and it is apparent that any conjugative interaction of the benzene ring with the cationic center should be completely absent.

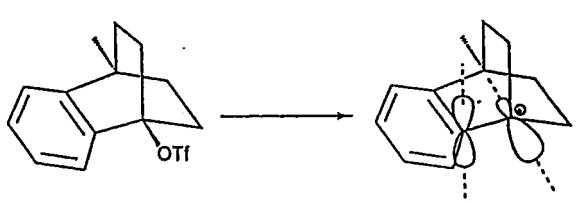

V-H-4 The Substituent Effect on the Acetolysis of Monosubstituted 2,2-Diphenylethyl Tosylates

Yasuyuki MAEDA,* Mutsuo GOTO,* Masaaki MISHIMA, Mizue FUJIO,* and Yuho TSUNO *(*Kyushu Univ.)*

The substituent effect on the acetolysis of mono-substituted 2,2-diphenylethyl tosylates was separated into respective effects of migrating and non-migrating groups. The application of the iterative non-linear least-squares method gives the following correlations for the X-phenyl-assisted pathway (k_M) and unsubstituted phenyl-assisted pathway (k_N).

$\log(k_M^X/k_M^H) = -3.658\ (\sigma^\circ + 0.58\Delta\bar{\sigma}_R^+)$

$\log(k_N^X/k_N^H) = -0.863\ (\sigma^\circ + 0.2\Delta\bar{\sigma}_R^+)$

The r_M for the aryl-assisted process is quite close to that for the neophyl system, and r_N value for the aryl-unassisted process is close to the r of 0.26 for σ constant.

Product analysis on the basis of the ^{13}C tracer method supports the dissection of the overall k_t into the two composite rates. It is concluded that this solvolysis involves two discrete pathways which are non-crossover.

V-H-5 The Substituent Effect on the Acetolysis of 2,2-Bis(aryl)ethyl Tosylates

Yasuyuki MAEDA,* Mutsuo GOTO,* Toshimitsu KOBAYASHI,* Masaaki MISHIMA, Mizue FUJIO,* and Yuho TSUNO *(*Kyushu Univ.)*

[*Memo. Fac. Sci., Kyushu Univ. Ser. C*, **18(1)**, 63 (1991)]

The substituent effect on the acetolysis of 2,2-bis(aryl)ethyl tosylats can be described in terms of the LArSR relationship, giving an r value of 0.52. This r value is quite close to that for neophyl system, suggesting the similarity of the transition state to that of the neophyl system. The correlation result can be reasonably accounted for on the basis of the accepted mechanism of this reaction, involving a rate-determining aryl-assisted transition state where only one aryl group of the two β-aryl groups participates.

V-H-6 Solvolysis of 1,1,3,3-Tetramethylindan-2-yl Sulfonates

Ken-ichi YATSUGI,* Yutaka TSUJI,* Mizue FUJIO,* and Yuho TSUNO *(*Kyushu Univ.)*

The solvolysis mechanism of 1,1,3,3-tetramethylindan-2-yl system was studied for various aspects. The substituent effect on the solvolysis of 5-substituted 1,1,3,3-tetramethylindan-2-yl triflates gave a small size ρ value of -1.1 with resonance-unexalted $(\sigma_p^\circ+\sigma_m)/2$, indicating the absence of homobenzylic participation by the ary ring. The solvent effect on the solvolysis of the unsubstituted triflate gave a reduced m value of 0.7 against Y_{OTf}, denying the k_c and/or k_s mechanisms and suggesting anchimerically assisted one. These results including product analysis suggest that solvolysis of this sulfonate may undergo by the neighboring methyl assisted mechanism.

V-H-7 The Study of ^{18}O-Scrambling on the Solvolysis of α-t-Butylbenzyl Tosylate

Yutaka TSUJI,* Ken-ichi YATSUGI,* Mizue FUJIO,* and Yuho TSUNO *(*Kyushu Univ.)*

The ^{18}O-scrambling within starting sulfonate during the solvolysis of α-t-butylbenzyl tosylate was determined in various solvent by use of ^{13}C-NMR method utilizing the split ^{13}C NMR signals of the alkoxy carbon induced by isotopic substitution $^{18}O/^{16}O$. The amount of ion-pair return, (1-F) value of ca. 0.5 in highly nucleophilic solvents such as aqueous ethanol and aq. acetone, and ca. 0.7 in less nucleophilic solvents such as acetic acid and aq. trifluorethanol were obtained. It has been found that large return to the starting tosylate from ion-pair intermediates occurs in the solvolysis of the present system which is classified as a limiting solvolysis. For the ion-pair return of both unsubstituted and m-Cl derivatives, nearly identical (1-F) value was obtained in each solvent, indicating that the ion-pair return is insensitive to substituent polarity. Therefore, the extent of ion-pair return does not affect the result of the substituent analysis of this substrate. Further, the examination with added salts revealed that the return mostly occurs from the intimate ion-pair.

V—I Organic Synthesis with Lanthanides

Recent progress on the utilization of lanthanides in organic synthesis has aroused a growing interest among organic chemists. Of these lanthanides, samarium has been one of the most attractive elements because of its unique properties. Samarium(II) diiodide has a moderate oxidation potential which falls between those of magnesium and zinc, being suitable for the reduction of a variety of organic functions. The oxophilicity of samarium, which falls between those of aluminum and titanium, is also significant. This property would be advantageous in the activation of oxygenated organic functions. In addition, it has high coordination number and quite large ionic radius compared to those of d-block transition metals. These properties should find some new reactions difficult to accomplish by any other existing methodologies. In this project, we have developed some SmI_2-promoted electron transfer reactions for the reduction and for the formation of carbon-carbon bonds.

V-I-1 A Facile Synthesis of *ortho*-Quinodimethanes

Junji INANAGA, Yuichi SUGIMOTO, and Takeshi HANAMOTO

Allenylsamarium compounds can easily be prepared from propargylic acetates by treating with SmI_2 in the presence of palladium catalyst under extremely mild conditions. When the mothod was applied to the reduction of suitably arranged (in 1,4-relationship) bifunctional propargylic acetates (e.g., derived from *ortho*-phthalaldehyde), the corresponding bis-allene compounds were produced and then readily underwent electrocyclic reaction with the migration of their double bonds to afford *ortho*-naphthoquinodimethanes as reactive and useful intermediates in organic synthesis. They were trapped intermolecularly with

a variety of dienophiles to give the corresponding Diels-Alder adducts (when R=H), caused [2+2] cycloaddition intramolecularly affording the naphthocyclobutene derivative (when R=Ph), or brought about 1,5-hydride shift to give the naphthalene derivative (when R=alkyl), respectively.

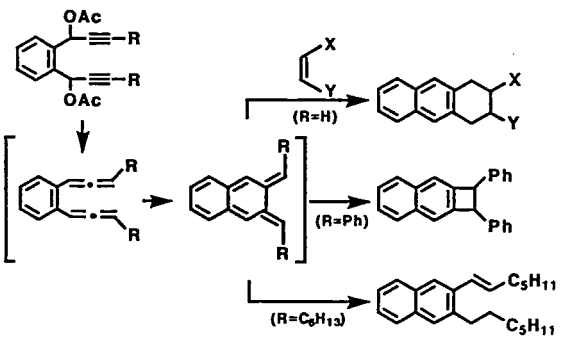

V-I-2 SmI_2-Promoted Ketyl Radical Addition to *O*-Benzyl Formaldoxime. A New Aminomethylation

Takeshi HANAMOTO and Junji INANAGA

[*Tetrahedron Lett.*, **32**, 3555 (1991)]

Reductive coupling of carbonyl compounds with *O*-benzyl formaldoxime was promoted by SmI_2 affording the corresponding aminomethyl alcohols under mild conditions. It is interesting from the mechanistic point of view that the reaction of 4-*tert*-butylcyclohexanone afforded a mixture of diastereomers with high axial-attack stereoselection, which may be interpreted in terms of the preferred configuration of the ketyl intermediate with orbital extension of the radical lobe in the axial direction. The N-benzyloxy group of the coupling products can easily be eliminated to form the corresponding free aminomethyl alcohols by platinum-catalyzed hydrogenolysis.

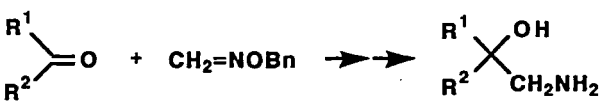

V-I-3 A Facile Reductive Dimerization of Conjugated Acid Derivatives with Samarium Diiodide

Junji INANAGA, Yuichi HANDA,* Takanori TABUCHI,* Kenji OTSUBO,* Masaru YAMAGUCHI,* and Takeshi HANAMOTO (**Kyushu University*)

[*Tetrahedron Lett.*, in press]

A variety of α,β-unsaturated esters instantaneously hydrodimerized at their β-position in either intermolecular or intramolecular fashion by use of the reduction system, SmI_2-THF-HMPA, in the presence of proton sources. The conjugated dienoic ester also dimerized at the γ-position with the migration of the remaining double bonds. The reaction of an α,β-unsaturated alkynic acid ester allowed an easy access to the 3,4-unsaturated adipic acid derivative. Very interestingly, a perfect stereoselection was realized in the reaction of N,N-dibenzyl crotonamide, in which the stereochemistry must be controlled on the coordination sphere of samarium.

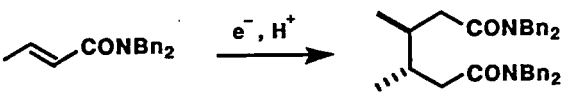

V-I-4 Selective Conjugate Reduction of α,β-Unsaturated Esters and Amides via SmI_2-Promoted Electron Transfer Process

Junji INANAGA, Shino SAKAI,* Yuichi HANDA,* Masaru YAMAGUCHI,* and Yasuo YOKOYAMA (**Kyushu University*)

[*Chem. Lett.*, in press]

α,β-Unsaturated esters and amides were rapidly and selectively reduced to the corresponding saturated ones under mild conditions without affecting coexisting isolated double or triple bonds by using the reduction system, SmI_2-N,N-dimethylacetamide-proton source. The use of bidentate ligands such as 1,2- or 1,3-diamine derivatives was also effective but in the presence of a tridentate chelating agent, N,N,N′,N″,N″-pentamethyldiethylenetriamine, by which the coordination sphere of samarium might be completely occupied, no reaction took place at all, which strongly indicates that the coordination of substrates to samarium(II) is crucial for the present electron transfer reaction.

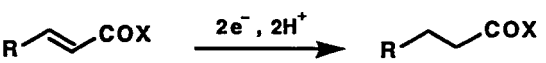

(X=OR', NR'_2)

V—J Development of New Organic Reactions Based on the Design of Reaction Intermediates

Some novel organic transformations which are designed on the basis of new reaction intermediates have been developed.

V-J-1 Utility of 3,4-Dimethoxybenzyl (DMPM) Glycoside. A New Glycosylation Triggered by 2,3-Dichloro-5,6-dicyano-*p*-benzoquinone (DDQ)

Junji INANAGA and Yasuo YOKOYAMA

A new type glycosylation which proceeds through the DDQ oxidation-triggered fragmentation of DMPM glycosides has been developed, the main features of which are: (i) DMPM group can be pivotally used as a protecting or an activating group; (ii) the activation is uniquely performed

via the formation of charge transfer complex; and (iii) the reaction is initiated at the remote position from Cl-carbon.

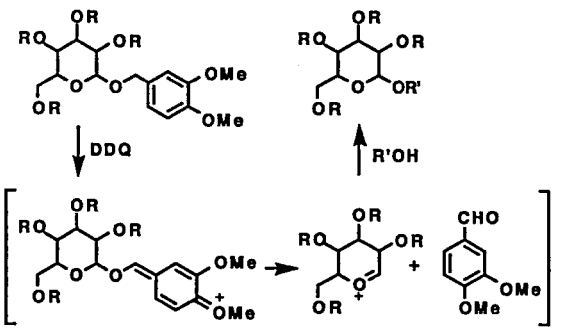

V-J-2 One-Pot Conversion of *O*-Acetylsugar Lactones into 2,3-Dideoxysugar Derivatives via Platinum-Catalyzed Hydrogenolysis

Junko KATSUKI and Junji INANAGA

[*Tetrahedron Lett.*, in press]

O-Acetylsugar lactones were cleanly converted into the corresponding 2,3-dideoxysugar derivatives at room temperature under an atmospheric pressure of hydrogen in the presence of triethylamine and platinum catalysts. The reaction seems to proceed through (i) elimination of the 3-acetoxyl group by triethylamine to give the 2-acetoxybutenolide (**A**), (ii) platinum-catalyzed hydrogenolysis of the 2-acetoxyl group leading to the butenolide (**B**), and (iii) hydrogenation of the remaining double bond. 2,3-Dideoxysugar lactones thus obtained would be useful for natural product synthesis not only as chiral synthons but also as templates for the preparation of other types of chiral nonracemic intermediates.

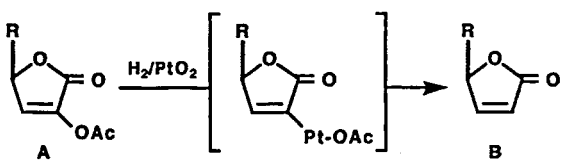

V-J-3 One-Carbon Reduction of Carbohydrates via Alkoxy Radical Fragmentation

Junji INANAGA, Yasuo YOKOYAMA, Takeshi HANAMOTO, and Yuichi SUGIMOTO

Generation and fragmentation of the alkoxy radical (**A**) of the hexopyranose (**1**) could nicely be promoted by iodobenzene diacetate and iodine under mild conditions to give the mixed acetal formate (**2**), which was further converted to the corresponding pentofuranose (**3**) by acid hydrolysis. The present one-carbon reduction offers a convenient and highly efficient route to lower carbohydrates with well-defined stereochemistry at the chiral centers.

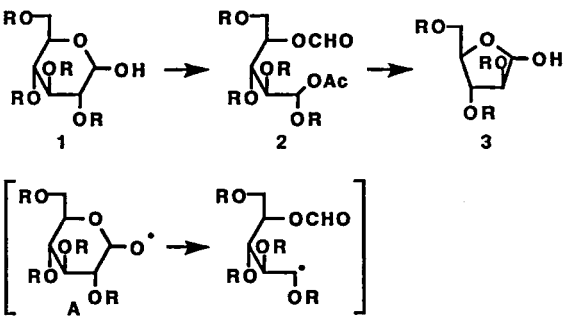

V-J-4 Phosphine(III)-Catalyzed Conjugate Addition of Alcohols to α,β-Unsaturated Alkynic Esters

Junji INANAGA, Yoshiyasu BABA, and Takeshi HANAMOTO

Conjugate addition of alcohols to α,β-unsaturated alkynic esters was easily performed with the aid of trialkylphosphine catalysts to give the corresponding 3-alkoxyacrylate derivatives, which are potentially useful synthetic intermediates with their contiguous three carbon unit of different oxidation states. Since phosphonium ester enolates, designed as new reaction intermediates, are readily prepared from α,β-unsaturated alkynic and alkenic acid derivatives under neutral conditions, they should find further applications. We are presently pursuing new synthetic reactions revolving around this strategy.

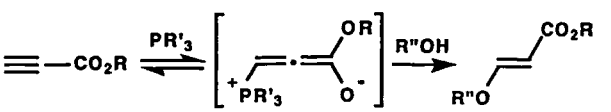

RESEARCH ACTIVITIES VI
Department of Vacuum UV Photoscience

VI—A Development of High-Resolution Laser Photoelectron Spectroscopy for Excited-State Molecules

During the last decade, in this Institute we have developed 'laser excited-state photoelectron spectroscopy' using REMPI (resonantly enhanced multiphoton ionization), and applied it to various jet-cooled molecules and molecular complexes. With such a laser photoelectron technique, it is possible not only to study radiative and non-radiative excited states but also to perform cation spectroscopy for various molecular species. [See, K. Kimura, *Adv. Chem. Phys.*, **60**, 161 (1985); *Intern. Rev. Phys. Chem.*, **6**, 195 (1987)].

Recently we have developed a compact and high resolution threshold photoelectron analyzer with which threshold photoelectrons are collected with a resolution of 1—2 cm^{-1} as a function of laser wavelength. The technique is equivalent to so-called ZEKE (zero kinetic energy) photoelectron spectroscopy. In this project we have concentrated mainly on 'cation vibrational spectroscopy' by means of a two-color (n+1') REMPI photoelectron technique, in which the excitation laser is fixed while the ionization laser is scanned during the threshold photoelectron measurements.

VI-A-1 MPI Ion-Current and Photoelectron Spectra of Jet-Cooled *p*-Phenylenediamines

Hiroyuki OZEKI, Katsuhiko OKUYAMA, Masahiko TAKAHASHI, and Katsumi KIMURA

[*J. Phys. Chem.* **95**, 4308 (1991)]

One- and two-color (1 + 1) resonant ionization experiments were carried out for *p*-phenylenediamine (PD), N,N-dimethyl-*p*-phenylenediamine (DMPD), N,N,N',N'-tetramethyl-*p*-phenylenediamine (TMPD) under conditions of isolated molecules. An MPI ion-current spectrum of PD shows many sharp bands consisting of several vibrational progressions with the S_1 origin (0_0^0) at 29824 cm^{-1}, while the photoelectron spectra due to the ground state (D_0) of PD^+ show a few progressions with the 0^+ peak at 54640 cm^{-1}. All these progressions have been interpreted in terms of the a_g vibrational modes in the S_1 and D_0 states of PD. The vibrational frequencies of the NH_2 out-of-plane mode are 489 cm^{-1} (S_0), 598 cm^{-1} (S_1), and 1034 cm^{-1} (D_0). An MPI spectrum of DMPD shows a well-resolved vibrational structure in the low-energy region and many congestion bands in the higher region; while that of TMPD shows no vibrational structure. These facts suggest that the geometrical changes in the S_1 state increases with the number of CH_3 groups. For a mixture of PD with acetonitrile in jets, a preliminary result supporting a molecular complex has been obtained, indicating a red shift of 207 cm^{-1} in the S_1 region of PD and a progression of 24 cm^{-1}, which is probably due to an intermolecular vibrational mode of the PD-acetonitrile complex.

VI-A-2 A New High-Resolution Threshold Photoelectron Analyzer: Observation of Rotational Structure of NO^+ Cation

Masahiko TAKAHASHI, Hiroyuki OZEKI, and Katsumi KIMURA

[*Chem. Phys. Lett.* **181**, 255 (1991)]

A new compact high-resolution photoelectron analyzer has been designed and constructed for the purpose of collecting threshold photoelectrons through a capillary plate.

Two-color (1+1') REMPI experiments have been carried out on jet-cooled NO via the A $^2\Sigma^+$ state (v'=0, N'=7). The resulting threshold photoelectron spectrum was obtained with a resolution of 4 cm^{-1}, as shown in Figure 1, indicating seven "rotational peaks" due to the v^+=0, N^+=4—10 levels of NO^+ ($^1\Sigma^+$) produced by ionization transition of ΔN=0, ±1, ±2 and ±3.

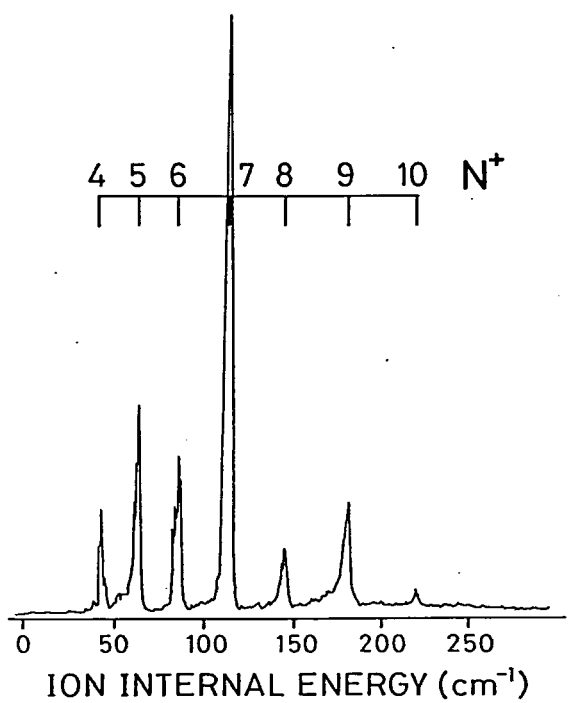

Figure 1. Threshold photoelectron spectra of NO obtained *via* the Rydberg $A^2\Sigma^+$ state (v'=0, N'=7) at several different pulsed electric fields: (a) −1, (b) −2, (c) −3, (d) −4, and (e) −5 V/cm. Each spectrum shows several rotational peaks due to the v^+=0 N^+=4 ~ 10 levels of NO^+ ($^1\Sigma^+$) produced by the ionization transitions of ΔN=0, ±1, ±2 and ±3.

VI-A-3 Molecular Ion Vibrational Spectroscopy by a Time-Resolved REMPI Threshold Photoelectron Technique

Masahiko TAKAHASHI and Katsumi KIMURA

[*Proceeding of the 5th Intern. Conf. on Time-Resolved Vibrational Spectroscopy* (Tokyo, 1991), in press]

We have successfully measured high-resolution threshold photoelectron spectra of several molecules with a few cm^{-1} of energy resolution using two new types of compact threshold photoelectron analyzers. One is a capillary-type[1] and the other is a deflection-type, as shown schematically in Figure 1. The deflection-type is 10 times brighter compared to the capillary-type, whereas the latter is easier to handle.

Two-color (1+1') REMPI threshold photoelectron spectroscopy has been applied to study the cation of the (phenol-water) complex. From the photoelectron spectrum obtained *via* the S_1 origin of the (phenol-water) complex, the adiabatic ionization potential has been determined as 64015 ± 4 cm^{-1}, which is 4606 cm^{-1} lower compared with phenol. The main photoelectron vibrational progression is due to the intermolecular stretching vibrational mode with a frequency of 240 cm^{-1}. From the anharmonicity of this mode, we have obtained the dissociation energy (hydrogen bond energy) of the (phenol-water)$^+$ complex cation; $D_e(D_0) = 6021$ cm^{-1}. In addition, we have obtained the dissociation energies of neutral phenol-water complex in the S_1 and S_0 state as follow, $D_e(S_1)$=1723, and $D_e(S_0)$=1367 cm^{-1}.

Reference

1) M. Takahashi, H. Ozeki and K. Kimura, *Chem. Phys. Lett.* **181**, 255 (1991).

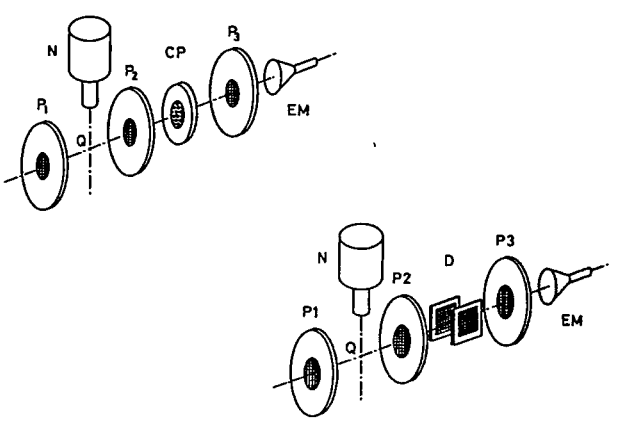

Figure 1. Two threshold photoelectron analyzers: (a) capillary-type and (b) deflection-type. The capillary-type analyzer consists of a pair of electrodes (P_1, P_2), a capillary plate (CP), a ground electrode (P_3), and an electron multiplier (EM Ceratron). A capillary plate of l/d=20 has been used, positioned 10 mm from the ionization point (Q), where l and d are the length and the diameter of the capillary hole, respectively. On the other hand, the deflection-type analyzer has a pair of deflection plates (D) in stead of the capillary plate.

VI-A-4 Vibrational Spectra of Jet-Cooled Ar-NO and Phenol-Water Cations

Masahiko TAKAHASHI and Katsumi KIMURA

Some low-frequency vibrational progressions have been successfully observed for the cations of the Ar-NO van der Waals complex and the phenol-H_2O complex formed in supersonic jets from two-color REMPI threshold photoelectron measurements.

Concerning the Ar-NO complex, the following evidences have been deduced. 1) The adiabatic ionization energy I_a=73869 ± 6 cm^{-1} (9.159 ± 0.01 eV). 2) The two low-frequency progressions give rise to ν_2^+=94 cm^{-1} and ν_3^+=79 cm^{-1}. 3) The ν_2^+ spacings are 94, 84, 78, and 72 cm^{-1}, while those of the ν_3^+ spacing are 79, 76, and 75 cm^{-1}, the both progressions showing considerable anharmonicities.

Concerning the phenol-H_2O complex, the following evidences have been deduced from the resulting threshold photoelectron spectrum shown in Figure 1. 1) I_a=64015 ± 4 cm^{-1}, given by $h\nu_1$ (35995 cm^{-1}) + $h\nu_2$ (28020 cm^{-1}), essentially the same as that (64025 ± 4 cm^{-1}) recently reported by Reiser *et al.*[1] 2) The spectrum in Figure 1 consists of four peaks with spacings of 241, 237, and 231 cm^{-1}, attributed to the intermolecular O-H stretching mode of the cation (phenol-H_2O)$^+$.

Reference

1) G. Reiser, O. Dopfer, R. Lindner, G. Henri, K. Müller-Dethlefs, E.W. Schlag and S.D. Colson, *Chem. Phys. Lett.* **181**, 1 (1991).

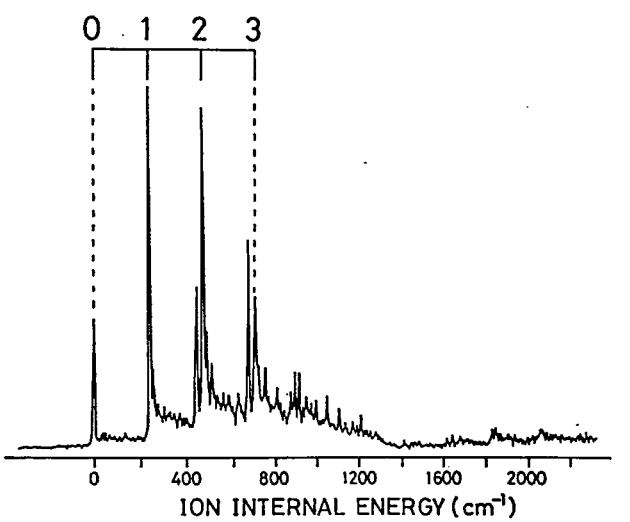

Figure 1. A two-color (1+1') REMPI threshold photoelectron spectrum of the phenol-H_2O complex, obtained *via* the lowest excited electronic state (S_1) at the intermolecular stretching vibrational level, v'=0, showing the vibrational progression of the cation (phenol-H_2O)$^+$.

VI-A-5 Two-Color Threshold Photoelectron Spectroscopy: Cation Vibrational Spectroscopy

Masahiko TAKAHASHI, Katsuhiko OKUYAMA, and Katsumi KIMURA

[*J. Mol. Struct.*, **249**, 47 (1991)]

It is demonstrated that a capillary-type threshold photoelectron analyzer capable of an energy resolution of $\pm 1-2$ meV in two-color (1+1′) resonance ionization is useful to study gas-phase cation vibrational spectroscopy, especially for studying low-frequency vibrational modes. The first example studied here is toluene. It has been found that several observed photoelectron vibrational bands due to the toluene cation show good correlation with our *ab initio* calculations.

The second example studied is *n*-propylbenzene. The rotational isomers *trans* and *gauche* of the *n*-propylbenzene cation have clearly distinguished from our threshold photoelectron measurements. It has been found that the *trans* and *gauche* isomers of this cation show quite different vibrational spectra in the low frequency region.

VI-A-6 REMPI Threshold Photoelectron Spectra of the *cis* and *trans* Rotational Isomers of Jet-Cooled *m*-Chlorophenol

Martin C.R. COCKETT, Masahiko TAKAHASHI, Katsuhiko OKUYAMA, and Katsumi Kimura

[*Chem. Phys. Letters*, in press]

Laser REMPI threshold photoelectron spectra have been recorded by exciting the origins of the S_1-S_0 transition for both the *cis* and *trans* rotational isomers of *m*-chlorophenol (see Figure 1). The most intense feature in each spectrum is the peak corresponding to the transition to the $v^+=0$ level in the ion, thereby satisfying the $\Delta v=0$ propensity rule. The position of each of these two peaks (ω_2=34041 $\pm$ 5 cm^{-1} and 34138 $\pm$ 5 cm^{-1}) represents the lowest energy required to ionize each isomer from its S_1 origin. The ionization energy I_a for each isomer can thus be calculated by adding these values to the energies of the respective S_1 band origins. This yields I_a values for the *cis* and *trans* isomers of 69810 $\pm$ 10 cm^{-1} (8.655 $\pm$ 0.001 eV) and 70027 $\pm$ 10 cm^{-1} (8.682 $\pm$ 0.001 eV), respectively. A provisional assignment of the vibrational structure recorded in the threshold photoelectron spectra for the two isomers is given in the figure. Threshold photoelectron spectra were also recorded by exciting the $10b_0^2$ and $9a_0^1$ levels in both isomers as well as the $6a_0^1$ level in the *cis* isomer only. In each case the dominant vibration excited in the ion retained the character of the vibrational mode pumped in the S_1 state.

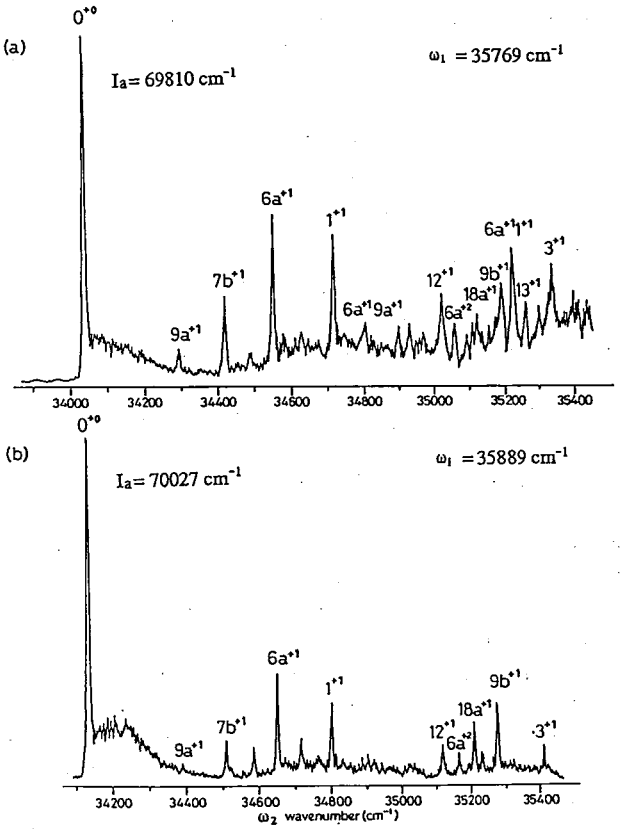

Figure 1. Threshold photoelectron spectra recorded by exciting the S_1 band origins of (a) the *cis* isomer and (b) the *trans* isomer of *m*-chlorophenol.

VI-A-7 Absence of Photoelectron Spectroscopic Evidence for 'Proton Tunneling' in the Cation Ground State of Jet-Cooled Tropolone

Hiroyuki OZEKI, Masahiko TAKAHASHI, Katsuhiko OKUYAMA, and Katsumi KIMURA

[*J. Chem. Phys*, in press]

Spectroscopic splittings showing the proton tunneling, so-called 'tunneling splitting', have been reported for molecules having intramolecular hydrogen bonds. Among these molecules, tropolone is the most typical one. In the present work, we measured high-resolution threshold photoelectron spectra of jet-cooled tropolone, combined with a two color REMPI technique, to investigate the proton tunneling in the cation ground state (D_0).

Two-color (1+1′) threshold photoelectron spectra obtained via S_1 0^0 and H^1 are shown in Figure 1, as a function of the total energy ($\omega_1+\omega_2$). The 0^0 and H^1 levels show the tunneling doublet in the S_1 state. If the proton tunneling occurs in the cation D_0 state, an energy shift should be observed between the 0^0 and H^1 excitation photoelectron spectra. This energy shift reflects the difference in the doublet separation between the S_0 and D_0 states. However, as shown from figure 1, the energy shift is not observed within our experimental accuracy of 2 cm^{-1}. The present experimental results represent the clear evidence of inhibition of proton tunneling in the cation D_0 state.

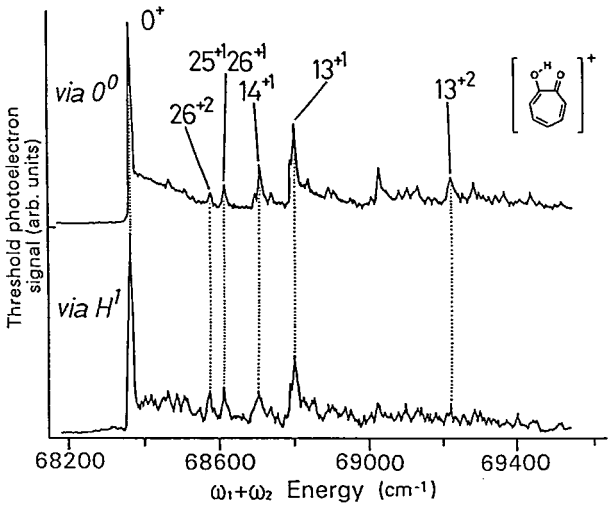

Figure 1. Threshold photoelectron spectra of jet-cooled tropolone obtained by (1+1′) REMPI via the S_1 0^0 and H^1 levels.

VI-A-8 Study on the Torsional Larg-Amplitude Motion of Diphenylacetylene in the Ground State of the Cation

Katsuhiko OKUYAMA, Martin C. R. COCKETT, and Katsumi KIMURA

The torsional large-amplitude motions of *p*-polyphenyl compounds are governed by the balance between the steric hindrance of orth hydrogens and the planarity due to π electron conjugation. In the case of diphenylacetylene (DPA), since the steric hindrance is negligibly small, the torsional motion largely depends on the π electron conjugation through the triple bond between the benzene rings. Therefore, the barrier height of the torsional motion or the internal rotation directly reflects strength of the conjugation. DPA is the simplest molecule valuable the strength. In the neutral DPA the barrier heights in the electronically excited states and the ground state have been reported as shown in Table 1.[1)]

Recently a compact high-resolution threshold electron analyzer has been developed in this laboratory.[2)] By using this analyzer we attempted to observe the torsional motion of DPA in its cation ground state. Figure 1 shows the whole feature of the threshold electron spectrum of jet-cooled DPA, obtained via the 0^0 level of the low-lying excited state ($^1B_{2u}$). The adiabatic ionization potential was obtained to be 63917 ± 4 cm^{-1} (7.925 ± 0.001 eV). The transition due to the torsional motion appears at 107 cm^{-1} that was assigned as its level with 2 quanta level of it. By exciting the T^4 level of the $^1B_{2u}$ state the energy level with 4 quanta was obtained at 213 cm^{-1}. From these frequencies we obtained a barrier height of 1980 cm^{-1} for the cation ground state.

References

1) K. Okuyama, T. Hasegawa, N. Mikami, and M. Ito, *J. Phys. Chem.*, **88**, 1711 (1984).
2) M. Takahashi, K. Okuyama, and K. Kimura, *J. Mol. Struct.*, **249**, 47 (1991).

Table 1. Comparison of barrier height to torsional motion

Electronic State	T_e (cm^{-1})	2 Quanta Level (cm^{-1})	Barrier Height (cm^{-1})	
D_0 ($^2B_{1g}$)	63917	107	1980	this work
($^1B_{1u}$)	35248	96	1590	ref. 1)
S_1 (^1A_g)	34960	79	1080	ref. 1)
($^1B_{1u}$)	~33000	86	1280	ref. 1)
S_0 (^1A_g)	0	34	202	ref. 1)

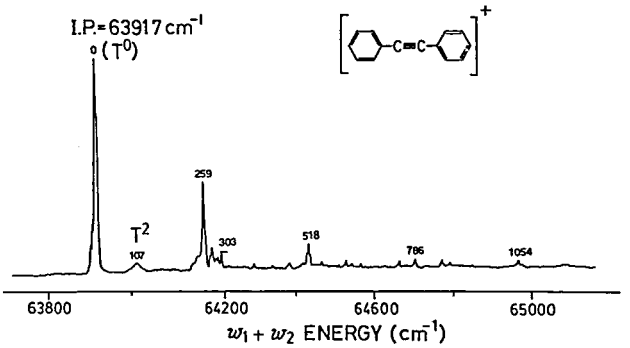

Figure 1. Threshold photoelectron spectrum obtained by REMPI with the 0^0 level in the low-lying $^1B_{2u}$ state of jet-cooled diphenylacetylene.

VI-A-9 Two-color (2+1′) REMPI Threshold Photoelectron Study of the Ar-NO van der Waals Complex: Observation of Intermolecular Vibrational Progressions of the Ar-NO$^+$ Cation

Masahiko TAKAHASHI

[Submitted, *J. Chem. Phys.*]

Two-color (2+1′) REMPI high-resolution threshold photoelectron spectroscopy has been applied to the Ar-NO van der Waals complex in a supersonic free jet. The resonant ionization process studied may be expressed by Ar-NO ($X^2\Pi_{1/2}$, $v''=0$) + $2h\nu_1$ → Ar-NO* ($C^2\Pi$, v') + $h\nu_2$ → Ar-NO$^+$ ($X^1\Sigma^+$, v^+). Two strong anharmonic vibrational progressions have been observed in the threshold photoelectron spectra which are shown in Figure 1 having frequencies of 79 and 94 cm^{-1}. These vibrations have been assigned to the intermolecular bending and stretching motions of the (Ar-NO)$^+$ complex cation. From the threshold photoelectron spectra, the adiabatic ionization potential of Ar-NO has been determined as 73869+6 cm^{-1} (86 cm^{-1} higher than previously reported[1)]), and the dissociation energy of the (Ar-NO)$^+$ cation has been calculated as 1001 cm^{-1}. The structural change of Ar-NO that occurs on photoionization has been calculated with the aid of simple Franck-Condon calculations, which suggest that the intermolecular bond distance of Ar-NO decreases by −1.03 A, while the O-N-Ar angle increases by 11.3 degrees.

Reference

1) K. Sato, Y. Achiba and K. Kimura, *J. Chem. Phys.* **81**, 57 (1984).

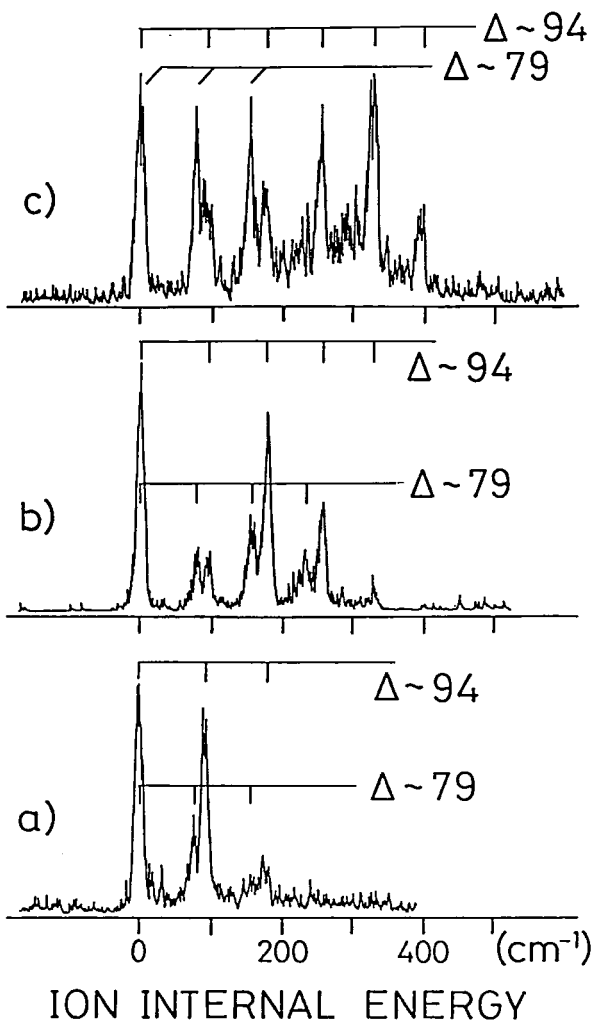

Figure 1. Two-color (2+1′) REMPI threshold photoelectron spectra of Ar-NO, obtained via the three intermolecular stretching vibrational levels in the $C^2\Pi$ state: (a) $v'=0$, (b) $v'=1$, and (c) $v'=2$.

VI-A-10 Two-Color (1+1′) REMPI Threshold Photoelectron Study of *trans*-Stilbene

Masahiko TAKAHASHI and Katsumi KIMURA

Two-color (1+1′) REMPI threshold photoelectron spectroscopy has been applied to *trans*-stilbene, which is the typical molecule with an isomerization channel in the S_1 state. The resulting threshold photoelectron spectra obtained via the 25^1, 25^2, and 25^3 levels in the S_1 state are shown in Figure 1. (The *ns* Nd-YAG pumped dye lasers were used as the excitation and ionization sources.) The photoelectron spectra were obtained at the S_1 state of *trans*-stilbene after its IVR has been completed. Some effects of IVR mainly appear around the $\Delta v=0$ bands as satellite bands in Figure 1, since the low frequency modes play an important role in IVR processes.

From the threshold photoelectron spectra obtained *via* the several vibrational levels in the S_1 state, the ionization potential of *trans*-stilbene has been determined to be 61379 ± 4 cm^{-1}. In addition, we have obtained the several vibrational frequencies of the *trans*-stilbene cation, on the basis of the threshold photoelectron spectra.

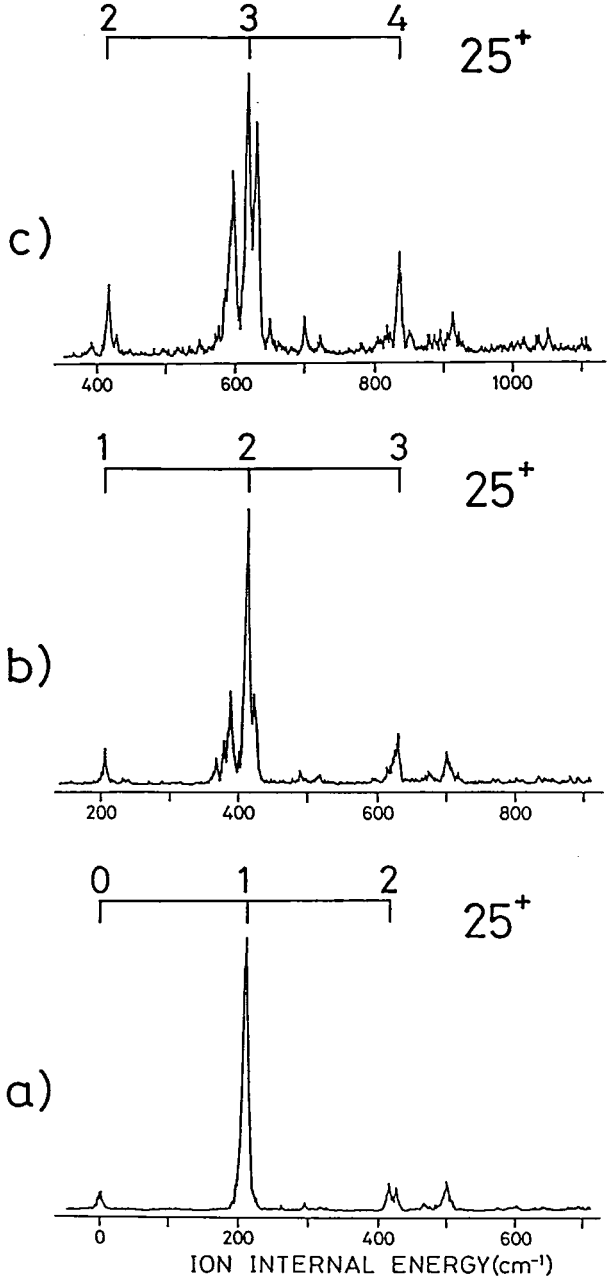

Figure 1. The resulting threshold photoelectron spectra of *trans*-stilbene obtained via the 25^1, 25^2, and 25^3 levels in the S_1 state.

VI-A-11 Two-Color (1+1′) REMPI Threshold Photoelectron Study of the Aniline-$(Ar)_n$ (n=1, 2) van der Waals Complex Cations: Observation of the van der Waals Vibrations

Masahiko TAKAHASHI, Hiroyuki OZEKI, and Katsumi KIMURA

Although the van der Waals (vdW) interaction plays an important role in the collisional and half-collisional relaxations of vibrationally excited molecules, there are few studies for molecular cations. Experimental information about the potential surface around the potential minima should be obtained from photoelectron vdW vibrational progressing in the low-frequency region. For this purpose, it is valuable to observe threshold photoelectron spectra of the vdW complexes. Threshold photelectron spectra of the aniline-$(Ar)_n$ complexes (n=1, 2) obtained via S_1 origins

are shown in Figure 1 around the ionization thresholds. The vdW vibrational progressions with frequencies of 16 and 11 cm^{-1} are observed in Figure 1 (b) and (c), respectively. We have tentatively assigned the former as the vdW bending vibration of the (aniline-Ar)$^+$ cation in which the Ar atom moves to the amino group, and the latter as the vdW bending vibration of the (aniline-Ar_2)$^+$ cation in which two Ar atoms move to the amino group symmetrically.

Another interesting point is the shift in the ionization potentials (I_a) of these vdW complexes. From the spectra in Figure 1, we have obtained shifts of 113 and 222 cm^{-1} for the aniline-Ar_n (n=1, 2), respectively. It seems that the I_a shift of aniline obey the additivity law of Ar.

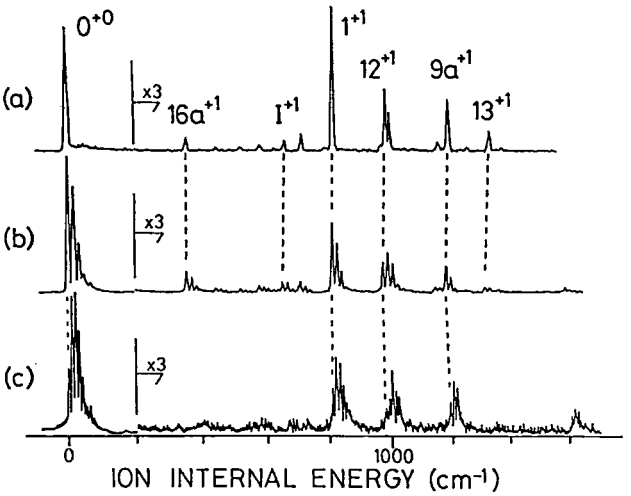

Figure 1. Threshold photoelectron spectra of aniline and the aniline-$(Ar)_n$ van der Waals complexes (n=1, 2), obtained by two-color (1+1') REMPI *via* the S_1 origins of (a) aniline, (b) the aniline-Ar complex, and (c) the aniline-Ar_2 complex.

VI—B Synchrotron Radiation Researches of Molecules and Molecular Clusters: Photoionization and Photoelectron Spectroscopy

The use of synchrotron radiation is attractive for studying photoionization and photoelectron spectroscopy of gaseous atoms, molecules and molecular clusters produced in supersonic jets. For this purpose, we have been using two kinds of synchrotron-radiation photoionization apparatuses connected with the 750-MeV electron storage ring (called UVSOR) in this Institute. One is a molecular-beam apparatus on beamline BL2B2 [K. Kimura, Y. Achiba and H. Shiromaru, *Rev. Sci. Instrum.* **60**, 2205 (1989)], using a multi-stage differential pumping system without using any window materials between the molecular-beam apparatus and the storage ring. The other is an undulator-radiation PEPECO apparatus on beamline 3A2 [K. Okuyama, J.H.D. Eland and K. Kimura, *Phys. Rev.* **A 41**, 4930 (1990)], constructed to study doubly charge ions of gasous atoms and molecules as well as to perform coincidence measurements of two photoelectrons.

VI-B-1 Energy Partitioning in the Dissociation Reaction $Ar_3^+ \rightarrow Ar_2^+ + Ar$

Kenji FURUYA, Takato HIRAYAMA *(Gakushuin Univ.)*, **and Katsumi KIMURA**

We have observed the threshold-photoelectron photoion coincidence (TPEPICO) spectra of argon clusters at several kinds of excitation energies on the beamline BL2B2 in the UVSOR Facility. Figure 1 shows Ar_2^+ peaks in the TPEPICO spectra at 80.00 nm and at the stagnation pressure of 2620, 1970, and 1310 Torr. All the peak shapes of the Ar_2^+ appearing in the TPEPICO spectra were simulated with two Gaussian functions, where one Gaussian function was used to simulate the component due to the ionization of argon dimer. The observed peak shapes agree very well with the simulated ones, this fact implying that the excess energy in the Ar_3 ionization and the successive dissociation is thermally or quasithermally partitioned into the translational energies of the fragment species. From the estimation of the average kinetic energies of Ar_2^+ we have found that the fraction of the total translational energy of the fragment species to the excess energy in Ar_3^+ depends on the excitation energy, and that the fraction is slightly smaller than the value expected from the statistical theory, 40%. We have also found that Ar_3^+ produced by single photon ionization of Ar_3 completely dissociates in the excess energy range 0.3–1.1 eV.

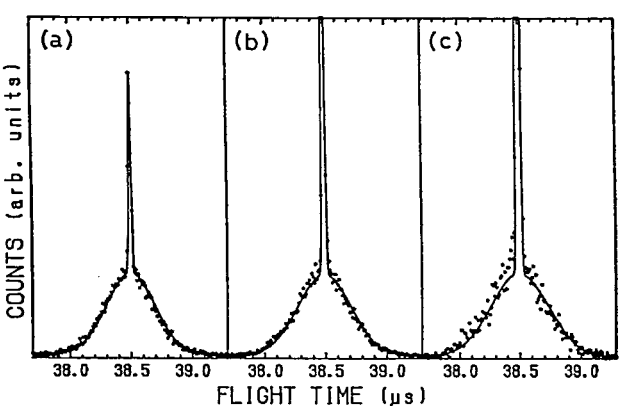

Figure 1. Ar_2^+ peaks in the TPEPICO spectra of Ar clusters at 80.00 nm under the stagnation pressure of (a) 2620 Torr, (b) 1966 Torr, and (c) 1310 Torr. Dot and solid lines are the observed and simulated peaks, respectively.

VI—C Molecular Beam Studies of Gas Phase and Surface Reaction Dynamics

In the present project we investigate dynamics of bimolecular reactions using a crossed molecular beam technique and surface reaction dynamics using molecule-surface scattering techniques. Experimental data obtained in this project are angular and velocity distributions of the scattered species detected by a rotatory quadrupole mass spectrometer using a TOF techniques as functions of reactant collision energy and, in the case of surface reactions, surface conditions such as substrate temperature, incident angle, and surface structure and coverage. We are interested in obtaining interaction energies between a molecule and a characterized surface in relation to the reactivities.

VI—D Vacuum UV Photochemistry of Molecules and Clusters

In the present project we seek to obtain detailed information about, 1) photodissociation dynamics of simple molecules, 2) production of emitting species from highly excited molecules, and 3) photochemistry of excited van der Waals (vdW) molecules and clusters formed in a supersonic expansion. The techniques applied are absorption and fluorescence spectroscopies of gaseous molecules and vdW molecules on an apparatus constructed on the beam line BL2A of UVSOR facility. In particular we use fluorescence excitation, fluorescence polarization, and dispersed fluorescence spectroscopies as our main detection techniques to identify the product species and obtain information on the dynamics of photochemical reactions.

VI-D-1 Absorption and Fluorescence Studies of Molecules and Clusters

Kosuke SHOBATAKE, Atsunari HIRAYA *(UVSOR),* **Kiyohiko TABAYASHI, and Toshio IBUKI** *(Kyoto Univ. of Education)*

[*Vacuum Ultraviolet Photodissociation of Molecules and Clusters*, ed. by C.Y. Ng (World Scientific, Singapore, 1991) p. 503]

Absorption and fluorescence spectroscopic studies of molecules and molecular clusters using vacuum UV light were reviewed. In particular the results obtained for the direct absorption spectra of benzene molecules and clusters and rare gas-chlorine molecular complexes on the gas-phase photochemistry apparatus on the beamline BL2A of UVSOR are presented along with the photodissociative excitation processes of various molecules in the gas phase, such as halogenated methanes, organometallic compounds, HNCO, and cynocompounds. Also included are polarization studies of and the deuterium isotope effects for photodissociative excitation processes, two-electron excitation processes in H_2 by Hatano and his coworkers, fluorescence from doubly charged ions, NO^{2+} and O_2^{2+}, and high-resolution absorption spectroscopy of Kr atom by Itoh and Namioka at Photon Factory (PF). At the end excimer formations in the reaction of photoexcited molecules and also fluorescence studies of photoexcited rare gas-dihalide van der Waals molecules are discussed.

VI-D-2 Photochemistry of Rare Gas-Dihalogen van der Waals Molecules. III. VUV Excitation Dynamics of Xenon Dichloride ($XeCl_2$)

Kiyohiko TABAYASHI, Atsunari HIRAYA *(UVSOR),* **and Kosuke SHOBATAKE**

So far, we have found the following two types of new van der Waals (vdW) molecular bands in the VUV region, originated from (1:1) Xe-Cl_2, in free jets of regulated Cl_2/Xe/Ne mixtures.

(A) The Xe-Cl_2 complex exhibits relatively strong broad structureless absorption bands (**A bands**) in the 125—150 nm region[1], with very weak fluorescence intensity from the relevant excitation (Figure 1a). The **A bands** have been assigned as excited states of ion-pair $XeCl^+Cl^-$ type. Very low quantum yields (less than 5%) for the fluorescent channels observed can be attributed to (pre-)dissociation of the photoexcited vdW complex to the non-fluorescent dissociation products (Xe+2Cl) via highly vibrationally excited states and then followed by curve-crossing to repulsive potential surfaces,

$$Xe\text{-}Cl_2 + h\nu \rightarrow XeCl^+Cl^-(v'=m) \rightarrow Xe + 2Cl.$$

(B) When only the fluorescence is monitored between 230 and 400 nm using a band-pass filter which covers the excimer emissions, XeCl(C-A, B-X) and $Cl_2(2^3\Pi_g\text{-}1^3\Pi_u)$, vibrationally structured Xe-Cl_2 bands (**B bands**) are observed in the excitation spectrum (Figure 1b). A large vibrational spacing of $\Delta\nu \simeq 640$ cm^{-1} is resolved for the **B bands**, which is indicative of the excited state of Rydberg-type Cl_2^* character. We propose that two kinds of excimer formation channels contribute to the emissions in the 230—400 nm region:

$$Xe\text{-}Cl_2 + h\nu \rightarrow Xe\text{-}Cl_2^* \rightarrow XeCl^* + Cl$$
$$\rightarrow Xe + Cl_2^*(2^3\Pi_g).$$

Reference

1) K. Tabayashi, A. Hiraya, and K. shobatake, *UVSOR Activity Report 1990*, **18**, 21 (1991).

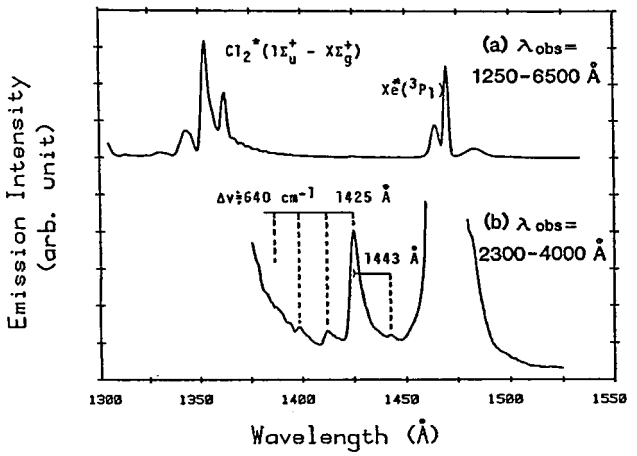

Figure 1. Fluorescence excitation spectra of free jets of Cl_2/Xe mixtures under two conditions for emission detection. **a)** Spectrum obtained using Hamamatsu R585MGF2 PMT which covers detection range 125–650 nm. Stagnation conditions: 4.6% Cl_2/Xe mixture at P_0=265 Torr and T_0=1°C. **b)** Spectrum obtained through a bandpass filter with transmission range 230–400 nm. Stagnation conditions: 2.4% Cl_2/Xe mixture at P_0=265 Torr and T_0=2°C.

VI-D-3 Vacuum UV Fluorescence Measurements of SOR-Light Excited Rg_n and Rg_n-Cl_2 by SMA Spectroscopy

Kiyohiko TABAYASHI, Atsunari HIRAYA *(UVSOR),* **and Kosuke SHOBATAKE**

A Spectrometric Multi-channel Analyzer (SMA) equipped with an MCP intensified CCD detector has been installed in BL2A system of UVSOR facility to measure dispersed radiation/fluorescence from energized gaseous species formed from UV photoexcited processes. It has been first applied to vacuum UV photochemical studies of Rg_n and Rg_n-Cl_2 clusters and complexes using a McPherson 218 Monochromator for UV/VUV fluorescence analyses.

Figure 1 shows a sample fluorescence spectrum from Xe_n* clusters (average size n ≃ 200), generated by free jet expansion of Xe gas and excited with monochromatized SOR light. Although the emission was analyzed with low spectral resolution (~3 nm) under selective excitation of Xe_n cluster band[1] at 148.2 nm, free-exciton (FE) emission in the resonant region and Stokes-shifted broad band emission of self-trapped (ST) exciton can be clearly seen. A relatively long-red tail of FE band is also indicative of a superimposition with phonon-coupled sidebands. The present results show the direct evidence that the same excitation and radiative relaxation mechanisms as in solid crystals are applicable in Xe_n clusters with $200 < n < 1000$.

Reference

1) K. Tabayashi, A. Hiraya, and K. Shobatake, *UVSOR Activity Report 1990,* **18,** 23 (1990).

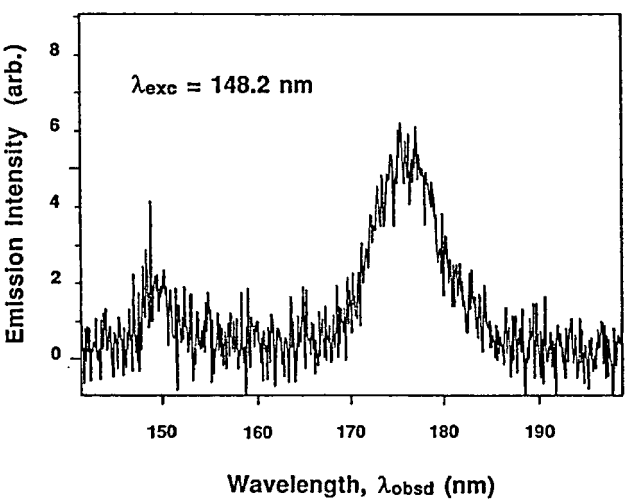

Figure 1. VUV emission spectrum of SOR-light excited Xe_n* clusters. Clusters were excited at 148.2 nm. Spectral resolution of SMA system is 3 nm.

VI—E Synchrotron Orbital Radiation-Excited Surface Reactions

In this project we study synchrotron radiation-excited surface reactions such as etching reactions of semiconductor materials and thin film formations by photochemical vapor deposition (photo-CVD). In the case of etching reactions of semiconductor surfaces we seek to clarify their mechanisms so that one can "control" or find the optimum conditions for the etching reactions and photochemical vapor depositions which are essentially of consecutive nature.

VI-E-1 Etchantless etching of SiO_2 by Synchrotron Radiation

Haruhiko OHASHI*, Kenichi KATO*, Akira YOSHIDA*, *(*Toyohashi Univ. of Tech.),* **and Kosuke SHOBATAKE**

Synchrotron radiation-excited etching of SiO_2 surface without using an etchant gas at ambient temperature was previously resported.[1] As more experiment was continued, it has been found that the etching rate defined as the etched depth divided by the accumulated dose (in the units of accumulated current · minute) was found to be not independent upon the accumulated dose. It was thus suspected that the etched depth measured by the wavelength dependence of the interference pattern might not correspond to the material removed but be due to a change in the refractive index given rise to by radiation. Therefore we measured the temperature dependence of the etching rate when SiO_2 surface was irradiated by pseudomonochromatic undulator radiation whose first order wavelength was 248 Å ($h\nu$=50 eV) as shown in Figure 1. The activation energy for the etching rate in the temperature range above 300°C was estimated to be 0.3 eV, which can be compared with a value (0.62 eV) obtained by Urisu and his coworkers when the white light was irradiated upon SiO_2 surface at PF. The quantum yield for etching reaction at 390°C was only 0.01%, which fact indicates the presence of very low fraction of predissociated Si-O by thermal excitation. This process is very fascinating and more experiments are underway.

Reference
1) H. Ohashi, K. Kato, A. Yoshida, and K. Shobatake, *UVSOR Activity Report*, (UVSOR, IMS, 1991) p.59.

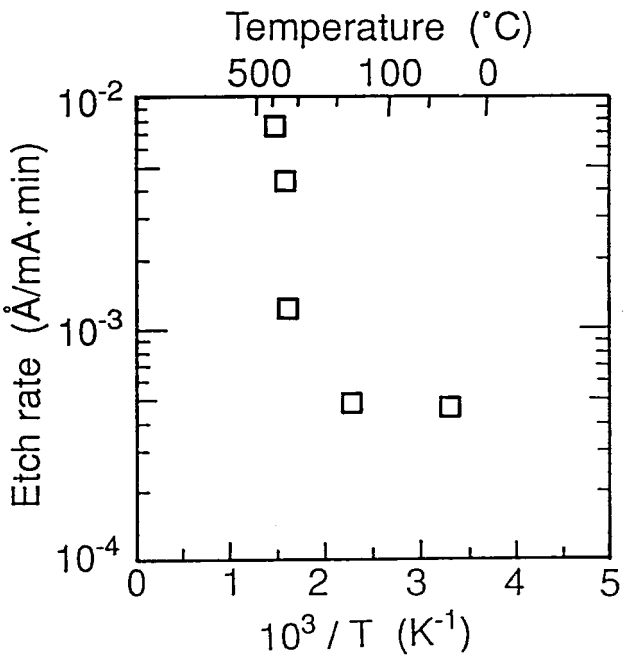

Figure 1. Etch rate vs. substrate temperature of undulator radiation-excited SiO_2 surface without an etchant at the excitation wavelength λ_{exc}=248 Å. The apparent activation energy above 300°C has been estimated as 0.3 eV.

VI-E-2 SF_6 Pressure Dependence of the Etch Rate of Synchrotron Radiation-Excited β-SiC(220) Oriented Polycrystalline Surface

Haruhiko OHASHI*, Akira YOSHIDA* *(*Toyohashi Univ. of Tech.)*, **Eiji ISHIGURO** *(City Univ. of Osaka and UVSOR)*, **Kazuo SANO**, Masaru KOEDA**, Tetsuya NAGANO**** *(**Shimadzu Corp.)*, **and Kosuke SHOBATAKE**

In order to obtain information upon the wavelength dependence of the etching rate of the β-SiC(220) oriented polycrystalline surface by SF_6, the pressure dependence of the etch rate was measured, though it is an indirect method to change the spectrum of irradiated photons upon the surface. Figure 1 shows the micrograph of the SiC surface with 500 lines/mm. Since an SiC surface is known to be hard to etch, the etch rate obtained is weaker than the SiO_2 surface by about a factor of 1/10. Although the data are scattered due to small number of runs, the etch rate tends to increase as the SF_6 pressure is raised, peaks at around 0.15 Torr, and sharply decreases at higher pressures. The results indicate the importance of the photo-excitation of surface layer by high energy photons.

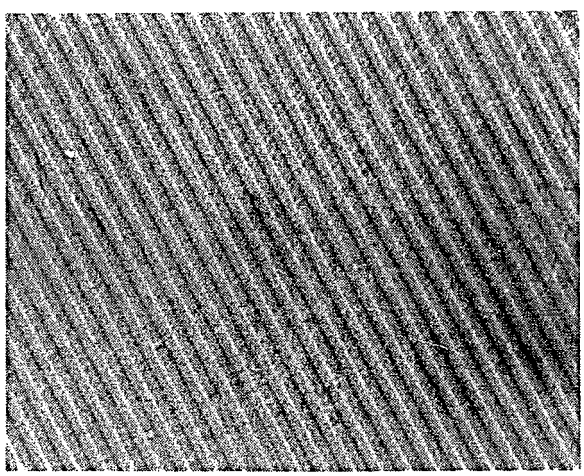

Figure 1. The micrograph of synchrotron radiation-excited β-SiC(220) oriented polycrystalline surface etched at ambient temperature in SF_6 (0.14 Torr). The line spacings are 1 μm.

VI—F Study of Ion-Pair Formation in the Vacuum Ultraviolet Region Using Synchrotron Radiation

Ion-pair formation is a very common process of highly excited molecules in the photon energy range of 10—50 eV. The detection of the counterpart negative ions is a sensitive probe to investigate the properties of Rydberg states lying in the vacuum ultraviolet region. We have measured the negative-ion efficiency curves using synchrotron radiation and obtained basic spectroscopic data and cross sections for the photodissociation into ion pairs. A great interest has also been taken in the dynamics of the ion-pair formation as half-collisional version of the electron transfer reaction.

VI-F-1 Negative-Ion Mass Spectrometric Study of Ion-Pair Formation in the Vacuum Ultraviolet. $CH_4 \rightarrow H^- + CH_3^+$ and $CD_4 \rightarrow D^- + CD_3^+$

Koichiro MITSUKE *(Univ. of Tokyo and IMS)*, **Shinzo SUZUKI** *(Tokyo Met. Univ.)*, **Takashi IMAMURA** *(IMS and Himeji Inst. of Tech.)*, **and Inosuke KOYANO** *(Himeji Inst. of Tech.)*

[*J. Chem. Phys.* **94**, 6003 (1991)]

Figure 1 shows a typical efficiency curve of H^- from CH_4 taken at wavelength intervals of 0.5—1.0 Å. Above an onset energy of 13.37±0.15 eV, there exists a broad peak arising from direct transitions to the ion-pair state of $^1T_2$ symmetry, which dissociates into $H^-(^1S_g) + CH_3^+(\tilde{X}^1A_1')$ (feature *F1*). The region above 19.8 eV contains two progressions: *P1* with poorly resolved structure and *P2* showing a long series of equally spaced peaks. The spectrum of D^- from CD_4 reveals a new progression (*P3*) starting at 21.744 eV besides *P1* and *P2*. The structures in *P1—P3* are considered to be due to the ν_1 progressions of npt_2

(n=3–5) Rydberg states converging to the $\tilde{A}^2A_1$ state of CH_4^+/CD_4^+. The $4pt_2$ and $5pt_2$ Rydberg states are observed here for the first time. The anomalously strong peak intensities of *P2* suggest that the $4pt_2$ state interacts strongly with a neutral repulsive state *D*.

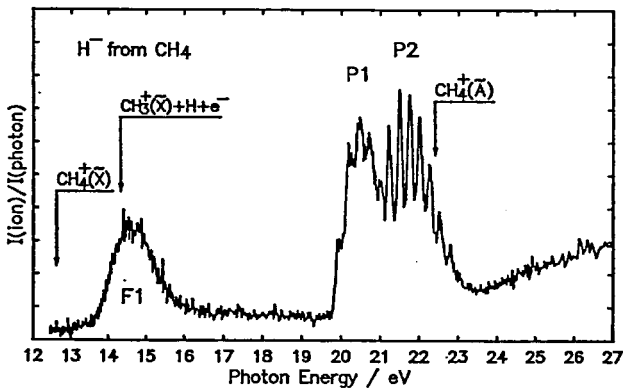

Figure 1. Photodissociation efficiency curve of H^- produced from CH_4 plotted as a function of the photon energy. The adiabatic ionization potentials for the $\tilde{X}^2T_2$ and $\tilde{A}^2A_1$ states of CH_4^+ and the appearance potential for the formation of CH_3^+ ($\tilde{X}^1A_1'$) + $H(^2S_g)$ + e^- are indicated.

VI-F-2 Nagative-Ion Mass Spectrometric Study of Ion-Pair Formation in the Vacuum Ultraviolet. $CF_4 \rightarrow F^- + CF_3^+$

Koichiro MITSUKE *(Univ. of Tokyo and IMS)*, **Shinzo SUZUKI** *(Tokyo Met. Univ.)*, **Takashi IMAMURA** *(IMS and Himeji Inst. of Tech.)*, **and Inosuke KOYANO** *(Himeji Inst. of Tech.)*

[*J. Chem. Phys.* **95**, 2398 (1991)]

Figure 1 shows the photodissociation efficiency curve of F^- from CF_4. The observed spectral features are identified as resonance peaks resulting from transitions to the Rydberg states converging to the five lowest ionic states of CF_4^+. Structureless peaks at the photon energies of 13.62 (feature *F1*) and 13.90 eV (feature *F2*) are assigned to CF_4^{**} ($1t_1 \rightarrow 3pt_2\ ^1T_2$) and CF_4^{**} ($4t_2 \rightarrow 3sa_1\ ^1T_2$), respectively. The $^1A_1$ components of these Rydberg states directly dissociate into a pair of the ground state F atom and a radical in Rydberg state, CF_3^{**}. The CF_3^{**} radical thus formed is electronically excited and decays radiatively by emitting the UV or visible fluorescence. The conversion to the ion-pair state occurs through avoided potential surface crossings between these repulsive CF_4^{**} states and the $^1A_1$ ion-pair potential that dissociates into $F^-(^1S_g)$ + $CF_3^+(\tilde{X}^1A_1')$. In contrast, the CF_4^{**} ($3t_2 \rightarrow npt_2\ ^1T_2$, $4 \leqq n \leqq 6$) Rydberg state shows a long series of the ν_1 vibrations in the F^- efficiency curve (features *F6* and *F7*). The $4pt_2$ Rydberg state is considered to have radiative decay channels to the dissociative Rydberg states converging to the $\tilde{X}$ and $\tilde{A}$ states, such as the $4t_2 \rightarrow 4pt_2\ ^1A_1$ and $1t_1 \rightarrow 4pt_2\ ^1T_2$ states.

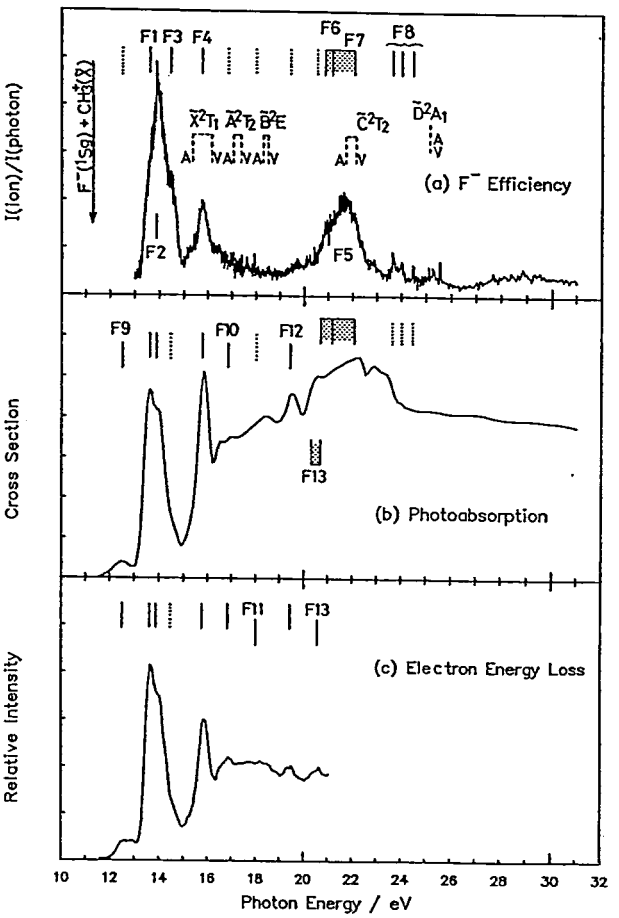

Figure 1. Comparison among (a) photodissociation efficiency curve of F^- produced from CF_4, (b) photoabsorption cross section curve of CF_4 (L.C. Lee *et al.*), and (c) electron-energy-loss spectrum of CF_4 (W.R. Harshbarger *et al.*). The adiabatic and vertical ionization potentials for the five lowest ionic states of CF_4^+ (C.R. Brundle *et al.*) are indicated by the dashed lines with marks *A* and *V*, respectively. The thermochemical threshold for the formation of $F^-(^1S_g)$ + $CF_3^+(\tilde{X}^1A_1')$ is also indicated.

VI—G Transition-State Spectroscopy by Photodetachment of Solvated Cluster Anions

Photodetachment spectroscopy of negative triatomic ions have been used by Neumark and coworkers to investigate the transition-state region of the corresponding neutrals in H-atom exchange reaction, X+HX → XH+X (X=Cl, Br, and I). Their photodetachment spectra exhibit characteristic progression in the particular vibrational mode, provided that a bound negative ion XHX^- upon photodetachment produces an unstable complex XHX the geometry of which is close to that of the transition state $XHX^‡$ for the above reaction. In the present study, we attempt to develop this methodology for photodetachment process of solvated cluster anions for the purpose of probing the transition-state region of chemical reactions in solution. Measurements will be made of the basic transition-state properties such as lifetime of the metastable states and coupling of dissociation coordinates with low-frequency intermolecular vibrational modes.

VI-G-1 Construction of Photodetachment Apparatus for Transition-State Spectroscopy of Cluster Anions

Koichiro MITSUKE

The schematic diagram of our apparatus, which is currently under construction, is illustrated in Figure 1. A gas mixture is expanded from a pulsed nozzle (*PN*). Negative cluster ions are produced by electron impact on the gas jet just outside the nozzle and sampled through a conical skimmer. Cluster ions are mass-selected with a beam-modulated time-of-flight mass spectrometer. The ion beam is modulated by applying to one of X-deflection plates (BD_X) a voltage varying in accordance with a step function. The risetime in switching the voltage from 0 to 50 V is estimated to be less than 15 ns. Any ions traveling between the deflection plates at the instant an electrical field change takes place (at time T_0) experience both downward and upward directed forces. Only the ions that happen to be exactly halfway between the deflection plates at T_0 can continue to move parallel to their initial direction of travel and will pass through a defining slit (*DS*) located at 80 cm downstream from the beam modulator. These ions separate into bunches according to their masses as they travel through a drift space. The cluster ion bunch of the desired mass is photoirradiated with a pulsed laser beam (the third or fourth harmonic of a Nd:YAG laser). The electrons produced by photodetachment are energy-analyzed by a time-of-flight spectrometer (*EEA*).

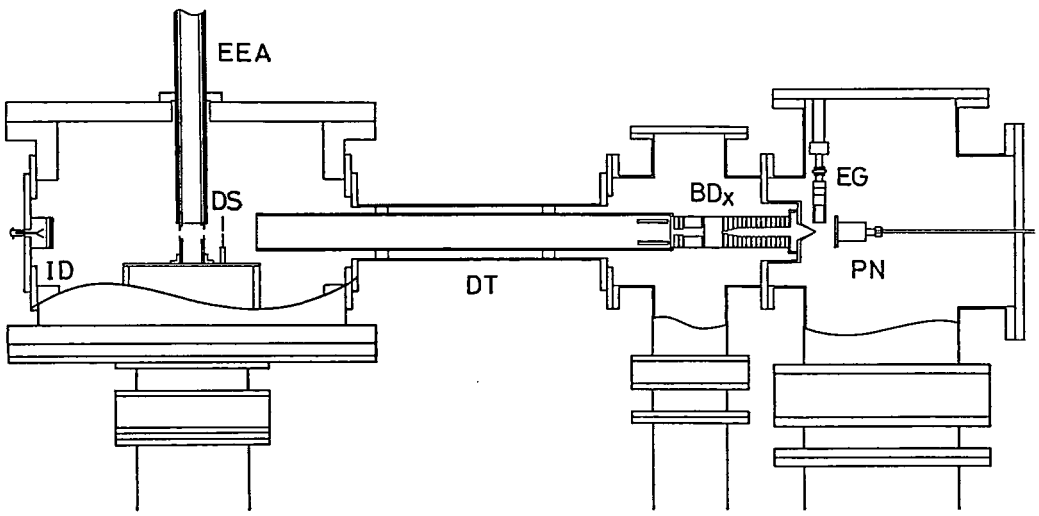

Figure 1. Schematic diagram of the apparatus. *PN*: pulsed nozzle, *EG*: electron gun, BD_X: X-deflection plates, *DT*: drift tube, *DS*: defining slit, *EEA*: time-of-flight electron energy analyzer, *ID*: ion detector.

VI—H Preparation and Characterization of Semiconductor Thin Films by New Excitation Processes

Crystalline and amorphous semiconductor thin films of high quality, especially prepared at low temperatures, are essential for the development of VLSI (very large-scale integration) and new functional devices in the near future. Synchrotron radiation-assisted, plasma-excited, and photon-activated CVD (Chemical Vapor Deposition) are believed to be powerful in this field. We have prepared elemental and compound semiconductor thin films by these excitation methods.

VI-H-1 High Quality Hydrogenated Amorphous Silicon Films by Windowless Hydrogen Discharge and Remote Plasma

Akira YOSHIDA, Haruhiko OHASHI*, Hiroshi TSUCHIMOTO*, Toshihiro KUGIMIYA*, and Kazuhito SUGURI* *(*Toyohashi Univ. of Tech.)*

Hydrogenated amorphous silicon films have been fabricated with vacuum ultraviolet (VUV) light through the direct photolysis of disilane gas. The VUV light was obtained from windowless hydrogen discharge. Optical properties and hopping transport of carriers have been investigated. The photosensitivity goes up to about 10^7 in the films prepared at 250°C, better than that of films obtained by conventional rf plasma-excited chemical vapor deposition. We have tried to clarify the degradation in the films under intense illumination of visible light.

References

1) A. Yoshida, K. Inoue, H. Ohashi, and Y. Saito, *Appl. Phys. Lett.*, **57** 484 (1990).
2) R. Kumar, A. Yoshida, R.M. Mehra, and K. Shimakawa, *Phys. Rev.*, **B43** 4174 (1991).

VI-H-2 Epitaxial Growth of Indium Nitride and Alloys by Microwave-Excited Metalorganic Vapor Phase Epitaxy

Akira YOSHIDA, Qi-Xin GUO*, and Osamu KATO* *(*Toyohashi Univ. of Tech.)*

Indium nitride, one of III-V compound semiconductors with wurtzite structure, is promising for visible light optoelectronic devices and highly efficient solar cells. InAlN and InGaN ternary alloys have attracted attention for luminescence devices emitting from blue to orange light. We have succeeded in preparing the epitaxial films of InN and InAlN on sapphire substrates by microwave-excited metal-organic vapor phase epitaxy for the first time. Trimethylindium and pure nitrogen were used as source materials. The emission spectra from the plasma in the reaction chamber were measured, in order to clarify the reaction process in the gas phase. The deposition conditions for this heteroepitaxial growth were made clear. The optical absorption and reflection spectra, and the electrical properties and microhardness of the films have been investigated.

References
1) A. Wakahara and A. Yoshida, *Appl. Phys. Lett.*, **54** 709 (1989).
2) A. Wakahara, T. Tsuchiya, and A. Yoshida, *J. Cryst. Growth*, **99** 385 (1990).
3) A. Wakahara, T. Tsuchiya, and A. Yoshida, *Vacuum*, **41** 1071 (1990).

VI-H-3 Thin Films of $CuInSe_2$ and $CuInGaSe_2$ Produced by RF Sputtering

Toshiyuki YAMAGUCHI *(Wakayama College of Tech.)*, **Jiro MATSUFUSA** *(Toyohashi Univ. of Tech.)*, **and Akira YOSHIDA**

I-III-VI_2 chalcopyrite semiconductors have been examined for a variety of optoelectronic device applications. Especially, $CuInSe_2$ and $CuInGaSe_2$ have shown great promise as the active material in thin-film solar cells. Structural, electrical and optical properties of these produced by rf sputtering from a stoichiometric target have been investigated by x-ray diffraction, Auger spectroscopy and x-ray photoelectron spectroscopy. The samples with intentional oxygen doping are different from those produced by a three-source elemental deposition procedure and subsequently oxidized in flowing oxygen. The electrical and optical properties of these films can be explained in terms of a mixture of $CuInSe_2$ and In_2O_3. SeO_2, CuO and In_2O_3 coexisting together at the surface.

Reference
T. Yamaguchi, J. Matsufusa, H. Kabasawa, and A. Yoshida, *J. Appl. Phys.*, **69** 7714 (1991).

VI-H-4 Low-Pressure MOCVD (Metalorganic Chemical Vapor Deposition) Growth of ZnTe and Observation of Gas Reaction

Mitsuhiro NISHIO*, Hiroshi OGAWA* *(*Saga Univ.)*, **and Akira YOSHIDA**

Zinc telluride is of great interest for fabricating purely green light emitting diodes. Very recently, several studies on MOCVD of ZnTe have been published. The growth characteristics of homoepitaxial layers of ZnTe on the substrates with different orientations have been investigated as a function of the transport rate of diethyltelluride(DETe) and dimethylzinc(DMZn). The surface of the layers on the (110) and (100) substrates is fairly smooth and flat at the high transport rate of DETe. The main reaction product is CH_4 at the high transport rate of DMZn, indicating that a large amount of methyl radicals is formed. The behavior of the growth rate is qualitatively explained with the Langmuir-Hinshelwood model, in which these radicals occupy the surface sites. We have tried to obtain the heteroepitaxial growth of ZnTe by synchrotron radiation-assisted process. The initial stages of growth have been investigated by RHEED (High Energy Electron Diffraction) and ESCA (Electron Spectroscopy for Chemical Analysis).

Reference
M. Nishio, H. Ogawa, and A. Yoshida, *Vacuum*, **41** 715 (1990)

VI-H-5 Construction and Operation of Ultrahigh Vacuum Chemical Vapor Deposition Epitaxial Reactor for Growth of Semiconductor and Metal

Akira YOSHIDA and Masahiro TOMIDA* *(*Toyohashi Univ. of Tech.)*

Low-temperature growth of silicon epitaxial layers is of great importance for large-scale integrated silicon devices. The limitation on growth temperature is very severe. An ultrahigh vacuum chemical vapor depositon (UHV/CVD) is potentially suitable for this application, because the residual gases in the reactor are detrimental on this growth. We have constructed a UHV/CVD growth system. Besides a purely thermal (pyrolytic) process, this system was designed to introduce the synchrotron radiation light and/or remote plasma into the reaction chamber.

VI—I Protochemistry of Organometallic Complexes Adsorbed on Solid Surfaces

Photochemistry of organometallic complexes adsorbed on solid surfaces has received increasing attention in recent years. The driving force behind this stems from its potential use in catalysis and microelectronics. Interest in the surface photochemistry also arises from the fact that its products are often quite different from those observed in gas phase or in liquid solution. We have studied the photolysis of metal carbonyls adsorbed on metal oxide powders and metals to investigate catalytic effects of the surface on a photochemical secondary process.

VI-I-1 IR Study on the Photochemistry and Adsorption States of Iron Carbonyls Adsorbed on Alumina

Shinri SATO and Tadayoshi OHMORI

[*J. Phys. Chem.*, **95**, 7778 (1991)]

The behavior of iron carbonyls adsorbed on alumina has been studied in the dark and under UV-illumination by FTIR spectroscopy. Photolysis products of adsorbed $Fe(CO)_5$ are affected by hydration of the surface as well as by their stability on alumina. On hydrated surfaces the photolysis leads to the formation of $[HFe_3(CO)_{11}]^-$, $[HFe(CO)_4]^-$, and $Fe(CO)_4$, which can be thermally produced at a lower rate by base catalysis. The photo- and thermochemical formation of $[HFe(CO)_4]^-$, requires stronger basic sites than that required for the formation of $[HFe_3(CO)_{11}]^-$. The photolysis of $Fe(CO)_5$ on dehydrated alumina results in predominant formation of $Fe_2(CO)_9$ with concomitant formation of a small amount of $Fe_3(CO)_{12}$, though the latter is exclusively formed under similar conditions on silica. This is because $Fe_3(CO)_{12}$ undergoes a disproportionation reaction on dehydrated alumina. These photo-products appear to be formed not at the outermost surface of alumina but inside the sample disc. The results are discussed with reference to those obtained for silica in terms of catalytic properties of oxide surfaces.

VI-I-2 Effects of Surface Basic Sites on the Photolysis of Iron Carbonyls Adsorbed on Silica

Tadayoshi OHMORI and Shinri SATO

[*J. Photochem. Photobio. A: Chem.*, in press]

Photolysis of iron carbonyls adsorbed on various types of silica was investigated by IR specroscopy. In the photolysis of $Fe(CO)_5$, $Fe_3(CO)_{12}$ was selectively produced on any silica samples. In the presence of gas phase water, a small amount of hydride species, $[HFe_3(CO)_{10}]^-$, was formed by the photolysis on one of the samples (denoted as Sample A), while the other samples still gave $Fe_3(CO)_{12}$ at a much smaller rate than in the absence of gaseous water. $Fe_2(CO)_9$ adsorbed on silica readily underwent a thermal disproportionation reaction to $Fe(CO)_5$ and $Fe_3(CO)_{12}$. Although adsorbed $Fe_3(CO)_{12}$ on silica samples was stable under illumination, the addition of gas phase water led to the formation of $[HFe_3(CO)_{10}]^-$, on Sample A and to decomposition of $Fe_3(CO)_{12}$ to $Fe(CO)_5$ on the other samples. The hydride formation was markedly suppressed by adsorption of a small amount of formic acid. Surface modification with a trace amount of pyridine, on the other hand, led to the photo-production of the hydride on any types of silica. These results indicate that the hydride formation on Sample A is due to a trace of weak basic sites induced by impurities.

VI-I-3 Photochemistry of Iron Pentacarbonyl Adsorbed on Titanium Dioxide

Yuji UKISU, Shinri SATO, and Tadayoshi OHMORI

[*Appl. Organomet. Chem.*, **5**, 243 (1991)]

The photolysis of iron carbonyl ($Fe(CO)_5$) adsorbed on titanium dioxide (TiO_2, anatase) was studied by FTIR spectroscopy. When adsorbed $Fe(CO)_5$ is illuminated by visible and near-UV light, the IR spectrum of its photolysis products is hardly observed, indicating that most of $Fe(CO)_5$ is photodecomposed to iron(0) or iron oxides on TiO_2. The carbon monoxide (CO) evolution rate upon illumination depends on the wavelength of light; 433 nm light is more effective for the CO evolution than 366 nm light. This result implies that the band-gap excitation of TiO_2 has little effect on the photolysis of adsorbed $Fe(CO)_5$, since the absorption edge of TiO_2 (anatase) lies at around 400 nm. The effects of substrates on the photolysis of adsorbed $Fe(CO)_5$ are discussed with reference to previous results obtained for alumina (Al_2O_3) and silica (SiO_2), on which the photolysis leads to the formation of $Fe_2(CO)_9$ or $Fe_3(CO)_{12}$.

VI-I-4 Reactivities and Adsorption States of $Fe(CO)_5$ Adsorbed on Reduced TiO_2

Yuji UKISU, Shinri SATO and Tadayoshi OHMORI

The adsorption states and reactivities of $Fe(CO)_5$ adsorbed on TiO_2 have been studied by FTIR spectroscopy. When $Fe(CO)_5$ is adsorbed on TiO_2 outgassed above 100°C, a significant red-shift of the IR bands of $Fe(CO)_5$ in the C-O stretching region and a remarkable increase in the adsorption amount of $Fe(CO)_5$ are observed. The new IR bands as well as the original ones readily disappear upon brief pumping at room temperature. The shift of IR bands is no longer observed after the TiO_2 samples are oxidized by O_2 at 400°C followed by outgassing at room temperature. These results indicate that a new adsorbed species of $Fe(CO)_5$ is formed on reduced TiO_2 surfaces. This surface species also exhibits a new absorption band at around 430 nm in the visible region, suggesting the formation of an electron-transfer complex on the surfaces.

Reactivities of the species have been examined for a ligand exchange reaction at room temperature. While $Fe(CO)_5$ adsorbed on Al_2O_3 or SiO_2 shows little activity for NO-CO ligand exchange, the species on TiO_2 is so active for this reaction that all carbonyls are readily exchanged with NO. $Fe(CO)_5$ adsorbed on reduced TiO_2 may be activated by an electronic interaction with Ti^{3+}.

VI-I-5 Photolysis of Iron Pentacarbonyl Adsorbed on Platinum

Shinri SATO and Yuji UKISU

$Fe(CO)_5$ adsorbed on platinum plate at 100–120 K was irradiated with SOR light, and the reaction products were analyzed by FTIR reflection absorption spectroscopy (IRAS) and temperature programmed desorption spectroscopy (TPD). On uncleaned Pt sample, the physisorption of $Fe(CO)_5$ is observed, while on the surface cleaned by Ar ion sputtering, $Fe(CO)_5$ is partly decomposed to form adsorbed CO and $Fe(CO)_{5-x}$. Irradiation with the SOR light of < 200 nm leads to a rapid decrease in the CO stretching band of $Fe(CO)_5$ in IRAS spectrum without an increase in any other bands, while TPD shows that the adsorbed $Fe(CO)_5$ in first monolayer is selectively decomposed to

$Fe(CO)_{5-x}$. Since IRAS gives the vibration mode perpendicular to the surface, these results suggest that the product has the vibration mode parallel to the surface, i.e., a planar structure of carbonyl.

VI-I-6 Reactivity of $Mo(CO)_6$ Adsorbed on Zeolite under Illumination

Yuji WADA *(Tokyo Inst. of Tech.)*, **Shinri SATO, and Yuji UKISU**

$Mo(CO)_6$ adsorbed on alkali-metal (Li, Na, and K) exchanged Y-zeolite shows different photocatalytic activity for olefin metathesis depending on the exchanged metal in the order Li-Y < Na-Y < K-Y. In connection with this, we have measured the rate of CO liberation from adsorbed $Mo(CO)_6$ in the dark and under illumination and found that the rate depends also on the exchanged metal in the same order as observed for the photometathesis. These results may be explained in terms of electrostatic field induced by alkali metal in zeolite cage.

VI-I-7 Construction of an Apparatus for Surface VUV-Photochemistry

Shinri SATO, Yuji UKISU, and Makoto WATANABE

To study the VUV-photochemistry of molecules adsorbed on solid surfaces, a new beam line of UVSOR was constructed last year. The beam line is equipped with a differential pumping chamber and a reaction and analysis chamber in which surface species are analyzed by polarization-modulation FTIR reflection-absorption spectroscopy. SOR light is introduced directly or through various type of filters to the apparatus. In this year, a focussing mirror was inserted to the beam line to improve beam intensity, and X-ray photoelectron and Auger electron spectroscopy, a sputter cleaning ion gun, and a sample load lock were added to the reaction and analysis chamber to improve surface analysis.

VI—J Studies on Catalysis for Automobile Exhaust and Energy Resources

The measures against global air pollution and the development of new energy resources instead of fossil fuel are current problems. Catalysts play important roles in the cleaning of exhaust gases from industrial factories and gasoline engines. We are now aiming the catalytic reduction of NO_x from diesel engines, and have recently found a new catalytic system hopeful for this purpose. A mechanistic study on the NO_x reduction is under progress in our laboratory. We have also studied a photocatalyst which converts light energy to chemical energy from the viewpoint of solar-to-chemical energy conversion.

VI-J-1 Surface Isocyanate Intermediate Formed during the Catalytic Reduction of Nitrogen Oxide in the Presence of Oxygen and Propylene

Yuji UKISU, Shinri SATO, Gyo MURAMATSU*, and Kiyohide YOSHIDA* *(*Riken Co. Ltd.)*

[*Catal. Lett.*, **11**, 177 (1991)]

IR spectroscopic measurements have revealed that an IR band ascribable to adsorbed isocyanate species grows up when alumina-supported Cu-Cs oxide catalyst is exposed to a mixture of NO, O_2 and C_3H_6 at room temperature and subsequently heated to 400°C in vacuum. The species produces N_2, CO_2 and CO in the ratio of ca. 2:1:1 in the presence of NO at 350°C. Alumina and alumina-supported Cu oxide catalyst are less active for the formation of isocyanate species.

VI-J-2 Infrared Study on Simultaneous Reduction of NO_x and Particulate Emissions from Diesel Engine Exhaust

Yuji UKISU, Shinri SATO, Gyo MURAMATASU*, and Kiyohide YOSHIDA* *(*Riken Co. Ltd.)*

We have found that the simultaneous removal of both NO_x and carbon particulate from the exhaust of diesel engines can be achieved by newly developed copper-containing catalysts. IR spectroscopic measurements in a model system have revealed that a key step is the reaction of activated NO_2 or N_2O_4 on the catalyst with carbon particulate, which gives N_2 and CO_2.

VI-J-3 Photocatalytic Activity of TiO_2 Films Prepared by Sol-Gel Method

Hisato KOSHIBA*, Noriyoshi KAKUTA*, Akifumi UENO*, Shinri SATO, and Yuji UKISU *(*Toyohashi Univ. of Tech.)*

TiO_2 films prepared on a quartz plate by a spin-on process of TiO_2 sols were photo-platinized in a H_2PtCl_6 solution and then submitted to the photocatalytic hydrogen evolution from an aqueous alcoholic solution. The yield of hydrogen increases with rise of calcination temperature up to 500°C and then decreases with further rise of calcination temperature as observed for powdered TiO_2 prepared from $Ti(OC_3H_7)_4$ or $TiCl_4$. The activity also increases with an increase in the thickness of film probably due to a decrease in the unfavorable effect of quartz substrate. The quantum yield of hydrogen evolution is smaller than those observed for powdered TiO_2.

VI—K Surface Molecular Dynamics Sensitive to the Structure of Reaction Sites

The structure of reaction sites is essential information for designing new functional catalyst surfaces. This should be analyzed through dynamic properties of surface processes, since it is not provided by structural information of non-reacting surface species. The spatial and velocity distributions of desorbing product molecules open new reaction dynamics sensitive to the structure. The spatial distribution depends on (a) the reactant density around the reaction site, (b) the arrangement of substrate atoms constituting the reaction site, and (c) the orientation. The velocity distribution is more sensitive to the site structure. We have succeeded in constructing a new apparatus for measurements of time-of-flight spectra of desorbing molecules during thermal desorption procedures. This method has advantages compared with molecular beams, since it can be applied to a wide range of reactant coverages.

VI-K-1 Co-Adsorption Phase Diagram of Carbon Monoxide and Oxygen on Palladium(100) and Angular Distribution of Reactive Carbon Dioxide Desorption

Tatsuo MATSUSHIMA *(IMS and Hokkaido Univ.)*, **Yuichi OHNO, Kiyoshi NAGAI** *(IMS and Komatsu Electronic Metal Co.)*, **and Hisakazu NOZOYE** *(National Chemical Laboratory for Industry)*

[submitted to *J. Chem. Phys.*]

The coadsorption structures of CO and oxygen on Pd(100) and the angular distribution of reactive CO_2 desorption were studied with angle-resolved thermal desorption and low energy electron diffraction. The CO_2 formation induced by heating the coadlayer was extended to lower temperatures with an increase in the coverages, yielding five peaks; P_1-(around 400 K), P_2-(~340 K), P_3-(~280 K), and P_4-(~240 K), and P_5-CO_2(~150 K). A coadsorption phase diagram was constructed from threshold coverages determined by the appearance of each CO_2 peak and the variation of LEED spot intensity. Each zone in the diagram is characteristic of separate domains of CO and oxygen, and different angular distribution of reactive CO_2 desorption.

VI-K-2 Orientation of Oxygen Admolecules on Platinum(110)(1×2) Reconstructed Surface: Near-Edge X-Ray-Absorption Fine-Structure Study

Yuichi OHNO, Tatsuo MATSUSHIMA *(IMS and Hokkaido Univ.)*, **Shin-ichiro TANAKA** *(UVSOR)*, **Eriko YAGASAKI** *(UVSOR)*, **and Masao KAMADA** *(UVSOR)*

[submitted to *Surface Sci.*]

The orientation of oxygen admolecules on a Pt(110) (1×2) reconstructed surface was studied with near-edge X-ray absorption fine-structure techniques. The molecular axis was determined to be lying on the surface and oriented along the surface trough.

VI-K-3 Velocity Distributions of Desorbing Products in the Oxidation of Carbon Monoxide on Palladium(110) Surfaces

Tatsuo MATSUSHIMA *(IMS and Hokkaido Univ.)*, **Kosuke SHOBATAKE, Yuichi OHNO, Kiyoshi NAGAI** *(IMS and Komatsu Electronic Metal Co.)*, **and Kiyohiko TABAYASHI**

[submitted to *Chem. Phys. Lett.*]

The velocity of desorbing product CO_2 from Pd(110) surfaces was measured by cross-correlation time-of-flight techniques combined with angle-resolved thermal desorption. Heating coadlayers of CO and oxygen yields five peaks of CO_2 formation in the range of 150 to 460 K. The translational temperature of CO_2 desorbing along the surface normal was estimated to be above 1600 K for all peaks. It increased with an increase in the reactant coverages, and decreased with increasing desorption angle. A typical time-of-flight spectrum of P_4-CO_2, which peaks at 230 K, is shown in Figure 1.

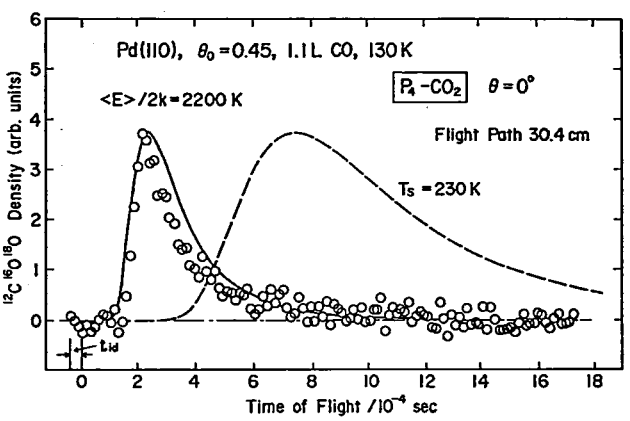

Figure 1. Typical time-of-flight spectrum measured for P_4-CO_2 desorbed in the normal direction. The translational temperature, <E>/2k, where <E> is the mean translational energy, was estimated to be 2200±150 K. The gate time of the chopper was 15 μs. The ion drift time, t_{id}, in the mass spectrometer was 40 μs. The dashed and solid curves represent Maxwellian distributions at the peak and translational temperature.

VI-K-4 Stability of Oxygen Admolecules on Various Noble Metal Surfaces and it's Orientation

Tatsuo MATSUSHIMA *(IMS and Hokkaido Univ.)* **and Yuichi OHNO**

[submitted to *Shokubai (Catalyst)*]

The stability of oxygen admolecules on various metal surfaces, Pd(111), Pd(110), Pd(100), Pt(111), Pt(110) (1×2) and Rh(111), was examined by means of thermal desorption combined with isotope tracer and low energy electron diffraction. It depends on the kind of metals, surface structures, surface modifications by oxygen adatoms, the oxygen coverage and the adsorption temperature. It was found that the admolecules on surfaces with a (111)

structure of the top-most layer are most stable and the stability is also modified by structures of the second layer. The orientation of the admolecule was also studied by using near-edge X-ray absorption fine-structure technique.

VI-K-5 Anisotropy of the Spatial Distribution of Reactive Carbon Dioxide Desorption from Narrow Terraces on Iridium(110)(1×2) Surfaces

Yuichi OHNO, Kiyoshi NAGAI *(IMS and Komatsu Electronic Metal Co.)*, **Tatsuo MATSUSHIMA** *(IMS and Hokkaido Univ.)*, **and Hirofumi MIKI** *(Science Univ. of Tokyo)*

The spatial distribution of reactive CO_2 desorption on Ir(110)(1×2) reconstructed surfaces was measured over a wide range of polar angles by means of angle-resolved thermal desorption. Two-directional desorption collimated along the terrace-surface normal was three-dimensionally represented. Each component of the desorption showed strong anisotropy in the spatial distribution. It is sharp along the terrace and much sharper perpendicular to the surface trough.

VI-K-6 Photoinduced Reaction of Oxygen Admolecules on Palladium(100) Surfaces

Nobuhiro OHTA *(Hokkaido Univ.)*, **Yuichi OHNO, Kiyoshi NAGAI** *(IMS and Komatsu Elecronic Metal Co.)*, **and Tastuo MATSUSHIMA** *(IMS and Hokkaido Univ.)*

Photoinduce desorption and dissociation of oxygen admolecules were studied on palladium(100) surfaces by using thermal desorption combined with an isotope tracer method. Both processes were enhanced with irradiation of photon energy above 3.1 eV. The cross section for the former process at ~300 nm was lower than that for the other.

RESEARCH ACTIVITIES VII
Coordination Chemistry Laboratories

In January, 1991, coordination chemistry laboratories welcomed Dr. Tamotsu Takahashi from the University of Tokyo as the associate professor of the laboratory of Functional Coordination Chemisty. An adjunct associate professor Ryuichi Ikeda of the laboratory of Complex Catalysis, who was an associate professor of Nagoya University, has been promoted to be a full professor of Tsukuba University in October, 1990, and thus he must be replaced by another associate professor of some other university. Dr. Kotaro Osakada, an associate professor of Tokyo Institute of Technology, has been appointed to be the adjunct associate professor for the rest one year after Prof. Ikeda. The adjunct professor Masanobu Hidai and adjunct associate professor Toshio Yamaguchi of the laboratory of Coordination Bond finished their term and returned to the University of Tokyo and Fukuoka University, respectively, at the end of March, 1991. Instead, Prof. Tasuku Ito of Tohoku University and associate professor Masatatsu Suzuki of Kanazawa University have been newly appointed to be an adjunct professor and an associate professor, respectively, after them. Dr. Atsushi Yagasaki, a technical associate of the laboratory of Complex Catalysis, moved to Kansei Gakuin University with the promotion to be a lecturer. We appreciated his cooperation during his stay in the coordination chemistry laboratories. Mr. Kenji Waizumi, who was working with us as a graduate student of Tohoku University and finished the doctor course at the end of March, has been employed as a technical associate after Dr. Yagasaki. Dr. Yusuke Tamura, an IMS fellow, left the Institute to industry. The staffs of the coordination chemistry laboratories are changing rather frequently, but the research activities are kept high as reported here.

VII—A Developments of Diastereoisomers of Metal Complexes Having Various Combinations of Chiral Elements

New metal complexes with various chiral elements as building blocks are synthesized and their molecular and crystal structures are determined.

The detailed comparison between those structures revealed sometimes the origin of the diastereoselectivities and the probable optical resolution mechanisms.

VII-A-1 Helically Chiral Trinuclear Complex with Ferrocene Group

Tatsuya KAWAMOTO and Yoshihiko KUSHI

A new class of heterometallic trinuclear complexes containing redox active ferrocene group have been synthesized from the ferrocenylbenzothiazoline as a starting material. The molecular structure of the helically chiral trinuclear Ni(II) complex is shown in the Figure. NMR, X-ray structure and cyclic voltammogram studies show some efficient interactions between intramolecularly linked functional groups. From the compairs on the crystal structure of spontaneously resolvable Pd(II) complex with that of hexahelicene, it is found that the complexes are a valuable model system for the optical discrimination mechanism related to the helical chirality.

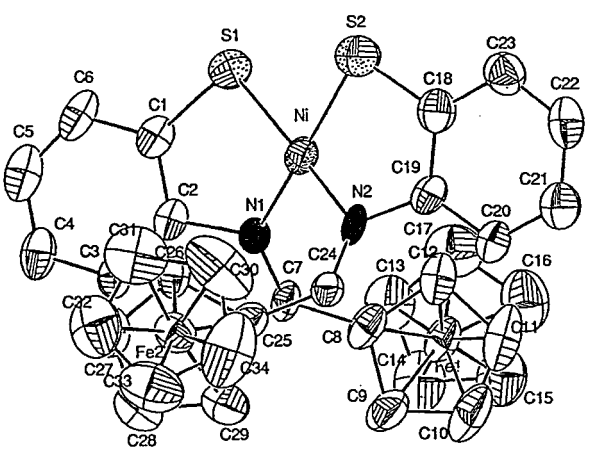

Figure 1. Helically Chiral Trinuclear Complex with Ferrocene Group.

VII-A-2 Stereoselectivity of the Metal Complex Having the Chiral Schiff Base Ligand

Tatsuya KAWAMOTO, Akira TAKEUCHI*, Hiro KUMA*, and Yoshihiko KUSHI *(*Osaka Univ.)*

New meridional tris-chelated cobalt(III) complexes with chiral Schiff base ligand having an asymmetric center at the N-terminal moiety are synthesized and the stereoselectivity of these complexes are studied. Diastereoselective crystallization of these complexes has been proved by X-ray crystal structure determinations.

VII-A-3 Stereoselectivity of the Metal Complex Having the Monodentate Chiral Amine and Cyclic Imidato Groups

Hiroshi SHIMOMURA, Seiko KOMORITA*, Hiro KUMA*, and Yoshihiko KUSHI *(*Osaka Univ.)*

Four trans-[Pd(chiral amine)$_2$(cyclic imidato)$_2$] complexes are synthesized and the stereoselectivities of these complexes are studied, where the chiral amine is 1-phenylethylamine(phenea) and the cyclic imidato are 3,3-dimethylglutarimidato(3,3-dmgluim, samples meso-(1) and optically active-(2)) and phthalimidato (phthal, samples meso-(3) and optically active-(4)) respectively. X-ray structural studies revealed that two unstable forms of the staggered rotamers of l-phenylethylamine ligand have been fixed in these crystals with the variations of co-existed cyclic imidato groups as shown in the figure (1)—(4).

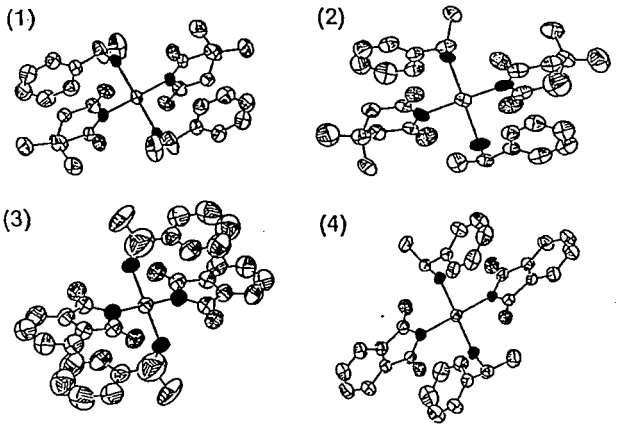

Figure 1. Stereoselectivity of the Metal Complex Having the Monodentate Chiral Amine and Cyclic imidato groups.

VII—B Static Aspects of Molecular Interactions in Solutions

Solute-solvent interactions including those of polymer solutes were studied from their static aspects. Much emphasis has been placed on 1) the selective solvation of ions in aqueous mixed solvent systems and 2) the volume changes accompanying stepwise complex formations. As for the former, we have divided the partial molar volume of an electrolyte MX V_2^0(MX) into cationic $V_2^0(M^+)$ and anionic $V_2^0(M^-)$ contributions in order to see the differences in the behavior of cation and anion in solutions. As for the latter, a method has been developed which enables us to evaluate the V_2^0 of reaction intermediates.

VII-B-1 Limiting Partial Molar Volumes of Ions in Water-Methanol and Water Acetonitrile

Fumio KAWAIZUMI, Yoshitomo INOUE*, and Hiroyasu NOMURA* *(*Nagoya Univ.)*

[*Bull. Chem. Soc. Jpn.*, **64**, 510 (1991)]

Measurements of densities of solution of $AgNO_3$ and $Ca(NO_3)_2$ dissolved in the mixed solvents water-methanol and water-acetonitrile were carried out at 25°C and the partial molar volumes V_2^0 of these electrolytes were determined from the density data. The ionic partial molar volumes of Ag^+, Ca^{2+}, and NO_3^- were evaluated by combining our results obtained earlier and those obtained in this work. The solvent composition dependence of V_2^0 of each ion was more remarkable in water-acetonitrile than in water-methanol and characteristic behaviors were observed for Ag^+ and Ca^{2+} ions in water-acetonitrile system.

VII-B-2 Sedimentation Potential Measurements and Partial Molar Volumes of Univalent Ions in Water-Acetone Mixtures

Fumio KAWAIZUMI, Hiromitsu HIRAKAWA *(Kagoshima Univ.)*, **Eiji KUBOTA** *(Shinshu Univ.)*, **and Hiroyasu NOMURA** *(Nagoya Univ.)*

[*Bull. Chem. Soc. Jpn.*, **64**, 2607 (1991)]

Sedimentation potentials and electrical conductivities were measured for NaCl, NaBr, sodium tetraphenylborate $Na[BPh_4]$ and tetraphenylphosphonium chloride $[Ph_4P]Cl$ dissolved in water-acetone system up to 50 wt% of acetone. Using the data obtained and the reported values of partial molar volumes V_2^0, the ionic division of V_2^0 was carried out. The values of $V_2^0(Na^+)$ evaluated for NaCl, NaBr, and $Na[BPh_4]$ were self-consistent and they work as references for ionic division of V_2^0(MX).

VII-B-3 Volume Changes Accompanying the Stepwise Complex Formation in Aqueous Solutions. Cu(II)-bpy Complexes

Fumio KAWAIZUMI and Kim A. BURKOV

[*Chem. Lett.*, 1755 (1991)]

The volume change ΔV associated with complex formation gives the dynamic information on reaction mechanism as well as the static information on interactions between complex ions and solvent molecules. We have tried to see quantitatively the ΔV of the stepwise complex formation between Cu^{2+} and bpy (bpy = 2,2'-bipyridine); Cu^{2+} + bpy → $[Cu(bpy)]^{2+}$ (**2**), $[Cu(bpy)]^{2+}$ + bpy → $[Cu(bpy)_2]^{2+}$ (**3**), $[Cu(bpy)_2]^{2+}$ + bpy → $[Cu(bpy)_3]^{2+}$ (**4**). Distribution of these complexes **2** - **4** in 0.01033 M of aqueous solutions of $Cu(NO_3)_2$ is illustrated in Figure 1. Densities of solutions were measured for systems of various concentrations of bpy indicated by the numbers ① — ⑫ in Figure 1.

The partial molar volumes V_2^0 were calculated for the hypothetical solute $[Cu(bpy)_i](NO_3)_2$, a solute which has the molar mass equal to the averaged value of molar masses of all ionic species at specified bpy concentrations in solutions. From the values of $V_2^0([Cu(bpy)_i](NO_3)_2)$, the $V_2^0([Cu(bpy)](NO_3)_2)$, $V_2^0([Cu(bpy)_2](NO_3)_2)$, and the $V_2^0([Cu(bpy)_3](NO_3)_2)$ were evaluated. Volume increment ΔV became gradually smaller with the number of ligand bpy coordinating to the Cu^{2+} ion.

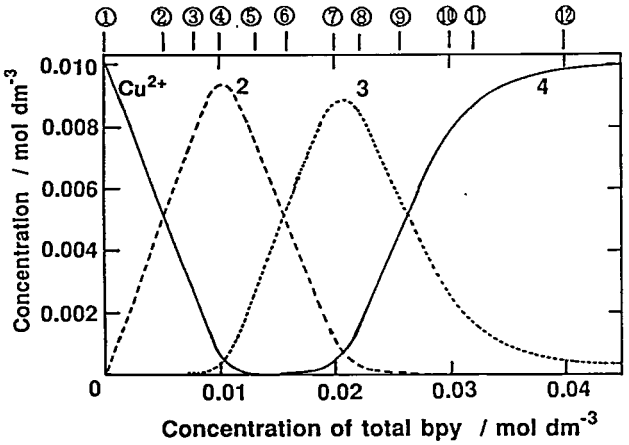

Figure 1. Distribution of Cu(II)-bpy Complexes in H_2O. Total concentration of Cu^{2+}=0.01033 mol/dm^3.

VII-B-4 Dissolved State of Ionene Polymers in Water-Acetone and Their Relation to Ionic Partial Molar Volumes and Partial Molar Adiabatic Compressibility

Fumio KAWAIZUMI, Shinobu KODA*, Masahiro KIMURA*, and Hiroyasu NOMURA* *(Nagoya Univ.)*

[*J. Solution Chem.*, in press]

Solution properties of water-soluble synthetic polymer, 3,3-ionene and 6,6-ionene chloride and bromide dissolved in water-acetone mixtures up to 50 wt% were investigated. Their partial molar volumes V_2^0 and partial molar adiabatic compressibilities K_s^0 were determined. Ionic additivity of V_2^0 with respect to the cation of backbone polymer chain and the counter-anion was confirmed quantitatively. The ionic additivity of V_2^0 is discussed along with the K_s^0 in their relation to the counterion binding of ionene polymers. Effects of ionic sites on the ionene are strong but they don't break the solvation layer.

VII-B-5 Hydration of Methyl Cellulose

Shinobu KODA*, Takeo HORI*, Hiroyasu NOMURA* *(*Nagoya Univ.)*, **and Fumio KAWAIZUMI**

[*Polymer*, **32**, 2806 (1991)]

Measurements of sound velocity and density of solutions of methyl cellulose(MC) have been carried out at 15, 25, 30, and 35°C. The partial molar volumes and partial molar adiabatic compressibilities have been determined as a function of degree of substitution, the number of $-OCH_3$ group in a cellulose unit. The partial molar volume of MC increased with the degree of substitution but it was independent of temperature. The amount of hydration of MC was calculated after evaluating the compressibility of the dehydrated MC which was estimated from the temperature dependence of the partial molar adiabatic compressibility. The hydration number of MC decreased with the degree of substitution.

VII—C Analysis of Microscopic Aspects of Fluid flow

Theoretical calculation was developed for fluid flow related to the complicated geometries with the intension of application for practical conditions.

VII-C-1 Theoretical Analysis of Turbulent Flow and Heat Transfer around a Surface-mounted Obstacle

Tsutomu ARAGAKI*, Shuichi IWATA*, Hideo TANGE*, Setsuro HIRAOKA*, Ikuho YAMADA* *(*Nagoya Institute of Technology)*, **and Fumio KAWAIZUMI**

[*J. Chem. Eng. Jpn.*, **24**, 171 (1991)]

A simple model based on the mixing-length hypothesis was developed. It was applied to two cases of turbulent flow, the one being the film flow on the outer wall of a vertical tube, and the other being the flow between parallel plates. Using the Galerkin finite element method, we have calculated the heat transfer and flow profiles around a surface-mounted obstacle. The reattachment length depends on Reynolds number and the maximum Nusselt number is observed on the upstream side of the reattachment point. The increase of heat transfer due to the obstacle is appreciable only in the ranges of low Reynolds number.

VII—D Structures of Solvated Metal Ions and Complexes in Solution

Structures of various metal complexes in aqueous and nonaqueous solutions have been investigated by the solution X-ray diffraction method.

VII-D-1 X-Ray Diffraction Studies on Ternary $MgCl_2$-KCl-H_2O and $MgCl_2$-CsCl-H_2O Solutions Saturated with the Corresponding Double Salts

Kenji WAIZUMI* *(*Tohoku University and IMS)*, **Yusuke TAMURA, and Hitoshi OHTAKI**

[*Z. Naturforsch.*, **46a**, 307 (1991)]

X-ray scattering measurements have been done on aqueous $MgCl_2$-KCl and $MgCl_2$-CsCl solutions saturated with their double salts of $MgCl_2 \cdot KCl \cdot 6H_2O$ and $MgCl_2 \cdot CSCl \cdot 6H_2O$, respectively, at 293 K. The Mg^{2+} ion was found to be coordinated with six water molecules at an Mg-O distance of 208—209 pm, whereas K^+ and Cs^+ ions where surrounded by both water molecules and chloride

ions in the first coordination sphere. The interatomic distance between the alkali cation and the chloride ion was 320 pm and 339 pm for K^+ and Cs^+, respectively, and the coordination numbers of K^+ and Cs^+ with respect to Cl^- were 2.4 and 2.0, respectively. The alkali metal-H_2O distance and the hydration number of the cation were 277 pm and 3.7, respectively, for K^+ and 315 pm and 4.7, respectively, for Cs^+. The structures of the solutions are discussed in connection with nucleation processes of the salts from aqueous solutions.

VII-D-2 Coordination Around Thorium(IV) in Aqueous Perchlorate, Chloride and Nitrate Solutions

Georg JOHANSSON *(Royal Inst. Technol. and IMS)*, **Mauro MAGINI** *(Division Chimica/TIB-ENEA, C.R.E.-Cassaccia)*, **and Hitoshi OHTAKI**

[*J. Solution Chem.*, **20**, 775 (1991)]

The coordination around the thorium(IV) ion in aqueous perchlorate, chloride and nitrate solutions has been determined from large angle X-ray scattering measurements. In perchlorate solutions, where inner-sphere complexes are not formed, the first coordination sphere contains 8.0±0.5 water molecules with Th-H_2O bond lengths of 2.48_5Å. In chloride solutions inner-sphere complexes are formed, which lead to an increase in the coordination number. In nitrate solutions the nitrate ions are bonded as bidentate ligands to the thorium ion. The bond lengths are similar to those found in crystalline hydrates of thorium nitrate. The coordination numbers found for thorium(IV) in solution are compared with previously reported values for lower charged ions of similar size.

VII-D-3 Structure of the Solvated Metal Ions in Nitrate and Chloride Solutions of Erbium(III) and Yttrium(III) in Dimethyl Sulfoxide

Georg JOHANSSON *(Royal Inst. Technol. and IMS)*, **Haruhiko YOKOYAMA** *(Yokohama City Univ.)*, **and Hitoshi OHTAKI**

[*J. Solution Chem.*, **20**, 859 (1991)]

X-ray diffraction measurements on 1M yttrium(III) and erbium(III) nitrate and chloride solutions in dimethyl sulfoxide (DMSO) have shown that Er(III) and Y(III) solutions of equal compositions are isostructural. The intensity difference functions can then be used to derive the detailed structure of the coordination sphere around the metal ions. The DMSO molecules are coordinated over oxygen with average M-O-S bond angles of about 130°. Two different conformations, corresponding to different relative orientations of the M-O and O-S bonds, seem to be prevalent. In the nitrate solutions an average of about 1.5 nitrate ions are coordinated as bidentate ligands to each metal ion. In the chloride solutions about 1.3 chloride ions belong to the inner-coordination sphere.

VII-D-4 A Structural Study on Saturated Aqueous Solutions of Some Alkali Halides by X-Ray diffraction

Hitoshi OHTAKI and Nobuhiro FUKUSHIMA *(Tokyo Inst. Technol.)*

[*J. Solution Chem.*, in press]

The structure of nearly saturated or supersaturated aqueous solutions of NaCl (6.18 mol (kg $H_2O)^{-1}$), KCl (4.56 mol (kg $H_2O)^{-1}$), KF (16.15 mol (kg $H_2O)^{-1}$) and CsF (31.96 mol (kg $H_2O)^{-1}$) has been investigated by means of solution X-ray diffraction at 298 K. In the NaCl and KCl solutions about 30% and 60%, respectively, of the ions form ion pairs and the Na^+-Cl^- and K^+-Cl^- distances have been determined to be 282 and 315 pm, respectively. The average hydration numbers of Na^+ and Cl^- ions are 4.6 and 5.3, respectively, in the NaCl solution and those of K^+ and Cl^- ions in the KCl solution are both 5.8. In the KF solution clusters containing some cations and anions, besides 1:1 ($K^+ \cdot F^-$) ion pairs, are formed. The K^+-F^- interatomic distance has been determined to be 269 pm, and nonbonding $K^+ \cdots K^+$ and $F^- \cdots F^-$ distances in the clusters are 388 and 432 pm, respectively, and the average coordination numbers n_{KF}, n_{KK} and n_{FF} have been estimated to be 2.3, 1.9, and 1.6, respectively. In the highly supersaturated CsF solution an appreciable amount of clusters containing several caesium and fluoride ions are formed. The Cs^+-F^- distance in the clusters has been determined to be 312 pm, while the nonbonding $Cs^+ \cdots Cs^+$ and $F^- \cdots F^-$ distances are estimated to be 442 and 548 pm, respectively, the distances being about $\sqrt{2}$ and $\sqrt{3}$ times the Cs^+-F^- distance, respectively. The coordination numbers n_{CsF}, n_{CsCs} and n_{FF} in the first coordination sphere of each ion are 3.3, 2.3 and 5.3, respectively, and the result shows the formation of clusters of higher order than 1:1 and 2:2 ion pairs. These ion pairs and clusters may be regarded as embryoes for the formation of nuclei of crystals and the results obtained in the present diffraction study support observations for the nucleation of alkali halide crystals studied by molecular dynamics simulations previously examined.

VII-D-5 Structure of Divalent Transition-Metal Complexes at Consecutive Steps of Interaction with Halide and Thiocyanate Ions in solution

Hitoshi OHTAKI

[*Indian J. Chem.*, in press]

All of the solvated Mn^{2+}, Co^{2+}, Ni^{2+}, Cu^{2+}, Zn^{2+}, Cd^{2+} and Hg^{2+} ions in various nonaqueous solvents, except for those in HMPA, have the octahedral structure and the final products of the complexes are tetrahedral. Structural changes occurring at the stepwise formation of the transition-metal complexes with halide and thiocyanate ions in aqueous and nonaqueous solutions are discussed on the basis of spectroscopic, calorimetric and solution X-ray diffraction data. The structures of some of the complexes $[MX_n]^{(2-n)+}$ (n=1–4) are determined by the solution X-ray diffraction method and the bond-length variations through the structural changes are shown. The step where the structure changes from octahedral to tetrahedral is thus shown from thermodynamic data, absorption spectra and structural analyses of the complexes. The importance of structures and properties of solvents in the complex formation reactions is especially emphasized.

VII—E Crystal Structures of Metal Complexes

Crystal structures of metal complexes have been determiend in order to obtain information by which the solution structure of the metal complexes can be connected with the solid state structure through the phase transition.

VII-E-1 In Situ Observation of the Phase Transition among Cobalt(II) Dichloride Hydrates and Crystal Structure of the Tetra- and Hexahydrates

Kenji WAIZUMI* *(*Tohoku Univ. and IMS)*, **Hideki MASUDA, Hitoshi OHTAKI, Katsuo TSUKAMOTO**, and Ichiro SUNAGAWA**** *(**Tohoku Univ.)*

[*Bull. Chem. Soc. Jpn.*, **63**, 3426 (1990)]

Transformation among cobalt(II) dichloride hydrates in aqueous solutions was studied by the optical microscopic method. Although there are three hydrates ($CoCl_2 \cdot 6H_2O$, $CoCl_2 \cdot 4H_2O$, and $CoCl_2 \cdot 2H_2O$) in the phase equilibrium diagram, the only solution mediated transformation between $CoCl_2 \cdot 6H_2O$ and $CoCl_2 \cdot 2H_2O$ could be observed under the present experimental conditions and it was confirmed that $CoCl_2 \cdot 4H_2O$ hardly formed compared with the other two hydrates. In order to investigate the reason why $CoCl_2 \cdot 4H_2O$ was hardly crystallized at the transformation from $CoCl_2 \cdot 6H_2O$ through $CoCl_2 \cdot 2H_2O$ and vice versa, the crystal structure of $CoCl_2 \cdot 4H_2O$ was investigated by the X-ray diffraction method. The structures of $CoCl_2 \cdot 6H_2O$ was reexamined because previously reported results had a relatively large *R*-factor. The crystal of $CoCl_2 \cdot 4H_2O$ is monoclinic, space group $P2_1/a$ with a=11.548(1)Å, b=9.342(1)Å, c=6.056(1)Å, β=110.79(1)°, and Z=4. The complex has a slightly distorted octahedral geometry about Co^{2+} ion and two Cl^- ions are located at the cis-position. The crystal of $CoCl_2 \cdot 6H_2O$ is monoclinic, space group $C2/m$ with a=10.380(2)Å, b=7.048(1)Å, c=6.626(1)Å, β=122.01(1)°, and Z=2. The geometry around the cobalt ion is also octahedral with four water molecules and two chloride ions at the equatorial and the axial positions, respectively. The remaining two water molecules are linked to the two Cl^- ions by hydrogen bonding. The difficulty of crystallization of $CoCl_2 \cdot 4H_2O$ crystals in solutions was explained in terms of the relatively unstable cis-dichloro structure of the $[CoCl_2(H_2O)_4]$ moiety and its crystal structure was stabilized by hydrogen bonding network between the cis-form moieties.

VII-E-2 Structure of $MgCl_2 \cdot RbCl \cdot 6H_2O$

Kenji WAIZUMI* *(*Tohoku Univ. and IMS)*, **Hideki MASUDA, Hitoshi OHTAKI, Kim A. BURKOV**, and Mikhail Y. SCRIPKIN**** *(**Leningrad Univ.)*

[*Acta Crystallogr.*, **C47**, 251 (1991)]

Magnesium rubidium trichloride hexahydrate, M_r=324.22, triclinic, $P\bar{1}$, a=6.672(5), b=13.282(15), c=6.639(5)Å, α=89.83(8), β=91.72(6), γ=90.41(8)°, V=588.0(14)Å^3, Z=2, D_x=1.831 Mgm^{-1}, $\bar{\lambda}$(Mo $K\alpha$) =0.71073Å, μ=5.17 mm^{-1}, F(000)=320, T=253 K, $R(F)$=0.078 for 2604 independent reflections with $|F_o|>3\sigma(|F_o|)$. The crystal consists of a network of top-sharing $[RbCl_6]$ octahedra and isolated $[Mg(H_2O)_6]^{2+}$ octahedra occupying holes in the $[RbCl_6]$ network. Rb^+ ions are coordinated with six Cl^- ions and each Cl^- ion is surrounded by two Rb^+ ions and four O atoms of water molecules. The Mg-O bond length varies from 1.982(14) to 2.115(13)Å in the $[Mg(H_2O)_6]^{2+}$ octahedron. Each H_2O molecule is hydrogen bonded to two Cl^- ions.

VII-E-3 Crystallographic Investigations of $[Mg(H_2O)_6]XCl_3$ Double Salts (X^+=K^+, Rb^+, Cs^+, NH_4^+): Crystal Structure of $[Mg(H_2O)_6]CsCl_3$

Kenji WAIZUMI* *(*Tohoku Univ. and IMS)*, **Hideki MASUDA, Hitoshi OHTAKI, Mikhail Y. SCRIPKIN**, and Kim A. BURKOV**** *(**Leningrad Univ.)*

[*Amer. Mineralogist*, **76**, 1864 (1991)]

The crystal structure of the $MgCl_2 \cdot CsCl \cdot 6H_2O$ double salt complex has been determined by single-crystal X-ray diffraction methods. The phase is the triclinic, space group $P\bar{1}$, with unit cell dimensions a=6.7507(7), b=13.495(2), c=6.750(1)Å, α=90.13(1), β=91.15(1), γ=90.18(1)°. The crystal structure consists of a network of corner-sharing $[CsCl_6]$ octahedra and isolated $[Mg(H_2O)_6]^{2+}$ octahedra which occupy holes in the $[CsCl_6]$ network. The atomic arrangement can be considered as a perovskite-type structure, where the large A-cation of the perovskite-type ABC_3 compound is replaced by the $[Mg(H_2O)_6]^{2+}$ complex. The structure is similar to that of $[Mg(H_2O)_6]RbCl_3$ and $[Mg(H_2O)_6]NH_4Cl_3$ although it differs from that of $[Mg(H_2O)_6]KCl_3$ (carnallite), which has a hexagonal $BaTiO_3$-type structure. To explain the existence of two structure types in the $[Mg(H_2O)_6]XCl_3$ (X^+=K^+, Rb^+, Cs^+, NH_4^+) compounds, the "tolerance factor", t, is calculated using the ionic radius of 2.90Å for $[Mg(H_2O)_6]^{2+}$ (estimated in this work). The calculated t values are 1.04, 1.00, 0.95 and 0.97 for the K^+, Rb^+, Cs^+ and NH_4^+ ions, respectively. The t value of the K^+ compound exceeds the stable region $0.80 \leq t \leq 1.00$ of the perovskite-type structure.

VII-E-4 Structure of Zinc(II) and Copper(II) Chloride *N,N*-Dimethylformamide Solvates

Honoh SUZUKI*, Nobuhiro FUKUSHIMA*, Shin-ichi ISHIGURO* *(Tokyo Inst. Technol.)*, **Hideki MASUDA, and Hitoshi OHTAKI**

[*Acta Crystallogr.*, **C47**, 1838 (1991)]

$[ZnCl_2((CH_3)_2NCHO)_2]$, dichlorobis (*N,N*-dimethylformamide)zinc(II), M_r=282.5, monoclinic, $C2/c$, a=13.296(4), b=13.254(4), c=14.702(6)Å, β=113.76(3)°, V=2371(2)Å^3, Z=8, D_x=1.583 g cm^{-3}, λ(Mo $K\alpha$)=0.71073Å, μ(Mo $K\alpha$)=25.5 cm^{-1}, F(000)=1152, T=226 K, R=0.035 for 2825 independent reflections. The zinc atom has a tetrahedral environment of two oxygen atoms from two *N,N*-dimethylformamide (DMF) molecules

and two chlorines, with Zn-O distances of 2.003(2) and 1.993(2)Å and Zn-Cl distances of 2.203(1) and 2.214(1)Å. $[CuCl_2((CH_3)_2NCHO)_2]_2$, di($\mu$-chloro)dichlorotetrakis (*N*, *N*-dimethylformamide)dicopper(II), M_r=561.3, monoclinic, $P2_1/n$, a=11.568(5), b=11.617(7), c=8.992(4)Å, β=111.87(5)°, V=1121(1)Å^3, Z=2, D_x=1.662 g cm^{-3}, λ(Mo $K\alpha$))=0.71073 Å, μ(Mo $K\alpha$)=24.1 cm^{-1}, F(000)=572, T=265 K, R=0.054 for 2577 independent reflections. The structure consists of centrosymmetric chlorine-bridged dimers, the bridging Cu-Cl distance being 2.61(2)Å. The coordination around copper is distorted tetragonal pyramidal with two *cis*-oxygen atoms (Cu-O=1.973(3) and 1.989(3)Å) and two chlorines (Cu-Cl=2.247(2) and 2.284(1)Å) in the basal plane and the bridging Cl axial. The Cu · · · Cu separation in the dimer is 3.613(2)Å. In both complexes, the DMF ligands are essentially planar and coordinated to the metal ion in the lone-pair direction of the oxygen donor atom.

VII—F Molecular Dynamics Simulations of Electrolyte Solutions

Molecular dynamics simulations have been employed to elucidate microscopic, dynamic behavior of ions in solution and dissolution and nucleation processes of ionic crystals.

VII-F-1 Dissolution of Alkali Fluoride and Chloride Crystals in Water Studied by Molecular Dynamics Simulations

Nobuhiro FUKUSHIMA* *(Tokyo Inst. Technol.)*, **Yusuke TAMURA, and Hitoshi OHTAKI**

[*Z. Naturforsch.*, **46a**, 193 (1991)]

The dissolution of cubic crystals of NaF, KF, CsF, LiCl, NaCl, and KCl consisting of 32 cations and 32 anions in an isolated box containing 216 water molecules was studied at 298 K by molecular dynamics simulations. The ion-ion, ion-water and water-water interactions were described in terms of the Tosi-Fumi, Kistenmacher-Popkie-Clementi, and Matsuoka-Clementi-Yoshimine potentials, respectively. During the simulation periods of 12 ps for NaF, CsF and LiCl and 20 ps for KF, NaCl and KCl cations did not dissolve, while anions *dissolved* from the CsF, LiCl and NaCl crystals but not from the NaF, KF and KCl crystals. The mass effect in the dissolution of CsF was examined by giving the caesium ions the atomic weight of the fluoride ion (18.998). In case of the "light" caesium ions the crystal fluctuated less far and again fluoride ions but no caesium ions were dissolved.

VII-F-2 Nucleation Processes of NaCl and CsF Crystals from Aqueous Solutions Studied by Molecular Dynamics Simulations

Hitoshi OHTAKI and Nobuhiro FUKUSHIMA *(Tokyo Inst. Technol.)*

[*Pure & Appl. Chem.*, **63**, 1743 (1991)]

Nucleation processes of NaCl and CsF crystals from supersaturated aqueous solutions of (a) 9.25, and (b) 15.42 mol (kg H_2O)$^{-1}$ NaCl and (c) 36.34 mol (kg H_2O)$^{-1}$ CsF have been studied by molecular dynamics simulations. The periodical boundary condition with the Ewald summation has been employed in the course of the simulation calculations. Numbers of cations (M^+), anions (X^-) and water (W) molecules in the systems (M^+:X^-:W) are (a) 56:56:336, (b) 80:80:288, and (c) 127:127:194. All ions and water molecules have been first randomly distributed in the cells and, except for (a), water molecules have been allowed to move until the thermal equilibrium attains between the water molecules and the ions which have been fixed at the given lattice points. Then, the simiulation for nucleation has been started. In (a) all water molecules and ions have been allowed to move feely in the pre-equilibrium step. Temperature has been kept constant at 298 K. Potential functions used in the simulations are the Fumi-Tosi, Kistenmacher-Popkie-Clementi, and Matsuoka-Clementi-Yoshimine potentials for ion-ion, ion-water, and water-water interactions, respectively. The simulation procedure has been continued for 18 ps with the time step Δt=1.0 fs. Formation of ion clusters in the systems was slow down after about 12 ps.

VII-F-3 An MD Simulation for Concentrated Aqueous Solutions of Caesium Iodide

Yusuke TAMURA, Hitoshi OHTAKI, and Isao OKADA *(Tokyo Inst. Technol.)*

[*Z. Naturforsch.*, in press]

Molecular dynamics simulations have been performed for concentrated aqueous CsI solutions with molar ratios CsI:H_2O = 1:20 (2.78 molal) at 298 K and 341 K and 1:10 (5.56 molal) at 349 K. Effects of temperature and concentration on the structures of the hydrated ions, the ion pairs, and ionic aggregates are discussed by comparing the results with X-ray diffraction data obtained under similar conditions.

VII—G Thermodynamic Studies of Metal Complexes in Nonaqueous Solutions

A parameter which can explain entropies of complex formaiton reactions in solution as a function of the parameter values has been newly introduced. Thus, enthalpies of the reactions have been interpreated in terms of donor and acceptor properties of solvents, while entropies of the reactions are well elucidated to be connected with the structuredness of solvents.

VII-G-1 An Attempt to Parameterize the Structuredness of Solvents

Hitoshi OHTAKI

[*J. Solution Chem.*, in press]

An attempt has been made to parameterize the structuredness of solvents from the view-point of intermolecular interactions, and the structuredness parameter S_p has newly been proposed. The enthalpy of vaporaization (ΔH^o_{vap}) of various solvents has been considered to consist of donor-acceptor interaction energy (DA), which can been estimated from Gutmann's donor and acceptor numbers, some other interaction energies (VDW), which may not be fully described in terms of the donor-acceptor interactions and may be related to the electronic distribution, the volume and shape of the molecule, the polarizability and ionization potential of atoms in the molecules, the energies of these interactions being usually considered to be of van der Waals type and possibly evaluated from the enthalpy of vaporization of n-alkanes, and the intermolecular interaction energy (STR) due to the three-dimensional molecular ordering in the liquid: ΔH^o_{vap}=DA+VDW+STR. The STR term obtained as the difference between ΔH^o_{vap} and (DA+VDW) is defined as the structuredness parameter S_p, which is a dimensionless quantity by diving the value with the (kJ mol^{-1}) unit. The entropies of formation ΔS^o_1 and $\Delta S^o_{\beta 4}$ of $[MX]^+$ and $[MX_4]^{2-}$ complexes, respectively, of divalent transition metals (Mn^{2+}, Co^{2+}, Ni^{2+}, Cu^{2+}, Zn^{2+}, Cd^{2+}, and Hg^{2+}) with halide and thiocyanate ions in aqueous and non-aqueous solvents could be represented as an almost linear funciton of the structuredness parameters S_p thus introduced.

Table 1. Enthalpies of vaporization ΔH^o_{vap}, the values of the DA and VDW terms of various liquids and the structuredness parameter S_p proposed.

Solvent	ΔH^o_{vap} kJ mol^{-1}	DA kJ mol^{-1}	VDW kJ mol^{-1}	S_p
Water	43.99	20.7	4.0	19.3
CH_3OH	37.43	19.7	9.0	8.7
C_2H_5OH	42.31	18.6	13.0	10.7
FA	64.98	24.0	9.7	31.3
DMF	47.51	17.8	19.0	10.7
AN	32.9	9.0	11.7	12.2
DMSO	52.88	24.1	15.8	13.0
TFE	43.97	13.5	16.1	14.4
Acetone	29	7.0	16.4	5.6
NB	47.3	2.3	22.8	22.2
NM	38.3	2.0	12.0	24.3

VII—H Developments of Novel Multi-functionalized Macrocycles and Their Metal Complexes

Novel functionalized macrocyclic polyamines are synthesized by renovating the classical structure of macrocyclic polyamines. These new ligands and their metal complexes have shown unique chemical properties.

VII-H-1 Roles of Zinc(II) Ion in Phosphatases. A Model Study with Zinc(II)-Macrocyclic Polyamine Complexes

Tohru KOIKE *(Hiroshima Univ.)* **and Eiichi KIMURA** *(Hiroshima Univ. and IMS)*

[*J. Am. Chem. Soc.*, **113**, 8935 (1991)]

The zinc(II) complexes of 1,5,9-triazacyclododecane (L_1, [12]aneN$_3$) and 1,4,7,10-tetraazacyclododecane (L_2, [12]aneN$_4$) promote the hydrolysis of tris(4-nitrophenyl) phosphate, TNP^0 (a neutral phosphotriester), and bis(4-nitrophenyl) phosphate, BNP^- (a monoanionic phosphodiester). Kinetic studies show that the reactive species are commonly L-Zn^{II}-OH$^-$ and the kinetically obtained pK_a values are almost identical to those obtained thermodynamically (pK_a(H_2O)). The comparative reactivities of OH^-, L_1-Zn^{II}-OH^-, and L_2-Zn^{II}-OH^- with different pK_a(H_2O) values of 15.7, 7.3, and 8.0 have been studied to understand the role of Zn(II) in *alkaline phosphatases*. For the neutral phosphotriester TNP^0, the second-order rate constants $M^{-1}s^{-1}$ at 25°C and I=0.20 are 10.7, 7.0, and 3.7, respectively, indicating free OH^- ion (the most basic OH^- species) is the best promoter. On the other hand, toward the anionic phosphodiester BNP^-, the L_1-Zn^{II}-OH^- becomes more efficient than free OH^- ion: the second-order rate constants ($\times 10^5$, $M^{-1}s^{-1}$) are 2.4, 8.5, and 2.1, respectively, at 35°C and I=0.20. A bifunctional ("hybrid") mechanism of Zn(II) (especially Zn^{II}-L_1 system) toward phosphates (especially the anionic phosphate), in which the Zn^{II}-bound OH^- acts as a nucleophile, while the vacant Zn(II) coordination site anchors the substrate P=O or P-O^- group, is well disclosed by comparing these kinetic results with the second-order rate constants (at 25°C and I=0.10) of 4-nitrophenyl acetate hydrolysis; 9.5, 4.1×10^{-2}, and 1.1×10^{-1} $M^{-1}s^{-1}$, respectively, where all of the OH^- species act merely as a nucleophile to the carbonyl group, as indicated by a linear relationship between the pK_a(H_2O) values and the rate constants. Phosphate anion affinity constants $K(A^-)$ (M^{-1}) with Zn^{II}-L_1 complex determined by pH titration are $10^{3.5}$ for phenyl phosphate and $10^{3.1}$ for 4-nbitrophenyl phosphate which are ca. 25 times larger than those with less acidic Zn(II)$_{aq}$ ion.

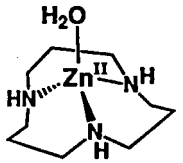

Zn^{II}-[12]aneN_3

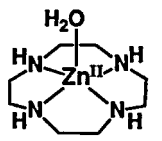

Zn^{II}-cyclen

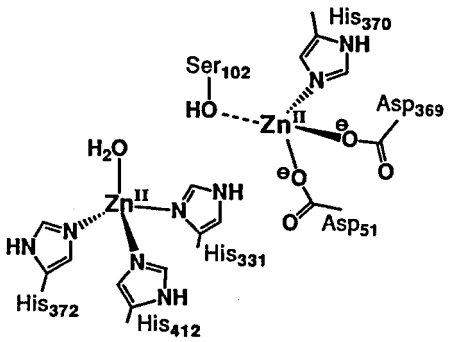

Alkaline Phosphatase

VII-H-2 Design of Discriminating Hosts for Noble Metal Ions with Double Functions of Thia and Amide Donors in Macrocyclic Structures

Eiichi KIMURA *(Hiroshima Univ. and IMS)*, **Yasuhisa KUROGI, Takashi TOJO, Mitsuhiko SHIONOYA** *(Hiroshima Univ.)*, **and Motoo SHIRO** *(Shionogi Research Labs)*

[*J. Am. Chem. Soc.*, **113**, 4857 (1991)]

A novel tetradentate, diamidedithia ("dioxo[14]-aneN_2S_2") **1** and a pentadentate, diamidetrithia macrocyclic ligand ("dioxo[16]aneN_2S_3") **2** have been synthesized, and their intelligent ligand properties were discovered. They smoothly encapsulate only divalent noble metal ions Pt(II) (to **3** and **5**, respectively) and Pd(II) (to **4** and **6**), but not other typical transition metal ions, Cu(II), Ni(II) or Co(II). Moreover, **1** and **2** can effectively snatch Pt(II) from *cis*-$[Pt^{II}(NH_3)_2Cl_2]$ to yield the Pt^{II}-in complexes **3** and **5**, respectively. The Pt(II) complex **5** possesses a four-coordinated, square planar geometry with $(N^-)_2S_2$ donors (N^- denotes a deprotonated amide anion), where the central S(4) atom is unbinding, as shown by the X-ray crystal structure resolved by the heavy-atom method using 2543 unique reflections with $|F_0| > 4\sigma(F_0)$. Final R and R_w were 0.040 and 0.060, respectively: monoclinic, space group $P2_1/c$ with a=11.7536(6), b=9.574(3) and c=19.183(9)Å, β=126.78(3)°, and V=1729(1)Å^3; ρ_c=2.096 g cm^{-3} for Z=4, and formamide (DMF) displays a 2e$^-$ oxidation at +0.81 V *vs.* SCE ($Pt^{II} \rightarrow Pt^{IV}$) and a 2e$^-$ reduction at +0.32 V ($Pt^{IV} \rightarrow Pt^{II}$), implying that Pt^{II} is stabilized by the square planar $(N^-)_2S_2$ coordination and Pt^{IV} by the octahedral $(N^-)_2S_3 \cdot$DMF coordination with additional S(4) and a DMF donor. The two amide anions in the Pt^{II}-in complexes **3** and **5** are reversibly protonated to the Pt^{II}-out complexes **7** and **8**. Treatment of **8** with an equimolar **2** yields a sandwich complex **9**. In **1** and **2** intelligent functions are endowed by the combination of the characteristic S donors and amide groups in the same macrocyclic skeletons to concerned work only on Pt(II) and Pd(II) ions.

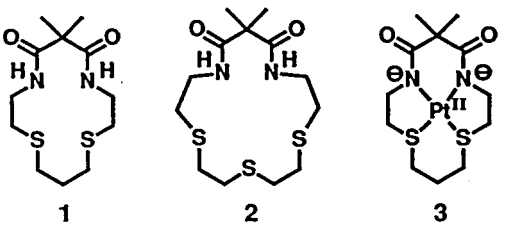

1 **2** **3**

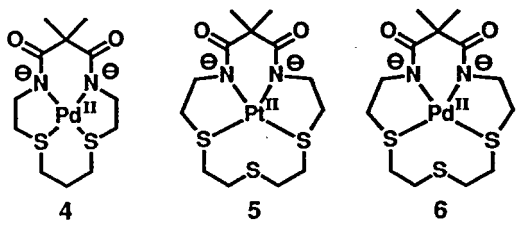

4 **5** **6**

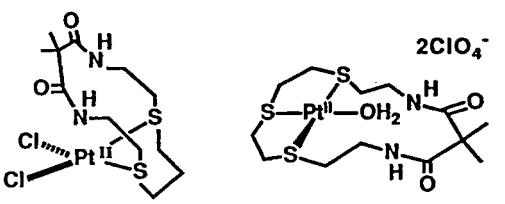

7 **8**

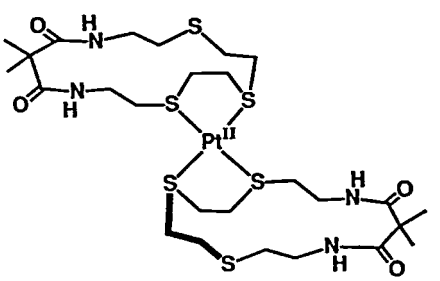

9

VII-H-3 The First Gold(III) Macrocyclic Polyamine Complexes and Application to Selective Gold(III) Uptake

Eiichi KIMURA *(Hiroshima Univ. and IMS)*, **Yasuhisa KUROGI, and Toshikazu TAKAHASHI** *(Hiroshima Univ.)*

[*Inorg. Chem.*, **30**, 4117 (1991)]

The hitherto unreported Au(III) complexes with cyclam (1,4,8,11-tetraazacyclotetradecane) **1**, phenol-pendant cyclam **2**, pyridyl-pendant cyclam **3**, monooxocyclam **4**, phenol-pendant monooxocyclam **5**, and pyridyl-pendant monooxocyclam **6** have been synthesized and characterized. Dissociation of a proton from one of the secondary amines in the "Au^{III}-in" cyclam complexes **7** readily occurs with pK_a values 5.0~5.4 and 25°C and I=0.1 ($NaClO_4$). Although monooxocyclam **4** does not accommodate Au(III), the donor-pendant monooxocyclams **5** and **6** enclose Au(III) with concomitant dissociation of an amide proton. As anticipated for the diamagnetic d^8 complexes, the pendant donors only weakly interact from an axial site. The outstanding acidity of Au(III) over common other metal ions in interaction with cyclam can be utilized for selective uptake of Au(III) using lipophilic cyclam derivatives **8**.

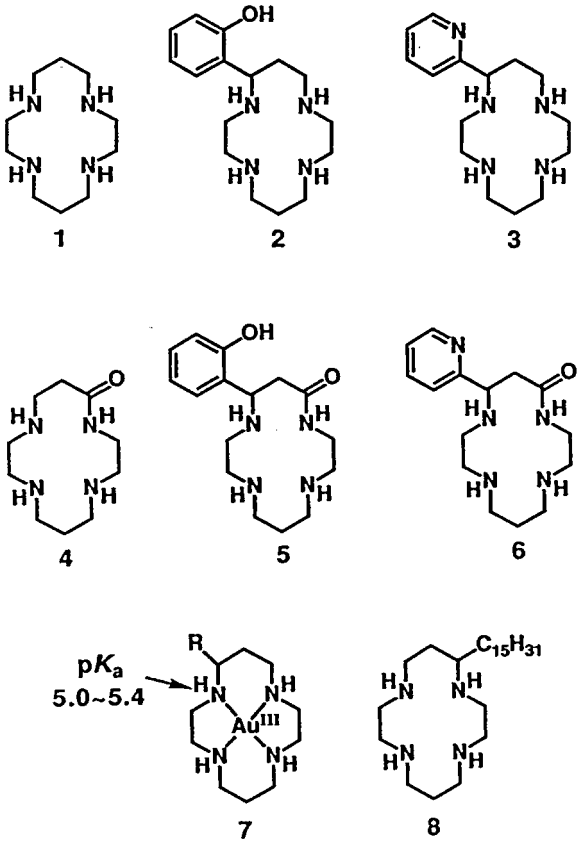

VII-H-4 Synthesis, Properties and Complexation of a New Imidazole-pendant Macrocyclic 12-membered Triamine Ligand

Eiichi KIMURA *(Hiroshima Univ. and IMS)*, **Yasuhisa KUROGI, Mitsuhiko SHIONOYA** *(Hiroshima Univ.)*, **and Motoo SHIRO** *(Shionogi Research Labs)*

[*Inorg. Chem.* **30**, 4524 (1991)]

A new 12-membered macrocyclic triamine with an imidazole-pendant, 2-(4-imidazoyl)-1,5,9-triazacyclododecane **1**, has been synthesized to study its complexation behaviors with Zn^{II} and Cu^{II}, along with the easiness with which the metal-bound imidazolate anion is generated. The Zn^{II} complex **2a** shows a close equatorial coordination of the imidazole (2.025Å) in a distorted trigonal bipyramidal structure with an additional chloride ion. Final R and R_w were 0.030 and 0.040, respectively: orthorhombic, space group $P_{na}2_1$ with a=14.574, b=9.079, c=13.506(Å), ρ_c=1.627 (g cm^{-1}) for Z=4, V=1787.0(Å^3). The proton dissociation most likely from the Zn^{II}- and Cu^{II}-coordinated imidazole occurs with pK_a values of 10.3 and 9.3, respectively, at 25°C. Mixtures of the Cu^{II}- (or Zn^{II}-) complex **2** and Cu^{II}- (or Zn^{II}-) [12]aneN$_3$ complex **3** in alkaline CH_3OH solution yield Cu^{II},Cu^{II}- (or Zn^{II} Zn^{II}-) dinuclear complexes bridged with the imidazolate anion, **4**. A boron complex **5** has been isolated during the diborane reduction of the monooxo precursor.

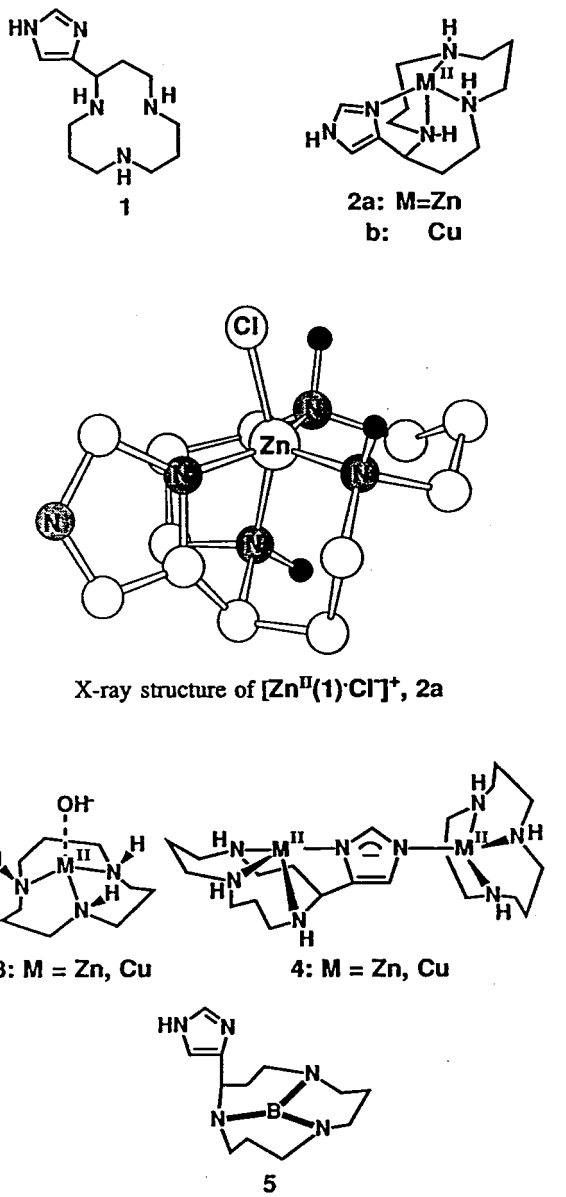

VII-H-5 The Proximal Imidazole Effect on Manganese(III)-Cyclam Complex

Eiichi KIMURA *(Hiroshima Univ. and IMS)*, **Mitsuhiko SHIONOYA** *(Hiroshima Univ.)*, **Tsuyoshi YAMAUCHI** *(Hiroshima Univ.)*, **and Motoo SHIRO** *(Shionogi Research Labs)*

[*Chem. Lett.*, 1217 (1991)]

The synthesis, X-ray structure, and chemical properties are reported of a new 5 coordinate Mn(III) complex with imidazole-pendant cyclam, which has been found to be an efficient catalyst for alkene epoxidation.

This novel catalyst more efficiently catalyzes the oxygen atom transfer from both PhIO and NaClO to the substrate than unsubstituted Mn(III)-cyclam and Ni(II)-cyclam complexes. The proximal imidazole increases the catalytic turnover, as found for porphyrins. Although we tentatively postulate an oxenoid intermediate, (*trans*-cyclam)Mn^{V}=O species, like the (porphyrin)Mn^{IV} or ^{V}=O and (cyclam) Ni^{IV}=O, detailed mechanistic studies are currently in progress.

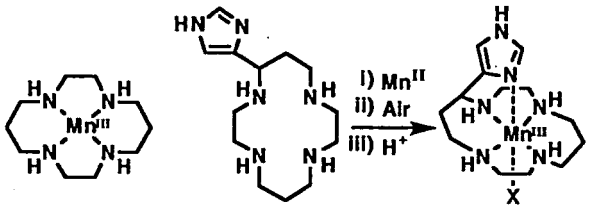

VII-I Structures and Chemical Properties of Organotransition Metal Complexes Relevant to Homogeneous Catalysis

Many synthetic organic reactions catalyzed by transition metal complexes involve organotransition metal complexes as the key intermediates. In this study, properties of various organotransition metal complexes, such as arylnickel complexes, hydrido(aryloxido)ruthenium complexes, nickel and palladium containing cyclic ester and amide complexes, and alkyl(alkoxido)platinum complexes, have been investigated by means of X-ray crystallography, spectroscopies, kinetic measurement, as well as calorimetric titration. Based on the results, mechanism of several synthetic reactions using metal complexes as catalyst has been elucidated, and novel catalytic carbonylative cyclization has been developed.

VII-I-1 Kinetic Study on C-C Coupling Reaction of Aryl Halides Using Ni(0) Complexes.

Kohtaro OSAKADA, Shoichiro WAKABAYASHI*, and Takakazu YAMAMOTO* *(*Tokyo Inst. Tech.)*

[*J. Organomet. Chem.* in press (1991)]

Coupling of aryl halides promoted by transition metal complexes is regarded as a crucial step of dehalogenative polycondensation of dihaloaromatic compounds to give poly(arylene)s which are utilized as organic semiconductors. The present study has revealed mechanism of Ni(0) complex promoted coupling reaction of aryl halides giving biaryls on the basis of the kinetic results.

Reactions of aryl halides, such as phenyl chloride, phenyl bromide, phenyl iodide, p-methylphenyl bromide, p-acetylphenyl bromide, p-methoxyphenyl bromide, with $Ni(cod)_2$(cod=1,5-cyclooctadiene) in the presence of 2,2'-bipyridine in DMF give the corresponding biaryl as the coupling product. The reaction obeys second-order kinetics to the nickel complex, and the obtained rate constants are independent from the concentration of the substrates. Kinetic parameters of the coupling of phenyl bromide are determined as $\Delta H^{\ddagger}$=60 kJ mol^{-1}, $\Delta G^{\ddagger}$=90 kJ mol^{-1}, and $\Delta S^{\ddagger}$=−90 J mol^{-1}K^{-1}, respectively, at 333 K. The above results indicate that the rate-determining step of the reaction lies in disproportionation of the intermediate Ni(Ar)(X)(bpy) to give $Ni(Ar)_2$(bpy) which is responsible for the C-C bond formation.

VII-I-2 Properties of Nickel- and Palladium Containing Cyclic Amide and Ester Complexes and Catalytic Carbonylative Cyclization of Unsaturated Carboxylic Acids Involving the above Complexes

Akio YAMAMOTO*, Takakazu YAMAMOTO*, Kohtaro OSAKADA, Kenji SANO, Myung-Ki DOH*, Fumiyuki OZAWA*, Sanshiro KOMIYA*, and Yoshihiko KUSHI *(*Tokyo Inst. Tech.)*

[*Organometallics*, **9**, 2197 and 2396 (1990)]

Zerovalent nickel and palladium complexes with phosphine ligands react with α, β- and β, γ-unsaturated carboxylic acids and amides to give various nickel and palladium complexes, such as π-coordinated olefin complexes, hydride complexes, and metal-containing cyclic amide or ester complexes, depending on the metal center, auxiliary phosphine ligands, and the substrates. X-ray crystallography has revealed molecular structures of a nickel containing cyclic amide complex and of a palladium containing cyclic ester complex, the latter of which is shown in Figure. These metallacycle compounds undergo reaction with CO to give five- or six-membered cyclic amides or cyclic esters accompanied by formation of zerovalent carbonyl complexes of nickel and palladium. The result is developed to palladium catalyzed carbonylative cyclization of β, γ-unsaturated carboxylic acids to give cyclic anhydrides. The selectivity of the catalytic reaction is discussed based on the reulsts of stoichiometric carbonylation of the above metallacycles.

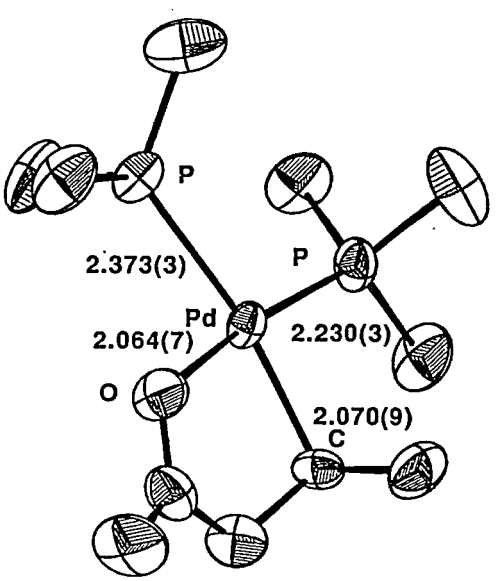

VII-I-3 Studies on Association of Fluoro Alcohol with Platinum Fluoroalkoxide Complex in the Solid State and in Solution. X-ray Crystallography, Calorimetric Titration, and NMR Measurement

Kohtaro OSAKADA, Masako TANAKA*, Yong-Joo KIM*, Shin-ichi ISHIGURO*, and Akio YAMAMOTO*
*(*Tokyo Inst. Tech.)*

[*Inorg. Chem.*, **30**, 197 (1991)]

Association of transition metal complexes with organic molecules through weak interaction such as hydrogen bonding and π-interaction is of recent interest relating to the structure of transition state of the homogeneous catalytic reaction.

Platinum alkoxide complex, cis-$PtMe(OCH(CF_3)_2)(PMe_3)_2$ **1**, reacts with hexafluoro-2-propanol to give cis-$PtMe(OCH(CF_3)_2)(HOCH(CF_3)_2)(PMe_3)_2$ **2** in toluene at room temperature. The X-ray crystallography of the complex **2** shows the structure having O-H...O hydrogen bonding between the coordinated oxygen atom and the OH group of the alcohol. The O...O distance is 2.63(5)Å which is reasonable for that of hydrogen bonded oxygen atoms. ^1H NMR observation of the reaction mixture of **1** with the fluoro alcohol indicates that the complexes **1** and **2** are in equilibrium although **2** is the major compound in the toluene solution at room temperature. Calorimetric titration is examined in order to reveal further details of the equilibrium. Results obtained at 25°C indicate that the complex **1** and the alcohol does not form 1:2 or higher adducts. The obtained thermodynamic parameters are $\Delta H°=-24.7$ kJ mol^{-1}, $\Delta G°=-10.9$ kJ mol^{-1}, and $\Delta S°=-46.0$ J $mol^{-1}K^{-1}$. These values agree well with the results obtained from ^1H NMR measurement.

VII-I-4 Preparation of Novel Ruthenium Aryloxide Complex from Dihydride Ruthenium Complexes and Phenols. Characterization of the Intermediate Ruthenium Complex with Dihydrogen Ligand and their Role in Hydrogenation of Olefin Catalyzed by Ru Complexes

Kohtaro OSAKADA, Kimitaka OHSHIRO*, and Akio YAMAMOTO* *(*Tokyo Inst. Tech.)*

[*Organometallics*, **10**, 404 (1991)]

Reaction of $RuH_2(PMe_3)_4$ with phenol and p-cresol at room temperature gives the corresponding hydrido (aryloxido)ruthenium complexes formulated as $RuH(OAr)(PMe_3)_4$. X-ray crystallography of the p-methylphenoxide complex confirmed the octahedral coordination around the ruthenium center and mutually cis coordination of the hydride and aryloxide ligands. This is probably the first crystallographic structure determination of mononuclear ruthenium alkoxide complex.

NMR(^1H and ^{31}P) spectra of the reaction mixture at lower temperature show initial formation of intermediate ionic complex formulated as $[RuH_3(PMe_3)_4]$ OAr followed by elimination of dihydrogen to give the above aryloxide complexes. T_1 value of the hydrogen atoms bonded to ruthenium in the above ionic intermediate suggests the coordination of a hydride and a molecular hydrogen ligands that undergo mutual exchange of the hydrogen atoms. The ionic ruthenium complex with dihydrogen complex shows much higher catalytic activity for the olefin hydrogenation than the starting netural hydride ruthenium complex probably due to lability of dihydrogen ligand of the former complex.

VII-I-5 Thermal Degradation of Zinc and Cadmium Methanethiolato Complexes to Give ZnS and CdS

Kahtaro OSAKADA and Takakazu YAMAMOTO*
*(*Tokyo Inst. Tech.)*

[*Inorg. Chem.* **30**, 2328 (1991)]

Thiolato zinc and cadmium complexes $[M(SR)_2]_n$ are prepared from reaction of thiol with $ZnEt_2$ or from the corresponding lithium thiolate with $ZnCl_2$ and $CdCl_2$. Analytical data agree well with the proposed formula although extremely low solubility due to the polymeric or nonmolecular structures prevented us from further characterization of the compounds by means of NMR and absorption spectroscopy.

Heating $[Zn(SMe)_2]_n$ and $[Cd(SMe)_2]_n$ at 260–300°C under argon or in vacuo causes formation of the corresponding metal sulfides, ZnS and CdS, accompanied by evolution of MeSMe. The solid products are characterized by X-ray crystallography and elemental analysis, and the gaseous product by GC and GC-MS. Thermogravimetric measurement indicates that the reaction obeys first-order kinetics or auto-catalytic type kinetics depending on the preparation method of the thiolato compounds. This difference of kinetic mode of decomposition is due to the difference of surface area of the thiolato compounds.

VII—J Synthesis of Optically Active Complexes and their Catalytic Use in the Asymmetric Oxidation

The enantioselective synthesis of organic compounds using chiral transition metal complexes has received attention. We are interested in the asymmetric epoxidation of olefins and oxidation of prochiral sulfides. In this project, the synthesis of new optically active complexes and their catalytic activities on the asymmetric oxidation reactions are investigated.

VII-J-1 Preparation and Characterization of Optically Active Quadridentate Schiff Base-Titanium(IV) Complexes and the Catalytic Properties of These Complexes on Asymmetric Oxidation of Methyl Phenyl Sulfide with Organic Hydroperoxides

Caori SASAKI*, Kiyohiko NAKAJIMA, Masaaki KOJIMA*, and Junnosuke FUJITA* *(*Nagoya Univ.)*

[*Bull. Chem. Soc. Jpn.*, **64**, 1318 (1991)]

Titanium(IV) complexes, [TiCl(Schiff base)$_2$]O, with quadridentate Schiff base ligands derived from optically active 1,2-diamines and salicylaldehyde were prepared by treating $TiCl_4$ with equimolar amount of the Schiff base ligand in wet pyridine. The complexes were characterized by their ^{13}CNMR, absorption, and circular dichroism spectra, and conductivity measurements. The complexes in dichlormethane take a μ-oxo dinuclear structure, and in methanol the complex break up into a mononuclear species, [Ti(OMe)(MeOH)(Schiff base)]Cl. The complexes catalyze the asymmetric oxidation of methyl phenyl sulfide into the sulfoxide with organic hydroperoxides; the highest enantiomeric excess (ee) was ca.60%. The kinetics conform to a rate law which is first order in the concentration of each sulfide, hydroperoxide, and complex catalyst.

VII—K Chemical Simulation to Nitrogen Cycle and Carbon Dioxide Fixation

Metal complexes which are capable of catalytic reduction of NO_3^- and NO_2^-, or CO_2 fixation have been investigated in order to simulate those biological redox reactions. Dissimilatory nitrite reductases reduce NO_2^- to afford N_2 through N_2O concomitant with a small amount of NO evolution. The mechanism of neither NO evolution nor N-N bond formation has been eludicated so far. Interconversion between NO_2^- and NO on a certain metal complex may afford a clue to solve the mechanism. In biological CO_2 fixation, CO_2 is fixed to positively polarized carbonyl carbons of organic molecules. Such a CO_2 fixation is expected to take place by reductive activation of CO_2 on coordinatively unsaturated metal complexes.

VII-K-1 Crystal Structure of *cis*-Carbonmonoxide-η^1-Carbondioxide-Bis(2,2'-bipyridyl)Ruthenium. An Active Species in Catalytic CO_2 Reduction Affording CO and $HCOO^-$

Hiroaki TANAKA, Hirotaka NAGAO, Shie-Ming PENG *(National Taiwan Univ.)*, **and Koji TANAKA***

An H_2O/EtOH (1:1 v/v) solution of $[Ru(bpy)_2(CO)_2](PF_6)_2$ turned to red by an addition of 2 equiv of Bu_4NOH, and single crystals of $[Ru(bpy)_2(CO)(COO)] \cdot 3H_2O$ were obtained. $[Ru(bpy)_2(CO)(COO)] \cdot 3H_2O$ displayed two strong IR bands at 1911 and 1242 cm^{-1} assignable to $\nu(C\equiv O)$ and $\nu(CO_2)$, and those bands were shifted to 1869 and 1213 cm^{-1}, respectively, by treatment of $[Ru(bpy)_2(CO)(COO)] \cdot 3H_2O$ with $H_2{}^{18}O$ (97%). Furthermore, an addition of an aqueous HCl solution to a methanolic solution of $[Ru(bpy)_2(CO)(COO)] \cdot 3H_2O$ quantitatively regenerated the colorless $[Ru(bpy)_2(CO)_2]^{2+}$. Thus, $[Ru(bpy)_2(CO)(COO)]$ reversibly reacts with H^+ to produce $[Ru(bpy)_2(CO)_2]^{2+}$ *via* $[Ru(bpy)_2(CO)C(O)OH]^+$ (eq.1 and 2). On the other hand, electrochemical reduction

$$[Ru(bpy)_2(CO)(CO_2)]+H^+ \rightleftarrows [Ru(bpy)_2(CO)C(O)OH]^+ \quad (1)$$

$$[Ru(bpy)_2(CO)C(O)OH]^+ + H^+ \rightleftarrows [Ru(bpy)_2(CO)_2]^{2+} \quad (2)$$

of $[Ru(bpy)_2(CO)_2]^{2+}$ at -1.10 V (*vs.* SCE) in dry CH_3CN under CO_2 atmosphere gives CO and $[Ru(bpy)_2(CO)(COO)]$ (eq.3).

$$[Ru(bpy)_2(CO)_2]^{2+} + CO_2 + 2e^- \rightarrow [Ru(bpy)_2(CO)(COO)] + CO \quad (3)$$

A selective formation CO and $HCOO^-$ in the electrochemical CO_2 reduction catalyzed by $[Ru(bpy)_2(CO)_2]^{2+}$, therefore, proceeds through rapid interconversions among $[Ru(bpy)_2(CO)_2]^{2+}$, $[Ru(bpy)_2(CO)C(O)OH]^+$, and $[Ru(bpy)_2(CO)(COO)]$ depending on activity of the proton source in the reaction media.

Molecular structure of $[Ru(bpy)_2(CO)(COO)]$

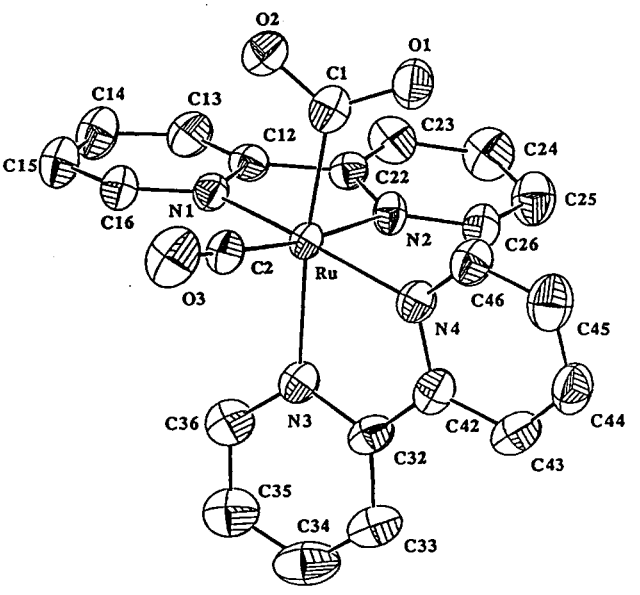

VII-K-2 Redox Behaviors of a Fe_4S_4 Cluster with Bulky Substituents in Aqueous Conditions

Hide KAMBAYASHI, Masami NAKAMOTO *(Osaka Municipal Technical Research Inst.)*, **Hirotaka NAGAO, and Koji TANAKA***

4Fe4S ferrodoxins mediate electron transfer between $[Fe_4S_4]^{+/2+}$ redox couples, while high potential iron-sulfur proteins (HiPIP) function as electron transfer catalysis using

$[Fe_4S_4]^{2+/3+}$ rodox couple. Thus, 4Fe4S iron-sulfur proteins can adopt three different oxidation levels, $[Fe_4S_4]^{1+/2+/3+}$. However, synthetic Fe_4S_4 clusters usually show only a reversible or quasi-reversible $[Fe_4S_4]^{+/2+}$ redox couple in ordinary solvents. It has been shown that three synthetic Fe_4S_4 clusters exhibit a stable $[Fe_4S_4]^{2+/3+}$ redox couple in organic solvents, but those clusters are labile in the $[Fe_4S_4]^{+}$ oxidation state. Accordingly, none of synthetic Fe_4S_4 cluster displays both $[Fe_4S_4]^{+/2+}$ and $[Fe_4S_4]^{2+/3+}$ redox couple. Cyclic voltammograms of $(Bu_4N)_2[Fe_4S_4(SAd)_4]$ (Ad=adamantane) show stable not only $[Fe_4S_4]^{2+/3+}$ but also $[Fe_4S_4]^{+/2+}$ redox couples at $E_{1/2}$=−0.28 and −0.90 V in aqueous nylon solution at pH 7.3. The $E_{1/2}$ value of the $[Fe_4S_4(SAd)_4]^{2-/3-}$ redox couple is shifted by −60 mV/pH, and has a tendency to level off above pH 9.1 and below pH 6.6. Similarly, the $E_{1/2}$ of the $[Fe_4S_4(SAd)_4]^{1-/2-}$ couple also shows a pH dependence and becomes a constant value between pH 6.6 and 7.2. These results are reasonably explained a successive protonation of the $[Fe_4S_4(SAd)_4]^{1-/2-/3-}$ state, as shown in Figure. The protonation of $[Fe_4S_4]^{2+}$ is also supported by a revesible change in the electronic absorption spectrum of $(Bu_4N)_2[Fe_4S_4(SAd)_4]$ in aqueous nylon solutions at various pH values.

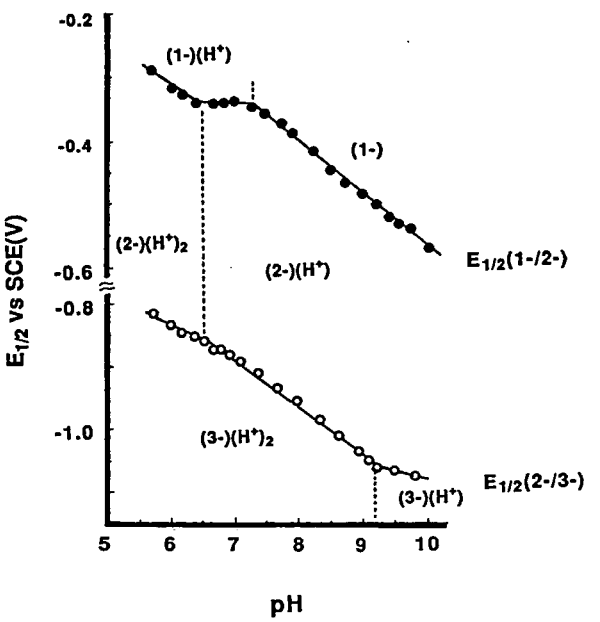

VII-K-3 Electrochemical Carbon Dioxide Fixation to Thioesters Catalyzed by $[Mo_2Fe_6S_8(SEt)_9]^{3-}$

Nobutoshi KOMEDA *(Osaka Univ.)*, **Hirotaka NAGAO, Tatsuji MATSUI** *(Osaka Univ.)*, **Ginya ADACHI** *(Osaka Univ.)*, **and Koji TANAKA***

A controlled potential electrolysis at −1.55 V *vs.* SCE of CO_2-saturated dry CH_3CN containing $(Bu_4N)_3[Mo_2Fe_6S_8(SEt)_9]$, $CH_3C(O)SEt$, Bu_4NBF_4, and molecular sieves 3A produced $CH_3C(O)COO^-$ with a current efficiency 27%. The similar electrolysis using $C_2H_5(O)SEt$ or $C_6H_5C(O)SEt$ also produces $C_2H_5C(O)COO^-$ or $C_6H_5C(O)COO^-$ catalytically with a current efficiency 49% or 13%, respectively (eq.1). The reaction (1) is essentially same as the CO_2 fixation catalyzed by photosynthetic bateria, where CO_2 is fixed at the carbonyl carbons of acetylcoenzyme A and succinyl-coenzyme A to generate pyruvate or α-keto glutarate (eq.2). Electrochemical study revealed that CO_2 is not activated one-electron reduced

$$RC(O)SEt + CO_2 + 2e^- \rightarrow RC(O)COO^- + EtS^- \quad (1)$$
(R=CH_3, C_2H_5, and C_6H_5)

$$RC(O)SCoA + CO_2 + 2e^- \rightarrow RC(O)COO^- + CoAS^- \quad (2)$$
(R=CH_3, $HO(O)CCH_2CH_2$; CoA=coenzyme A)

Fe_4S_4 cluster, while the two-electron reduced MoFeS cluster can activate CO_2, which reacts with thioesters to afford the corresponding α-keto acids (eq.1). Carbon dioxidie as an electrophile presumably binds to basic sites of the MoFeS cluster in the initial stage in the reaction (1). Not only $[Fe_4S_4(SR)_4]^{3-}$ but also $[Mo_2Fe_6S_8(SR)_9]^{5-}$ are reversibly protonated in aqueous micellar solutions, but the basicity of the latter ($pK_a \approx 11$) is much stronger than the former ($pK_a \approx 9$). In addition, a pK_a value of the core sulfur of $[Fe_4S_4(SC_6H_4-p-t-Bu)_4]^{3-}$ (pK_a=8.80) is higher than that of the terminal one of $[Fe_4S_4(SC_6H_4-p-t-Bu)_4]^{2-}$ (pK_a=5.85) in aqueous conditions, suggesting that a core sulfur is a strong base compared with a terminal sulfur of Fe_4S_4 cluster. The most possible site for an electrophilic attack of CO_2 to $[Mo_2Fe_6S_8(SEt)_9]^{5-}$, therefore, may be a core-sulfur of the two-electron reduced MoFeS cluster, where CO_2 is activated through an intramolecular electron transfer from $[Mo_2Fe_6S_8(SEt)_9]^{5-}$ *via* S-CO_2 bond.

VII-K-4 Synthesis and Characterization of bis(2,2'-bipyridyl)nitrocarbonylruthenium(II) Complex

Hiroaki TANAKA, Hirotaka, NAGAO, and Koji TANAKA*

Orange crystals of $[Ru(bpy)_2(CO)(NO_2)]PF_6$ were obtained in a 70% yield by refluxing a CH_3OH/H_2O solution containing $[Ru(bpy)_2(CO)Cl]PF_6$ and $NaNO_2$ for 24 h, followed by cooling the solution to room temperature. The IR spectrum of $[Ru(bpy)_2(CO)(NO_2)]PF_6$ showed a $\nu(C\equiv O)$ at 1983 cm^{-1}, and $\nu_a(NO_2)$ and $\nu_s(NO_2)$ at 1372 and 1316 cm^{-1}, respectively, and the IR absorption bands of $\nu_a(^{15}NO_2)$ and $\nu_s(^{15}NO_2)$ of $[Ru(bpy)_2(CO)(^{15}NO_2)]PF_6$ were observed at 1345 and 1293 cm^{-1}. An addition of Bu_4NOH in CH_3OH to a dry CH_3CN solution of $[Ru(bpy)_2(CO)(NO_2)]PF_6$ results in an increase in an absorption band at 290 nm with an isosbestic point at 310 nm, and the electronic spectrum of $[Ru(bpy)_2(CO)(NO_2)]^+$ was regenerated by neutralization of the solution using an aqueous $HClO_4$. The IR spectrum of a product obtained in the reaction of $[Ru(bpy)_2(CO)(NO_2)]PF_6$ with 2 mole of KOH in CH_3OH showed a strong band at 1650 cm^{-1}, together with a weak $\nu(C\equiv O)$ band at 1983 cm^{-1} due to a contamination of $[Ru(bpy)_2(CO)(NO_2)]PF_6$, suggesting that $[Ru(bpy)_2(CO)(NO_2)]^+$ reversibly reacts with OH^- to form $[Ru(bpy)_2(C(O)OH)(NO_2)]$ (eq.1).

$$[Ru(bpy)_2(CO)(NO_2)]^+ + OH^- \rightleftarrows [Ru(bpy)_2(C(O)OH)(NO_2)] \quad (1)$$

The structure of $[Ru(bpy)_2(CO)(NO_2)]PF_6$ determined by X-ray analysis is represented in Figure. Carbon monoxide and nitro on Ru(II) are in cis-position. The Ru-C and C-O bond distances are 1.94(1) and 1.02(2)Å, respectively, with a slightly distorted Ru-C-O angle, 170(1)°. The Ru-N5 (trans to CO) distance, 2.11(1)Å, is same as the Ru-N2 (trans to NO_2) distance. In addition, the Ru-N4 (trans to bpy) bond length, 2.07(1)Å, is also almost consistent with the Ru-N3 (trans to bpy) one, 2.06(1)Å. The equivalence in the bond length between not only Ru-N4 and Ru-N3 but also Ru-N5 and Ru-N2 suggests that carbonyl and nitro ligands of $[Ru(bpy)_2(CO)(NO_2)]^+$ give a similar electronic influence on Ru-bpy bonds.

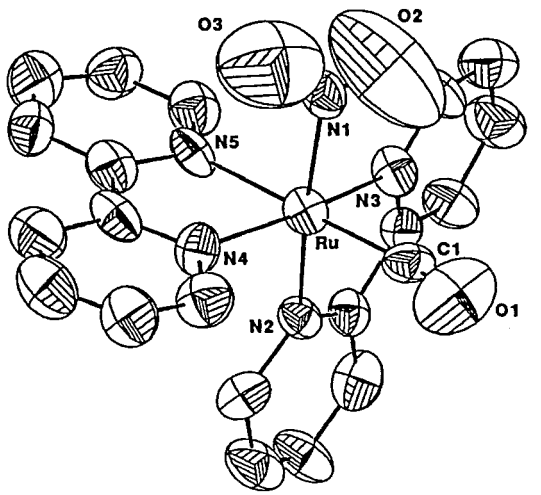

Molecular structure of $[Ru(bpy)_2(CO)(NO_2)]^+$.

VII—L Selective Reactions Using Early Transition Metal Compounds

Highly selective reactions of early transition metal complexes such as zirconium(II)-alkene complexes have been investigated. Not only stoichiometric reactions but also catalytic reactions have been developed.

VII-L-1 Remarkably "Pair"-Selective and Regioselective Carbon-Carbon Bond forming Reactions of Zirconacyclopentane Derivatives with Grignard Reagents

Tamotsu TAKAHASHI, Takashi SEKI*, Yu NITTO*, Masahiko SABURI*, Christophe J. ROUSSET, and Ei-ichi NEGISHI**** *(*The Univ. of Tokyo, **Purdue Univ.)*

[*J. Am. Chem. Soc.*, **113**, 6266 (1991)]

Treatment Cp_2ZrCl_2 with 2 equiv of EtMgBr followed by addition of alkenes, such as 1-decene, styrene and (E)-β-methylstyrene, gives α-aryl- and/or β-alkyl-substituted zirconacyclopentane derivatives in a highly regioselective manner. Their treatment with EtMgBr (1 equiv) produces regioselectively 1-aryl- and /or 2-alkyl-substituted butylmagnesium bromides with concomitant formation of Cp_2Zr-ethylene, which has been trapped with PMe_3, to give $Cp_2Zr(CH_2{=}CH_2)(PMe_3)$. The discrete stoichiometric processes described above can be combined to provide a Zr-catalyzed process for converting alkenes and EtMgBr into 1-aryl-and/or 2-alkyl-substituted butylmagnesium bromides in good yields.

VII-L-2 Zirconium-Catalyzed Highly Regioselective Hydrosilation Reaction of Alkenes and X-Ray Structures of Silyl(hydrido)zirconocene Derivatives

Tamotsu TAKAHASHI, Maki HASEGAWA,* Noriyuki SUZUKI,* Masahiko SABURI,* Christophe J. ROUSSET, Phillip E. FANWICK**, and Ei-ichi NEGISHI**** *(*The Univ. of Tokyo, **Purdue Univ.)*

[*J. Am. Chem. Soc.*, in press]

Dialkylzirconocenes, generated in situ from Cp_2ZrCl_2 and alkylmetals, such as EtMgBr or BuLi, catalyze hydrosilation reactions of alkenes with H_2SiPh_2., Alkyldiphenylsilanes containing n-Oct(75%), n-Decyl(70%), $PhCH_2CH_2$(78%), and $Ph(CH_2)_3$(65%) were obtained in the yields shown in parentheses. The available data indicate that alkene-zirconocenes are likely intermediates. These species undergo oxidative addition with H_2SiPh_2 to produce a silyl(hydrido)zirconocene species as a presumed and elusive active species. In the presence of PMe_3 or an excess of H_2SiPh_2, the reaction yielded $Cp_2Zr(PMe_3)(H)(SiHPh_2)$ or $[Cp_2Zr(H)(SiHPh_2)]_2$, respectively. These complexes are yellow crystalline species and have been fully identified by spectroscopic means including X-ray analysis. The complex $Cp_2Zr(PMe_3)(H)(SiHPh_2)$, reacted with 1-octene to give n-OctSiHPh$_2$. The results show not only the feasibility of generating silyl(hydrido)zirconocene derivatives from dialkylzirconocenes and H_2SiPh_2 but also their ability to effect hydrosilation of alkenes.

VII-L-3 Catalytic Hydrogenation of Alkenes Using Zirconocene-Alkene Complexes

Tamotsu TAKAHASHI, Noriyuki SUZUKI*, Motohiro KAGEYAMA*, Yu NITTO*, Masahiko SABURI*, and Ei-ichi NEGISHI** *(*The Univ. of Tokyo, **Purdue Univ.)*

[*Chem. Lett.*, 1579 (1991)]

Hydrogenation reactions of alkenes were catalyzed by zirconium-alkene complex derivatives which were prepared from Cp_2ZrCl_2 (Cp=η^5-C_5H_5) and n equiv. of RR'CHCH$_2$M (M=MgX or Li). By the use of three or more equiv. of EtMgBr relative to Cp_2ZrCl_2, the product yield of hydrogenation of 1-decene was remarkably improved most likely due to the stabilization of the Zr(II) species.

VII—M Novel Reactivity of Molybdenum and Tungsten Dinitrogen Complexes

Reactivity of coordinated dinitrogen in molybdenum and tungsten complexes of the type $[M(N_2)_2(L)_4]$ (M=Mo, W; L=phosphine) has been investigated.

VII-M-1 Silylation of Coordinated Dinitrogen by Silylcobalt Complexes

Andrew C. STREET*, Yasushi MIZOBE*, Fumisato GOTOH*, Izumi MEGA*, Hiroyuki OSHITA* *(*Tokyo Univ.),* **and Masanobu HIDAI** *(Tokyo Univ. and IMS)*

[*Chem. Lett.*, 383 (1991)]

The silylcobalt complexes $[R_2R'SiCo(CO)_4]$ (R, R'=Ph, Me) reacted with dinitrogen complexes of the type $[M(N_2)_2(P)_4]$(M=Mo, W; P=tertiary phosphine) to give new silyldiazenido complexes *trans*-$[M(NNSiR_2R')(P)_4][(\mu\text{-OC})Co(CO)_3]$, which were further converted to silylhydrazido(2−) complexes such as *trans*-$[WX(NNHSiR_2R')(dpe)_2][Co(CO)_4]$ by treatment with HX (dpe=$Ph_2PCH_2CH_2PPh_2$; X=OH, OMe, Br).

VII-M-2 Regioselective Mono- and Di-C-acylation of Tungsten Diazoalkane Complexes via Alkenyldiazenido Complexes

Hidekazu MIYAGI*, Youichi ISHII*, Takayuki AOSHIMA*, Yasushi MIZOBE* *(*Tokyo Univ.),* **and Masanobu HIDAI** *(Tokyo Univ. and IMS)*

[*Chem. Lett.*, 611 (1991)]

Tungsten alkenyldiazenido complexes reacted with isocyanates, isothiocyanate, and diphenylketene to give regioselectively α-acylated diazoalkane complexes after protonation. In the reaction of *trans*-$[WF(NNCMe{=}CH_2)(dpe)_2]$ (dpe=$Ph_2PCH_2CH_2PPh_2$) with excess aryl isocyanates, α, α-diacylated diazoalkane complexes such as *trans*-$[WF\{NN{=}CMeCH(CONHPh)_2\}(dpe)_2][BF_4]$ were obtained, whose structure was determined by the X-ray analysis.

VII—N Study of Dinuclear and Polynuclear Metal Complexes

There are many polynuclear metalloproteins in biological system. We devised various types of polynucleating ligands to prepare model complexes for metalloproteins.

VII-N-1 Synthesis and Characterization of a Novel Dimer of Di(μ-oxo)manganese Dimers with Two Coordinated Water molecules Molecules in (III,IV,III,IV) Oxidation State

Masatatsu SUZUKI *(Kanazawa Univ. and IMS),* **Yoshihito HAYASHI*, Kazutoshi MUNEZAWA*, Machiko SUENAGA*, Hitoshi SUNDA*, and Akira UEHARA*** *(*Kanazawa Univ.)*

[*Chem. Lett.*, 1991, 1929]

A dimer of di(μ-oxo)dimanganese(III,IV) dimers with two coordinated water molecules, $[\{Mn_2(tmdp)(O)_2(H_2O)\}_2](CF_3SO_3)_4 \cdot 6H_2O$, was synthesized as a model for manganese cluster of oxygen-evolving center (OEC) in photosystem II (PS II), where Htmdp is 1,5-bis[bis(2-pyridylmethyl)amino]-3-pentanol. X-ray structure analysis reveals that the complex consists of two di(μ-oxo)Mn_2 dimers which are linked by two tmdp bridges to form a dimer of dimers with a bilayered structure (Figure 1). The most striking feature of the complex is that it has two water molecules coordinated to manganese(III) ions, which are separated only by ca. 3.3Å. Such coordinated water molecules in close proximity must be of a key importance for modelling manganese center of OEC in PS II. This is the first example of tetranuclear complex which contains two di(μ-oxo)Mn_2(III,IV) dimers and two coordinated water molecules.

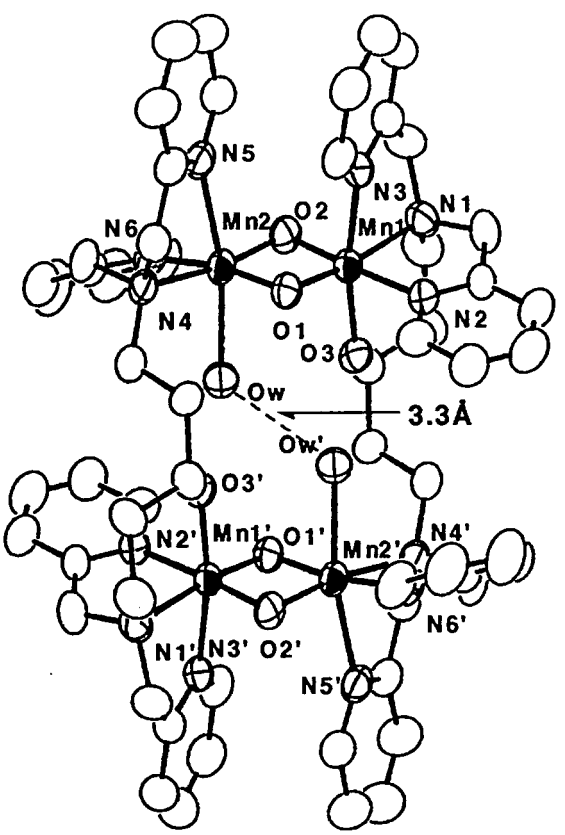

Figure 1. Molecular structure of $[\{Mn_2(tpdp)(O)_2(H_2O)\}_2]^{4+}$.

VII-N-2 Reversible Oxygenation of (μ-alkoxo) Diiron(II,II) Complexes of Dinucleating Ligand, Me-tpdp, 1,3-bis{bis[2-(6-methylpyridyl)methyl]amino}-2-propanolate

Yoshihito HAYASHI*, Masatatsu SUZUKI *(Kanazawa Univ. and IMS)*, **Akira UEHARA*, Yasuhisa MIZUTANI, and Teizo KITAGAWA** *(*Kanazawa Univ.)*

[*Chem. Lett.*, in press]

Two types of (μ-alkoxo)diiron(II,II) complexes with hindered dinucleating ligand Me-tpdp, $[Fe_2(Me\text{-}tpdp)(RCOO)]^{2+}$ (RCOO=C_6H_5COO or CF_3COO) and $[Fe_2(Me\text{-}tpdp)Cl_2]^+$, were synthesized and the structure of benzoato derivative was determined by X-ray analysis (Figure 1). The complexes showed reversible oxygenation in dichloromethane. The presence of methyl groups in the 6-position in pyridyl rings in Me-tpdp plays an essential role for the oxygenation and reversibility. Resonance Raman study of the oxygenated species suggests an unsymmetrical μ-η^1-η^1 binding of peroxo group toward diiron center. The oxygen affinities of the complexes were determined by electronic spectral change under various oxygen partial pressures: $P(O_2)_{1/2}$ of benzoato, trifluoroacetato, and dichloro complexes are 6, 43, and 46 torr, respectively.

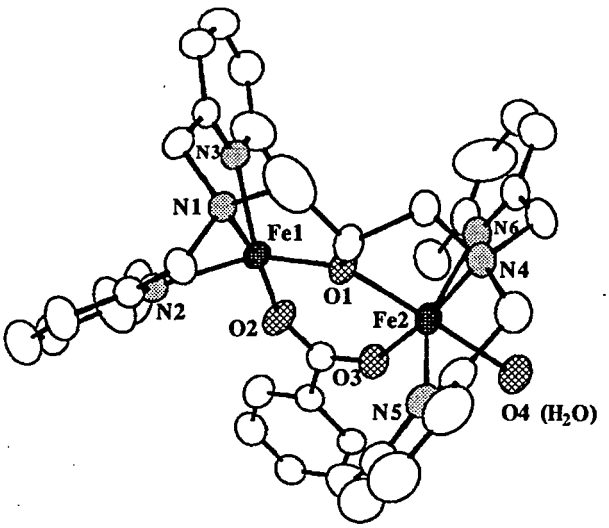

Figure 1. Molecular structure of $[Fe_2(Me\text{-}tpdp)(C_6H_5COO)]^{2+}$

RESEARCH ACTIVITIES VIII
Computer Center

VIII—A Theoretical Investigations of Structures and Properties of Molecular Assemblies

Structures and properties of molecular clusters, liquids, solutions and solids are studied using the molecular dynamics and the Monte Carlo technique. A new intermolecular potential function for the molecular simulations is developed based on the *ab initio* molecular orbital theory.

VIII-A-1 Monte Carlo Simulation of Liquid Ammonia and an Evaluation of Thermodynamic Properties

Kazuhiko HONDA, Kazuo KITAURA, and Kichisuke NISHIMOTO *(Osaka City Univ.)*

Monte Carlo simulations are performed on liquid ammonia using the potential function expressed by the intermolecular overlap integrals and fractional point charges on the atoms. The N-N radial distribution function is shown in Figure 1. The peak at 3.2 Å is due to the hydrogen bonding between molecules. A broad shoulder at 3.8 Å (the arrow in Figure 1) suggests that there are non-bonding molecules in the first shell. Thermodynamic properties are estimated using a partition function whose parameters are obtained by referring to the results of the Monte Carlo simulation. The calculated thermodynamic properties well reproduce the experiments.

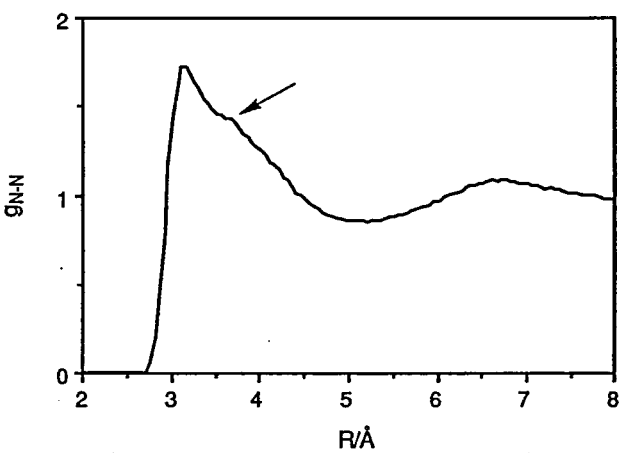

Figure 1. N-N radial distribution function at 273 K, 0.63 gcm^{-3}.

VIII-A-2 Density of States of Large Size Matrix

Umpei NAGASHIMA

The calculation of density of state (DOS) of large size matrix usually requires a large amount of computer memory space (order of N^2) and relatively long CPU time because matrix is directly diagonalized to obtain eigenvalues and eigenvectors. Because of this condition, the size of matrix N is limited in general to a few thouthands. In addition, standard routines of matrix diagonalization yield poor accuracy for large size matrix, especially for the eigenvalues which are around zero: small absolute value. The method employed in the present work, introduced by Williams and Maris[1], and developed by Yakubo et al[2], enables us to treat the matrix diagonalization of very large matrix. This algorithm requires less memory space (order of N) and is suitable for supercomputers. This method is based on the physical analogy that the eigen frequency of the system satisfies the resonance condition when applying the periodic external force (frequency O) to the system. In the present work, the method is developed to treat general standard eigenvalue problem.

In Figure 1, DOS of cyclic polyacene ($C_{20000}H_{10000}$) calculated by the present program is depicted with the analytical DOS for infinitely large cyclic polyacene[3]. The singular points of analytical DOS for infinity system are reproduced in calculated DOS. CPU time required is 115 seconds on Hitac S820/80. Memory size is only 1M byte because all-nonzero matrix elements are kept with index (i,j) on disk space.

References

1) M.L. Williams and H.J. Maris, *Phys. Rev.* **B31**, 4508 (1985).
2) K. Yakubo and T. Nakayama, *Phys. Rev.* **B40**, 517 (1989).
3) H. Hosoya, M. Aida, R. Kumagai, and K. Watanabe, *J. Comput. Chem.* **8**, 358 (1987).

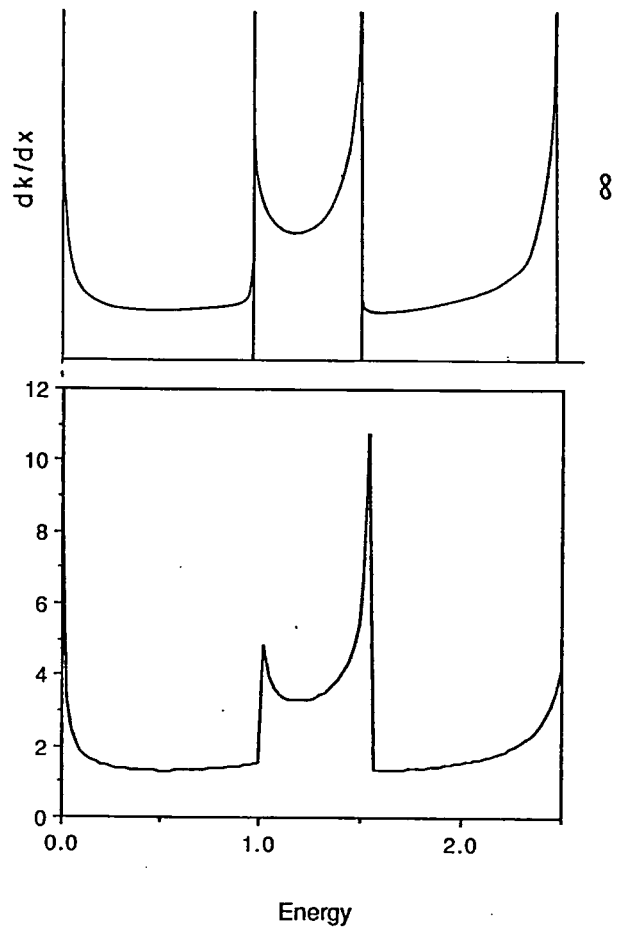

Figure 1. Density of states for cyclic polyacene. Upper one is analytical solution for infinity system obtained by Hosoya et al[3]. Lower one is numerical result for $C_{20000}H_{10000}$.

VIII-A-3 Analysis of Numerical Error for Eigenvalue Problems of Large Matrix

Umpei NAGASHIMA

[*Supercomputer Rev.* in press]

The remarkable progress on CPU performance by the emergence of supercomputer has brought us a drastic change in numerical computation. This allowed us to accomplish larger size calculations which accuracy is hard to evaluate.

In order to develop new program of matrix diagonalization, numerical error and the corse of the error was analyzed by using some typical matrix which analytical solutions were well known.

Maximum and averaged numerical error of Frank matrix is depicted in Figure 1. Matrix elements and eigenvalues are given by

$a_{ij}=n+1-\max(i,j)$

and

$e_i=0.5(1.0-\cos((2i-1)\pi/(2n+1)))^{-1}$,

respectively. Eigenvalues of Frank matrix do not degenerate.

Householder-Bisection (HBS) and Householder-QR (HQR) methods are examined with the convergence threshold $\varepsilon=1.0e^{-12}$. Dimension of matrix is changed from 100 to 2000 by 100. Hitac S820/80 in IMS computer center is used.

Errors seem to be proportional to square root of matrix size. Though both methods give almost the same maximum error, HQR seems to give more accurate result than HBS. For the eigenvalues around 0.0: small absolute values, these methods yield poor accuracy. This is unsuitable for our problem because the position of HOMO and LUMO is closest to 0.0.

Main cause of the numerical error is the loss of trailing digits and the cancelation of significant digits. Both causes can be easily avoid by using larger bits to a word.

The calculations of the order of 1000 dimension are not difficult on supercomputer but the accuracy of the results should be carefully evaluated because degeneracy of eigenvalues is usually happen in the actual calculation and corse serious numerical error.

Supercomputer based on 128 bits or larger bits for a word is essential for high accurate calculation.

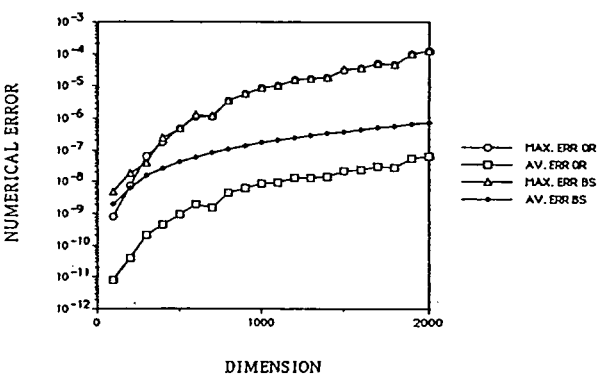

Figure 1. Maximum and averaged numerical error of eigenvalues of Frank matrix. Maximum errors are almost the same between HQR (-○-) and HBS (-△-). Average error of HQR (-□-) is smaller than that of HBS (-◇-). Errors seem to be proportional to square root of matrix size (n).

VIII-A-4 Fluorescence Properties of the Allenic Carotenoid Fucoxantin: Analysis of the Effect of Keto Carbonyl Group by Using a Model Compound, all-*trans*-β-apo-8′-Carotenal

Mamoru MIMURO *(NIBB)*, **Yoshinobu NISHIMURA** *(Hokkaido Univ.)*, **Iwao YAMAZAKI** *(Hokkaido Univ.)*, **Tetsuya KATOH** *(Kyoto Univ.)*, **and Umpei NAGASHIMA**

[*J. Luminescence* in press]

The fluorescence spectrum of a linear carotenoid, all-*trans*-β-apo-8′carotenal (β-apo-8′-carotenal (BAC)) at 20°C is reported for the first time. This pigment contains a keto carbonyl group and thus is regarded as a model compound of fucoxantin, a main light-harvesting carotenoid in marine algae. When BAC was excited at 460 nm, fluorescence originating from plural states was simultaneously detected; one being located close to the 0-0 absorption band and the other, around 750 nm at its maximum.

Locations of the fluorescence maxima were solvent dependent; the emission from the former varied its location in accordance with the locations of the absorption maximum, countrary to the emission from whose location was only

slightly affected by solvents. Relative intensities of both emissions were also solvent dependent; in a solvent with small polarizability (n-hexane), emission solely came from the former, on the other hand, in a solvent with high polarizability (CS_2 and CCl_4), the emission from the latter was stronger.

These difference can be explained by an interaction between BAC and solvent. When we simiulate solvent molecules with a sphere model, CS_2 and CCl_4 can be seen to hold a negatively charged atmosphere, and n-hexane, a positively charged atmosphere. CS_2 and CCl_4 interact attractively with hydrogen atoms of BAC, giving rise to the formation of a large cluster. In the excited state this cluster will facilitate an increase of dipole moment, which consequently induces a large Stokes shift. As shown in Figure 1, the main emission in n-hexane comes from the S_2, thus the energy gap between the S_1 and S_2 is relatively large with a similar Frank-Condon factor. On the other hand, in CS_2 and CCl_4, the potential surface of the S_1 is largely shifted, giving rise to crossing with the potential surface of the S_2. These suggest that the fluorescence of BAC originates both from the lowest (S_1) and second (S_2) singlet states.

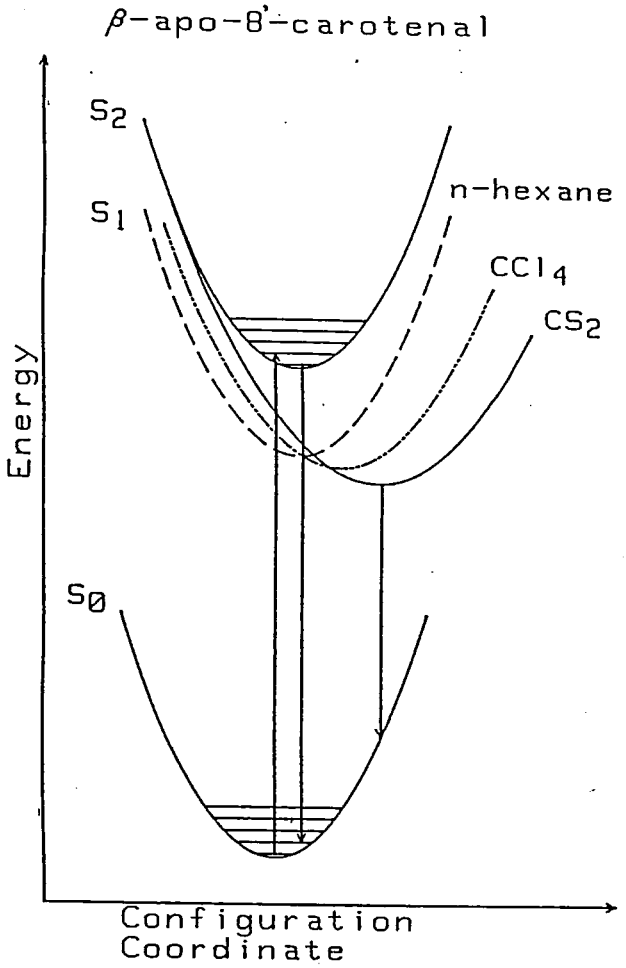

Figure 1. Schematic energy level diagram for β-apo-8'-carotenal in various solvents. Light absorption corresponds to the S_0-S_2 transition (full straight line). Three different S_1 potential surfaces correspond to individual solvents shown in Figure. In the case of n-hexane (----), the emission originates from the S_2, as shown by a straight line (left side). In CS_2 (—), the main emission comes from the S_1 (straight line, right side).

Chemical Materials Center

VIII-B Preparation and Properties of Novel Heterocyclic Compounds Giving Organic Conductors

Heterocyclic compounds containing sulfur or nitrogen atoms are useful as components of functional materials such as organic conductors because heteroatoms in their rings are helpful to stabilize ions or ion-radical species, and intermolecular interactions caused by heteroatom contacts may form unique molecular assemblies. In this project novel electron acceptors and donors based on heterocycles were synthesized and their properties including those of the charge-transfer complexes or ion-radical salts were investigated.

VIII-B-1 A Facile Preparation of Tetrathiafulvalenes Having Alkylthio Groups from 1,3-Dithiole-2-thiones Using a High-pressure Reaction

Yoshiro YAMASHITA, Shoji TANAKA, and Masaaki TOMURA

[*J. Chem. Soc., Perkin Trans. 1* 3358 (1989)]

The simplest route for the synthesis of bis(ethylenedithio)tetrathiafulvalene (BEDT-TTF) **1a** is desulfurization of the readily available 1,3-dithiole-2-thione **2a** with trivalent phosphorous compounds. However, the reaction is smooth only under photochemical conditions, and the thione **2a** is usually converted into the corrsponding 1,3-dithiol-2-one by reaction with $Hg(OAc)_2$ followed by deoxygenation. We have now examined desufurization of the thiones **2a-d** under high pressure and found that the reaction to afford the TTF derivatives **1a-d** is accelerated by high pressure. The yields of **1a-d** under 400 MPa at 80°C were 78, 50, 60 and 30%, respectively.

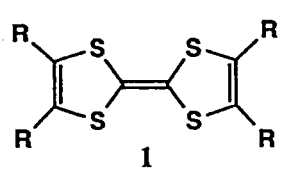

1

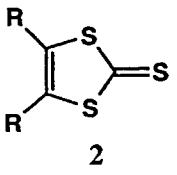

2

a: R=SCH_3
b: R=$S(CH_2)_9CH_3$
c: R,R=SCH_2CH_2S
d: R=H

VIII-B-2 Tetrathio-Derivatives of *p*-Quinodimethanes Fused with 1,2,5-Thiadiazoles. A Novel Type of Organic Semiconductors

Yoshiro YAMASHITA, Shoji TANAKA, Kenichi IMAEDA, and Hiroo INOKUCHI

[*Chem. Lett.* 1213 (1991)]

Bis[1,2,5]thiadiazolo-*p*-quinobis(1,3-dithiole) (BTQBT) was prepared by a Wittig-Horner reaction of 2-dimethylphosphono-1,3-dithiole with 4H,8H-benzo[1,2-c;4,5-c']bis[1,2,5]thiadiazole-4,8-dione. BTQBT is a red-violet crystal with a high melting point and the conductivity is unusually high (10^{-3} S cm^{-1}) as a single component. The X-ray structural analysis reveals that the molecule is completely planar and forms a sheet-like network by short S---S contacts (3.26 Å) as shown in Figure 1. The good conductivity is attributed to the strong intermolecular interactions suggested by the crystal structure as well as the very low ionization potential in solid state.

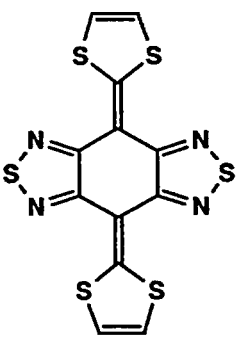

BTQBT

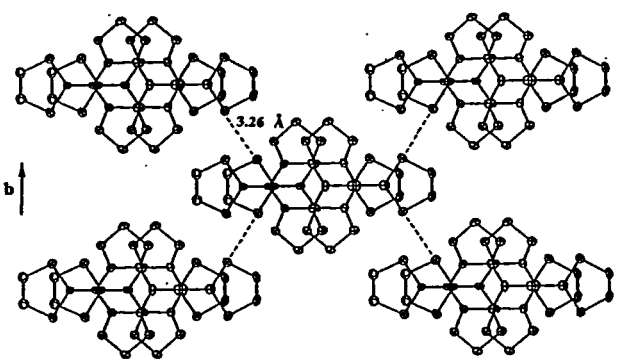

Figure 1. Crystal strucure of BTQBT.

VIII-B-3 5,8-Bis(1,3-dithiol-2-ylidene)-5,8-dihydroqunoxalines: Novel Electron Donors with Low Oxidation Potentials

Yoshiro YAMASHITA, Shoji TANAKA, Kenichi IMAEDA, Hiroo INOKUCHI, and Mizuka SANO* *(*International Cristian Univ.)*

[*J. Chem. Soc., Chem. Commun.* 1132 (1991)]

Bis(1,3-dithiole) donors with extended π-conjugation are of interest as components of organic conductors due to the highly donating properties as well as the decreased Coulombic repulsion. Although a *p*-quinodimethane analogue **1** of tetrathiafulvalene (TTF) is a typical example, **1** was unstable and rapidly decomposed in solution. We have now prepared pyrazine-fused derivatives **2a-d** as air-stable solids using a Wittig-Horner reaction and a retro-Diels-Alder reaction. The cyclic voltammetry showed that they are stronger electron donors than TTF in spite of the presence of the electron-withdrawing heterocycle. The X-ray structural analysis of **2d** revealed that the molecule is almost planar and short contacts between the S of the dithioles and the N of the pyrazines exist. The donor **2b** gave a highly conducting TCNQ complex and cation radical salts.

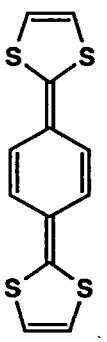

1

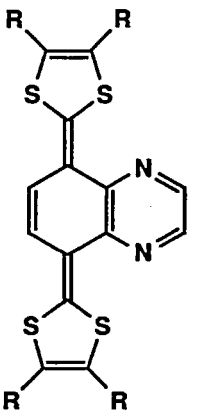

2a; R=H
2b; R=Me
2c; R,R=SCH_2CH_2S
2d; R,R=benzo

VIII-B-4 Preparation and Properties of Tetracyanoquinodimethane Anion Radical Salts with Azaazulenium and Diazaazulenium Ions

Yoshiro YAMASHITA, Takanori SUZUKI*, Yasuo KOBAYASHI*, Toshio MUKAI*, and Tsutomu MIYASHI* *(*Tohoku Univ.)*

[*Snthetic Metals* in press]

1-Aza- and 1,3-diazaazulenium ions, stable heterocyclic cations, were easily prepared. They afforded conducting salts of tetracyanoquinodimethane anion radical ($TCNQ^{-\cdot}$) by metathesis with $Li^{+}TCNQ^{-\cdot}$. Some salts exhibit good conductivities in spite of 1:1 salts. The nitrile stretching frequencies of the salts obtained here are not linearly correlated with the degrees of charge transfer due to strong interactions between the nitrile groups and heteroatoms of

the cations. The X-ray strucural analysis of 2-imino-3-thia-1-azaazulenium-TCNQ salt reveals the novel crystal structure as shown in Figure 1, in which a ribbon-like network is formed by short interheteroatom contacts and hydrogen bondings.

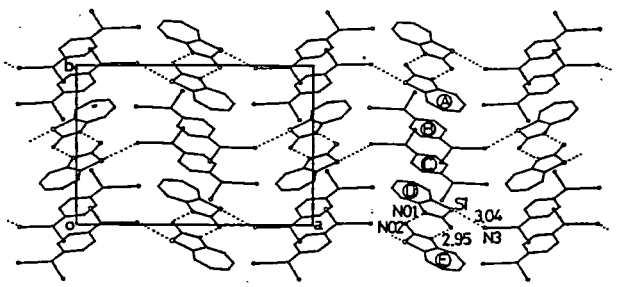

Figure 1. Crystal structure of 2-imino-3-thia-1-azaazuleniumion-TCNQ. Molecules A-D form a tetrad with face-to-face overlapping Cations D and E form a coplanar dyad by hydrogen bonding (N01---N02 2.95 Å). Tetrads are connected by S1---N3 contacts (3.04 Å) forming a ribbon-like network.

VIII-B-5 Synthesis and Electropolymerization of 4,6-Di(2-thienyl)thieno[3,4-c][1,2,5]thiadiazole

Shoji TANAKA, Masaaki TOMURA, and Yoshiro YAMASHITA

Aromatic-quinonoid copolymer systems are promising candidates for narrow band gap materials in the undoped state. We prepared a novel conjugated copolymer **2** containing thiophene units as an aromatic part and thieno[3,4-c][1,2,5]thiadiazole units as a quinoid part. The monomer **1** was synthesized by the coupling reaction of 4,6-dibromothieno[3,4-c][1,2,5]thiadiazole with 2-thienyl magnesium bromide catalyzed by Ni(dppp)Cl_2. Compound **1** displays a reduced HOMO-LUMO separation compared to related systems; its lowest π-π^* transition is at 618 nm [compared to 354 nm for α-terthienyl]. The E_p^{ox} and $E_{1/2}^{red}$ of **1** are +0.85 V and −0.93 V (vs. SCE), respectively. The polymer **2** was prepared by the electrochemical oxidation of **1**. The obtained polymer is easily p-doped as well as n-doped (E_p^{ox}=+0.7 V and E_p^{red}=−1.1 V vs. SCE). The band gap, determined from the thresholds for p-type and n-type doping, is about 0.9 eV. This gap is about 1 eV lower than that for polythiophene.

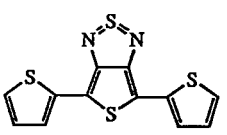

1

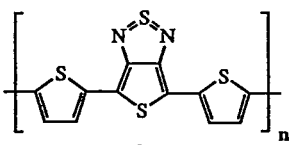

2

VIII-B-6 Synthesis, Structure, and Properties of the TTF Derivative Fused with 1,2,5-Thiadiazole Rings

Masaaki TOMURA, Shoji TANAKA, and Yoshiro YAMASHITA

Tetrathiafulvalene derivatives fused with heterocycles have received much attention as materials of two- or three-dimensional organic conductors. We have synthesized bis[1,2,5]thiadiazolotetrathiafulvalene **1** by the reaction of [1,2,5]thiadiazole-1,3-dithiole-2-thione with triphenylphosphine under refluxing toluene for 72 h in 63% yield. The cyclic voltammogram of **1** in dichloromethane shows two oxidation waves at +1.42 (reversible) and +1.63 V (irreversible) vs. SCE. Due to the high oxidation potential, no complex of **1** with tetracyanoquinodimethane or 2,3-dichloro-5,6-dicyano-1,4-benzoquinone was formed. The molecular structure of **1** was determined by X-ray crystallographic analysis (Figure 1). The short intermolecular S ... S and S ... N contacts within the sum of the Van der Waals radii were observed in the crystal of **1**.

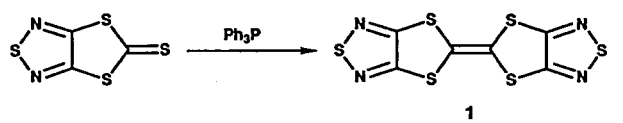

1

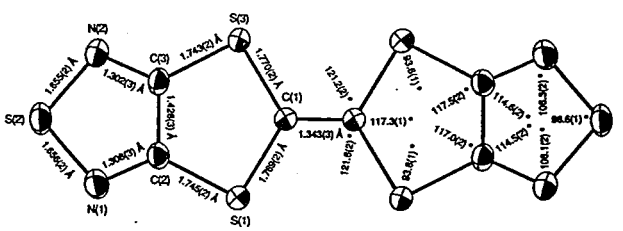

Figure 1. Molecular structure of 1.

Instrument Center

VIII—C Studies of Solvated Metal Clusters

Solvated metal ions and metal cluster ions afford a particularly interesting collection of systems for study because they bridge the gap between bare, isolated ions and ionic solids and electrolyte solutions. From the point of view of cluster chemistry, the questions of charge delocalization, the formation of solvation shells, and the interaction of solvent with metal surfaces appear especially attractive.

In this project we investigate the photoionization and photodissociation processes of various kinds of solvated metal atom (ion) clusters to unveil the microscopic aspect of solvation.

VIII-C-1 Photoionization of Solvated Cs Atoms

Fuminori MISAIZU, Keizo TSUKAMOTO, Masaomi SANEKATA, and Kiyokazu FUKE

[*Chem. Phys. Lett.* in press]

Cesium atom solvated by polar solvents, $Cs(H_2O)_n$, $Cs(NH_3)_n$, and $Cs(CH_3CN)_n$, are studied by one-photon ionization and time-of-flight mass spectroscopy. These species are considered to be a model of alkali metal solution. In the bulk ammonia and water, alkali metal is dissolved and produces the ground state of the solvated electron plus the solvated Cs^+ ion. This state is expected to correlate with the ion-pair state of the cluster. In order to understand the solvation process of alkali atom in bulk fluids, photoionization threshold (IP) was measured for $Cs(NH_3)_n$ ($n \leqq 31$), $Cs(H_2O)_n$ and $Cs(CH_3CN)_n$ with $n \leqq 21$. Determined IPs are plotted in Fig. 1 as a function of $(n+1)^{-1/3}$, which is approximately inversely proportional to the cluster radius. IPs of $Cs(H_2O)_n$ and $Cs(CH_3CN)_n$ are found to be constant for $n \geqq 4$ (3.1 eV) and $n \geqq 12$ (2.4 eV), respectively. These results seem to indicate that the electronic character of $Cs(H_2O)_n$ ($n \geqq 4$) and $Cs(CH_3CN)_n$ ($n \geqq 12$) clusters in the ground state changes from the covalent to ion-pair type. This conclusion is strongly supported by the following arguments. In the photoionization mass spectrum, enhanced stability at n=20 is observed for the $Cs(H_2O)_n$ clusters. This anomaly seems to be ascribable to the stability of neutral $Cs(H_2O)_{20}$ cluster. From the analogy of the magic behavior of these clusters with that of $H_3O^+(H_2O)_n$, this cluster is expected to have the ion core with an ion-chlathrate structure like $H_3O^+(H_2O)_{20}$ and the excess electron is distributed outside the core. Thus, the ground state of this cluster is expected to have an ion-pair nature. On the other hand, the IP for $Cs(NH_3)_n$ decreases monotonously with increasing n to a limit value coincides with the bulk value of 1.4 eV, indicating that the above change may occur at $n \geqq 30$ or succeedingly with n for $Cs(NH_3)_n$.

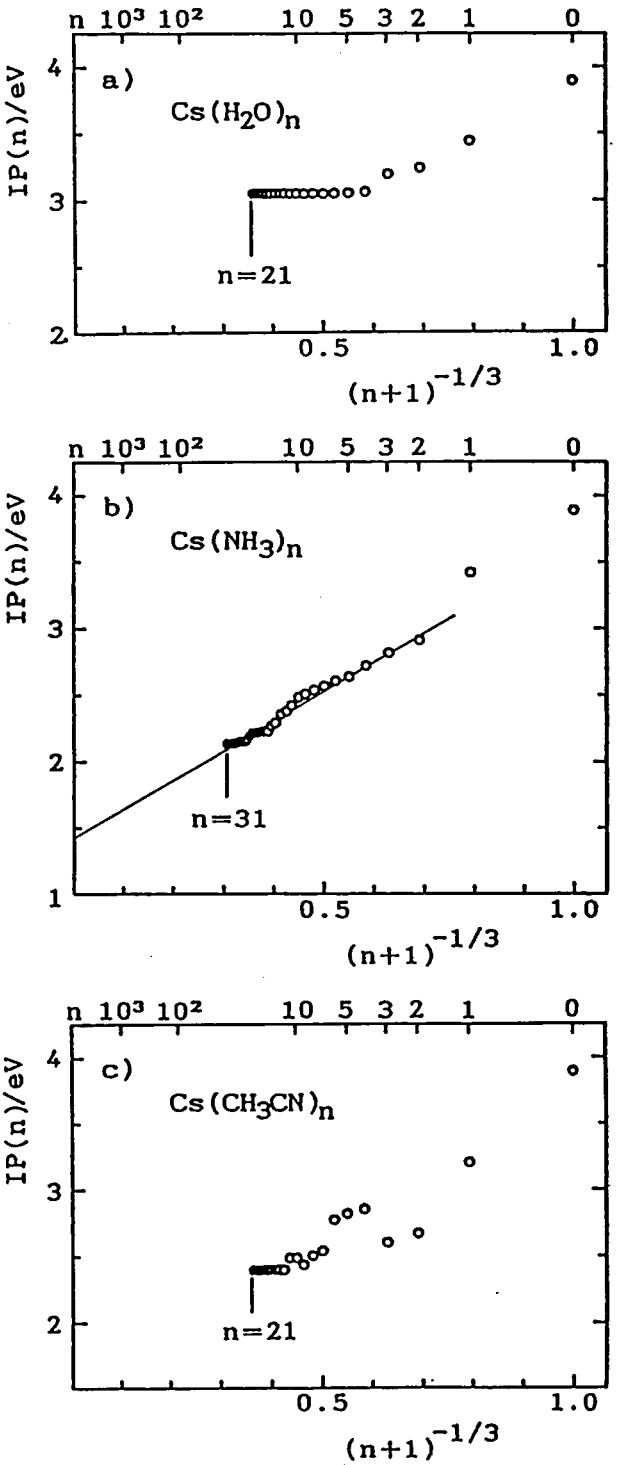

Figure 1. Ionization potentials (IP(n)) of CsM_n clusters plotted vs. $(n+1)^{-1/3}$. a) M=H_2O ($n \leqq 21$). b) M=NH_3 ($n \leqq 31$). The result of the least square fitting for $n \geqq 2$ is also shown. The extrapolated value to $(n+1)^{-1/3}=0$ ($n \to \infty$) is 1.41 eV. Correlation coefficient of the fitted line, r=0.990. c) M=CH_3CN ($n \leqq 21$).

VIII-C-2 Photodissociation of Size-selected $Mg^+(H_2O)_n$ Ions

Fuminori MISAIZU, Masaomi SANEKATA, Keizo TSUKAMOTO, and Kiyokazu FUKE

[*J. Phys. Chem.* to be submitted]

Electronically excited states of magnesium-water cluster ions, $Mg^+(H_2O)_n$ are studied by photodissociation after

mass selection of these ions. Parent cluster ions are produced by laser vaporization and accelerated by pulsed electric fields. UV or visible laser was irradiated to a given size of cluster ions at the end of the first drift region of the reflectron time-of-flight mass spectrometer, and the fragment ions were detected after mass-analyzed in the second drift region. Relative dissociation cross sections are measured as a function of wavelength for n=1 (250–370 nm), 2 (280–470 nm) and 5 (440–720 nm), as shown in Figure 1. The spectra show peaks at 28300, 30500, and 38500 cm^{-1} for n=1 and 25000 and 29400 cm^{-1} for n=2. For n=1, the lowest two transitions have energies consistent with the prediction of ab-initio calculation[1] and are expected to be localized at the Mg^+ ion. In addition to the loss of H_2O molecules, intramolecular dissociation process to produce Mg^+OH are also observed for n=2. The branching ratio between the H_2O evaporation and the intramolecular dissociation is strongly dependent on the photon energy: The process to produce Mg^+OH overcomes the evaporation process in the energy region higher than 30000 cm^{-1}. This observation implies that the reactive potential surface correlated to $Mg^+OH + H + H_2O$ may cross the excited state potential surface of $Mg^+(H_2O)_2$ at this energy. In contrast to the case of n=1 and 2, broad dissociation spectrum is observed with the photon energy of higher than 14000 cm^{-1} for n=5. Only the doubly charged ion, Mg^{2+}, is stable in the bulk aqueous solution, and therefore, the ion-pair state, $Mg^{2+}(H_2O)_n^-$, is expected to be stabilized at large n. The spectrum for n=5 has a possibility to contain transitions to such ion-pair states.

Reference

1) C.W. Bauschlicher, Jr. and H. Partridge, *J. Phys. Chem.* **95**, 3946 (1991).

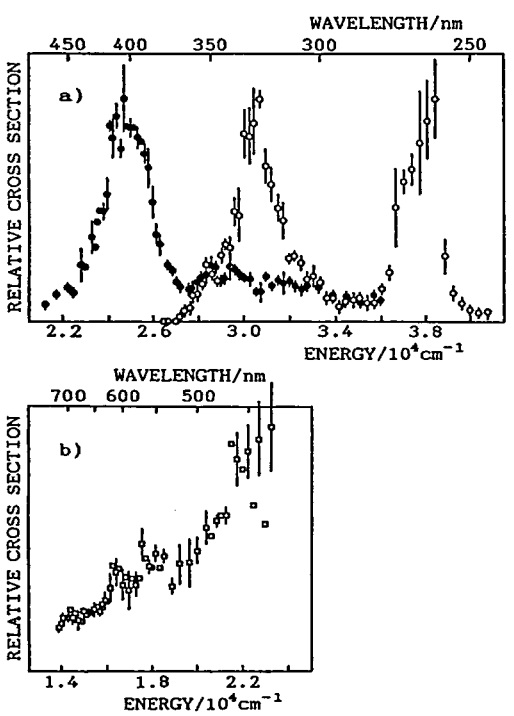

Figure 1. Photodissociation spectra of $Mg(H_2O)_n$. a) n=1 (○) and 2 (●). The dissociation cross sections are normalized at their peaks. b) n=5 (□).

VIII-C-3 Photoionization of Aluminum-water Clusters

Fuminori MISAIZU, Keizo TSUKAMOTO, Masaomi SANEKATA, and Kiyokazu FUKE

The clusters of alminum atom solvated by water molecules and their ions are investigated by photoionization-mass spectroscopic method. Figure 1 shows a typical mass spectrum of $Al(H_2O)_n$ clusters ionized by irradiation of 213 nm (5.82 eV) photons. The Al^+ ion is not observed in this mass spectrum because ionization potential of aluminum atom is 5.98 eV. The solvated cluster ions, $Al^+(H_2O)_n$, are intensely observed up to n=4. Especially, an outstanding peak is observed for the ion of n=3. On the other hand, intense peaks around n=5–10 are observed in the mass spectrum of the ions which are produced directly in the laser vaporization source. Therefore, the intensity gap between n=4 and 5 is expected to be ascribed to the abundance of neutral clusters and not to the stability of cluster ions. Photoionization thresholds determined for n=1–4 are as follows: 5.07(2) (n=1), 4.66(4) (n=2), 4.46(4) (n=3), and 4.41(4) eV (n=4). According to the results of the recent ab-initio calculations, Al atom and Al^+ ion bound with water molecules via interactions between the 3p orbitals of Al atom (ion) and the nonbonding orbitals of oxygen atoms, and no stable structure is found for Al atom plus equivalent 3 water molecules and also for Al^+ ion plus equivalent 4 water molecules[1]. Therefore, the observed magic number at n=3 may be ascribable to the stability of the cluster ions.

Referenece

1) S. Iwata, private communication.

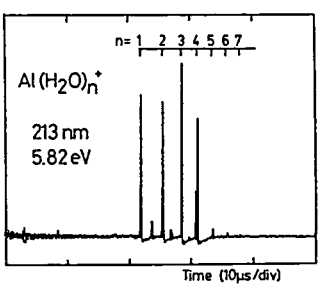

Figure 1. Typical photoionization mass spectrum of $Al(H_2O)_n$. Ionization wavelength is 213 nm (5.82 eV).

VIII-C-4 Photodissociation of Size-selected $Al^+(H_2O)_n$ Ions

Fuminori MISAIZU, Masaomi SANEKATA, Keizo TSUKAMOTO, and Kiyokazu FUKE

Photodissociation of alminum-water cluster ions, $Al^+(H_2O)_n$, are investigated after size selection. Instrumentation of the cluster ion formation, size selection, and detection after photodissociation was already shown in the preceding chapter. Photons at wavelengths of 193–308 nm were irradiated to the cluster ions of n=1–10. For Al^+H_2O, fragement Al^+ ion is observed at 193 nm but not at 248 nm and longer wavelength. Also for n≧2, fragment ions produced by loss of H_2O molecules are uniquely observed at

245–265 nm. Figure 1 shows mass spectra of photofragment ions produced from $Al^+(H_2O)_3$ at wavelengths of 245–265 nm. For n=3, intensities of the fragment ions decrease with increasing the wavelength from 245 to 265 nm. At 308 nm, photofragmentation is observed for n=8–10 but not for smaller cluster ions. Since the lowest allowed transition of Al^+, $3^1P \leftarrow 3^1S$, is known to be observed at 167.1 nm, the observed absorptions of cluster ions for n=1–7 seem to be assigned to the transitions localized on the Al^+ ion. In the photofragment ions produced by dissociation of the ions of n=4–10, the $Al^+(H_2O)_3$ ion is most intensely observed. This result indicates that $Al^+(H_2O)_3$ is eminently stable, as predicted by a recent thoretical work[1].

Reference

1) S. Iwata, private communication.

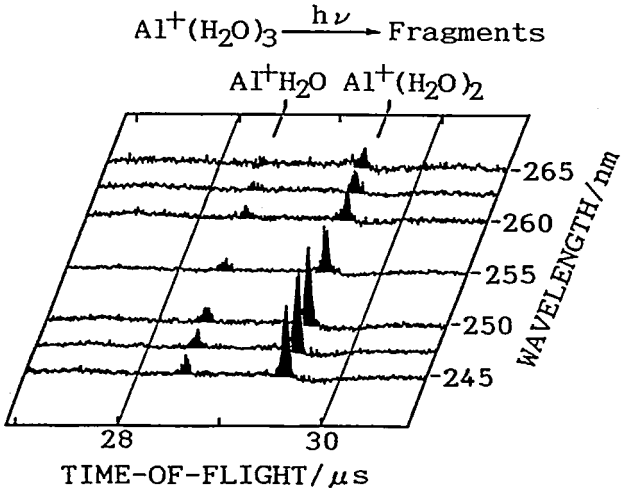

Figure 1. Time-of-flight mass spectra of photofragment ions produced from $Al^+(H_2O)_3$ at wavelengths of 245–265 nm.

VIII—D Dynamics of Proton-Transfer Reaction in a Model Hydrogen-Bonded Base Pair

Proton-transfer reaction (PTR) has known to play a predominant role in many chemical and biological systems. With the advent of a picosecond laser spectroscopy, a wealth of kinetic data in solution has been accumulated and produced a good qualitative description of the PTR process in the form of reaction mechanism. However, a dynamical aspect of PTR still remains to be unveiled, especially, the role of cooperative motion of proton and a frame of heavy nuclei. To manifest the dynamics of PTR, we have been studying the PTR of model hydrogen-bonded base pairs such as 7-azaindole and 1-azacarbazole (1-AC) dimers and their heterodimer in supersonic jet by using a laser induced fluorescence method. In this issue we report on the picosecond realtime study of the PTR of jet-cooled 1-AC dimer.

VIII-D-1 Picosecond Measurements of Vibrationally-Resolved Proton-Transfer Rate of Jet-Cooled 1-Azacarbazole Dimer

Kiyokazu FUKE, Fuminori MISAIZU, Keizo TSUKAMOTO, and Koji KAYA* *(*Keio Univ.)*

[*J. Chem. Phys.* **95**, 4074 (1991)]

Studies that afford a vibrationally resolved rate are basic to the understanding of PTR dynamics on a multidimensional potential energy surface. In the present work, we conducted the direct, time-resolved measurements of the population of both the product and precursor dimer by monitoring the emissions at 500 nm and 370 nm, respectively, and also the vibrationally resolved rates for the excited-state PTR of jet-cooled 1-AC dimer.

The time-resolved data for the reactant and product populations clearly show that the PTR process precedes other nonradiative processes including IVR, and that the back reaction is negligible in the excited-state PTR of 1-AC dimer. These results strongly support the reaction mechanism presumed in the condensed-phase works. We have studied the time-resolved PTR dynamics of 8 intermolecular vibrational levels of 1-AC dimer as summarized in Figure 1. PTR is strongly mode specific and is dramatically promoted by the intermolecular symmetric stretching vibration, which has a vibrational frequency of 109 cm^{-1}. The other modes such as intermolecular bending-type vibrations (55 cm^{-1} and 67 cm^{-1}) rather suppress PTR. The mechanism of this enhancement was explained in terms of the dynamic coupling of proton motion with the intermolecular vibrational motion by assuming the two dimensional model potential.

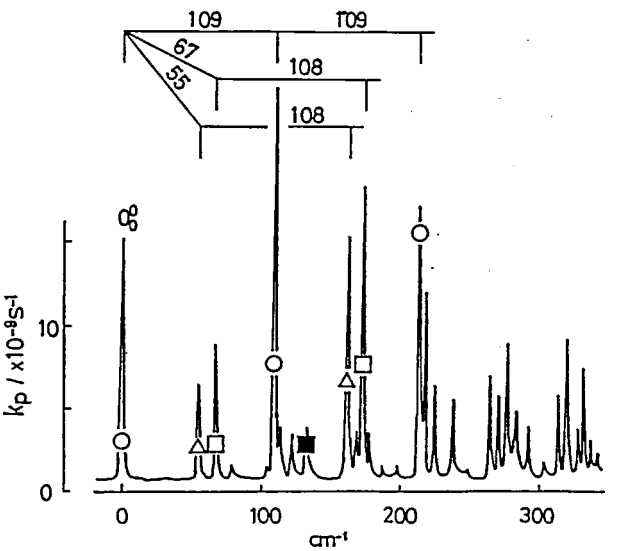

Figure 1. Visible monitoring spectrum of 1-AC dimer and the plots of PTR rates. O, Δ and □ are for the origin and the 109 cm^{-1} vibration, the fundamentals of the 55 and 67 cm^{-1} vibrations, and the combination bands with the 109 cm^{-1}, respectively. ■ is for the overtone of the 67 cm^{-1} vibration. The excitation of 109 cm^{-1} vibration enhances PTR, while the excitations of the 55 and 67 cm^{-1} vibrations suppress the reaction.

VIII-E Interatomic Potentials and Intramultiplet Mixing of Cd

The collisional quenching of electronically excited metal atoms has been the subject of extensive studies because of its importance in photophysics and photochemistry. In the present project we seek to obtain more detailed information about the dynamics of deactivation processes of the group IIB metal atoms.

VIII-E-1 The Intramultiplet Relaxation of $Cd(5^3P_2)$ by H_2 and D_2

Hironobu UMEMOTO, Akira MASAKI, Toshiharu OHNUMA, Youichi WADA *(Tokyo Inst. of Tech.)*, **Fuminori MISAIZU, and Kiyokazu FUKE**

[*J. Chem. Phys.* **94**, 7951 (1991)]

The deactivation processes of $Cd(5^3P_2)$ by H_2 and D_2 were studied by employing pulsed laser techniques. The cross sections for the intramultiplet relaxation to produce $Cd(5^3P_1)$ and $Cd(5^3P_0)$ were determined as follows:

$Cd(5^3P_2) + H_2 \rightarrow Cd(5^3P_1) + H_2$; 6.3,
$Cd(5^3P_2) + H_2 \rightarrow Cd(5^3P_0) + H_2$; 1.0,
$Cd(5^3P_2) + D_2 \rightarrow Cd(5^3P_1) + D_2$; 4.4,
$Cd(5^3P_2) + D_2 \rightarrow Cd(5^3P_0) + D_2$; 0.9,

in units of 10^{-16} cm^2 at 630 K. The cross section for the overall deactivation of $Cd(5^3P_2)$ by H_2 and D_2 were determined to be 9.8×10^{-16} cm^2 and 6.9×10^{-16} cm^2, respectively. These values are compared with the calculated results based on a semiclassical curve crossing mechanism. It is suggested that electronic-to-rotational energy transfer without sharp resonances plays an important role in the deactivation of $Cd(5^3P_2)$.

VIII-E-2 The Intramultiplet Relaxation of $Cd(5^3P_2)$ Induced by Collision with N_2 and CO

Akira MASAKI, Toshiharu OHNUMA, Youichi WADA, Hironobu UMEMOTO *(Tokyo Inst. of Tech.)*, **Fuminori MISAIZU, and Kiyokazu FUKE**

[*J. Chem. Phys.* **95**, 372 (1991)]

The intramultiplet relaxation of $Cd(5^3P_2)$ was studied by using pump-and-probe techniques. The following cross sections were obtained for the $^3P_2 \rightarrow {}^3P_1$ and $^3P_2 \rightarrow {}^3P_0$ transitions induced by collisions with N_2 and CO at 630 K: $\sigma_{21}(N_2)$=4.6, $\sigma_{20}(N_2)$=1.2, σ_{21}(CO)=20.9, σ_{20}(CO)=7.6 in units of 10^{-16} cm^2. Comparison of these cross sections with those for the overall deactivation shows that the intramultiplet relaxation processes are the major exit channels and that the deactivation to the ground state is minor. The curve crossing probabilities were calculated for the $Cd(5^3P_2)$+N_2 collisions by employing a semiclassical model. It was revealed that Cd^+—N_2^- ionic complexes play an important role.

VIII—F Studies of Ultrafine Particles

The structural and magnetic properties of magnetic fine particles are affected by the finite size effect due to the number of atoms or molecules including in a particle, the number which is less than *ca.* 10^4, or more effective less than 10^3, corresponding to the particle size 10 nm to several nm. These properties are studied as functions of particle size and time scale of measurement method.

VIII-F-1 Structural Phase Transition of Ultrafine MnF_2 Particles Induced by Size Reduction

Shunji BANDOW

[*Jpn. J. Appl. Phys.* **30**, 788 (1991)]

The metastable phase of MnF_2 (MnF_2-IV, α-PbO_2 type) is formed with particles smaller than about 10 nm. The concentration of the MnF_2-IV phase increases with decreasing particle size, and finally the MnF_2-IV phase becomes dominant in 5 nm particles, in which very weak X-ray diffraction peaks of rutile-type MnF_2 (MnF_2-I) are detected. The largest particles (d~14 nm) are dominated by the MnF_2-I phase.

The powdered rutile-type MnF_2 (Rare Metallic Co., LTD. 99.99%) was used as a starting material, and the compressed pellet of them was put into a tungsten basket for evaporation. Preheating of the pellet for degasing was executed in advance. Helium was used as an inert gas, and its pressure was changed from 0.3 to 5 Torr to produce the various sizes of particles. The average size of the particles was checked by the width of the Debye-Scherrer rings of X-ray diffraction and by the electron micrograph of a TEM (transmission electron microscope). Figure 1 is the size dependence of the structural phase transition. In bulk, only the MnF_2-I phase can be detected by X-ray diffraction. On the other hand, the X-ray diffraction peaks from the MnF_2-IV phase can be found in 10 nm particles. These peaks gradually increases with decreasing particle size, while the diffraction peaks from the MnF_2-I phase decrease. The study of the formation mechanism of the metastable phase of ultrafine MnF_2 particles is an interesting subject as a nucleation and a structural relaxation.

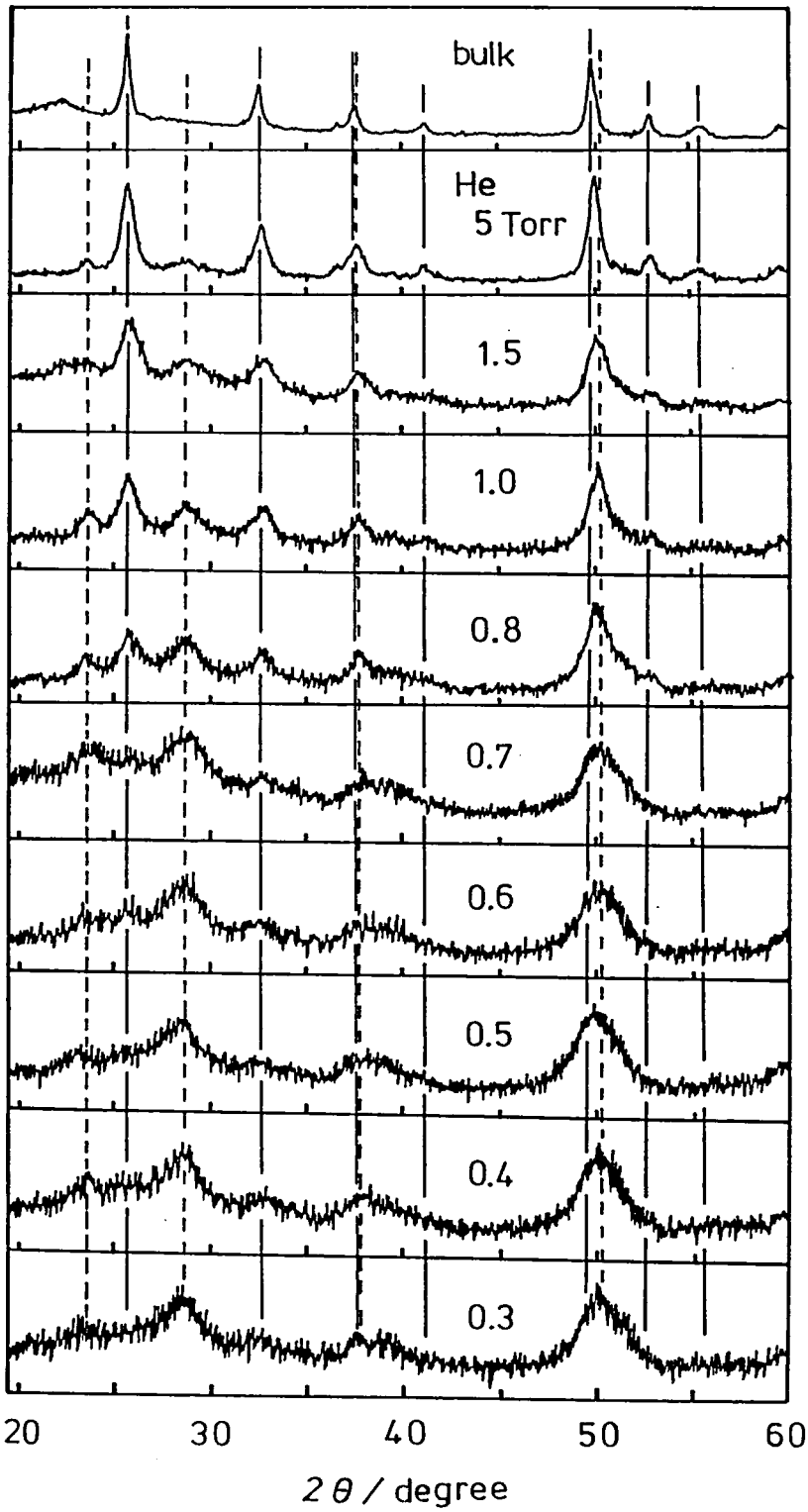

Figure 1. Size dependence of the X-ray diffraction patterns (CuK_α irradiation). Numerical values in the figure are the environmental pressure of He gas, corresponding to the size of about 14, 10, 8.5, 8.0, 7.5, 7.1, 6.7, 6.2, 5.6 nm, respectively, from the top of the figure. Diffraction peaks from MnF_2-IV phase (positions are indicated by the broken lines) become stronger when the size decreases. Solid lines are the positions corresponding to the diffraction peaks of MnF_2-I phase.

VIII-F-2 Static Magnetic Properties of Ultrafine MnF_2-IV Particles

Shunji BANDOW

The metastable MnF_2-IV particles can be prepared by the vacuum deposition or the gas evaporation method.[1] The magnetic properties of these particles examined by ESR were reported in the previous report:[2] ESR linewidth ΔH was diverged at the certain temperature and we can determine the Néel temperature T_N from this divergence of ΔH. T_N showed the size dependence with a functional relation d^{-3}. In the present study, we performed the static magnetic susceptibility measurement to investigate the temperature dependence of effective magnetic moment. The result is shown in Figure 1 for various size of particles. For the bulk sample, we can see a clear bend at the temperature corresponding to Néel point determined from ESR. However, other samples do not indicate this kind of bend at T_N determined from ESR (marked by arrows in the figure); decreasing monotonously toward zero. We consider that this comes from the time scale difference between the measurement methods: Observation time for the ESR is considered to be 10^{-9}~10^{-10} s for X-band (9 GHz) operation. On the hand, the time scale for static magnetic susceptibility is considered to be infinite. Hence, the phenomenon faster than above time scale will be averaged in the measurement, but slower phenomenon can be resolved in a time scale. From such a reason, we consider that the short-range spin-order will fluctuate in a time scale longer than the ESR observation time but shorter than that of static magnetic susceptibility.

References
1) S. Bandow, *Jpn. J. Appl. Phys.* **30**, 788 (1991).
2) S. Bandow and K. Kimura, *IMS Ann. Rev.* 188 (1990).

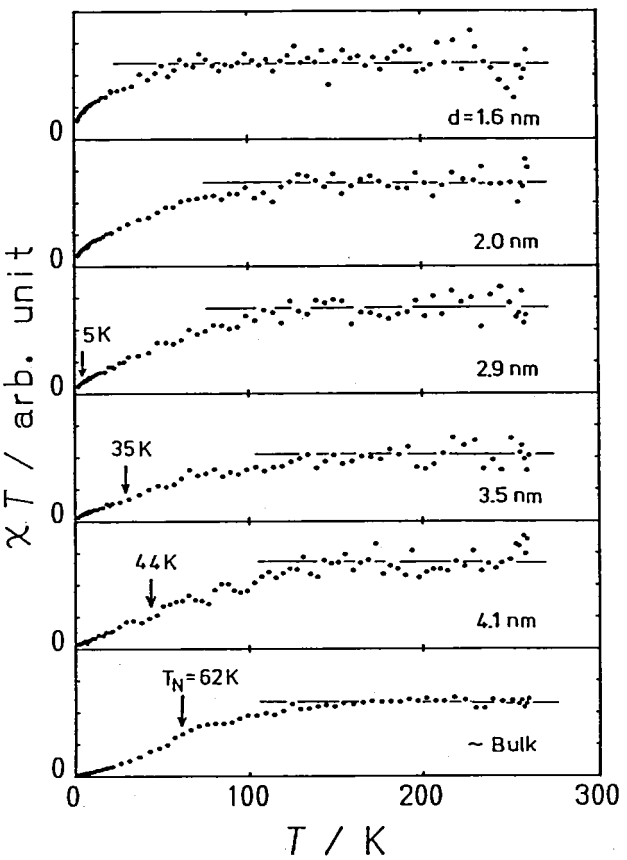

Figure 1. Temperature dependence of effective magnetic moment. χT represents effective magnetic moment. The symbol d is the particle size and T_N indicated by arrows is the Néel temperature determined by ESR.[2]

VIII-F-3 Production of Small Fe Particles Dispersed in MgO Film

Masahiro SAKAI and Shunji BANDOW

Nanoscale iron crystallites have been prepared with the interest of the magnetic properties. We made composite films by controlling the size and the separation distance of crystallites. The films were prepared by a simiultaneous vacuum deposition technique, which was applied to produce metallic small particles by Nagao *et al.*[1]

Figure 1 is a schematic illustration of apparatus for simultaneous vacuum deposition. The deposition of iron and magnesium oxide was carried out by resistance and electron beam heatings, respectively. The vacuum chamber is evacuated to 8×10^{-3} Pa. The deposition rate of iron and MgO were 0.1~0.9 nm/s and 0.1~1.0 nm/s, respectively, which were measured by a quartz thickness monitor. In order to prevent the oxidation or the other chemical reaction to Fe, 10 nm thick of MgO was deposited before and after the simultaneous deposition. A shutter was used as a deposition selector. In this way, sandwiched film of MgO/Fe/MgO can be prepared for the purpose of studying the magnetic properties.

Reference
1) M. Nagao, N. Tanaka and K. Mihama, *Jpn. J. Appl. Phys.* **25**, L614 (1986).

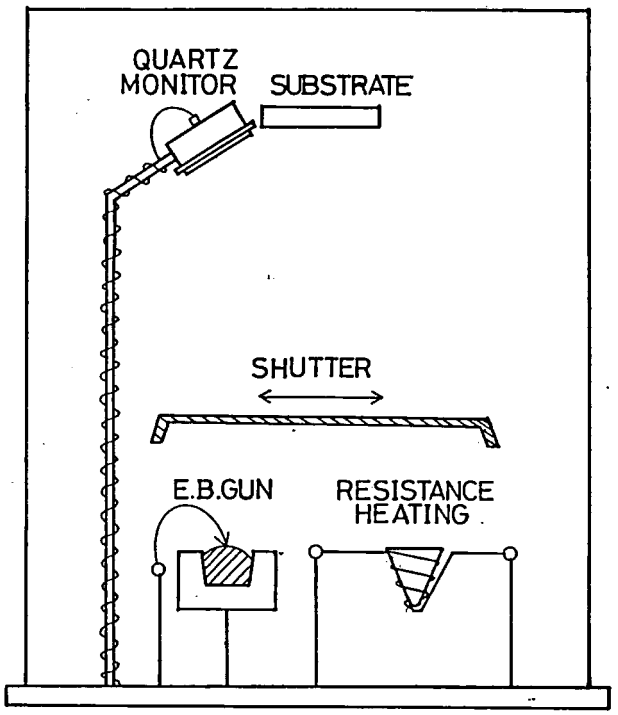

Figure 1. Schematic illustration of the simultaneous vacuum deposition system. Resistance and electron beam heatings are used to evaporate Fe and MgO, respectively. A quartz thickness monitor are always exposed to measure the deposition rate. A shutter is used as a deposition selector.

VIII—G Formation and Physical Properties of Fullerenes

Apparatus for the preparation of C_{60} and related compound was designed as a project of new material research of supporting facilities in IMS. The separation of the fullerenes from eluant is also conducting by using high-pressure liquid chromatography. Physical properties of fullerenes were studied mainly from the magnetic side.

VIII-G-1 Construction of New Apparatus for Fullerenes by the Gas-Flow Arc Discharge Evaporation

Nobuo MIZUTANI, Shunji BANDOW, Masaaki NAGATA, Hiroshi KITAGAWA, Tadaoki MITANI, Shinzo SUZUKI*, and Yohji ACHIBA *(*Tokyo Metropolitan Univ.)*

The Fullerenes, spheroidal carbon clusters, can be produced by means of gas evaporation technique under 100 Torr of He ambient. This technique is widely used in the area of small particle physicists: The carbon rods are evaporated in a depressurized He quenching gas by the direct electro-heating or arc discharge. Under such condition, carbon atoms or molecules collide with the quenching gas and lose their translational energy. Then the supersaturated carbon vapor will form around the carbon rod and will nucleate into clusters or fine particles. In such processes, the fullerenes will be formed as a part of fine smoke.

In this project, we designed the apparatus for the formation of fullerenes and related compound based on the gas evaporation method. Figure 1 is the schematic drawing for the apparatus, which is constructed by two parts: One is the preparation chamber and the other the collection chamber. The carbon rods (10 mm in diameter) are held horizontally at the center of the preparation chamber and are evaporated by DC arc discharge (35 V, 300 A). The He gas is flew below the gap of the carbon rods to make the continuous stream. This stream is evacuated by the rotary pump to guide the smoke to the collection chamber. On the way to flow to the collection chamber, the vapor of organic solvents (hexane, benzene and toluene, etc.) is inlet into the gas stream and is condensed on the cold wall cooled by liquid nitrogen together with the fine smoke. Then it collected in a stock bottle by removing liquid nitrogen. Further, we are planning the metal doping into fullerenes by the simultaneous gas evaporation of metal using resistance heating.

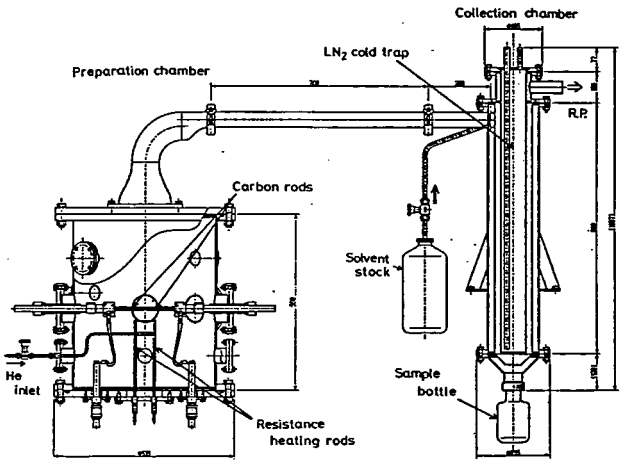

Figure 1. Apparatus for the formation and collection of fullerenes. The carbon rods are evaporated by the DC arc discharge in the depressurized continuous He stream (100 Torr). The electrodes from the bottom of flange is also available to the gas evaporation of metal for the purpose of doping the metal into fullerenes. The carbon smoke including fullerenes is trapped on the cold wall (LN_2 temperature) with solvent. The sample stock bottle can be attached at the bottom of collection chamber.

VIII-G-2 Magnetic Susceptibility of Pristine C_{60}

Shunji BANDOW, Hisanori SHINOHARA,[a] Hideo NAGASHIMA *(Toyohashi Univ. of Tech.)*, **Masato OHKOUCHI,[b] Yoshinori ANDO** *([b]Meijo Univ.)*, **and Yahachi SAITO** *([a]Mi'e Univ.)*

Diamagnetic susceptibility χ_d of chromatographed C_{60} from different kind of eluants was measured by the Faraday balance in the temperature range between 2 and 270 K. All samples had the Curie term. Hence, the magnetic susceptibility χ_g increased with decreasing temperature. The values of χ_d determined from the slope of $\chi_g T$ vs T plot and Curie constant for the samples from different eluants are listed in Table 1. Each Curie term probably comes from the spurious origins, because the C_{60} is large bandgap (2.5 eV)[1] insulator and the Curie term depends on sample to sample. The χ_d also depends on sample to sample, but these values are all smaller than that expected from the aromatic system; Pauling free electron model, −1972 emu p.p.m/mol.[2] This latter fact is the same as the other workers reported.[3,4] The difference of values in χ_d listed in the table might be the effect of contaminants due to solvents.

References

1) S. Saito, "*Clusters and Cluster Assembled Materials*", e.d. R.S. Averback, D.L. Nelson and J. Bernholc, in press.
2) R.C. Haddon and V. Elser, *Chem. Phys. Lett.* **169**, 362 (1990).
3) R.C. Haddon, *et al.*, *Nature* **350**, 46 (1991).
4) R.S. Ruoff, *et al.*, *J. Phys. Chem.* **95**, 3457 (1991).

Table 1. The values of diamagnetic susceptibility and Curie constant. The values are the C_{60} molar quantity.

C_{60}	χ_d (10^{-6} emu/mol)	Curie constant (10^{-5} emu-K/mol)
Benzene	−295	419
HCl	−330	710
Toluene	−189	1480
300	−387	1790

Benzene: from Hexane/Benzene solution.
HCl: refluxed the sample "Benzene" by HCl solution to remove impurities.
Toluene: from Hexane/Toluene solution.
300: heated the sample "Toluene" up to 300°C.

VIII-G-3 Superconducting Properties of K-doped C_{60} Evaluated by the Magnetic Susceptibility and Magnetization Curve

Shunji BANDOW, Noboru AKUZAWA *(Tokyo National College of Tech.)*, **Hisanori SHINOHARA,[a] Masato OHKOUCHI,[b] Yoshinori ANDO** *([b]Meijo Univ.)*, **and Yahachi SAITO** *([a]Mi'e Univ.)*

The magnetization curves of K-doped C_{60} ($K_{3.8}C_{60}$) in the temperature range between 18 and 2 K (T_c=18.4 K) were measured by the Faraday balance with the magnetic field up to 50 kOe. This system behaves as Type-II superconductor with upper critical field H_{c2} higher than 50 kOe at the temperatures lower than 10 K. H_{c2} at 13.5 K can be roughly estimated to be 40~50 kOe. This value allows to evaluate $H_{c2}(0)$ equals 100~130 kOe by the relation $H_{c2}(0)=0.69(\partial H_{c2}/\partial T)T_c$[1] and the correspondent coherence length ξ at zero-temperature is about 5 nm by $H_{c2}(0)=\Phi_o/2\pi\xi^2$, where Φ_o is the fluxoid quantum. H_{c1} is estimated to be about the order of a hundred Oe at the temperature lower than 6.4 K. These values are in the same order reported by Holczer *et al.*;[2] H_{c2}=490 kOe and ξ=2.6 nm.

References

1) N.R. Werthamer, E. Helfand and P.C. Hohenberg, *Phys. Rev.* **147**, 295 (1966).
2) K. Holczer, O. Klein and G. Gruner, *Phys. Rev. Lett.* **67**, 271 (1991).

Low-Temperature Center

VIII—H Ferromagnetic Interaction in Molecular Crystal

The study of the ferromagnetic intermolecular interaction in organic molecular solids should bring us important knowledge, not only to the establishment of molecular ferromagnet but also to the understanding about radical reactions. In the present project, we investigate the factors controlling ferromagnetic and antiferromagnetic behaviors in the solids.

VIII-H-1 Pressure-Induced Enhancement of the Ferromagnetic Intermolecular Interaction of an α-Nitronyl Nitroxide Organic Radical

Kunio AWAGA and Yusei MARUYAMA

[*Chem. Mater.*, **2**, 535 (1990)]

The effect of high pressure on the ferromagnetic properties of a crystal of an organic radical, 2-(4-nitrophenyl-4,4,5,5-tetramethyl-4,5-dihydro-1*H*-imidazolyl-1-oxy-3*N*-oxide (**I**) has been studied with the use of the combined system of a Faraday susceptometer and a Be-Cu high-pressure clamp cell. The magnetic susceptibility of the crystal **I** remarkably increases with increasing pressure at low temperatures, and furthermore, its increment increases monotonically with decreasing temperature down to about 5 K. The Weiss constant under the pressure of 9 kbar corresponds to the 40% increase in the ferromagnetic intermolecular interaction in the crystal of **I**, and the magnetization at 9 kbar also comes to saturation more rapidly compared with the behavior under an ambient pressure. The simple calcualtion of the intermolecular overlap integrals between the frontier orbitals, can semiquantitatively interpret the pressure-induced enhancement of the ferromagnetic coupling in the crystal of **I**.

VIII-H-2 Ferromagnetic Coupling in a New Phase of the *p*-Nitrophenyl Nitronyl Nitroxide Radical

Philipe TUREK*, Kiyokazu NOZAWA*, Daisuku SHIOMI*, Kunio AWAGA, Tamotsu INABE, Yusei MARUYAMA, and Minoru KINOSHITA* *(*Univ. Tokyo)*

[*Chem. Mater.*, **2**, 535 (1991)]

p-Nitrophenyl-α-nitronyl nitroxide (p-NPNN) is know to crystallize in the two different polymorphs, α and β phases, both of which exhibit FM intermolecular interactions. In this work, we discovered a new phase of p-NPNN, γ-phase. γ-phase crystallizes in the triclinic $P\bar{1}$ space group, while α and β phases do in the monoclinic $P2_1/c$ and in the orthorhombic *Fdd2*, respectively. In γ-phase, there are 1-D molecular stacks along *c* axis in which the molecules are related by the translation operation and are connected by the intermolecular NO...NO_2 contacts. Such NO...NO_2 interaction is also found in the crystal of α or β phase. In addition to the stacking chain along *c* axis, γ-phase has the side-by-side and head-to-tail stacks along the [011] direction, which are due to the hydrogen bonds.

Temperature dependence of the paramagnetic susceptibility of γ-phase follows the Curie-Weiss law with a positive Weiss constant of 2.4 K. γ-phase exhibit an FM interaction, as well as α and β phases.

VIII-H-3 An Organic Radical Ferromagnet

Minoru KINOSHITA*, Philippe TUREK*, Masafumi TAMURA*, Kiyokazu NOZAWA*, Daisuke SHIOMI*, Yasuhiro NAKAZAWA*, Masayasu ISHIKAWA*, Minoru TAKAHASHI*, Kunio AWAGA, Tamotsu INABE, and Yusei MARUYAMA *(*Univ. Tokyo)*

[*Chem. Lett.*, 1225 (1991)]

The γ-phase crystal of 2-(4-nitrophenyl)-4,4,5,5-tetramethyl-4,5-dihydro-1*H*-imidazolyl-1-oxy 3-*N*-oxide is shown to become a ferromagnet below about 0.65 K from the measurements of magnetization, magnetic susceptibility, and heat capacity.

VIII-H-4 High-Pressure Effects on the Canted Ferromagnetism in Manganese(II) Phthalocyanine

Kunio AWAGA and Yusei MARUYAMA

[*Phys. Rev. B*, **44**, 2589 (1991)]

The effect of high pressures up to 10 kbar, on the magnetization of a canted ferromagnet, β-form manganese(II) phthalocyanine (MnPc), has been studied at *ca.* 30 kOe in the temperature range of 3-250 K. In the paramagnetic state above the transition temperature of T_c=8.6 K, the magnetization shows a remarkable increase with increasing pressure. At a constant pressure, the increment, ΔM, increases with decreasing temperature down to *ca.* 25 K. This pressure and temperature dependence indicates the strength of the ferromagnetic intermolecular interaction. The pressure-induced enhancement of the ferromagnetic coupling can be semiquantitatively interpreted by the pressure dependence of the distance of the Mn-N...Mn superexchange pathway. However ΔM decreases below *ca.* 25 K and becomes negative below *ca.* 10 K. The applied pressure slightly decreases the 30 kOe magnetization in the ordered state below T_c. The magnetization curve at 9 kbar at 4.8 K showed that the pressure effect also depends on the magnetic field. The pressure increases the magnetization at lower fields below *ca.* 2 kOe, in contrast to the negative change above it. This effect is similar to that of decreasing temperature, suggesting the increase in T_c with pressure.

Equipment Development Center

VIII—I Studies of Quasi-1-D Mixed-Valence Systems

VIII-I-1 A New 1-D Conducting State Stabilized by Strong H-Bondings in Halogen-Bridged Metal Complexes

Hiroshi OKAMOTO, Koshiro TORIUMI, Kaoru OKANIWA, Tadaoki MITANI, and Masahiro YAMASHITA *(Nagoya Univ.)*

[*Synth. Met.*, **42**, 2791 (1991)]

The 1-D brome-bridged Ni complex with strongly enhanced 2-D H-bond network has the Mott-Hubbard-type electronic state, in which the electron-electron repulsive energy is responsible for gap-opening. In spite of the large optical gap (ca. 1.3 eV), the conductivity is fairly high (ca. 0.2 S/cm at R.T.) suggesting the presence of low energy carriers induced by the 1-D charge density instability. The possibility of the phase transition from the Peierls system to the Mott-Hubbard system has been checked by the hydrostatic-pressure effect on Raman scattering of the bromo-bridged Pd compelx.

VIII-I-2 Control of the CDW State in the Halogen-Bridged Metal Complexes

Hiroshi OKAMOTO, Koshiro TORIUMI, Kaoru OKANIWA, Tadaoki MITANI, and Masahiro YAMASHITA *(Nagoya Univ.)*

Chemical modifications of the one-dimensional halogen-bridged mixed-valence metal complexes have been made in order to control an amplitude of the CDW state in -M-X- chain (M=Pt, Pd or Ni, and X=Cl, Br or I). By changing chemical parameters, such as strength of hydrogen bonds between ligands and counter anions, and radii of M and X ions, the characteristic diagram of the amplitude of the CDW state has been obtained as a function of the M-X-M distances. This provides a new basic idea for understanding of the 1-D electronic state of the M-X compounds especially related to dynamical phenomena originated in the charge transfer instability in the optically excited state and the ground state as well.

VIII-I-3 IR and Near-IR Photo-Induced Absorption of the Halogen-Bridged Metal Complexes

Hiroshi OKAMOTO, Tadaoki MITANI, Koshiro TORIUMI, and Masahiro YAMASHITA *(Nagoya Univ.)*

To study dynamical behaviors of the excited states such as the polaron and soliton generated during the relaxation process of the photo-excited states in the quasi-one-dimensional semiconductors, the photo-induced absorption (PA) spectra in the mid-gap region gives us much important information. We measured the IR and near-IR PA spectra in the range of 12000 cm^{-1}—1000 cm^{-1} in detail on the 1-D halogen-bridged metal complexes by using the FTIR spectrometer modified for the PA measurements.

From the results of time-dependence of the PA spectra, it has been revealed that in the $[Pt(en)_2I](ClO_4)_2$ crystal, both the polaron and the soliton are generated during the relaxation process. On the other hand, in the $[Pt(chxn)_2Br]Br_2$ crystal, only the polaron has been found to be generated. Such a difference between the relaxation processes of the two complexes is attributable to the difference of the interchain interactions. Because of the development of the 2-D ordering of CDW, the excitation energy of the soliton is so high that dissociation of the photo-excited electron-hole pair to the soliton pair hardly occurs in the $[Pt(chxn)_2Br]Br_2$ crystal.

VIII-J Studies of H-Bonded Organic CT Complexes

VIII-J-1 Optical Studies of H-Bonded 1-D Conductor, DAP-TCNQ

Kaoru OKANIWA, Hiroshi OKAMOTO, Tadaoki MITANI, Tamotsu INABE, Hironori OGATA, Kunio AWAGA, and Yusei MARUYAMA

The DAP-TCNQ crystals have segregated stacks of charge-transfer (CT) molecules, which are bridged by H-bonds. The electrical conductivity at room temperature is considerably high (10 S/cm), although the activation energy is relatively large of 0.24 eV in comparison with other segregated stacked CT complexes. In order to clarify these characteristic electric properties, the electronic structure has been studied using the polarized reflection spectra in infrared region. There observed several absorption bands in this energy region. Compared with the spectra of K-TCNQ, which is a typical half-filled CT complex, a structure observed near 1 eV in the direction of stacking can be assigned to CT transition between $TCNQ^-$ ions ($TCNQ^-+TCNQ^-\rightarrow TCNQ^0+TCNQ^{2-}$). The lower structures found at around 0.15 and 0.5 eV are attributable to the optical transition from the carrier induced states accompanied by lattice relaxation.

VIII-J-2 Intra- and Inter-Molecular Charge Transfer Interactions in H-Bonded DTPP Crystals

Kaoru OKANIWA, Hiroshi OKAMOTO, Tadaoki MITANI, Tamotsu INABE, Jiro TOYODA, Yasushi MORITA, Kazuhiro NAKASUJI, Hiroshi YAMAMOTO*, Takashi DENO*, and Seiji HONMA* *(*Ciba-Geigy Japan Ltd.)*

The DTPP (1,4-dithioketo-3,6-diphenyl-pyrrolo-[3,4c]-pyrrole) has donner- and acceptor-like components in the molecule. In the β-form crystal, the molecules are stacked in *b* axis with a considerable overlapping of the donner- and acceptor-like components. And intermolecular H-bonds exist along *c* axis. The spectra of polarized reflec-

tivity and excitation of photoconductivity of β-DTPP crystal have been measured. Despite of one dimensional stacking structure, highly efficient photoconductivity was observed along the both axes of the stacking(*b*) and of the H-bonds(*c*). The spectral shapes of the excitation spectra for the both axes, however, are considerably different and dependent on the direction of applied electric field. These photoconducting properties are discussed in terms of charge transfer (CT) along the stacking axis and the charge screening effect through a displacement (or transfer) of protons in H-bonds.

VIII-J-3 Design and Construction of New Molecular Systems Based on Cooperation of Transition Metal Chain and CT Stack *via* Intermolecular H-Bonds

Hiroshi KITAGAWA, Tadaoki MITANI, Hiroshi OKAMOTO, Masahiro YAMASHITA *(Nagoya Univ.)*, **Jiro TOYOTA, and Kazuhiro NAKASUJI**

The formation of the H-bond network in solids provides a unique opportunity for construction of novel molecular assemblies, in which many electronic systems are combined *via* intermolecular H-bonds.[1] The molecular system proposed consists of several characteristic components, M is a transition metal (M=Ni, Pd, and Pt), L stands for a ligand, and A (or D) molecule works as an acceptor (or a donor) of electron against the 1-D M-L system. Dynamical property of protons (H) in H-bonds might sensitively depend on a degree of the charge transfer between the M-L chain and the A (or D) segregated-stack. This system implicitly includes many interesting aspects concerning with the instability of the low dimensional systems. As the first demonstration of this system, the optical and transport measurements on [M(H_2DAG)(HDAG)]TCNQ (M=Ni, Pd, Pt, H_2DAG: diaminoglyoxime) single crystals have been made. The results show unusual behaviors around room temperatures. Detailed investigations including the high pressure effect are under way.

Reference

1) T. Mitani, *Mol. Cryst. Liq. Cryst.*, **171** 343, (1989).

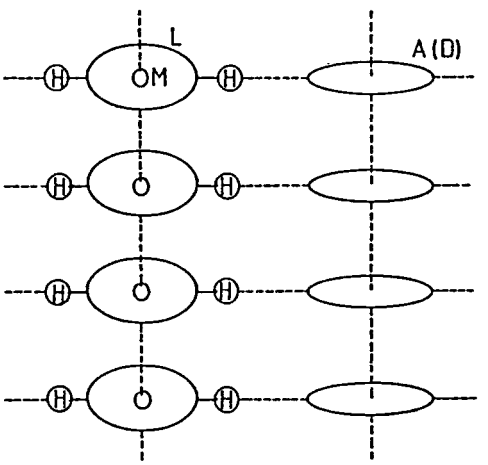

VIII—K Development of Experimental Devices

VIII-K-1 Development of Switching Circuits for the Pockels Cell

Hisashi YOSHIDA

In the experiments using the mode-locked Q-switched laser, it is sometimes necessary to switch the stable pulse train out of the laser output. In the Passively mode-locked Q-switched Nd:YAG laser made in IMS, the output pulses in the early stage of the pulse train is unstable, as seen in Figure 1 (a). An effective method for switching out only the stable pulse train is to use the Pockels cell as an optical shutter.

We made the switching circuits to apply a high voltage pulse of about 3 kV across the Pockels cell. A fast rising time of the voltage less than 10 nsec is necessary to switch out the laser pulses sharply. To produce such pulses, the transistor (2N5551, Motorola) was used in the avalanche mode. This transistor has the relatively high breakdown voltage (>220 V) and the first rising time (<2 nsec). Ten pieces of the transistor were connected in series to produce the sufficient voltage. In order to obtain the fast rising time, the transistors were selected to have the same breakdown voltage within ±2 V. The serious problem is that even small stray capacitance should spoil the rising of the pulses, since the output impedance of the circuit is high (2MΩ). To minimize stray capacitance, the circuit board was directly connected to the Pockels cell. The obtained pulse is fairly good, having the amplitude of 2.2-3.4 kV and the rising time of about 7 nsec. Time jitter is only ±1 nsec. Figure 1 (b) shows the stable pulse train successfully switched out of the output laser pulses by using this switching circuits.

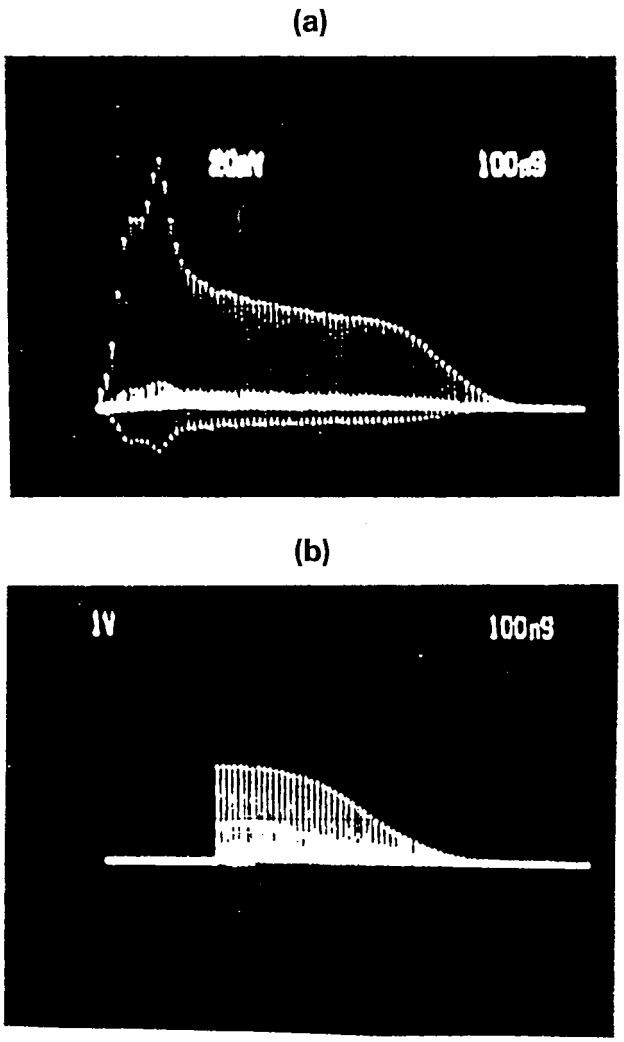

Figure 1. (a) The output wave form of the passively mode-locked Q-switched Nd:YAG laser. (b) The pulse train switched out by the Pockels cell.

VIII-K-2 Development of High-Temperature Pulsed Nozzle

Norio OKADA and Toshio HORIGOME

Fuel injectors for automobiles have been used as a supersonic pulsed nozzle. The operation of this type of nozzles has a limitation of temperature above about 120°C, and we have newly developed a nozzle which can be operated at high temperatures up to about 600°C using the advantages of the fuel injectors.

A cross-section of the nozzle is shown in Figure 1. The spring and the parts 10, 11, 12 and 13 were taken from the original fuel injector. Material to be vaporized is loaded by opening the top flange (ICF-34), and heating of the nozzle is done by a sheath-heater bobbin. Several different attachments can be fitted to the top flange according to the shape and the size of the required jet beam. The driving solenoid is protected from heat by the water jacket mounted on the main tube. By unscrewing the sealing joint (9) the nozzle body can be easily disassembled for cleaning.

The beam intensity profile vs. time is shown in Figure 2, where the temperature of the sample chamber was 500°C, and the beam repetition rate was 10 Hz.

The newly developed pulsed nozzle is useful for beam experiment where high temperature is needed to vaporize sample materials such as polymers and metal oxides.

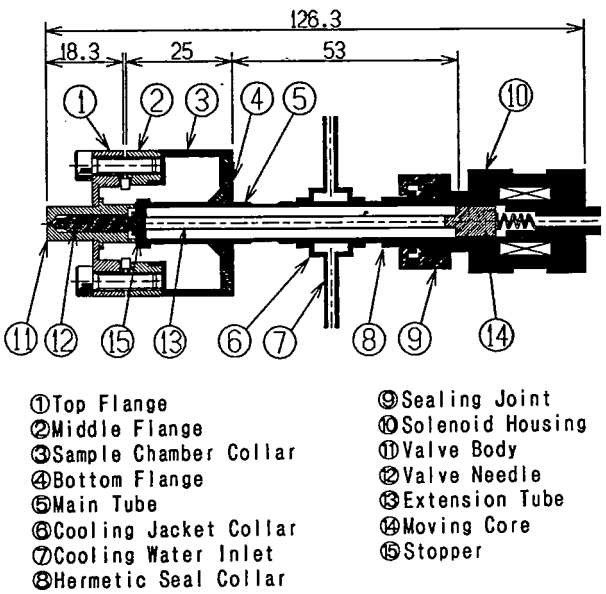

Figure 1. Cross-section of high temperature pulsed nozzle.

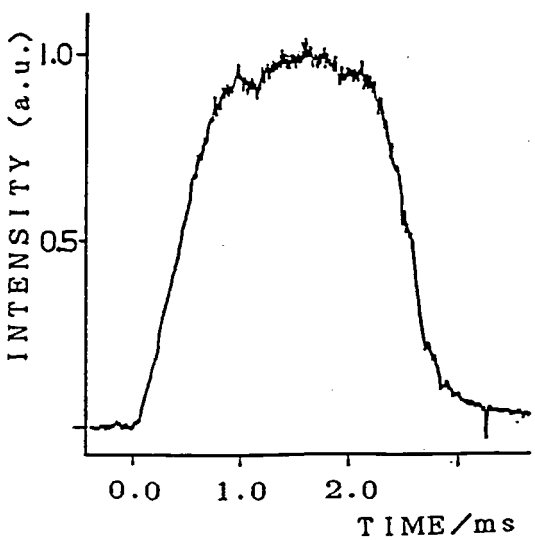

Figure 2. Beam intensity profile as a function of time.

VIII—L New Materials Research

VIII-L-1 Separation and Purification of C_{60} and C_{70} Fullerenes

Masaaki NAGATA, Hiroshi KITAGAWA, Tadaoki MITANI, Shinzo SUZUKI*, Yohji ACHIBA*, Shoji TANAKA, and Yoshiro YAMASHITA, *(*Tokyo Met. Univ.)*

The efficient macroscopic preparation, separation, and purification of C_{60}, C_{70}, and other fullerens have been a subject rapidly to be solved in the field of carbon cluster research. The soot-like material containing fullerites and fullerides (C_{70}, C_{72}, C_{84},..., presumably including $C_{x>100}$) was prepared by arc heating of graphite. Crude benzene-soluble products were extracted from the carbon soot by Soxhlet extractor using toluene for 24 hours. A preparative HPLC (Model LC-908 with Jaigel 1H and 2H, Japan Analytical Industry Co., Ltd.) was used to separate several kinds of fullerens from concentrated extract. Benzene was used as a eluted solution because of good solubility compared with other solution, such as hexane, chloroform, or THF. Its flow rate and each auto-injection amount was 5 ml/min and 5 ml, respectively. The UV-absorption separation (at 270 nm) of C_{60} and C_{70} fullerens by HPLC is very excellent in using of benzen as an elute. In our HPLC system, 0.5 g of C_{60} and C_{70} fullerens per day can be obtained. In coping with a carbon-arc-type carbon-fullerens generator, which is approaching completion, we will raise the HPLC capability of treatment amount up to 5 g/day. Preparations of carbon-cluster single crystals are indispensable and in progress.

Ultraviolet Synchrotron Orbital Radiation Facility

VIII—M Development of UVSOR Light Source

VIII-M-1 Production of an Ultra-Short Bunched Beam in the UVSOR Storage Ring

Hiroyuki HAMA, Shiro TAKANO, and Goro ISOYAMA

We have studied a possibility to control the bunch length of the UVSOR storage ring. The bunch length is proportional to the square root of the momentum compaction factor α, which is given by the integral of the dispersion function η in bending magnets. The bunch length of the UVSOR storage ring is controlled by changing α. The experiment has been carried out at 600 MeV electron energy. In the normal operation mode, the bunch length is 300 ps (FWHM) and the corresponding α is 0.034. The momentum compaction factor was varied by changing a value of the dispersion function in the long straight sections while the horizontal and the vertical betatron wave numbers were kept constant. The positive and the negative parts of η in a bending magnet cancel each other and α is reduced. The momentum compaction factor was estimated from displacement of the horizontal beam position made by changing the RF frequency by the relation $\delta x=(\eta/\alpha)\times(\delta f/f)$, where we use the calculated value for η at the position monitors in the short straight sections. The momentum compaction factor is also proportional to the square root of the synchrotron frequency.

Figure 1 shows the momentum compaction factor as a function of the dispersion function in the long straight sections. Both of the experimental values are in good agreement with each other, and also agree with the calculated value. We measured the bunch length by the single photon counting method using a micro-channel plate. The preliminary result seems to confirm that the bunch length is controlled, and the shortest bunch ever realized is less than one tenth of the normal value. The investigation of shorter bunch length is going on.

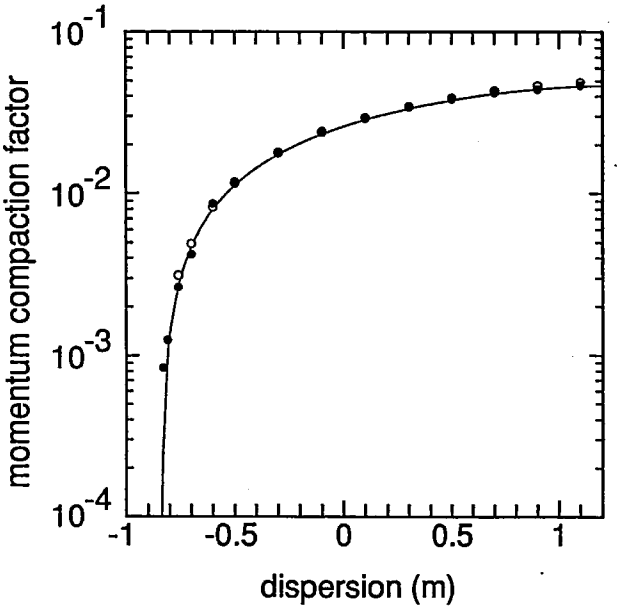

Figure 1. The momentum compaction factor as a function of the dispersion function in the long straight sections. Closed and open circles show the experimental value deduced from the displacement of the horizontal beam position by changing the RF frequency and from the synchrotron frequency, respectively. The calculated momentum compaction factor is shown by the line. Errors of the experimental value are comparable to circle size.

VIII-M-2 FEL Gain Measurement on the UVSOR Storage Ring

Shiro TAKANO, Hiroyuki HAMA, Goro ISOYAMA, Akihiko LIN *(Aishin Seiki)*, **and Nikolay A. VINOKUROV** *(Institute of Nuclear Physics, USSR)*

We have measured a free electron laser (FEL) small-signal gain on the UVSOR storage ring at the optical wavelength of 488 nm for the electron energy of 500 MeV. A conventional permanent magnet undulator is employed,

which is installed in one of the long straight sections of the storage ring. The period length and the number of periods of the undulator are 111 mm and 19, respectively. Electrons are stored in one of the 16 RF buckets (the single bunch operation) by the full energy injection. An argon ion laser of 1 W (CW) output power is used as the external light, which is injected through a glass window into the straight section. The theoretical small-signal gain per pass is estimated to be 1×10^{-3}(I/10 mA). Figure 1 shows the measured gain (filled circles) as a function of the undulator full gap as well as a fit using an theoretical gain curve calculated from the spontaneous emission spectrum (Maday's theorem). The measured maximum peak gain is 7×10^{-4} for the stored beam current I of 10 mA, which is in agreement with a theoretical estimation.

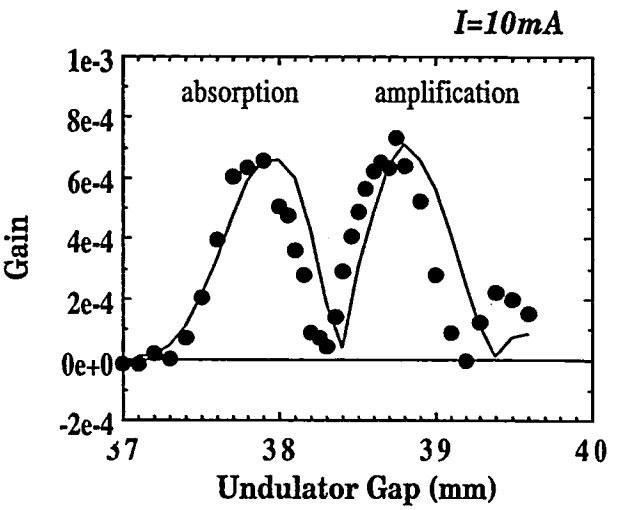

Figure 1. The measured gain (filled circles) and the fitted theoretical gain (solid line) as a function of undulator full gap.

VIII—N Development of Beamlines and Equipment for UVSOR

VIII-N-1 Construction of Focusing Soft X-Ray Beamline BL1A at UVSOR

Atsunari HIRAYA, Toshio HORIGOME, Norio OKADA, Nobuo MIZUTANI, Kusuo SAKAI, Osamu MATSUDO, Masami HASUMOTO, Kazutoshi FUKUI *(Fukui University)*, **and Makoto WATANABE**

A focusing soft X-ray beamline equipped with a focusing premirror and a double crystal monochromator (DXM) has been constructed at BL1A in the UVSOR. Figure 1 shows the plan and side views of the beamline. An elliptically bent cylindrical mirror was used as the focusing premirror in order to attain both horizontal and vertical focusing at the sample position. Ray tracing calculations show that size and shape of the X-ray beam focused by an elliptically bent cylindrical mirror are almost identical with that by an ellipsoidal mirror. Measured spot size of the monochromatic X-ray beam at the sample position was about 2 mm wide and 1 mm high, which is in good agreement with the result of ray tracing. Monochromatic X-rays were observed up to 4 keV even after reflection at platinum coated premirror with grazing angle of 1°.

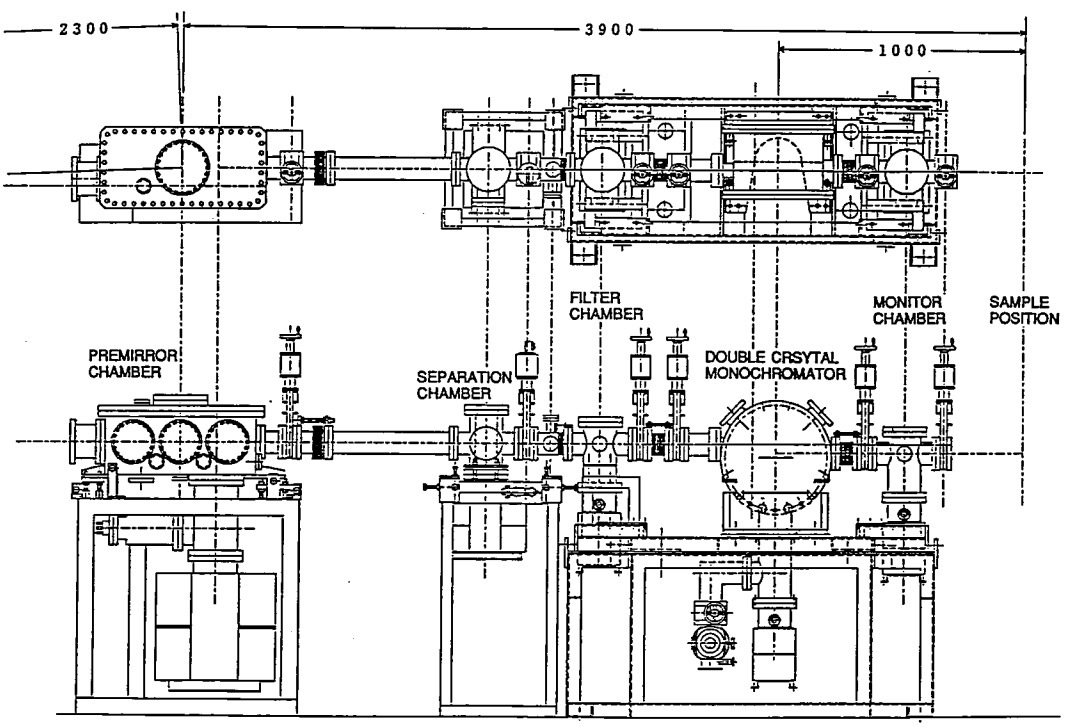

Figure 1. Plan and side views of the focusing soft X-ray beamline BL1A.

VIII-N-2 Fabrication and Characterization of Reactive Ion-Beam Etched SiC Gratings

Eiji ISHIGURO *(Osaka City Univ. and IMS)*, **Koujun YAMASHITA** *(ISAS)*, **Haruhiko OHASHI** *(Toyohashi Univ. of Technology and IMS)*, **Makoto SAKURAI** *(NIFS)*, **Osamu AITA** *(Univ. of Osaka Prefecture)*, **Makoto WATANABE, Kazuo SANO*, Masaru KOEDA*, and Tetsuya NAGANO*** *(*Shimadzu Corp.)*

A SiC holographic laminar grating has been fabricated by means of reactive ion-beam etching in $Ar+CHF_3$ mixture and by using photoresist as an etching mask. The etch rates of SiC and photoresist depend on the CHF_3 concentration in $Ar+CHF_3$ mixture. The maximum value for a ratio of the etch rate of SiC to that of photoresist was found to be 1.29 for $67\%Ar+33\%CHF_3$ mixture.

Diffraction efficiency of the ion-beam etched grating coated with Au was measured by using monochromatized light from a PGM installed into the BL5B beam line of UVSOR and the Al-Kα emission line from a X-ray tube. Figure 1 shows diffraction efficiencies for the -1 to 5 orders as a function of the grazing angle for various wavelength between 8.34 Å and 120 Å. The maximum values measured for the efficiency in the $+1$ order were 4.5—9.3% in the soft X-ray region between 8.34 Å and 120 Å, which could be compared with previously reported values for a laminar grating coated with Au[1,2]. The efficiency for the $+2$ order was below 10% of the $+1$ order. The value is also comparable with experimental[2] and theoretical[3] results. In addition, the intensity of the scattered light component for the grating was estimated to be as low as for a SiC mirror coated with Au. This means that the etched suface of the grating is kept smooth.

We conclude from the results obtained in this experiment that a combination of a holographic technique and reactive ion-beam etching is very useful for fabrication of SiC gratings which are applicable to high power soft X-ray beam.

References

1) R.L. Johnson, *Nucl. Instrum. Methods* **152**, 117 (1978).
2) R.P. Haelbich, C. Kunz, D. Rudolph and G. Schmahl, *Nucl. Instrum. Methods*, **152**, 127 (1978).
3) M. Neiere, J. Flamand and J.M. Lerner, *Nucl. Instrum. Methods*, **195**, 183 (1982).

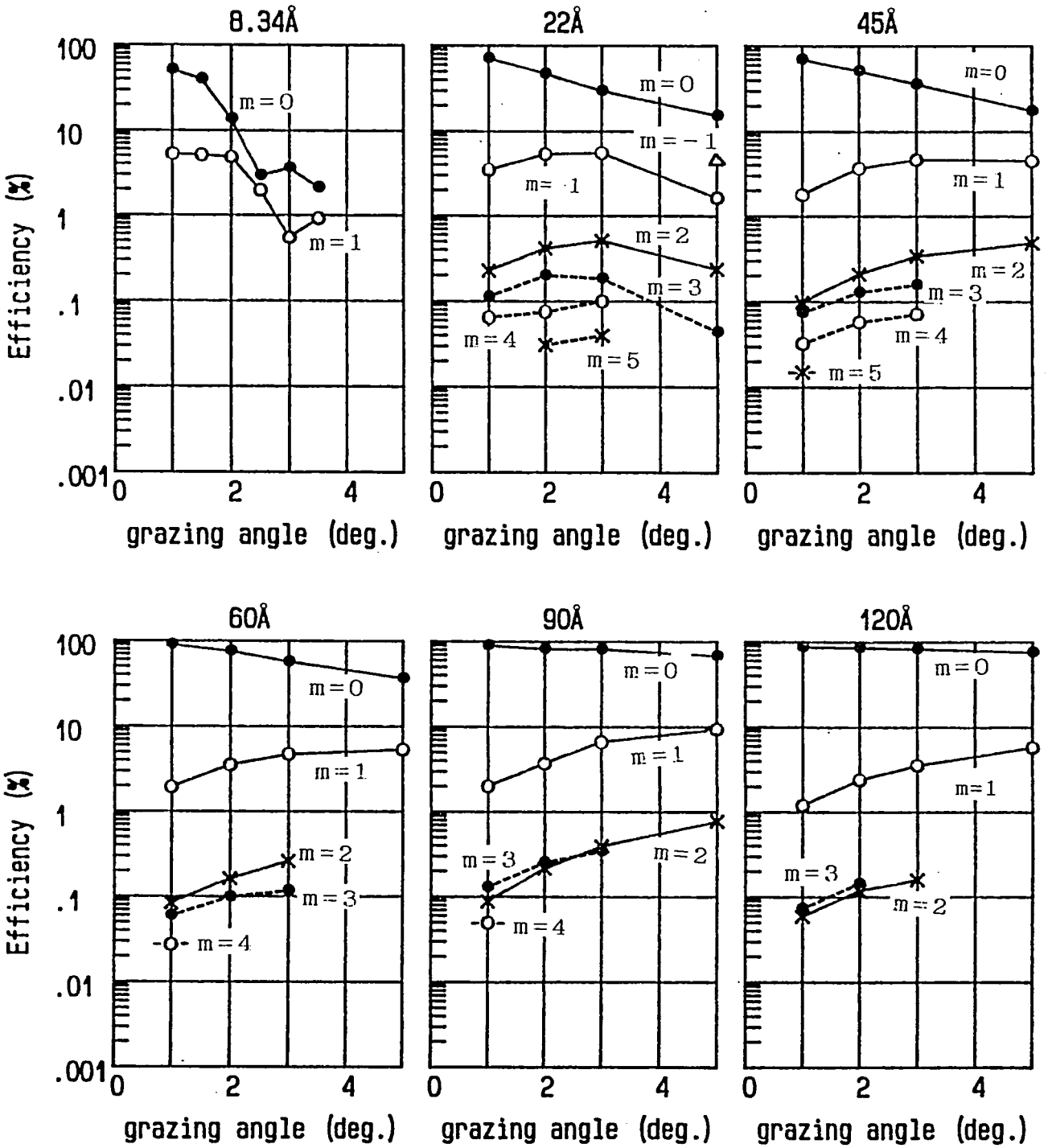

Figure 1. Efficiency of a SiC laminar grating coated with Au of 750 Å thickness for the -1st to 5th order. The groove density is 1200 l/mm, the groove depth, 75 Å and the groove spacing, 0.5.

VIII—O Researches by the Use of UVSOR

VIII-O-1 Temperature Dependence of Ultraviolet Emission from CN^- in Surface Layers of NaCl and KCl

Masao KAMADA and Sayumi HIROSE

[*J. Phys. Soc. Jpn.*, **60**, 3178 (1991)]

Temperature dependence of ultraviolet (uv) emission from CN^-, which was introduced into surface layers of NaCl and KCl crystals by electron irradiation, was investigated. From the comparison with uv emission from electron- and X-ray irradiated NaCl: CN and KCl:CN, it was found that temperature dependences of uv emission from surface and bulk CN^- are much different from each other, in spite of good agreement in the spectral shape. It was also found that there is a good correspondence among uv emission from surface CN^-, thermally stimulated exoelectron emission and desorption of constituent atoms. It is suggested that thermal instability of surface defects plays an important role on the emission mechanism of surface CN^-.

VIII-O-2 Surface Core Exciton in LiCl Studied by Photoelectron Spectroscopy

Kouichi ICHIKAWA*, Osamu AITA*, Masao KAMADA, and Kenjiro TSUTSUMI** *(*Univ. Osaka Pref., **Setsunan Univ.)*

[*Phys. Rev.* **B43**, 5063 (1991)]

The surface core exciton as well as the bulk core exciton were observed by means of photoelectron spectroscopy for the (001) surface of a LiCl single crystal by using polarized light from a storage ring. Constant-initial-state spectra with the initial state at the valence band were measured with various angles of incidence of the exciting light for photoemission. Spectra show two peaks around the excitation photon energy of the Li 1s core exciton. The intensity of the lower-energy peak relative to that of the higher-energy one, which has been attributed to the bulk core exciton, increases drastically with the increase of the angle of incidence. The origin of the lower-energy peak is attributed to the decay of the surface core exciton.

VIII-O-3 Photon-Stimulated Desorption of Excited-State Alkali Atoms from Alkali Halides Irradiated with Undulator Radiation

Sayumi HIROSE and Masao KAMADA

[*J. Phys. Soc. Jpn.*, **60**, 4376 (1991)]

Photon-stimulated desorption of excited-state alkali atoms from sodium- and potassium-halides has been investigated by using a strong quasi-monochromatic undulator-radiation from an electron storage-ring as a light source. The atomic emission (Na D-line) due to the transition from desorbed excited-state sodium atoms was observed on NaF more strongly than on NaCl, but not appreciable on NaBr and NaI, while the intensity of the atomic emission line from excited-state potassium atoms was found to be larger in the order of KI, KBr and KCl. This result is in the good correspondence with the recent models for the defect formation and intrinsic luminescence, and may be interpreted in terms of the lattice instability due to the electronic excitation in the surface layer.

RESEARCH FACILITIES

For the sake of brevity the present issue includes only the newly installed facilities and the activities since September 1990. Concerning the activities and facilities before September 1990, please refer to older IMS Annual Review issues (1978 ~ 1990).

Computer Center

The main computers at the Center are a supercomputer HITAC S-820/80 and a main-frame computer HITAC M-680H. About 40 % of the computer time is used by the research staff at IMS, and the remaining 60 % is given out as research grants to scientists outside the Institutes in molecular science and related fields. As of March 1991, the number of project groups was 256, consisting of 733 users.

In December 1990, a system for making video movies has been adopted to S-820/80. Using this system, one can make video movies of one minute long in one job on S-8720/80. The system is especially useful for the visualization of molecular dynamics simulations. In August 1991, the computers have been linked to international networks through Tokyo University International Science Network(TISN).

The library programs of the Center amount to 704. Among them, about 200 programs can be executed immediately. Recent additions include GAUSSIAN 88 and 90 and MDH208(molecular dynamics simulations for liquid water).

The Quantum Chemistry Literature Database(QCLDB) has been developed by the Center in collaboration with the QCDB Group. The databases, CMQCA, IR2, STERIC, and QCBDB are also available at the Center.

Chemical Materials Center

The Chemical Materials Center plays an important role in the synthesis and purification of chemical substances in IMS. The scientists and technical associates of this facility support other people in IMS to carry out the above works. Upon request, technicians carry out elemental and mass spectrometric analyses of new compounds prepared at IMS. They also carry out their own researches on synthesis of new interesting compounds, developments of new selective chemical transformations, elucidation of reaction mechanisms, and application of new methodologies developed in IMS to the analysis of chemical substances and reactions. Part of the scientific activities are presented in the Section VIII.

Instrument Center

For the efficient use of instruments, the Center is equipped with various types of instruments for general use.[1] One instrument has been newly installed in 1991.

Scanning Tunneling Microscope (Digital Instruments, NanoScope II)

Three-dimensional images of surfaces of conducting samples can be observed with an atomic-resolution at atmospheric pressure. The system is composed of the microscope with a piezoelectric scanner, the scan control unit, and the computer workstation.

Reference

1) *List of Instruments*, No.7, IMS Instrument Center (1989).

Low-Temperature Center

The helium liquefier system installed in 1989 is in steady operation without any serious troubles, and the total monitoring system for liquefying conditions was completed in 1991. The supplied amount of liquid helium in 1990 was 17,662 *l*.

Equipment Development Center

A number of research instruments have been designed and constructed by making use of the mechanical, electric and glass-blowing technologies at this Facility. Representative instruments developed during this fiscal year of 1990 are listed below.

Far-infrared Microspectroscopy for UVSOR Beamline
Double Crystal Monochromator
Beam Source for TOF-MS Spectrometer
Cell for Photoacoustic Raman Spectroscopy
Detector Stage for Infrared Microspectroscopy
20-ch Photon Counting Detector Head
Low-temperature STM Unit
Optical Guide for Deep UV Lasers
Programmable Pulse Generator for NMR

Molecular Beam Valve Controller
Fast Rising High Voltage Pulse Generator
Pockels Cell Driver for Mode-locked Nd:YAG Laser
Data Processing System for Triple Coincidence Studies
Laser Cavity Length Feedback Circuit
Combustion Tube Made of Ceramics
Reaction Cell with a Spiral Discharge Tube
Quartz Cell for Electrochemistry

Cooperative Unit for Advanced Engineering

The cooperative unit for advanced engineering made a start this year. In this unit planning and designing of research instruments with unique idea is performed, and development of new technologies necessary for it is also promoted. The production of these machines (called "IMS Machines") is carried out in collaboration with the present machinery sections.

Ultraviolet Synchrotron Orbital Radiation Facility

The UVSOR light source is usually operated at an electron energy of 750 MeV with an initial current of 200 mA and a beam lifetime of about 200 min. A part of the control system of the accelerators has been replaced with a new computer control system. Three beamlines have been newly constructed. They are BL1A equipped with a double crystal monochromator, BL4B for photo-assisted etching and BL6B for far-infrared microspectroscopy.

SPECIAL RESEARCH PROJECTS

IMS has special research projects supported by national funds. Three projects presently in progress are:

(1) Development and evaluation of molecular synergistic systems and their application to chemical energy conversion (1990-).

(2) Materials science on molecular devices (1990-).

(3) Molecular science of primordial chemical evolution and selforganization (1987-1991).

These projects are being carried out with close collaboration between research divisions and facilities. Collaborators from outside also make important contributions. Research fellows join these projects. The results in 1990 are reviewed in this report.

(1) Development and Evaluation of Molecular Synergistic Systems and their Application to Chemical Energy Conversion

(1) Studies on Dynamical Processes of Highly Excited Atoms and Molecules

(2) Studies of Laser Cooling and Trapping of Atoms

Norio MORITA, Asuka FUJII, and Mitsutaka KUMAKURA

Theoretical analysis on the spectra of doubly excited states of Ca atom so far observed has been continued through the R-matrix calculation and multichannel quantum defect theory. The behavior of the electron correlation has extensively been investigated by drawing charge density plots (see II-A-3).

Experimental studies on superexcited Rydberg states of the NO molecule have been continued with interest in their autoionization and predissociation properties. The Rydberg states are excited by two UV lasers and then the fragment nitrogen and oxygen atoms generated by the predissociation are detected through laser multiphoton ionization with another UV laser. In this experiment, the dependence of each final state of the fragment atoms on the initial NO states has extensively been studied (see II-A-1 and II-A-2).

The construction of an apparatus for the laser cooling of the He atom has been completed. It is schematically shown in Fig. 1. Using this apparatus, the laser deceleration of a helium atomic beam in the $2s^3S_1$ metastable state has been realized (see II-B-1). An experiment for the laser trapping of the He atom is now in progress, and some improvements of the system has been continued to achieve it.

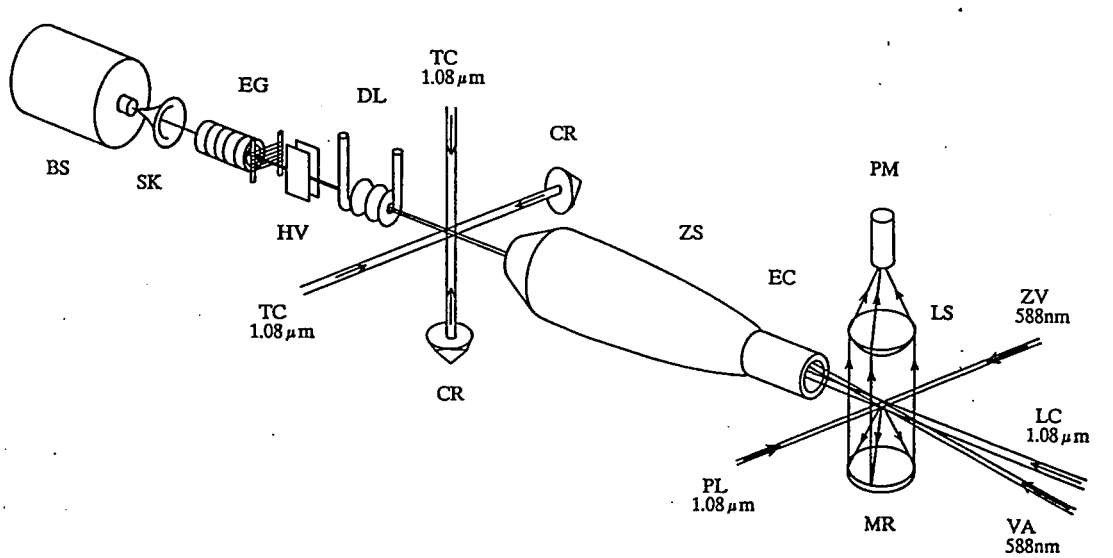

Figure 1. Schematic diagram of the experimental setup. BS: liquid-nitrogen-cooled nozzle, SK: skimmer, EG: electron gun, HV: high-voltage electrodes, DL: helium discharge lamp, TC: transverse-cooling laser, CR: corner reflector, ZS: Zeeman-tuning solenoid, EC: extraction coil, PM: photomultiplier, LS: lens, MR: concave mirror, PL: pumping laser for the velocity analysis, ZV: zero-velocity-marking laser, VA: velocity-analysis laser, and LC: longitudinal-cooling laser.

Mechanism of Oxygen Activation by Cytochrome Oxidase in a Respiratory Chain

Teizo KITAGAWA, Takashi OGURA, Satoshi TAKAHASHI, and Shinya YOSHIKAWA *(Himeji Inst. Tech.)*

Cytochrome oxidase is the terminal enzyme of the electron transfer chain and located in energy transducing membrane of aerobic organisms. This enzyme contains two heme A groups (Fe_A and Fe_B) and two copper ions (Cu_A and Cu_B) as the redox active metal centers and couples the dioxygen reduction reaction with proton translocation across the membrane. A functional unit containing the Fe_A and Cu_A ions serves as an electron transfer protein from cytochrome *c* to another functional unit containing the Fe_B-Cu_B binuclear dioxygen reducing site. A mechanism of dioxygen reduction by the Fe_B-Cu_B is a current topic of spectroscopic studies. We investigated reaction intermediates present in the time interval between 0.1 and 5.4 ms after initiation of the reaction by using time-resolved resonance Raman spectroscopy combined with our original Artificial Cardiovascular System. At 0.5 ms, we observed a new oxygen-isotope sensitive band at 356 cm^{-1} for $^{16}O_2$ which shifted down to 341 cm^{-1} for $^{18}O_2$. The temporal behavior of this band was found to be very close to that of another oxygen-isotope sensitive band at 788 cm^{-1} which had been assigned previously to the Fe^{IV}=0 stretching mode of the ferryloxo intermediate. However, the fact that the 788 cm^{-1} band shifts to a higher frequency (802 cm^{-1}) in D_2O, taken together with the present detection of two oxygen-isotope sensitive bands, prompts us to suggest an alternative assignment; namely, that these bands arise from the O^--O^- (788 cm^{-1}) and Fe^{III}-O^- (356 cm^{-1}) stretching modes of the Fe^{III}-O^-O^--H intermediate. This conclusion will force a reconsideration of the currently accepted view of cytochrome oxidase catalysis.

In order to develop a new method for probing the Cu_A site, a Raman system using a CCD (Charge Coupled Device) detector and Ti-supphire laser was constructed. The spectra of cytochrome oxidase excited at 830 nm yielded the amide bands and the side chain modes of aromatic residues of protein irrespective of the oxidation state. However, additional Raman bands were observed around 330 cm^{-1} only for the oxidized enzyme, and were assigned to Cu_A-S(Cys) and Cu_A-N(His) stretching modes on the basis of deuteration sensitivity.

Development of Non-Linear Spectroscopy for Studies on Ultrafast Phenomena

Hiromi OKAMOTO, Ryoji INABA *(Univ. of Tokyo and IMS)*, **Tohru KOBAYASHI, Yoshihiro TAKAGI, Vaclav KUBECEK, Shigeichi KUMAZAKI, and Keitaro YOSHIHARA**

Firstly, we have constructed a femtosecond time-resolved coherent anti-Stokes Raman scattering (FSCARS) measuring system, which has the capability of performing polarization experiments. Duration of the excitation laser pulse is typically 85 fs. We have studied vibrational relaxation of simple molecules (acetonitrile etc.) in liquid and solutions as well as large molecules (carotenoids etc.) in various kinds of environments (solvents, biological systems, etc.). It has been demonstrated that the vibrational phase relaxation reflects liquid state structures and dynamics. The details are described in III-D.

Secondly, we have found, by femtosecond fluorescence up-conversion method, an ultrafast intermolecular electron transfer on the order of 100 fs with the dye/electron donating liquid solvent systems. A new mechanism for a possible contribution of vibrational motion of molecules (ultrafast) to electron transfer rather than rotational fluctuations (relatively slow) is emphasized. The details are described in III-B.

Thirdly, all solid state widely tunable laser source of ultrashort light pulses for spectroscopy has been developed and improved. A feedback controlled mode-locking operation of flashlamp pumped neodymium laser generates long flat pulse trains which synchronously pump an optical parametric oscillator (OPO). The OPO outputs widely tunable energetic picosecond pulses. The details are described in III-E.

Picosecond Reaction Dynamics of Excited Molecules in Clusters

Hrvoje PETEK and Keitaro YOSHIHARA

While the understanding of reaction dynamics in isolated molecules has greatly advanced in recent years, similar progress in understanding of reaction dynamics in solution awaits development of more powerful experimental and theoretical techniques. A fruitful approach for studying condensed phase reactions is to investigate well characterized solvent-solute clusters under supersonic molecular beam conditions. This approach is particularly useful because it can reveal specific solvent-solute interactions that are otherwise obscured, and because such well characterized systems can be modeled by theoretical methods. We have made preliminary measurements on *cis*-stilbene isomerization in Ar and Kr clusters using picosecond pump-probe techniques. Although, the isomerization rate was measured by monitoring the fluorescence from the *trans*-stilbene product, no information was gained about the cluster size distribution. This year we have constructed a time-of-flight mass spectrometer. By using picosecond pump-probe multiphoton ionization, we can measure picosecond time scale dynamics of clusters with a specific composition. Since excess energy in excitation and ionization is likely to lead to fragmentation of cluster ions before they can be detected, it is necessary to excite the cluster near the threshold for ionization. For this purpose, we have modified our picosecond laser system so that two independently tunable colors can be generated, by picosecond continuum amplification.

Studies of Laser-Induced Photochemistry on Solid Surfaces

Yoshiyasu MATSUMOTO and Kyoichi SAWABE

A new apparatus has been constructed for the observation of laser-induced reactions on well-defined solid surfaces. The apparatus is equipped with a low energy electron

diffraction(LEED) and Auger electron spectrometer(AES), a quadrupole mass spectrometer (QMS), an ion gun, a precision XYZ sample manipulator mounted on a differentially-pumped rotary platform, a sample holder, a gas doser, and inlet and outlet windows for laser beams. The main chamber is evacuated by a tandem turbo molecular pump and the housing of the QMS is differentially pumped by another tandem turbomolecular pump. The base pressure of the apparatus is kept below 2×10^{-10} Torr. The sample temperature can be cooled from 1300 to 80 K in a few minutes. Impurities on the surface of samples can be removed by Ar ion sputtering and the impurity level is checked with AES. Surface order is determined with LEED. The quadrupole mass spectrometer is used for temperature-programmed desorption and time-of-flight measurements of neutral species desorbed from surfaces.

External Magnetic Field Effects upon Chemical Reactions

Masaharu OKAZAKI *(Gov. Ind. Res. Inst., Nagoya and IMS)*, **Ryoichi NAKAGAKI, Minoru SUMITANI, and Saburo NAGAKURA** *(Grad. Univ. for Adv. Studies)*

In this research project the magnetic field effects on the recombination fluorescence as well as the optically detected ESR(ODESR) for X-ray irradiated ethylene-propylene rubber (EP-rubber) doped with pyrene have been observed. Through the analysis of these observations we concluded that the charge recombination occurs mainly through electron hopping (by tunneling) between the doped pyrenes when the concentration is as high as 1.0 wt%. At elevated temperatures hopping of hole can also contribute to the recombination process.

Continued efforts have been also made on the clarification of the mechanism of the magnetic field effects on the emission intensity of NO in the $B^2\Pi$ state. Direct laser excitation from the NO $X^2\Pi$ state has been used to populate the $B^2\Pi$ state, instead of the production of this state by use of chemical reactions previously studied in our group.

Fragmentation and Extension of Cube Size in Integrated Cubane-Type Oxide Clusters

Kiyoshi ISOBE, Yoshiki OZAWA, and Bateer WANG

Recently, we have synthesized new classes of organometallic oxide clusters which have a novel structure with integrated cubane-type frameworks. The triple cubane-type oxide cluster, $[(RhCp^*)_4(MoO_4)_4]$, can react with organic compounds with the acidic proton, for example, CH_3OH and CH_3SH to give a trishomocubane-type cluster, $[(RhCp^*)_2Mo_3O_9(OMe)_4]$, and a tetranuclear compound, $[(RhCp^*)_2Mo_2O_5(SMe)_6]$. At first stage of these reactions the hydrogen bond interaction was formed at the bridge oxygen atoms of the clusters, and then the $M\text{-}O_{(bridge)}$ bonds were cleaved selectively followed by the degradation of the cube size. The trishomocubanetype cluster couples itself in CH_2Cl_2 to extend the cube size to a lienar quadruple cubane-type cluster, $[(RhCp^*)_4Mo_6O_{22}]$. On the other hand, the tetranuclear complex is converted to $[(RhCp^*)_2(SMe)_3]_2\{[Mo_6O_{19}]\}$ in CH_2Cl_2.

Structure and Stability of Organic Ions

Masaaki MISHIMA and Yuho TSUNO

Gaseous thermochemical data such as acidity and basicity of organic molecules provide valuable information regarding intrinsic effects of molecular structure on the stability of ions. Such data serve as the most precious basis for investigation of an essential relationship between structure and chemical reactivity which has played an important role in the development of organic reaction theory. In the present project, thermodynamic stabilities of a variety of ionic species which are believed to be intermediates of reactions in solution have been determined by measuring equilibrium constants of H^+, Me_3Si^+, and electron transfer reactions using a pulsed ion cyclotron resonance spectrometer. Substituent effects on stabilities of ions where the direct π-interaction between the aryl and ionic center is possible, have been found to be successfully described in terms of our LArSR equation. Furthermore, a comparison of the substituent effect for stabilities of ions with that for reactions in solution of relevant substrates has provided a new insight into the basic concept for relating the transition states to intermediate ions. Details of the work are given in Section V-G.

Development of New Asymmetric Auxiliaries, Ligands, and Catalysts for Remote Asymmetric Induction

Junji INANAGA, Takeshi HANAMOTO, Yasuo YOKOYAMA, and Naohide MATSUMOTO* *(*Kyushu University)*

Asymmetric space-expansion by the introduction of aromatic rings into optically active compounds at suitable positions is thought to be effective for remote asymmetric induction. As a preliminary study, we have introduced *p*-biphenyl and *m*-terphenyl group to the 8-position of (R)-(+)-pulegone to give the corresponding (1R,2S,5R)-8-*p*-biphenylmenthol (**1**) and (1R,2S,5R)-8-*m*-terphenylmenthol, respectively. The X-ray crystallographic analysis of **1** revealed that the hydroxyl group is placed in front of the plane of the aromatic ring (conformation A). Although MM2 calculation of the corresponding acetate does not support that the type-A conformer is most stable in ground state, the ^1H NMR analysis in deuteriochloroform revealed that proportion of the conformer is so large that the methyl protons of the acetyl group appear at ca. 0.5 ppm upper field than those of menthyl acetate. It may be stabilized through hyperconjugative interaction between the acetyl methyl and the phenyl group. In the case of 8-*p*-biphenylmenthyl-2,4-hexadienoate, not only olefinic protons but also vinylic methyl protons, which are far away from the asymmetric carbon C(1), were found to be considerably shielded (ca. 0.2 ppm) by the biphenyl moiety, suggesting the contribution of π-stacking structure. This might be a promising sign for the remote asymmetric induction.

Excited-State Photoelectron Spectroscopy for Studying Photophysical and Photochemical Behaviors of Molecules and van der Waals Complexes

Katsumi KIMURA, Katsuhiko OKUYAMA, Masatoshi TAKAHASHI, Hiroyuki OZEKI, and Martin C.R. COCKETT

Excited-state photoelectron spectroscopy combining a UV/visible pulse laser technique and a supersonic molecular beam technique has been developed in this Institute since 1980 (Kimura et al., *IMS Annual Review,* 1980-1990). The method which is often called "MPI or REMPI photoelectron spectroscopy" has made it possible to study dynamic behavior of excited-state species which include nonradiative electronic states. Photoelectron spectra originating from various molecular excited states have been investigated from photophysical and photochemical points of view. The information deduced from excited-state photoelectron spectra have been found to be unique and important.

In this project, we have develped a compact and high resoltuion threshold photoelectron analyzer with which threshold photoelectrons are collected with a resolution of 1-2 cm^{-1} as a function of laser wavelength. The technique is equivalent to so-called ZEKE (zero kinetic energy) photoelectron spectroscopy. In this project, furthermore, we have applied this high resolution analyzer to two-color (n+1') REMPI threshold photoelectron experiments of various molecules and molecular complexes. [See].

Construction of an Apparatus for Velocity Distribution Measurements of Desorbing Molecules during Thermal Desorption

Tatsuo MATSUSHIMA *(IMS and Hokkaido Univ.),* **Kosuke SHOBATAKE, Yuichi OHNO, and Kiyoshi NAGAI** *(IMS and Komatsu Electronic Metal Co.)*

The apparatus consists of a reaction chamber, a chopper chamber and an analyzer chamber, as shown in Figure 1. A sample crystal was set on the top of a L-shaped manipulator. It can be rotated at the top to change the desorption angle. Further, the sample can be cooled to 100 K. The desorption of product molecules was induced by heating co-adlayer of reactants. A chopper blade has slots of unit width (1mm×6mm) distributed in a psedo-random sequence. Time resolution of 15 μs was obtained at a rotation rate of 130.72 Hz. The arrival times at the ionizer of a mass spectrometer in the analyzer chamber were registered on a homemade multichannel analyzer running synchronously with the chopper blade. The signal counting for the temperature range of each thermal desorption peak was stored separately. It was controlled by a micro-computer monitoring the output of a thermocouple spot-welded on the crystal.

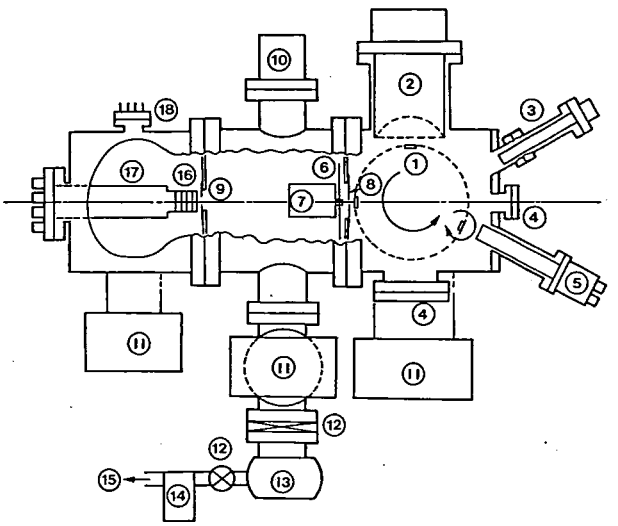

Figure 1. Schematic of a time of flight spectrometer combined with angle-resolved thermal desorption. (1) sample crystal, (2) LEED-AES optics, (3) mass spectrometer, (4) window, (5) ion gun, (6) chopper and photocell, (7) motor, (8) slit 1, (9) slit 2, (10) cryo-element, (11) ion pump, (12) gate valve, (13) turbomolecular pump, (14) oil diffusion pump, (15) rotary pump, (16) ionizer, (17) mass spectrometer, and (18) ionization gauge.

Development of Computer Program for Molecular Simulations

Kazuo KITAURA and Umpei NAGASHIMA

A Computer program has been developed for molecular simulations. The program has been expanded to use the Lennard-Jones potentail and the Buckingham potential, in addition to the new intermolecular potential which is expressed by intermolecular overlap integrals. The program has been coded for calcualting the derivatives of these potentail functions with respect to coordinates.

The functions of the program are geometry optimizations, normal mode analysises and Monte Carlo simulations for molecular clusters and liquids. It is also possible to calculate packing structures of molecular crystals by the program. The structure and the thermodynamic propeties of liquid annmonia have been studied using the program. The details is described in VIII-A-1.

(2) Materials Science on Molecular Devices

Study of Novel Organic Semi- and Conductors

Hiroo INOKUCHI

In this period, 1990-1991, we are joining to this special research project to find novel organic semiconductors and/or conductors. We found the third single-component organic semiconductor, BTQBT, with Yamashita's school. BTQBT, [Bis[1,2,5]-thiadiazolo-p-quinobis(1,3-dithiole)], shows a fairly high electronic conduction, $10^3\Omega$cm ~ $10^5\Omega$cm, having semiconductive activation energy (~0.2 eV). We could succeed to observe a Hall voltage; from this value we estimate the value of Hall mobility, 4 cm^2/v.sec. We also are studying the change of semi-conductivity of cytochromes as a function of structure. (See page 117)

d-π Interaction in Molecular Metals

Kyuya YAKUSHI, Hideo YAMAKADO, Takashi IDA, Atsushi KAWAMOTO, Akito UGAWA, and Kentaro IWASAKI

We have undertaken a systematic study on the solid molecular systems in which transition metals are embedded in a π-conjugated system from the viewpoint of the future design of the superconducting material. The most attractive materials are the one-dimensional solid based on phthalocyanine molecules. Through the systematic study of the optical spectra of phthalocyanine radical salts (see IV-A-2), we have claimed that $CoPc(AsF_6)_{0.5}$ has a unique double-chain structure where a half-filled Hubbard type Co chain and a π-type Pc chain are linked by a magnetic exchange interaction (see IV-A-1). It is not clear now that this magnetic interaction plays an important role in the solid state properties of this salt, since the magnitude of this exchange interaction is not known. We are now conducting the experiment to determine the exchange energy using model compounds.

Coupled Proton and Electron Transfer in the Crystals of Salicylideneaniline Derivatives and their Complexes

Tamotsu INABE, Hironori OGATA, Naomi HOSHINO *(Hokkaido Univ.)*, **Kaoru OKANIWA, Hiroshi OKAMOTO, Tadaoki MITANI, and Yusei MARUYAMA**

Our interest in this particular area of research on molecular devices lies in the possibility of furnishing molecular assemblies with novel physical properties through an appropriate modification of the constituent molecules. Proton-transfer process was chosen as the molecule-based function, and its coupling to the assembly-based properties has been investigated. A framework of salicylideneaniline has such a function of intramolecular proton transfer. The thermochromic behavior observed in many of the derivatives gives a clue for changes in the π-electron state accompanying the proton transfer. Thus, the work has been devoted to the crystal structure determination at varied temperature and elucidation of possible cooperation in proton- and electron-transfer processes in the crystal of these compounds by means of optical measurements. Since the assembly-based properties depend largely on the intermolecular interaction, some derivatives have been employed as a donor component of the charge-transfer complexes with various acceptors in order to introduce stronger intermolecular interaction. The structural and optical studies of the complexes have provided the information about the correlation between the proton motion and the electronic state, which suggests possibilities of constructing a novel type of electrical conductors. Similarly, the structures and the optical and electrical properties of some charge-transfer complexes with intermolecular hydrogen-bonds have been studied. Details of the work are given in Section IV—F.

Fabrication of Novel Organic Molecular Assemblies with the Use of the Molecular Beam Epitaxy Technique

Yusei MARUYAMA, Hajime HOSHI, Naoki NAKAMURA *(Toyota Motor Corp. and IMS)*, **and Tamotsu INABE**

In order to prepare new materials which could be useful for molecular devices elements, we have started to design and fabricate ultra-thin organic multi-layered systems. In the first palce, we have prepared ultra-thin single component phthalocyanine thin films to investigate epitaxial growth conditions on alkali halide single crystals. Fairly well oriented, uni-or bi-directionally, crystalline films are obtainable on the alkali halide substrates. Based on this kind of mono-film, we are going to fabricate a multi-layered system.

The SHG and-or THG of the films are investigated from the view point of the molecualr structure and the epitaxial or orientational structure of the films.

Fabrication of High T_c Metal Oxide-Superconducting Films by Layer-by-Layer Deposition from Multi-electron-Beam Gun Sources

Toshifumi TERUI and Yusei MARUYAMA

Successive deposition of each component of metal oxides has been undertaken to achieve the layer-by-layer construction for high T_c oxide superconductors. The high vacuum evaporation machine is equiped with three electron-beam guns and it can be operated under a differential pumping when oxygen inclusion is required. As an initial trial, La-Sr-Cu-O system is now invesigated.

Exploration of New Cooperative Proton-Electron Transfer (PET) Systems

Kazuhiro NAKASUJI, Kenichi SUGIURA, Jiro TOYODA, and Yasushi MORITA

Search for new molecular materials based on cooperative interactions between hydrogen bonding and charge transfer in the solid stete has been actively continued. Our particular attention in this research project is concentrated on the

phase transition found for 1,4-benzoquinhydrone under pressure. The phase transition can be regarded as a cooperative proton-electron transfer (PET) phenomenon. The final PET state can be characterized as a molecular assembly of *H-bonded neutral radicals.* We are now developping a general strategy to explore new molecular materials based on PET phenomena. The stepwise consideration leads to two reasonable molecular design strategies to realize such cooperative phenomena under milder conditions in the solid state: the exaploration of (a) a quinone-hydroquinone pair with a smaller intermolecular CT gap and/or (b) an electronic modification to stabilize H-bonded neutral radicals. As a former approach (a), we have already reported the synthesis and solid state properties of four extended conjugated quinhydrones. As a next step, the design and synthesis of new extended conjugated quinhydrone, including heterocyclic conjugated quinhydrones, are now actively performed. As a latter approach (b), the prototype, benzoquinhydrone, is modified by introducing the electron donor and the acceptor substituents. Such a modification turned out to prevent the formation of the quinhydrone type complexes. As this can be partly attributed to the formation of intramolecular hydrogen bonded species in the hydroquinone components, we are now designing molecules more precisely to eliminate such an unfavorable factor.

Dynamics of Solvated Metal Cluster Ions

Kiyokazu FUKE and Fuminori MISAIZU

Metal ions are intimately involved in chemistry and biochemistry and play a crucial role in many reactions. Although there has been extensive progress in the thermodynamic and kinetic studies of solvated metal ions, the study of microscopic aspect of solvation dynamics has been rather limited. Spectroscopic studies of the solvated metal ion clusters as a specific function of cluster size can provide detailed information on energetic and dynamics of solvation. The advent of mass spectrometer and metal cluster beam techniques in conjunction with laser probes now allow an attack on the problem for the solvation of metal ions and metal cluster ions through studies that probe energy levels and dynamical processes occurring in solvated metal clusters.

In the present research project, we have investigated the photoionizaiton of cesium atom solvated by polar solvents such as water, ammonia, and acetonitrile relating with the excess electron in bulk fluids (see VIII-C-1). We are also studying the photoionization and photodissociation of water clusters involving the Group II and III metal atoms in order to obtain information about the cluster-size dependence of geometrical and electronic structures, and its reactivities. The details are described in VIII-C-2, 3, and 4.

Novel Electron Donors and Acceptors Containing Fused-heterocycles

Yoshiro YAMASHITA, Shoji TANAKA, and Masaaki TOMURA

Electron donors and acceptors containing fused heterocycles such as thiadiazole and pyrazine are of interest since the presence of the fused heterocycles enlarges the π-electron ring system and reduces Coulombic repulsion. Intermolecular interactions can be also expected by heteroatom contacts. We have now prepared several novel compounds containing a fused [1,2,5]thiadiazole or a pyrazine ring. For example, bis[1,2,5]thiadiazolo-*p*-quinobis(1,3-dithiole) (BTQBT) was prepared by using a Wittig-Horner reaction. BTQBT was found to show an unusually high conductivity (10^{-3} S cm^{-1}) as a single component. The X-ray structural analysis revealed that the molecule is completely planar and forms a sheet-like network by short S—S contacts (3.26 Å). 5,8-Bis(1,3-dithiol-2-ylidene)-5,8-dihydroqunoxalines which are TTF analogues with a quinoid structure were also prepared. They were stronger donors than TTF inspite of the presence of an electron-withdrawing heterocycle.

Details of these works are described in VIII-B section.

A New Molecular System: Cooperation of Transition Metal Chain and CT Stack *via* Intermolecular H-Bonds

Tadaoki MITANI, Hiroshi KITAGAWA, and Hiroshi OKAMOTO

Recent years, our studies have been concentrated on the H bond network in solids, which provides a unique opportunity for construction of novel molecular assemblies.[1] The presence of cooperative proton-electron transfer (PET) systems in the H-bonded charge-transfer (CT) complexes was recently confirmed.[2] While, it has been found that strengthening the interchain H-bonds in the 1-D mixed-valence metal complexes leads to the stabilization of a new type of 1-D electronic states.[3),4] Very recently, it has been proved that the quantum mechanical motion of protons is enhanced by doping electrons into the 1-D H-bonded system. The proposal in this project is how efficiently to cooperate these characteristic H-bonded electronic states, i.e. the CT electronic states, the 1-D transition-metal electronic states, and the electron-proton interaction system, in order to create a new molecular function. (See XXX) As the first demonstration of this proposal, the optical and transport measurements on [M(H_2DAG)(HDAG)]TCNQ (M=Ni, Pd, Pt, and H_2DAG: diaminoglyoxime) single crystals have been made. The results show a unique possibility to control the 1-D metallic state *via* the electron-proton interaction in H-bonds. Synthesis of new conducting materials by chemical modification of these complexes is in progress.

References

1) T. Mitani, *Mol. Cryst. Liq. Cryst.*, **171** (1983) 343.
2) K. Nakasuji, K. Sugiura, T. Kitagawa, J. Toyota, H. Yamamoto, H. Okamoto, K. Okaniwa, T. Mitani, H. Yamamoto, I. Murata, A. Kawamoto, and J. Tanaka, *J. Am. Chem. Soc.*, **113** (1991) 1863.
3) K. Toriumi, Y. Wada, T. Mitani, S. Bandow, M. Yamashita, and Y. Fujii, *J. Am. Chem. Soc.*, **111** (1989) 2341.
4) H. Okamoto, K. Okaniwa, T. Mitani, K. Toriumi, and M. Yamashita, *Solid State Commun.*, **77** (1991) 465.

(3) Molecular Science of Primordial Chemical Evolution and Self-organization

Determination of Light Inhibition/Induction Efficiency of Chemical Oscillations in the Batch and Flow Reactors

Ichiro HANAZAKI

Light irradiation on chemical oscillators sometimes inhibit or induce chemical oscillation. Although several works had been reported, there had been no acculate determination of wavelength-dependence of the efficiency until our papers[1),2)] appeared recently. In these papers, we have derived a relation to determine the efficiency experimentally. It seems to be desireable to obtain more general relations which can be applied both to the batch and CSTR experiments. Therefore we have derived a general treatment to obtain efficiency $\alpha(\lambda)$ as a function of wavelength λ as

$$\alpha(\lambda) \propto [D/P_0^c(\lambda)]\,[1-\exp(-2.303D)]^{-1}$$

where $P_0^c(\lambda)$ is the experimentally determined threshold light power to inhibit or induce chemical oscillation. This relation is common for the batch and CSTR experiments. In addition, we have found that the same "stationary" concentrations can be attained in CSTR if the experimental parameters such as input concentrations, flow rates and reactor dimension are varied under the "equivalent" constraint. Using this result, we have found the dependence of P_0^c on the reactor dimension is

$$P_0^c \propto AL/R$$

commonly for the batch and CSTR, where AL is the reactor volume, L is the optical pathlength and $R \equiv (L/2.303D)\,[1-\exp(-2.303D)]$.

References

1) P.K. Srivastava et al., *Chem. Phys. Letters*, **177**, 213 (1991).
2) Y. Mori et al., *Chem. Letters*, **669** (1991).

Mechanism of Photo-inhibition in Ruthenium-Catalyzed Belousov-Zhabotinskii Reaction

Prem Kumar SRIVSTAVA, Yoshihito MORI, and Ichiro HANAZAKI

To study the basic mechanism of photo-inhbition in the catalyzed Belousov-Zhabotinskii (BZ) reaction, we have chosen ruthenium-catalyzed BZ reaction. Irradiation of the acidic $Ru(bpy)_3^{2+}$ solution by the 455 nm light causes oxidation. The dark reaction of acidic $Ru(bpy)_3^{2+}$ with BrO_3^- has been known to be autocatalytic with an induction period. Our study has shown that irradiation of this system at 455 nm increases the rate of the autocatalytic reaction and reduces the induction period. The efficiency spectrum of photo-inhibition in this reaction is in good agreement with absorption spectrum of the reduced state of the catalyst. We have verified experimentally that the critical power necessary to inhibit the oscillation varies as a linear function of the concentration of reduced state of the catalyst as shown in the figure. The above observation suggests that $Ru(bpy)_3^{2+}$ absorbs light. The most probable mechanism for the inhibition is that $Ru(bpy)_3^{2+}$ is photo-oxidised to $Ru(bpy)_3^{2+}$ which in turn reacts with substrate and brominated substrate to produce Br^-. As has been postulated in the literature, excess Br^- keeps the system in the reduced state by inhibiting the autocatalytic step in the redox cycle. Increase in the concentration of Br^- under irradiation has been verified experimentally.

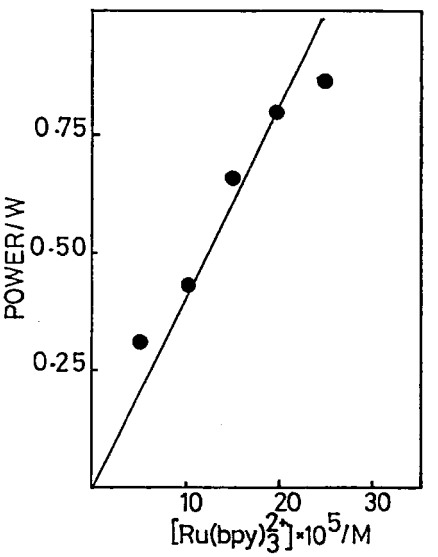

Figure 1. Dependence of the critical power for inhbition of oscillation on the $Ru(bpy)_3^{2+}$ concentration when solution is irradiated through a band pass (380-570 nm) filter. Initial conditions are; $[\text{malonic acid}]_0$=0.025 M $[BrO_3^-]_0$=0.025 M, $[H_2SO_4]_0$=1.0 M, k_o=0.0373 min^{-1} and temperature = 25°C.

Mechanism of Uncatalysed Chemical Oscillation

Prem Kumar SRIVASTAVA, Yoshihito MORI, and Ichiro HANAZAKI

The chemical oscillators reported upto now are mostly based on oxidation reduction reactions. Orbon et al.[1)] have reported a list of organic substrates which oscillate with bromate alone. We have investigated the species responsible for oxidation reduction reaction in aromatic substrates. In order to identify the species responsible for oxidation reduction cycle, we have analysed the intermediates in well-studied phenol-BrO_3^--H_2SO_4 system by the rapid scan spectrophotometric technique. The intermediate species shows an absorption band at 392 nm. The intensity of this band increases during the induction period and then decreases in oscillatory pattern and finally disappears. The oscillation is in-phase with that of the redox potential. The difference spectrum (reduced minus oxidized states) has a broad absorption band at 392 nm, which is assumed to be due to the phenoxy radical (Figure 1). On the other hand the difference spectrum (oxidized minus reduced states) has a broad absorption band at 435 nm which may be due to a semiquinone species. These results have been discussed on the basis of the mechanism we have reported[2)], where the phenoxy radical plays an important role as a "catalyst" as

well as a substrate.

References

1) M. Orbon and E. Koros, *J. Phys. Chem.* **84**, 1330 (1980).
2) P.K. Srivastava, Y. Mori and I. Hanazaki, *Chem. Phys. Letters*, **177**, 213 (1991).

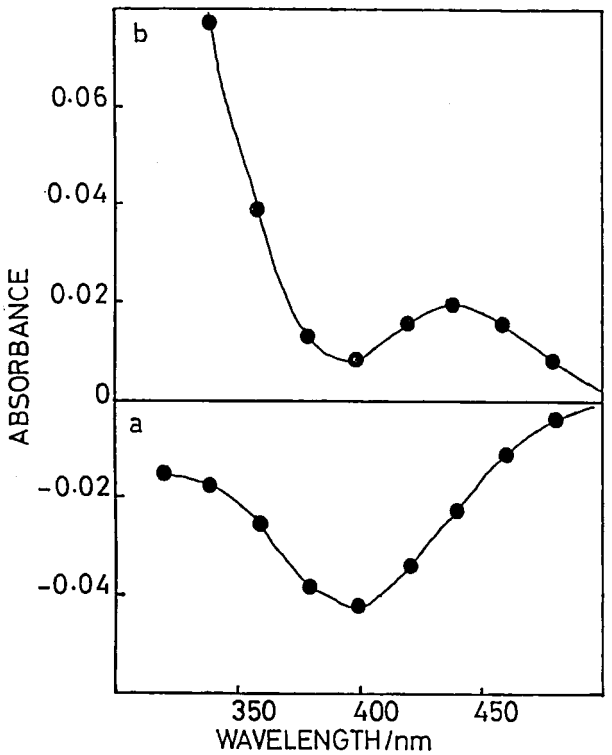

Figure 1. (a) Difference spectra (reduced minus oxdized states). (b) Difference spectra (oxdized minus reduced states). Initial concentrations: $[phenol]_0$=[0.002 M], $[BrO_3^-]_0$=0.025 M, $[H_2SO_4]_0$=1.0 M and temperature = 25°C.

Asymmerical Coupling of Chemical Oscillators

Minoru YOSHIMOTO *(Nagoya Univ.)*, **Kenichi YOSHIKAWA** *(Nagoya Univ.)*, **Yoshihito MORI, and Ichiro HANAZAKI**

Synchronization of coupled nonlinear chemical oscillators has so far been studied with reactors coupled by holes or semipermeable membranes to reveal various modes of synchronization. All these experiments have been done for the symmetrical coupling (coupling among equivalent reactors). In this report, we focused on *asymmetrical* coupling, i.e., coupling between nonequivalent reactors. Two reactors are coupled with mass transfer by a pump to observe modes of synchronization as a function of the rate of mass transfer. This experimental setup is capable of varying continuously the rate of mass transfer between two reactors, fascillitating the determination of the range of mass-transfer rate in which each mode of synchronization realizes.

In both symmetrically and asymmetrically coupled reactors, we have observed three modes of synchronization by varying the rate of mass transfer; namely, quasi in-phase (Figure 1a), out-of-phase (Figure 1b) and in-phase (Figure 1c). It was found that the out-of-phase coupling occurred in a wider range of mass-transfer rate in the asymmetrically coupled system than in the symmetrically coupled one.

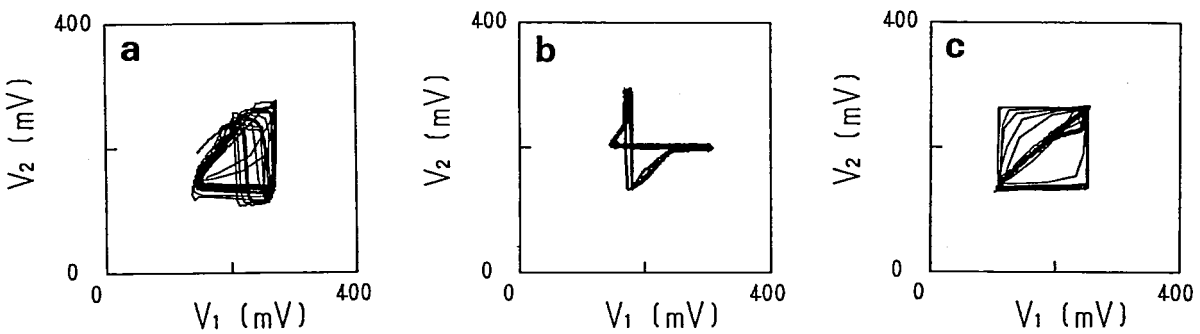

Figure 1. Synchronization of coupled oscillators. Redox potential of reactor 1 is plotted against that of reactor 2. (a) quasi in-phase, (b) out-of-phase, (c) in-phase

Enhancement of Water Shell Stabilities and Stackings of Hydrophobic Substances in Aqueous Environment

Nobuyuki NISHI

Mass spectrometric analyses of liquid fragments in the form of molecular clusters made it possible to study the nature of solute-solute association and solute-solvent interaction in aqueous environments. Despite of its original meaning, "hydrophobic" groups show a property that breaks its original meaning; this is sometimes termed "hydrophobic hydration", for entropically unfavorable solution of apolar residues of amphiphilic molecules in water. Cluster mass spectra of the aqueous solutions of $CH_3(-CH_2-)_mOH$ (m=0~5), their isomers, phenol, cyclohexanol, $CH_3(-CH_2-)_nOH$ (n=0~3), and $HO(-CH_2-)_{n(=2,5)}OH$ were measured up to m/Z=1300. Linear chain alkyl alcohols or alkyl carboxylic acids exhibited dramatic enhancement of hydration networks around alkyl groups, while the displacement of the end methyl group of n-hexanol by another hy-

droxy group (yielding $HOCH_2CH_2CH_2CH_2OH$) had comperably less stable hydration shells in spite of the introduction of a strong hydrophilic character. With increasing size of hydrophobic groups, the alcohols or carboxylic acids developed a tendency to stack the hydrophobic groups with diret contact(s) in the water shells. This tendency was also found to be related to the size of the contact area of the hydrophobic groups. Even in $10^{-2} \sim 10^{-3}$ mol/mol solutions, many of hydrocarbon molecules with one hydrophilic group were found to form "micro-micelles" with higher order hydration and stacking structures.

Carbon Dioxide Fixation Catalyzed by Homogeneous Catalysts

Koji TANAKA, Hirotaka NAGAO, Hiroaki TANAKA, Hide KAMIBAYASHI, and Nobutoshi KOMEDA *(Osaka Univ.)*

Selective reduction of CO_2 to either CO or HCOOH is achieved by taking advantage of a reversible interconversion between CO_2 and CO ligated on ruthenium metal complexes. Carbon dioxide fixation to organic molecules accompanied by carbon-carbon bond formation, however, is much more important than reduction of CO_2 affording CO and/or HCOOH from the viewpoint of utilization of CO_2 as a C_1 building block. Biological CO_2 fixation is always accompanied by carbon-carbon bond formation. For example, four molecules of CO_2 are fixed in one turn of reductive carboxylic acid cycle by photosynthetic bacteria in the presence of reduced ferredoxins (iron-sulfur proteins) generated photochemically; two of them are fixed to the β-carbons of carbonoyl groups of organic molecules to form β-keto acids, and the other two molecules of CO_2 are introduced to carbonyl carbons to afford α-keto acids, which is further converted to amino acids. We have been studying CO_2 fixation as a model reaction of photosynthetic bacteria, and succeeded in a catalytic formation of α- and β-keto acids by artificial CO_2 fixation using FeS and MoFeS clusters. So, we are now investigating not only the mechanism of those artificial CO_2 fixation directed toward the elucidation of the mechanism of biological CO_2 fixation but also a new tupe of CO_2 fixation by using ruthenium complexes.

Solvation Structure and Properties of Ions in Supercritical Water

Hitoshi OHTAKI, Yusuke TAMURA, Atsushi YAGASAKI, Georg JOHANSSON *(Royal Inst. Technol., Sweden and IMS)*, **and Toshio YAMAGUCHI** *(Fukuoka Univ. and IMS)*

An X-ray diffractometer with a beryllium cell, which can be used under high pressure ($<$ 8000 atm.) and high temperature ($<$ 400°C) where water becomes a supercritical fluid, has been constructed and tested. There are some points to be improved to obtain reliable data. The apparatus constructed is shown in Fig. 1. As the first investigation pure water under supercritical conditions will be done to study the temperature and pressure effects on the water structure.

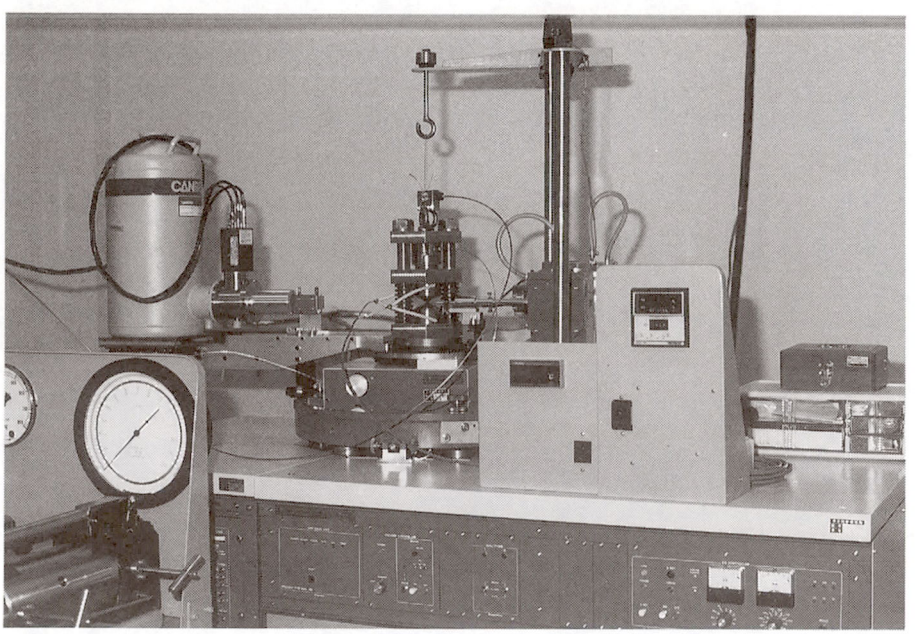

Figure 1. Solution X-ray diffractometer for supercritical fluids.

OKAZAKI CONFERENCES

"Okazaki Conferences" are principal symposia at IMS, which are held on the subjects related to the "Special Research Projects". They are held two or three times a year, with a moderate number of participants around 50, including several invited foreign speakers. The formal language for the conference in English. Outlines of the thirty-eighth, thirty-ninth, and fortieth conferences are as follows.

The Thirty-eighth Okazaki Conference

Structures and Dynamic Aspects of Metal Complexes in Biological Systems
(October 16-18, 1990)

Organizers: O. YAMAUCHI *(Nagoya Univ.)*, **I. MORISHIMA** *(Kyoto Univ.)*, **and T. KITAGAWA** *(IMS)*
Invited Speakers: R.J.P. WILLIAMS *(Univ. of Oxford)*, **T.M. LOEHR** *(Oregon Grad. Inst. of Sci. and Tech.)*, **G.H. NANCOLLAS** *(State Univ. of New York, Buffalo)*, **I. BERTINI** *(Univ. of Florence)*, **H. SIGEL** *(Univ. of Basel)*, **T.V. O'HALLORAN** *(Northwestern Univ.)*

Metal complexes in biological systems have a stationary structure specific to their physiological functions. However, dynamical features of a structure are requisite for the proteins to carry out their functions. In their active sites, the metal ions interact with proteins or nucleic acids in one hand and with substrates or oxygen on the other, catalyzing the electron transfer or the migration of chemical groups. Such biosystems involving metal ions would provide new themes for material science. Accordingly, the conference was organized so that metallochemists, physical chemists, organic chemists, biochemists, and biophysicists could discuss together the following three topics;

1) Interactions between metal ions and biomolecules,
2) Active site structure and reaction mechanism of metalloenzymes, and their chemical modelling,
3) Electronic process of biosystem.

The conference consisted of 24 invited talks and 13 poster presentations. Registered participants were 64 from outside and 39 from inside of IMS.

The Thirty-ninth Okazaki Conference

Development of Molecular Functions and Control of Assembly Structures Toward Molecular Devices *(October 24-27, 1990)*

Organizers: T. SHIMIDZU *(Kyoto Univ.)*, **T. KOBAYASHI** *(Tokyo Univ.)*, **and Y. MARUYAMA** *(IMS)*
Invited Speakers: J. SIMON *(ESPCI-CNRS)*, **J.L. BREDAS** *(Univ. Mons)*, **C. FLYTZANIS** *(Ecole Polytech.)*, **and L.E. BRUS** *(AT & T Bell)*

We planned to have an overview of present and future status of "Molecular Devices" through the discussion on the following three points.

1. Highly functional conducting macromolecular materials: The studies of functional Macromolecular Materials based on conducting polymers are one of the most direct approach to the actual construction of molecular devices. One example of this type approach is to embed or attach functional device element to have the corresponding functions. This is also directly related to the development of highly functionalized conducting polymers.
2. Nonlinear optical materials and phenomena: Nonlinearity is a key factor for advanced materials, and in this conference the discussion was focused to the basic physical properties and the corresponding device characteristics, such as photo-ferroelectricity or ultrafast photo-response, of nonlinear optical organic materials including polymers.
3. Control of assembly structure − thin films: Organization or systematization of molecular arrangements is required to realize the device or assembly functions based on the individual molecular functions. In this respect, the discussion will be focused to the fabrication, characterization and property measurement of organic thin-films. LB-films and vacuum-deposition-films were main interest, and the probles in organization and control of the structure and the mechanisms of their exotic properties were discussed.

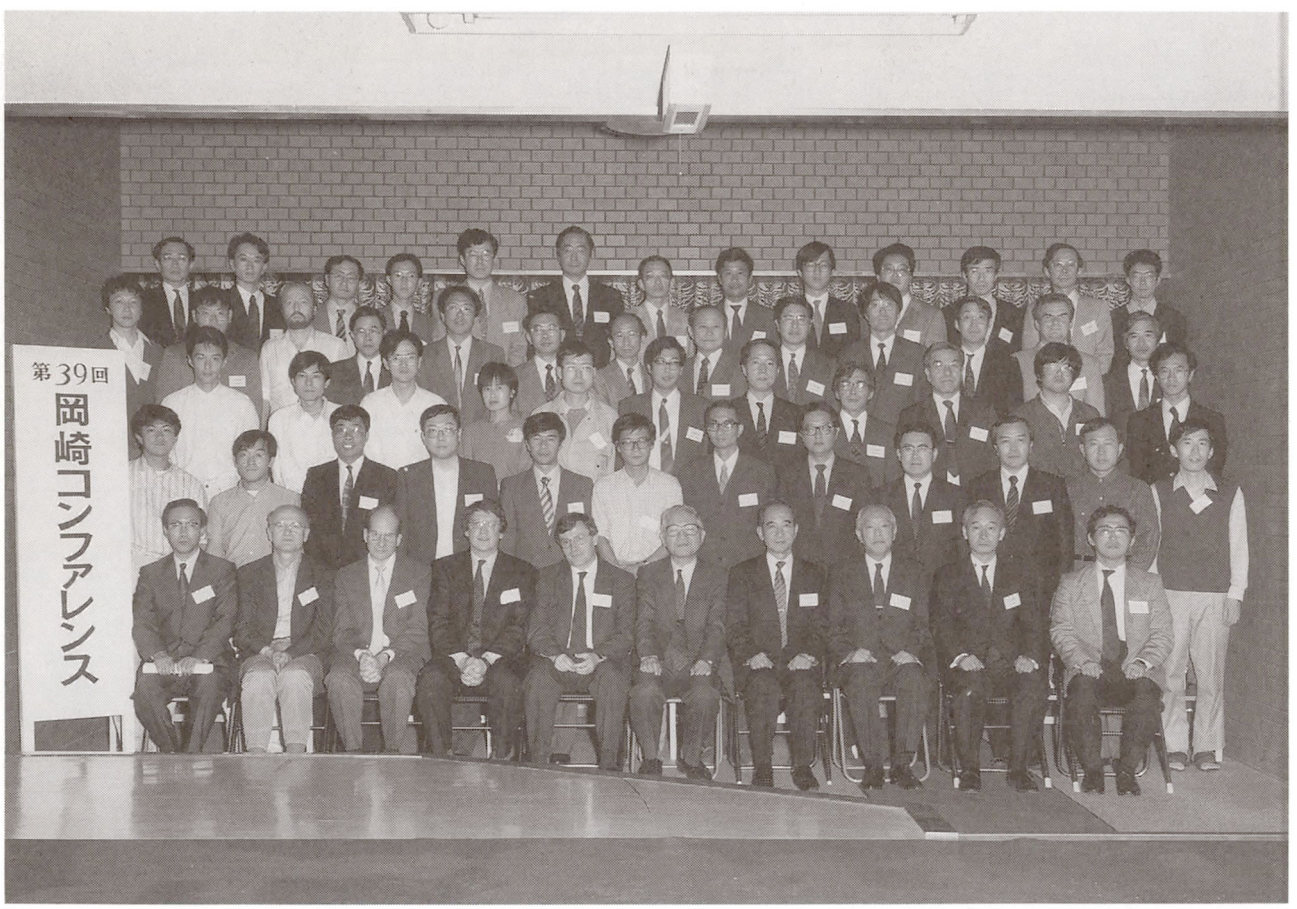

The Fortieth Okazaki Conference

Non-linear Chemical Reaction and Self-organization *(January 23-25, 1991)*

Organizers: I. HANAZAKI *(IMS)*, **K. YOSHIKAWA** *(Nagoya Univ.)*, **K. KITAHARA** *(Tokyo Inst. Tech.)*, **and H. NAKAMURA** *(Nagoya Univ.)*
Invited Spepakers: A. ZHABOTINSKII *(Natl. Sci. Centre of Hematology, USSR)*, **J.P. LAPLANTE** *(Royal Millit. Coll., Canada)*, **I.R. EPSTEIN** *(Brandeis Univ., USA)*, **K. SHOWALTER** *(W. Virginia Univ., USA)*, **R. LARTER** *(Purdue Univ., USA)*, **R.H. HARDING** *(W.R. Grace & Co., USA)*, **and G.J.D. DEWEL** *(Univ. Libre Bruxelles, Belgium)*

This conference was proposed for discussing the nature of non-linear chemical reactions and various kind of self-organizing phenomena (temporal oscillations and spatial pattern formations). The phenomenon manifests itself in a wide variety of human and natural science such as chemistry, physics, biology, ecology, and social sciences, being the basis of time evolution and structure of organizations in nature and human societies. We have intended in this conference to have a chance for the scientists in various fields altogether to discuss what kind of problems are existing and what is common in various fields of science. We believe it was successful with foreign scientists listed above together with informal attendants, **J. GORECK** *(Inst. Phys. Chem., Poland)*, **M. MOREAU** *(Univ. Pierre & Marie Curie, France)* and **M.I. TRIBELSKY** *(Landau Inst. Theor. Phys., USSR)*, and more than 50 domestic attendants.

JOINT STUDIES PROGRAMS

As one of the important functions of an inter-university research institution, IMS undertakes joint studies programs for which funds are available to cover research expenses as well as travel and living expenses of individuals. The proposals from domestic scientists are reviewed and controlled by the inter-university commitee. The programs are carried out under one of five catagories:

1) Joint Studies on special projects (a special project of significant relevance to the advancement of molecular science can be carried out by a team of several groups of scientists).
2) Research Symposia (on timely topics in collaboration with both outside and IMS scientists).
3) Cooperative Research (carried out in collaboration with both outside and IMS scientists).
4) Use of Facility (the Computer Center, Instrument Center and other research facilities at IMS are open to all researchers throughout the country).
5) Joint studies programs using UVSOR facilities.
   a) Special Project, b) Cooperative Research, c) Use of UVSOR Facility.
   In the fiscal year 1990, numbers of joint studies programs accepted amounted to 2, 10, 112, and 287 for categories 1)-4), respectively 3, 28 and 105 for 5a)-5c), respectively.

1) Special Projects

Static and Dynamic Solvent Effects in Elementary Reactions

Coordinators: **Okitsugu KAJIMOTO** *(Kyoto Univ.)*, **Tadamasa SHIDA** *(Kyoto Univ.)*, **Hisanori SHINOHARA** *(Mie Univ.)*, **Masaru NAKAHARA** *(Kyoto Univ.)*, **and Keitaro YOSHIHARA, Nobuyuki NISHI**

This research project aims at the molecular-level understanding of both static and dynamic solvent effects by means of recently developed techniques such as molecular beam, supercritical solution and pico-second Raman spectroscopy.

1. Solvent Dynamics Studied by Pico-second Raman Spectroscopy

In order to infer the dynamics of solvent molecules immediately after the excitation of reactant molecules (or the start of reaction), the time-dependence of the spectral shfit in their electronic transitions has been measured with pico-second time resolution. However, such kind of approach gives no information about the actual motion of solvent molecules around a reactant molecule. For more specific and local information, time-dependent Raman spectroscopy is much favorable because spectral shfit in vibrational transitions could reflect the specific interaction between solvent molecules and a given vibrational mode of the reactant molecule.

An output of a mode-locked YAG − dye laser system was amplified using a two stage amplifier pumped by a Cu vapor laser. The frequency-doubled photons were used for exciting reactant molecules while the photons of fundamental frequency were utilized for the resonance Raman spec-

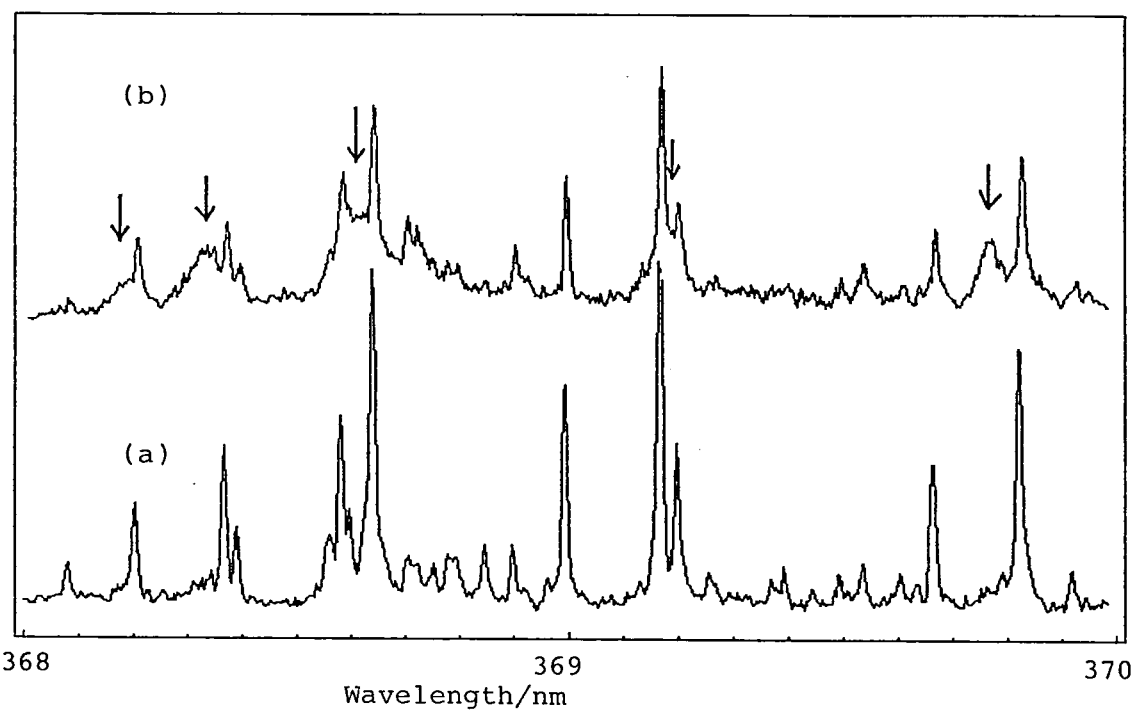

Figure 1. The LIF excitation spectra of AA and AA-H_2O complexes. (a) AA only, (b) AA and AA-H_2O (The peaks of AA-H_2O are indicated by ↓).

troscopy. The solvent dynamics following the photoionization of tetramethylphenylendiamine (TMPD) was the first target of this experiment. Although the Raman spectra with ps time resolution is not yet obtained due to the problem in the Cu vapor laser, the Raman spectra of TMPD cation was observed using ns pulsed laser.

2. Pico-second Dynamics of the CT State Formation in van der Walls Clusters with Specific Number of Solvent Molecules

9-Anthrylaniline (AA) was synthesized for the first time and the clusters including AA and solvent molecules were formed in a free jet. Figure 1 exhibits a part of the LIF spectra showing the peaks of bare AA and its van der Walls complex with water. We are now observing the emission spectra of the various complexes of AA and measuring their lifetimes in order to clarify the nature of the excited state of these complexes.

3. Solvent Effects in Photo-induced Ion-molecule Reactions

Cationic clusters between benzene and ethylene molecules were found to be formed on γ-ray irradiation in the freon matrix at 77 K. Subsequent photo-irradiation of the clusters gave the octatetraene cations in various isomeric form. The photo-induced ionic reaction is quite sensitive to the environment.

We are further planning to form 1:1 benzene-ethylene van der Waals clusters in a free jet and to investigate the fate of the cluster cations to be formed by photo-ionization. From the comparison between the features observed in the matrix and in the free jet, we try to clarify the microscopic mechanism of the environmental effect.

References

1) K. Honma, K. Arita, K. Yamasaki and O. Kajimoto, *J. Chem. Phys.*, **94**, 3496 (1991).
2) O. Kajimoto, S. Hayasmi and H. Shizuka, *Chem. Phys. Lett.*, **177**, 219 (1991).
3) Y. Fujisaka, M. Makino, J. Takahashi, T. Shida, K. Roth, R. Straut and T. Bally, *J. Phys. Chem.*, to be submitted.
4) T. Shida, *Ann. Rev. Phys. Chem.*, **42**, 55 (1991).

Studies on Photo-responsive Chemical Oscillators

Coordinators: **Kenichi YOSHIKAWA** *(Nagoya Univ.)*, **Ichiro HANAZAKI** *(IMS)*, **Kazuo KITAHARA** *(Tokyo Inst. Tech.)*, **Takeko MATSUMURA** *(Nara Educ. Univ.)*, **Hiroyuki NAGASHIMA** *(Shizuoka Univ.)*, **Tetsuo UEDA** *(Hokkaido Univ.)*, **and Hidetoshi MIIKE** *(Yamaguchi Univ.)*

In nonlinear open systems, checmial reaction sometimes shows an oscillating time evolution as well as a spatial pattern formation, which are due to the system's intrinsic nonlinearity. They have also been interested for their close relation to the biological phenomena. We have measured the action spectra for the photo-inhibiton and -induction of chemical oscillation to identify the initial process responsible for the effect. Interaction of chemical oscillators has also been studied to determine the phase relation between two chemical oscillators connected by a pumped flow. Spatial pattern formation in chemical oscillators have been studied useing an artificial pacemaker to control the pattern formation and explained by a numerical analysis. An equipment for the 3-dimensional pattern analysis is being developed as well as the theoretical study of the relation between elementary reaction process and the macroscopic diffusion-reaction treatments. Oscillation in physarum polycephalum has also been studied and analyzed in view of the highly organized collection of chemical oscillators.

2) Research symposia

1. Organic Molecules in Action. Analysis and Functional Design in Organic Chemistry
   (November 30th-December 1st, 1990)
   Organizer: E. Nakamura (Tokyo Inst. of Technology)
2. Interaction of Ultrafine Particles with Light
   (January 1st, 1991)
   Organizer: K. Kimura (IMS)
3. Design Concepts of Molecular Systems
   (January 28th-30th, 1991)
   Organizer: M. Kotani (Gakushuin Univ.)
4. Structures and Properties of Cytochromes
   (February 2nd, 1991)
   Organizer: H. Inokuchi (IMS)
5. Chemistry and Physics on Phthalocyanine
   (February 14th, 1991)
   Organizer: Y. Maruyama (IMS)
6. Molecular Science of Cytochrome Oxidase
   (February 21st, 1991)
   Organizer: T. Ogura (IMS)
7. Theoretical Chemistry Meeting for Young Molecular Scientists
   (May 7th, 1991)
   Organizer: M. Baba (Kyoto Univ.)
8. Mini Symposium on "Nonlinear Optical Materials"
   (June 1st, 1991)
   Organizer: H. Yakushi (IMS)
9. Application of Raman Spectroscopy to Investigations of Excited States
   (June 10th, 1991)
   Organizer: T. Kitagawa (IMS)
10. Conference for the Development of "IMS Machines" — Newest Trends of Technology
    (June 29th, 1991)
    Organizer: S. Asaka (IMS)
11. Possible New Development of Molecular Science by the New Particles Involving Antiproton
    (July 30th, 1991)
    Organizer: H. Nakamura (IMS)

3) Cooperative Research

This is one of the most important programs IMS undertakes for conducting its own research of the common interest to both outside and IMS scientists by using the facilities at IMS. During the first half of fiscal year of 1990 ending on September 30, 53 outside scientists including 1 invited collaborated with IMS scientists; and during the second half

of the fiscal year, 59 outside scientists and 2 invited scientists worked in collaboration with IMS scientists, the names and the affiliations of these collaborators are found in the Research Activities.

4) Use of Facility

The number of projects accepted for the Use of Facility Program of the Computer Center during the fiscal year of 1990 amounted to 210 (594 users) and the computer time spent for these projects is 7920 hours (converted to the HITAC M-680H time), and amounted to 58% of the total annual CPU time used.

Sixty seven projects (121 users) were accepted for the Use of Facility Program of the Instrument Center during the fiscal year of 1990.

5) UVSOR

In the UVSOR Facility with the 750 MeV electron storage ring, there are nineteen beam lines available for synchrotron radiation research (see "Activity Report", *UVSOR*, 1991), including four new beam lines and one beam line which belongs to the Institute of Nuclear Fusion Science. Under the following programs, a number of SR studies have been carried out by many users outside and inside IMS: a) the UVSOR Special Projects, b) the UVSOR Cooperative Research Projects, c) the UVSOR Invited Research Projects, and d) the Use-of-UVSOR Projects. Furthermore, the 11th UVSOR User's Symposium was held at Okazaki during the period November 30 — December 1, 1990.

5-a) UVSOR Special Project

Development of the Infrared and Far-infrared Spectroscopy Using Synchrotron Radiation

Coordinators: **Kyuya YAKUSHI, Akito UGAWA, Hideshi ISHII*, Tadaoki MITANI, Hiroshi OKAMOTO, Takao NANBA**, Makoto WATANABE, and Kusuo SAKAI** *(*Univ. of Tokyo, **Kobe Univ.)*

Application of Synchrotron Radiation (SR) for infrared spectroscopy has been performed at the beamline BL-6A1 of the UVSOR facility in IMS. We are planning and conducting three projects for the use of infrared region of SR using the characteristic natures of SR such as a high collimation, high brilliance, wide-range tunability, and pico-second pulse width. (1) These natures are the ideal properties as the light source of a microspecrophotometric apparatus. We have designed a microspectrophotometer to measure optical reflectivity of a small (~ 20 μm) single crystal in the wide range of 50 cm^{-1} — 13000 cm^{-1} (see IV-D-1). This apparatus will be mainly used for the study of organic conductors and superconductors. (2) Delay-time modulation spectrometer has been designed and constructed using the pico-second light pulse of SR synchronized with a cw mode-locked Nd-YAG lasser. This method has been be applied to the transient photo-induced absorption measurement in the infrared region. This spectrometer is combined with FT-IR to increase the sensitivity. (3) The future plan is the grazing-angle infrared spectroscopy for the surface absorbed molecules. This optical system uses also the high collimation and high brilliance of SR.

Photoionization Spectroscopy of Molecular Mixed Clusters in Supersonic Jets.

Coordinator: **Katsumi KIMURA**

In this project, we attempted to further apply our molecular-beam photoionization technique to jet-cooled atomic and molecular clusters including rare-gas-atom clusters as well as hydrogen-bonded water mixed clusters, by using the molecular beam photoionization apparatus on beam line BL2B2 [K. Kimura *et al.*, Rev. Sci. Instrum. 60, 2205 (1989)]. This apparatus contains a threshold-photoelectron photoion coincidence (TPEPICO) spectrometer which collect threshold photoelectrons as a function of wavelength through a capillary array by angular and TOF electron discrimination. With this beam line, we have obtained TPEPICO spectra of argon van der Waals molecules, and estimated the average kinetic energies of Ar_2^+ which are produced by dissociation from Ar_3^+. So far, we have also studied van der Waals molecules formed between Ar and molecular oxygen and several kinds of water mixed clusters with other molecular species.

Studies of Dissociation Processes in Inner-shell and Multiple Ionized Molecular Ions

Coordinator: **Inosuke KOYANO** *(Himeji Institute of Technology)*

The objective of this three-year project is to udnerstand the dissociation mechanisms of molecules following the inner-shell and multiple (double and triple) photoionization in the vacuum ultraviolet, the multiple photoionization including both the direct type and via-Auger type processes. For this purpose the apparatus on beamline 3A2[1] is utilized to obtain angle-resolved TOF mass and PIPICO spectra of ionic products of dissociation in the wavelength range 30—140 eV. The project is successfully in progress owing to the tremendous efforts of the members of the project, notably Drs. T. Masuoka, S. Nagaoka, T. Imamura, and T. Ibuki. Two scientists from abroad, C.E. Brion and B.H. Boo, have also contributed to the project.

This year, which is the second year of the project, emphasis has been placed on the following three subjects.

(i) Comparison between the valence and inner-shell ionization. Difference between the fragmentation patterns following valence and inner-shell ionization has carefully been examined in, for example, SiF_4, and the new dissociation channels F^++SiF_2^{2+}, F^++SiF^{2+}, and F^++Si^{2+} have been found to occur, in addition to the dominant process F^++SiF^{2+}, when the Si:2p electrons are ionized.[2].

(ii) Angular distribution of fragment-ion pairs originating from direct double photoionization of valence elecrons. This is most conspicuously manifested in the angular dependence of the spectral profiles of PIPICO peaks and thus could successfully been measured for the first time with our apparatus. From the analysis of such spectral profiles

measured at θ=0° and 90°, where θ is the angle from the direction of polarization (electric vector) of the incident photon, interesting results have been obtained for OCS.[3].

(iii) Search for site-specific dissociation. Search has been made for site-specific decomposition processes, which are important in the synchrotron-radiation-assisted CVD and material synthesis, using some organometallic compounds. Although definite site-specificity has not been recognized in these wavelength regions, interesting fragmentation patterns have been observed in $Al_2(CH_3)_3Cl_3$[4] and $Si_2(CH_3)_3Cl_3$[5], following the Al:2p and Si:2p inner-shell ionization, respectively.

References

1) T. Masuoka, T. Horigome, and I. Koyano, *Rev. Sci. Instrum.* **60**, 2179 (1989).
2) T. Imamura, C.E. Brion, I. Koyano, T. Ibuki, and T. Masuoka, *J. Chem. Phys.* **94**, 4936 (1991).
3) T. Masuoka, I. Koyano, and N. Saito, *Phys. Rev. A* **42**, in press (1991).
4) S. Nagaoka, I. Koyano, T. Imamura, and T. Masuoka, *Appl. Organometall. Chem.* **5**, in press (1991).
5) S. Nagaoka, J. Ohshita, M. Ishikawa, T. Masuoka, and I. Koyano, to be published.

5-b) UVSOR Cooperative Research Projects

Under this joint-study program, many synchrotron radiation experiments have been carried out with the beam lines of in-house staff in cooperation with scientists who were invited from other institutions. The total number of the projects in this category was 28 in the fiscal year of 1990.

5-c) The UVSOR Invited Research Projects

Under this joint-study program, several scientists were invited from other institutions to help for construction of new beam lines and improvement of the UVSOR storage ring and others. The total number of the projects in this category was 4 in the fiscal year of 1990.

5-d) The Use-of-UVSOR Projects

Ten out of the total of nineteen UVSOR beam lines are available for general users outside and inside IMS for their synchrotron radiation studies in the field of molecular science. The total number of the projects in this category was 105 in the fiscal year of 1990.

FOREIGN SCHOLARS

Vistors from abroad play an important role in research activities and are always welcome at IMS. The following is the list of foreign scientists who visited IMS in the past year (Aug. 1990 — July 1991). The sign *[1] indicates an attendant to an Okazaki Conference, *[2] an IMS or Japan Society for the Promotion of Science Invited Foreign Scholar, *[3] an IMS councillor, *[4] an IMS visiting scientist*[5] an IMS adjunct professor or associate professor from abroad (period of stay is from 9 to 12 months). Scientists who wish to visit IMS under programs 2 and 5 are invited to make contact with an IMS faculty in a related field.

Dr. P. Lablanquie*[4]	Centre Univ. Paris-Sud	(France)	Apr. 1990 - Oct. 1991
Prof. Kee Hag Lee*[2]	Won Kwang Univ.	(Korea)	Jun. - Aug. 1990, Jun. 1990 -
Dr. A. Douhal *[2], *[4]	Kadi Ayad Univ.	(Morocco)	Jun 1990 -
Prof. Nam-Soo Lee	Chungbuk Natl. Univ.	(Korea)	- Aug. 1990
Prof. M.H. Palmer	Univ. of Edingburgh	(UK)	Aug. 1990
Prof. Ding Fu-Jiang*[2]	Chengdu Inst. of Organic Chem. Chinese Acad. of Sci.	(China)	Aug. 1990
Dr. Jing-Nan Liu*[4]	Fudan Univ.	(China)	Aug. 1990 - Apr. 1991
Prof. V. Kubecek*[2]	Tech. Univ. of Prague	(Czechoslovakia)	Aug. 1990 - Aug. 1991
Prof. Tseng. Poh-Kun*[4]	Natl. Taiwan Univ.	(Taiwan)	Sep. 1990, Jun. 1991
Mr. Hsu, Shen Nung	Synchrotron Radiation Research Center	(Taiwan)	Sep. 1990
Prof. June-Rong Chen	Synchrotron Radiation Research Center	(Taiwan)	Sep. 1990
Dr. M. LeDourneuf*[2]	Observatory of Paris	(France)	Sep. 1990
Dr. J.-P. Pique	CNRS	(France)	Sep. 1990
Prof. C.B. Moore	Univ. of California, Berkeley	(USA)	Sep. 1990
Prof. R.W. Hay*[2]	Univ. of St. Andrews	(UK)	Sep. 1990
Prof. J.C. Fuggle	Res. Inst. for Materials, Univ. of Nijmegen	(The Netherlands)	Sep. 1990
Dr. K. Zachariasse	Max-Planck Inst.	(Germany)	Sep. 1990
Ms. T.C. Kavanaugh*[4]	Massachusetts Inst. of Tech.	(USA)	- Sep. 1990
Dr. A. Labeque	LURE	(France)	Oct. 1990
Dr. A. Flamini*[2]	CNR	(Italy)	Oct. 1990
Prof. A. Magneli	Univ. of Stockholm	(Sweden)	Oct. 1990
Mr. Zongrong Xu	Chengdu Univ. of Sci. & Tech.	(China)	Oct. 1990 - Jan. 1991
Dr. R. Bhattacharjee*[2]	St. Edmund's Coll.	(India)	Oct. 1990 - Mar. 1991
Dr. Chaoyuan Zhu	Inst. of Nuclear Phys., Acad. Sinica, Shanghai	(China)	Oct. 1990 -
Dr. N.C. Handy	Unv. of Cambridge	(UK)	Nov. 1990
Dr. A.J. Bell*[2]	Southampton Univ.	(UK)	Nov. 1990 - Nov. 1991
Prof. Yuan T. Lee	Univ. of California, Berkeley	(USA)	Nov. 1990
Mr. M. Fogliani	Univ. of Pavia	(Italy)	Nov. 1990
Prof. J.C. Polanyi	Univ. of Toronto	(Canada)	Nov. 1990
Prof. Zheng Huang*[2]	Shanghai Jiao Tong Univ.	(China)	Nov. 1990 - Apr. 1991
De. Bongsoo Kim*[4]	Univ. of California, Berkeley	(USA)	Nov. 1990 -
Mr. M. Dupui	IBM Corp., Kingston Lab.	(USA)	Dec. 1990
Prof. A.Vazquz*[2]	Univ. of Alcala de Henares	(Spain)	- Dec. 1990
Prof. Y. Do*[2]	KAIST	(Korea)	Dec. 1990 - Feb. 1991
Dr. A.A. Zakhidov*[5]	USSR Acad. of Sci.	(USSR)	Dec. 1991 -
Prof. K.-P. Huber	Natl. Res. Council	(Canada)	Jan. 1991
Prof. E.I. Rashba	Landau Inst.	(USSR)	Jan. 1991
Prof. J. Sighn	North-Tersitony Univ.	(Austraria)	Jan. 1991
Dr. T.J. Gammel	Bayreuth Univ.	(Germany)	Jan. 1991
Prof. S.K. Song	Ottawa Univ.	(Canada)	Jan. 1991
Prof. B.H. Boo*[2]	Chungnam Natl. Univ.	(Korea)	Jan., Jul. 1991
Prof. K.A. Burkov	Leningrad State Univ.	(USSR)	Jan. - Jul. 1991
Dr. M.C.R. Cockett	Univ. of Southampton	(UK)	Jan. 1991 -
Dr. Zhan Mingsheng	Anhui Inst. of Optics & Fine Mechanics, Acad. Sinica	(China)	Feb. 1991
Prof. Zhou Shikang	Laser Spectroscopy Lab. Chinese Acad. of Sci.	(China)	Feb. 1991
Prof. M. Wikstrom	Univ. of Helsinki	(Finland)	Feb. 1991

Prof. M. Brunori	Univ. of Rome 'La Sapienza'	(Italy)	Feb. 1991
Dr. J.J. Ewing	Spectra Tech.	(USA)	Feb. 1991
Dr. N.A. Vinokurov*[2]	Inst. of Nuclear Phys.	(USSR)	Feb. 1991
Prof. V.P. Skulachev	Moscow State Univ.	(USSR)	Feb. 1991
Prof. V.G. Stankevitch	I.V. Kurchatov Inst. of Atomic Energy	(USSR)	Feb. - Mar. 1991
Dr. J. Moc*[2]	Univ. of Wroclaw	(Ploand)	Feb. 1991 -
Dr. R.A. Rooth	N.V. KEMA	(The Netherlands)	Mar. 1991
Prof. R.L. Whetten	Univ. of California	(USA)	Mar. 1991
Prof. I.V. Hertel	Univ. Freiburg	(Germany)	Mar. 1991
Prof. P. Day*[2]	Univ. of Oxford	(UK)	Mar. 1991
Prof. J.D. Baldeschwieler	Calif. Inst. of Tech.	(USA)	Mar. 1991
Prof. V. Aquilanti	Univ. of Perugia	(Italy)	Mar. 1991
Prof. M. Baer*[2]	Soreq Nuclear Res. Center	(Israel)	Mar. - May 1991
Dr. J.L. Anchell*[2]	Univ. of Utah	(USA)	Mar. 1991 -
Dr. K. Kemnitz*[4]	ERATO	(Germany)	Mar. - Aug. 1991
Prof. K.-M. Zhao*[4]	Inner Mongolia Norm. Univ.	(China)	Mar. 1991 -
Prof. T.-W. Zhu*[4]	Inner Mongolia Norma. Univ.	(China)	Mar. 1991 -
Prof. B. Wang *[4]	Inner Mongolia Norm. Univ.	(China)	Mar. 1991 -
Dr. K.R. Bauchspiess	Photon Factory, Natl. Lab. for High Energy Phys.	(Japan)	Apr. 1991
Prof. G.G. Balint-Kurti*[2]	Univ. of Bristol	(UK)	Apr. 1991
Dr. D.V. O'Connor	Polytech. of Central London	(UK)	Apr. 1991
Prof. O.P. Charkin	Inst. for New Chem. Problems Acad. of Sci.	(USSR)	Apr. 1991
Prof. A.D. Bandrauk	Univ. of Sherbrooke	(Canada)	Apr. 1991
Prof. B.C. Eu	McGill Univ.	(Canada)	Apr. 1991
Prof. P.P. Pashinin	Inst. of General Phys., Acad. of Sci., USSR	(USSR)	Apr. 1991
Prof. B.B. Krynetsky	Inst. of General Phys., Acad. of Sci., USSR	(USSR)	Apr. 1991
Dr. Jingui Qin	Wuhan Univ.	(China)	Apr. 1991
Prof. Y. Zhenxin	Zhongshan Univ.	(China)	Apr. 1991
Prof. Xu, Chaoyin*[2]	Univ. of Sci. & Tech., Chi. (USTC)	(China)	Apr. - May 1991
Prof. J. Kincaid*[2]	Marquette Univ.	(USA)	Apr. - Jun. 1991
Dr. D.G. Musaev	Inst. of New Chem. Problems Acad. of Sci.	(USSR)	Apr. 1991 -
Prof. Xue-Kue Li*[4]	Inst. Theo. Chem., Jilin Univ.	(China)	Apr. 1991 -
Dr. D.H. Kerridge*[2]	Univ. of Southampton	(UK)	May 1991
Dr K. Tominaga	Univ. of Minnessota	(USA)	May 191
Prof. G.R. Flemig	Univ. of Chicago	(USA)	May 1991
Prof. S. Mukamel	Univ. of Rochester	(USA)	May 1991
Dr. J. Aaviksoo	Estonian Acad. of Sci.	(USSR)	May 1991
Dr. V.M. Agranovich	USSR Acad. of Sci.	(USSR)	May 1991
Dr. M.V. Alfimov	USSR Acad. of Sci.	(USSR)	May 1991
Dr. E.M. Dianov	USSR Acad. of Sci.	(USSR)	May 1991
Dr. E.L. Frankevich	USSR Acad. of Sci.	(USSR)	May 1991
Dr. G.V. Kozlov	USSR Acad. of Sci.	(USSR)	May 1991
Dr. T.A. Loskova	USSR Acad. of Sci.	(USSR)	May 1991
Dr. R.I. Personov	USSR Acad. of Sci.	(USSR)	May 1991
Dr. E.A. Vinogradov	USSR Acad. of Sci.	(USSR)	May 1991
Dr. V.S. Dneprovskii	Moscow State Univ.	(USSR)	May 1991
Prof. W. Rettig	Tech. Univ. Berlin	(Germany)	May 1991
Prof. J. McGarvey	Univ. of Belfast	(UK)	Jun. 1991
Prof. R.L. Christensen*[4]	Bowdoin Coll.	(USA)	Jun. 1991
Prof. C.S. Parmenter	Indiana Univ.	(Usa)	Jun. 1991
Prof. S. Schneider	Erlangen Univ.	(Germany)	Jun. 1991
Dr. V.V. Kvach	BSSR Acad. of Sci.	(USSR)	Jun. 1991
Prof. S. Han	Kangweon Natl Univ.	(Korea)	Jun. 1991
Dr. M. Stockburger	MPI, Gottingen	(Germany)	Jun. 1991
Dr. V. Kamalov	The inst. of Chem. Phys. Acad. of Sci., USSR	(USSR)	Jun. 1991

Prof. T. Gustafson	Ohio State Univ.	(USA)	Jun. 1991
Dr. T. Brack	Univ. of Arizona	(USA)	Jun. 1991
Prof. K.-J. Paeng*4	Yonsei Univ.	(Korea)	Jun. 1991
Prof. Pong, Way-Faung*4	Tamkang Univ.	(Taiwan)	Jun. 1991
Prof. J. Frederick*4	Univ. of Nevada	(USA)	Jun. - Jul. 1991
Prof. Sungyul Lee	Kyung Hee Univ.	(Korea)	Jan. - Mar., Jun. - Aug. 1991
Dr. D.-J. Jang*2	KSRI	(Korea)	Jun. 1991 -
Prof. M.C. Lin*2	Emory Univ.	(USA)	Jul. 1991
Prof. S.-K. Kim	Seoul Natl. Univ.	(Korea)	Jul. 1991
Prof. K.-H. Jung	KAIST	(Korea)	Jul. 1991
Prof. Sung-Ho Such Salk	Pohang Inst. of Tech.	(Korea)	Jul. 1991
Dr. Hong Ku Shim	KAIST	Korea)	Jul. 1991
Dr. P. Ruani	CNR Inst. of Mol. Spectroscopy	(Italy)	Jul. 1991
Prof. J.-S. Huang	Fujian Inst. Res. on Structure of Matter Chin. Acad. of Sci.	(China)	Jul. 1991
Prof. Z.-D. Chen	Fujian Inst. Res. on Structure of Matter Chin. Acad. of Sci.	(China)	Jul. 1991
Prof. J.-Q. Huang	Fuzhou Univ.	(China)	Jul. 1991
Prof. B.-S. Kang	Fujian Inst. Res. on Structure of Matter Chin. Acad. of Sci.	(China)	Jul. 1991
Prof. S.-F. Lu	Fujian Inst. Res. on Structure of Matter Chin. Acad. of Sci.	(China)	Jul. 1991
Mrs. Y.-F. Zhang	Fujian Inst. Res. on Structure of Matter Chin. Acad. of Sci.	(China)	Jul. 1991
Prof. S.-W. Lu	Dalian Inst. Chem. Phys. China. Acad. of Sci.	(China)	Jul. 1991
Prof. X.-Q. Xin	Nanjing Univ.	(China)	Jul. 1991
Prof. J.-Q. Xu	Jiling Univ.	(China)	Jul. 1991
Porf. Y.-Q. Yin	Lanzhou Inst. Chem. Phys. Chin. Acad. of Sci.	(China)	Jul. 1991
Prof. L.-S. Zheng	Xiamen Univ.	(China)	Jul. 1991
Mr. H.-S. Qiu	Chin. Acad. of Sci.	(China)	Jul. 1991
Prof. Xin Sun*5	Fudan Univ.	(China)	- Jul. 1991
Dr. N.J. Fitzpatrick*4	Univ. Coll. Dublin	(Ireland)	Jul. 1991 -
Dr. G.S. Lodha*4	Centre Advanced Tech., Indore	(India)	Jul. 1991 -
Prof. Shie-Ming Peng	Natl. Taiwan Univ.	(Taiwan)	Jul. 1991 -
Dr. P.K. Srivastava	Banaras Hindu Univ.	(India)	- Oct. 1991

AWARD

Mr. Hayasaka's Technical Contributions to Cryogenics

Mr. Keiichi Hayasaka, Technical Section Chief of Low-Temperature Center, received the Award of the Cryogenic Association of Japan for 1991 for his contribution to the development of the Association and the research in superconductivity cryogenics.

Mr. Hayasaka is one of the pioneer in cryogenics in Japan. He started his contribution to cryogenics since 1961 in the Institute for Solid State Physics, The University of Tokyo, and he was operating the first helium liquefier made in Japan in the Institute. He made great contribution to improve the machine and also helium gas recycling systems. He moved to the Institute for Molecular Science, Okazaki, and again he had developed a stable and efficient system for supplying liquid helium.

For all these contributions, the Cryogenics Association of Japan awarded him the special prize in May 1991.

LIST OF PUBLICATIONS

N. KOGA, T. OZAWA, and K. MOROKUMA, "Origin of Exo Selectivity in Norbornene. An Ab Initio MO Study.", *J. Phys. Org. Chem.* **3,** 519 (1990).

S. SAKAKI, N. KOGA, and K. MOROKUMA, "Ab Initio MO and SD-CI Study of Ni $(PH_3)_2(CO_2)$. Electron Correlation Effects on Geometry, Binding Energy, and Electronic Structure.", *Inorg. Chem.* **29,** 3110 (1990).

N. KOGA and K. MOROKUMA, "A Simple Scheme of Estimating Substitution or Substituent Effects in the Ab Initio MO Method Based on the Shift Operator.", *Chem. Phys. Lett.* **172,** 243 (1990).

S. YABUSHITA and K. MOROKUMA, "Ab Initio Potential Energy Surfaces for Rotational Excitation of CN Product in the A-Band Photodissociation of ICN.", *Chem. Phys. Lett.* **175,** 518 (1990).

N. KOGA and K. MOROKUMA, "Comparison of Biradical Formation between Enediyne and Eneyne-Allene. Ab Initio CASSCF and MRSDCI Study.", *J. Am. Chem. Soc.* **113,** 1907 (1991).

K. MOROKUMA and W.T. BORDEN, "Ab Initio Calculations on $(H_3P)_2Pt(C_2H_4)$. The Effect of Alkene Pyramidalization on Internal Rotation and Alkene Binding Energies", *J. Am. Chem. Soc.* **113,** 1912 (1991).

N. KOGA and K. MOROKUMA, "Structure of Dinuclear Complex $(Cp^*Rh)_2(CH_3)_2(\mu\text{-}CH_2)_2$ and CC Coupling Reaction of its Model Complexes. An Ab Initio MO Study.", *Organometallics* **10,** 946 (1991).

Y. AMATATU, S. YABUSHITA, and K. MOROKUMA, "Ab Initio Potential Energy Surfaces and Trajectory Studies of A-Band Photodissociation Dynamics: $CH_3I^* \rightarrow CH_3+I$ and CH_3+I^*.", *J. Chem. Phys.* **94,** 4858 (1991).

E. NAKAMURA, S. YAMAGO, S. EJIRI, A.E. DORIGO, and K. MOROKUMA, "Reversible Generation of Trimethylenemethanes by Mild Thermolysis of Dialkoxymethylenecyclopropanes.", *J. Am. Chem. Soc.* **113,** 3183 (1991).

K. KAMIYA and K. MOROKUMA, "Potential Energy Surface for Unimolecular Dissociation and Rearrangement Reactions of the Ground Electronic State of HFCO.", *J. Chem. Phys.* **94,** 7287 (1991).

I. OHMINE and H. TANAKA, "Potential Energy Surfaces for Water Dynamics II; Vibrational Mode Excitations, Mixing and Relaxations," *J. Chem. Phys.* **93,** 8138 (1990).

I. OHMINE and M. SASAI, "Relaxation, Fluctuation, Phase Transitions and Chemical Reactions in Liquid Water," *Prog. Theor. Phys. Supplement* **108,** 61 (1991).

I. OHMINE and H. TANAKA, "Dynamics of Liquid Water; Fluctuations and Collective Motions," in *"Molecular Dynamics Simulations"* ed. by F. YONEZAWA, Springer Verlag (1991).

I. OHMINE, "Fluctuation and Collective Motions in Liquid Water," *Buseikenkyu* **56,** 269 (1991) in Japanese.

A. OHSAKI and H. NAKAMURA, "Hyperspherical Coordinate Approach to Atom-Diatom Chemical Reactions in the Sudden and Adiabatic Approximations", *Physics Reports* **187,** 1 (1990).

H. SUN and H. NAKAMURA, "Theoretical Study of the Dissociative Recombination of NO^+ with Slow Electrons", *J. Chem. Phys.* **93,** 6491 (1990).

M. IWAI and R. D. LEVINE, "Anharmonic Collective Vibrational Modes in ABA Triatomic Molecules", *Phys. Rev.* **A42,** 3991 (1990).

K. SOMEDA and H. NAKAMURA, "Separation of Collisional and Vibrational Variables in Chemical Reactions: Decoupling Surface in Phase Space", *J. Chem. Phys.* **94,** 4260 (1991).

H. NAKAMURA, "What are the Basic Mechanisms of Electronic Transitions Molecular Dynamic Processes", *Intern. Reviews in Phys. Chem.* **10,** 123 (1991).

K. NASU, "Discontinuous Change of Superconducting Transition Temperature from BCS Type to Bipolaron Type in Strongly Coupled Electron-Phonon Systems." *Phys. Rev.* **B42,** 6076 (1990).

X. SUN, Z. SHUAI, R. FU, K. NASU, X. LI, D. LIN, and T. GEORGE, "The Spectrum of Third-order Non-linear Susceptibility of Trans-polyacetylene", *J. Phys. Condens. Matter* **2,** 9713 (1990).

K. NASU, "Theory for Many-Body Problems in Strongly Coupled Electron-Phonon Systems" ed. N. Tuda, Electron Conduction in Oxides (*Springer-Verlag,* Berlin, 1990) p.43.

S. NAGASAKA and K. NASU, "Dichotomization Process of Self-trapped Exciton into Asymmetric Electron-hole Pair", *Review of Solid State Science* **4,** 411 (1990).

S. YAMAMOTO, K. YAMAGUCHI, and K. NASU, "Ab initio MO Studies on Electron Correlation Effects in CuO_6 Cluster Relating to High-Tc Superconductivity", *Phys. Rev.* **B42,** 266 (1990).

A. FUJII and N. MORITA, "Detection of Nitrogen Atoms Produced by Predissociation of Superexcited Rydberg States of NO", *Chem. Phys. Lett.* **182,** 304 (1991).

N. MORITA and M. KUMAKURA "Laser Cooling of a Helium Atomic Beam", *Jpn. J. Appl. Phys.* **30,** L1678 (1991).

K. KAWAGUCHI, E. HIROTA, T. ISHIWATA, and I. TANAKA, "A Reinvestigation of the NO_3 1492 cm^{-1} Band", *J. Chem. Phys.* **93,** 951 (1990).

K. TANAKA, Y. AKIYAMA, T. TANAKA, C. YAMADA, and E. HIROTA, "Millimeter-wave Spectroscopy of the GeF^+ Ion", *Chem. Phys. Lett.* **171,** 175 (1990).

H. ITO, E. HIROTA, and K. KUCHITSU, "Laser-induced Fluorescence Spectroscopy of the $\tilde{A}^1A''$-$\tilde{X}^1A'$ Transition of HGeCl", *Chem. Phys. Lett.* **175,** 384 (1990).

K. KAWAGUCHI, K. KAJITA, K. TANAKA, and E. HIROTA, "Diode Laser Spectroscopy of the ν_3 (CN Stretch) Band of HC_3NH^+", *J. Mol. Spectrosc.* **144,** 451 (1990).

S. KODA, Y. ENDO, S. TSUCHIYA, and E. HIROTA, "Branching Ratios in O(^{3}P) Reactions of Terminal Olefins Studied by Kinetic Microwave Absorption Spectroscopy", *J. Phys. Chem.* **95,** 1241 (1991).

H. ITO, E. HIROTA, and K. KUCHITSU, "Laser-induced Fluorescence Spectroscopy of the $\tilde{A}^1A''$-$\tilde{X}^1A'$ Transition of HGeBr", *Chem. Phys. Lett.* **177,** 235 (1991).

T. SUZUKI, H. KANAMORI, and E. HIROTA, "Infrared Diode Laser Study of the 248 nm Photodissociation of CH_3I", *J. Chem. Phys.* **94,** 6607 (1991).

K. KAWAGUCHI, T. ISHIWATA, I. TANAKA, and E. HIROTA, "Fourier-transform Infrared Spectroscopy of the NO_3 Radical", *Chem. Phys. Lett.* **180,** 436 (1991).

Y. KAWASHIMA, C. YAMADA, and E. HIROTA, "Microwave Spectrum of Alkali Metal Tetrahydroborate. I. Rotational Transitions and Molecular Structure of $NaBH_4$ in the Ground Vibrational State", *J. Chem. Phys.* **94,** 7707 (1991).

E. HIROTA, K. KAWAGUCHI, T. ISHIWATA, and I. TANAKA, "Vibronic Interactions in the NO_3 Radical", *J. Chem. Phys.* **95,** 771 (1991).

Y. MIZUTANI, K. KAMOGAWA, T. KITAGAWA, A. SHIMIZU, Y. TANIGUCHI, and K. NAKANISHI, "Solution Structures and Phase Separation in Fluoroalcohol/Water Mixtures; A Study with Raman Difference and ^{13}C NMR Spectroscopy", *J. Phys. Chem.* **95,** 1790 (1991).

M. NAKAGAWA, A. MAEDA, T. OGURA, and T. KITAGAWA, "Identification of the Long-lived L' Species of Bacteriorhodopsin to the N Intermediate by Raman/absorption Quasi-simultaneous Measurements", *J. Mol. Struct.* **242,** 221 (1991).

K. KAMOGAWA and T. KITAGAWA, "Evidence for Direct Intermolecular Interactions as an Origin of the Hydration Shifts of the C-H Stretching Vibrations; 1,4-Dioxane/Water System", *Chem. Phys. Lett.* **179,** 271 (1991).

T. EGAWA, T. OGURA, R. MAKINO, Y. ISHIMURA, and T. KITAGAWA, "Observation of the O-O Stretching Raman Band for Cytochrome P-450$_{cam}$ Under Catalytic Conditions", *J. Biol. Chem.* **266,** 10246 (1991).

M. NAGAI, Y. YONEYAMA, and T. KITAGAWA, "Unusual CO Binding Geometry in Abnormal Subunits of Hemoglobins M Boston and Hb M Saskatoon", *Biochemistry* **30,** 6495 (1991).

K. IMAI, K. FUSHITANI, G. MIYAZAKI, K. ISHIMORI, T. KITAGAWA, Y. WADA, H. MORIMOTO, I. MORISHIMA, D. T.-b SHIH, and J. TAME, "Site-directed Mutagenesis in Haemoglobin. Functional Role of Tyrosine-42(C7)α at the α1-β2 Interface.", *J. Mol. Biol.* **218,** 769 (1991).

T. OGURA, S. TAKAHASHI, K. SHINZAWA-ITOH, S. YOSHIKAWA, and T. KITAGAWA, "Time-resolved Resonance Raman Investigation of Cytochrome Oxidase Catalysis: Observation of a New Oxygen-Isotope Sensitive Raman Band", *Bull, Chem. Soc. Jpn.* **64,** 2901 (1991).

M. NAGAI, T. KITAGAWA, and Y. YONEYAMA, "Molecular Pathology of Hemoglobin M Saskatoon Disease", *Biomed. Biochim. Acta* **49,** 2/3 S317 (1990).

S. HASHIMOTO, Y. MIZUTANI, Y. TATSUNO, and T. KITAGAWA, "Resonance Raman Characterization of Ferric- and Ferrylporphyrin π Cation Radicals and the Fe^{IV}=O Stretching Frequency", *J. Am. Chem. Soc.* **113,** 6542 (1991).

V. FIDLER, T. OGURA, S. SATO, K. AOYAGI, and T. KITAGAWA, "Resonance Raman Study on Photoreduction of Iron-porphyrins: a Novel Insight into the Ligand-aided Process", *Bull. Chem. Soc. Jpn.* **64,** 2315 (1991).

T. KITAGAWA and T. OGURA, "Resonance Raman Spectra of Transient Species of a Respiration Enzyme Detected with an "Artificial Cardiovascular System" and Raman/absorption Simultaneous Measurement System", *'Laser Applications in Life Sciences'* SPIE Vol. **1403,** Part 2, 563 (1991).

M. ASANO and Y. KAIZU, "Relaxation Processes of Excited Metalloporphyrins", *J. Spectrosc. Soc. Jpn.* (in Japanese) **39,** 149 (1990).

T. KITAGAWA and S. KAMINAKA "Ultraviolet Resonance Raman Spectroscopy and Its Application for Investigation of Protein Structures", *J. Spectrosc. Soc. Jpn.* (in Japanese) **40,** 193 (1991).

K. KEMNITZ and K. YOSHIHARA, "Free-Volume Effect of Dye Monomers in the Adsorbed State." *J. Phys. Chem.* **94,** 8805 (1991).

S.R. MEECH and K. YOSHIHARA, "Picosecond Dynamics at the Solid Liquid Interface: A Total Internal Reflection Time Resolved Surface Second-Harmonic Generation Study.", *Chem. Phys. Lett.* **175,** 423 (1990).

H. PETEK, K. YOSHIHARA, Y. FUJIWARA, and J.G. FREY, "Isomerization of cis-Stilbene in Ar and Kr Clusters: Direct Measurements of trans-Stilbene Formation Rates on a Picosecond Time Scale", Ultrafast Phenomena VII, eds. C.B. Harris, E.P. Ippen, G.A. Mourou, A.H. Zewail, Springer-Verlag, Berlin, 1990, p444.

H. OKAMOTO and K. YOSHIHARA, "Theoretical Study on Polarized Time-Resolved Resonance Coherent anti-Stokes Raman Scattering: Effect of Ultrafast Molecular Rearrangement in the Electronically Excited State", *Chem. Phys. Lett.* **172,** 323 (1990).

K. KEMNITZ and K. YOSHIHARA, "Diffusionless Electron Transfer of Xanthene Dyes in Nonpolar and Weekly Polar Donor- and Acceptor-Solvents", *Chem. Lett.* 645 (1991).

K. KEMNITZ and K. YOSHIHARA, "Entropy-Driven Dimerization of Xanthene Dyes in Nonpolar Solution and Temperature-Dependent Fluorescence Decay of Dimers", *J. Phys. Chem.* **95,** 6095 (1991).

S.R. MEECH and K. YOSHIHARA, "The Photoreaction of a Rhodamine 6G Monolayer Adsorbed on Quartz Studied by Surface Second Harmonic Generation", *Photochem. Photobiol.* **53,** 627 (1991).

H. PETEK, K. YOSHIHARA, and R.L. CHRISTENSEN, "Spectroscopic and Dynamical Studies of the S_1 and S_2 States of Decatetraene in Supersonic Molecular Beams", *J. Chem. Phys.* **95,** 4739 (1991).

H. OKAMOTO and K. YOSHIHARA, "Femtosecond Time-resolved Coherent Raman Scattering from β-carotene in Solution. Ultrahigh Frequency (11 THz) Beating Phenomenon and Subpicosecond Vibrational Relaxation", *Chem. Phys. Lett.* **177,** 568 (1991).

J.H. FREDERICK, Y. FUJIWARA, J.H. PENN, K. YOSHIHARA, and H. PETEK, "Models for Stilbene Photoisomerization: Experimental and Theoretical Studies of the Excited State Dynamics of 1,2-Diphenylcycloalkenes", *J. Phys. Chem.* **95,** 2845 (1991).

Y. SHICHIDA, H. KANDORI, T. OKADA, T. YOSHIZAWA, N. NAKASHIMA, and K. YOSHIHARA, "Differences in the Photobleaching Process between 7-*cis*- and 11-*cis*-Rhodopsins: A Unique Interaction Change between the Chromophores and the Protein during the Lumi-Meta I Transition", *Biochem.* **30,** 5918 (1991).

A. K. CAMPEN, A.J. REST, and K. YOSHIHARA, "Luminescence Spectra and Lifetimes of tris-(2,2'-bipyridine) Ruthenium (II) Dichloride and Potassium Hexacyanochromate (III) in Polymer Films and Hydrocarbon Mulls at Approximately 77K: Evaluation of Alternative Host Media for Studying Unstable Species in Photochemical Reaction Pathways Originating from Non-volatile Substrates", *J. Photochem. Photobiol. A: Chem.* **55,** 301 (1991).

T. KOBAYASHI, Y. TAKAGI, H. KANDORI, K. KEMNITZ, and K. YOSHIHARA, "Femtosecond Electron Transfer in Diffusionless, Weakly Polar Solvent Systems: Nile Blue in Aniline and N,N-Dimethylaniline", *Chem. Phys. Lett.* **180,** 416 (1991).

R. INABA, H. OKAMOTO, K. YOSHIHARA, and M. TASUMI, "Femtosecond Time-resolved Coherent Anti-Stokes Raman Scattering from Acetonitrile: Solvent Effects on the Vibrational Dephasing of the C≡N Stretching Band", *Chem. Phys. Lett.* **185,** 56 (1991).

K. HONDA, M. TAKAYANAGI, T. NISHIYA, H. OHOYAMA, and I. HANAZAKI, "Reaction of H_2O with H Produced by the 266 nm Photolysis of HI", *Chem. Phys. Lett.* **180,** 321 (1991).

Y. MORI, P.K. SRIVASTAVA and I. HANAZAKI, "Spatiotemporal Pattern in Coupling between Convective Instability and Autocatalytic Photochemical Reaction", *Physica D* **50,** 59 (1991).

P.K. SRIVASTAVA, Y. MORI, and I. HANAZAKI, "Wavelength-dependent Photo-inhibition of Chemical Oscillation: Uncatalyzed Oscillators with Phonol and Aniline as Substrates", *Chem. Phys. Lett.* **177,** 213 (1991).

Y. MORI, P.K. SRIVASTAVA, and I. HANAZAKI, "Wavelength Dependence of Light-induced Chemical Oscillation. Hexacyanoferrate (II)-Hydrogen Pereoxide-Sulfuric Acid System", *Chem. Lett.* 669 (1991).

P.K. SRIVASTAVA, Y. MORI, and I. HANAZAKI, "Dual-frequency Chemical Oscillator with Acetylphenols as Substrates", *J. Phys. Chem.* **95,** 1636 (1991).

N. NISHI and K. YAMAMOTO, "Molecular Clusters Isolated from Aqueous Solutions by Adiabatic Expansion of Liquid Jets: a New Approach for Molecular Association in Solutions", *Chem. Phys of Atomic and Mol. Clusters; Soc. Italiana Fisica,* **CVII Corso,** 797 (1990).

F. MISAIZU, H. SHINOHARA, N. NISHI, T. KONDOW, and M. KINOSHITA, "Two color 2+2 Photon Resonance-enhanced Ionization of Benzene-Carbon Tetrachloride Binary Clusters", *Int. J. Mass Spectry. Ion Processes* **102,** 99 (1990).

T. MUNEGUMI, N. NISHI, and K. HARADA, "Oxydation of Ethylamine to Glycine in Aqueous Solution induced by KrF Excimer Laser Irradiation" *J. Chem. Soc. Chemical Communications* 1689 (1990).

H. SHINOHARA, H. SATO, F. MISAIZU, K. OHASHI, and N. NISHI, "Metastable Dissociation Dynamics of Molecular Cluster Ions", *Z. Phys. D, Atoms, Molecules and Clusters* **20,** 197 (1991).

K. OHASHI and N. NISHI, "Photodissociation Spectroscopy of Benzene Cluster Ions: $(C_6H_6)_2^+$ and $(C_6H_6)_3^+$", *J. Chem. Phys.* **95,** 2999 (1991).

K. SUZUKI, T. KONDOW, and K. KUCHITSU, "Dissociative Electron Attachment to BrCN in the Reaction with Autoionizing High-Rydberg Atoms", *J. Phys. Chem.* **94,** 6615 (1990).

M. SUMITANI, H. ABE, and S. NAGAKURA, "External Magnetic Field Effects on the β Band Emission of NO", *J. Chem. Phys.* **94,** 1923 (1991).

H. ITO, K. SUZUKI, T. KONDOW and K. KUCHITSU, "Electronic Transition Moment for the $B^2\Sigma^+ - X^2\Sigma^+$ Emission of CN. Analysis of Dependence on the Internuclear Distance", *J. Chem. Phys.* **94,** 5353 (1991).

M. OKAZAKI, K. TORIYAMA, Y. TAI, and K. NUNOME, "Excimer formation of Pyrene as a Probe to Inverstigate the Recombination of Geminate Pairs (III): The Effect of Charge Hopping Process on Fluorescence and ODESR Spectra in X-irradiated Ethylene Propylene Rubber Doped with Pyrene", *Appl. Magn. Reson.* **1,** 213 (1990).

K. YAKUSHI, H. YAMAKADO, T. IDA, and A. UGAWA, "*d*-π Interaction in Conducting Phthalocyaninatocobalt Hexafluoroarsenate, CoPc $(AsF_6)_{0.5}$", *Solid State Commun.* **78,** 919 (1991).

K. YAKUSHI, T. IDA, A. UGAWA, H. YAMAKADO, H. ISHII, and H. KURODA, "Polarized Reflectance Spectra of Single Crystal of the Phthalocyanine Radicals $NiPc(AsF_6)_{0.5}$, $H_2Pc(AsF_6)_{0.5}$, and LiPc", *J. Phys. Chem.* **95,** 7636 (1991).

A. UGAWA, K. IWASAKI, A. KAWAMOTO, K. YAKUSHI, Y. YAMASHITA, and T. SUZUKI, "Metallic Behavior stable against Peierls Instability in the One-Dimensional Organic Conductor Tetraselenotetracene-Bis (1,2,5-thiadiazolo)tetracyanoquinodimethane [(TSeT)-(BTDA-TCNQ)]", *Phys. Rev.* **B43,** 14718 (1991).

A.G. SWANSON, J.S. BROOKS, M. TOKUMOTO, A. UGAWA, and K. YAKUSHI, "Transport and Magnetization Studies of β''-$(BEDT\text{-}TTF)_2AuBr_2$", in *Organic Superconductivity,* edited by V.Z. Kresin and W.A. Little, Plenum, pp.191-200 (1990).

M. TAMURA, R. MASUDA, T. NAITO, H. TAJIMA, H. KURODA, A. KOBAYASHI, K. YAKUSHI, R. KATO, H. KOBAYASHI, M. TOKUMOTO, N. KINOSHITA, and H. ANZAI "Reflectance Spectra of Some Two-dimensional Organic Metals based on BEDT-TTF and $[Ni(dmit)_2]$", *Synth. Met.* **41-43,** 2499 (1991).

A.A. ZAKHIDOV, A. UGAWA, K. IMAEDA, K. YAKUSHI, H. INOKUCHI, K. KIKUCHI, I. IKEMOTO, S. SUZUKI, and Y. ACHIBA, "Evolution of Superconductivity of K_xC_{60} upon K-dopig: Microwave Low-Field Signal and ESR Study", *Solid State Commun.* **79,** 939 (1991).

Y. MARUYAMA, T. INABE, L. HE, T. TERUI, and K. OSHIMA, "Electrical Conductivity of Black Phosphorus-Germanium Compound", *Bull, Chem. Soc. Jpn.* **64,** 811 (1991).

T. INABE, "Proton Transfer in *N*-Salicylideneanilines. An Approach to Controlling the Charge Transport in Molecular Materials", *New J. Chem.* **15,** 129 (1991).

T. INABE, I. GAUTIER-LUNEAU, N. HOSHINO, K. OKANIWA, H. OKAMOTO, T. MITANI, U. NAGASHIMA, and Y. MARUYAMA, "Structure and Optical Properties of Thermochromic Schiff Bases. Charge Transfer Interaction and Proton Transfer in the *N*-Tetrachlorosalicylideneaniline and *N*-Tetrachlorosalicylidene-1-pyrenylamine Crystals", *Bull. Chem. Soc. Jpn.* **64,** 801 (1991).

P. WANG, T. INABE, S. BANDOW, Y. MARUYAMA, H. INOKUCHI, N. IWASAWA, G. SAITO, and D.B. ZHU, "Electrical and Magnetic Properties of Tetrakis(methylseleno)tetrathiafulvalene $(TSeC_1\text{-}TTF)_xHgBr_2$ Complex Salt", *Synth. Met.* **41-43,** 1949 (1991).

T. INABE, Y. MARUYAMA, and T. MITSUHASHI, "Approaches to Controlling the Dimensionality in Molecular Conductors. Axially Substituted Phthalocyanines and Twin-Type Molecules", *Synth. Met.* **41-43,** 2629 (1991).

Y. MARUYAMA, T. INABE, L. HE, and K. OSHIMA, "Electrical Conductivity of Black Phosphorus-Germanium Compound", *Synth. Met.* **41-43,** 4067 (1991).

H. HOSHI and Y. MARUYAMA, "Epitaxial Growth of Chloroaluminum and Vanadyl Phthalocyanine Films on Alkali Halide Single Crystals by the Molecular-Beam-Epitaxy Technique", *J. Appl. Phys.* **69,** 3046 (1991).

Y. ACHIBA, T. NAKAGAWA, Y. MATSUI, S. SUZUKI, H. SHIROMARU, K. YAMAUCHI, K. NISHIYAMA, M. KAINOSHO, H. HOSHI, Y. MARUYAMA, and T. MITANI, "Visible, UV, and VUV Absorption Spectra of C_{60} Thin Films Grown by the Molecular-Beam Epitaxy (MBE) Technique", *Chem. Lett.* 1233 (1991).

H. HOSHI, N. NAKAMURA, Y. MARUYAMA, T. NAKAGAWA, S. SUZUKI, H. SHIROMARU, and Y. ACHIBA, "Optical Second- and Third-Harmonic Generations in C_{60} Film", *Jpn. J. Appl. Phys.* **30,** L1397 (1991).

Y. MORI, Y. MARUYAMA, H. MORI, and G. SAITO, "Electronic Structure of $(BEDT\text{-}TTF)_2X$ Salts Studied by Scanning Tunneling Spectroscopy", *Jpn. J. Appl. Phys.* **30,** L358 (1991).

K. IMAEDA, T. MITANI, C. NAKANO, H. INOKUCHI, and G. SAITO, "Infrared Spectra of Tetrakis(alkylthio)tetrathiafulvalenes", *Chem. Phys. Lett.* **173,** 298 (1990).

K. IMAEDA, T. MORI, C. NAKANO, H. INOKUCHI, N. IWASAWA, and G. SAITO, "Crystal Structures and Electrical Conductivities of TXC_n-TTF (X=Sulfur, Selenium, Tellurium; n=2,3)·TCNQ Charge-Transfer Complexes", *Bull. Chem. Soc. Jpn.* **64,** 2159 (1991).

T. MORI and H. INOKUCHI, "Synthesis, Structure, and Electrical Properties of $Ag_{1.2}$(2,5-dimethylthio-*N,N'*-dicyanoquinonediimine)," *Chem. Lett.* 2077 (1990).

T. MORI and H. INOKUCHI, "Band Structure and Fermi Surface of Organic Conductors," *Synth. Met.* **42,** 2447 (1991).

H. MORI, S. TANAKA, K. OSHIMA, G. SAITO, T. MORI, Y. MARUYAMA, and H. INOKUCHI, "Electrical Properties and Crystal Structures of Mercury (II) Thiocyanate Salts Based upon BEDT-TTF with Li^+, K^+, NH_4^+, Rb^+, and Cs^+," *Synth. Met.* **42,** 2013 (1991).

H. MORI, I. HIRABAYASHI, S. TANAKA, T. MORI, Y. MARUYAMA, and H. INOKUCHI, "Preparation, Crystal and Electronic Structures, and Physical Properties of New Ambient-Pressure Organic Superconductor, κ-$(BEDT\text{-}TTF)_2Ag(CN)_2H_2O$," *Synth. Met.* **42,** 2255 (1991).

K. OSHIMA, T. MORI, H. INOKUCHI, H. MORI, H. YAMOCHI, and G. SAITO, "Fermi Surface Modulation by Pressure in κ-$(BEDT\text{-}TTF)_2Cu(NCS)_2$," *Synth. Met.* **42,** 2175 (1991).

N. KINOSHITA, M. TOKUMOTO, K. MURATA, K. TAKAHASHI, H. ANZAI, T. MORI, and K. HONDA, "Electronic Structure of α-$(BEDT\text{-}TTF)_2Cu(NCS)_2$," *Synth. Met.* **42,** 2107 (1991).

H. MORI, S. TANAKA, T. MORI, Y. MARUYAMA, H. INOKUCHI, and G. SAITO, "Structural and Physical Properties of $(BEDT\text{-}TTF)_3Li_{0.5}Hg(SCN)_4(H_2O)_2$ and α''-$(BEDT\text{-}TTF)_2CsHg(SCN)_4$," *Solid State Commun.* **78,** 49 (1991).

H. MORI, I. HIRABAYASHI, S. TANAKA, T. MORI, Y. MARUYAMA, and H. INOKUCHI, "A New Ambient-Pressure Organic Superconductor, κ-(BEDT-TTF)$_2$Ag(CN)$_2$H$_2$O," in *"Advances in Superconductivity III,"* ed. by K. Kajimura and H. Hayakawa, *Springer*, Berlin (1991) p.323.

K. KAMIYA, H. INOKUCHI, M. OKU, S. HASEGAWA, C. TANAKA, J. TANAKA, and K. SEKI "UPS of New Type Polyacetylene," *Synthetic Met.* **41-44,** 155 (1991).

C. NAKANO, K. IMAEDA, T. MORI, Y. MARUYAMA, H. INOKUCHI, N. IWASAWA, and G. SAITO, "Phase Transion of Tetrakis(octylthio)tetrathiafulvalene (TTC$_8$-TTF) and Crystal Structure Analysis", *J. Mater. Chem.* **1,** 37 (1991).

I. KANAZAWA, S. TANIGAWA, R. SUZUKI, M. SANO, and H. INOKUCHI, "Three-dimensional Positron-electron Momentum Distribution in Single-crystal Graphite", *Phys. Rev.* **B 42,** 583 (1990).

N. UNENO, K. SEKI, K. SUGITA, and H. INOKUCHI, "Nature of the Temperature Dependence of Conduction Bands in Polyethylene", *Phys. Rev.* **B 43,** 2384 (1991).

E.A. SILINSH and H. INOKUCHI, "On Charge Carrier Photogeneration Mechanisms in Organic Molecular Crystals", *Chem. Phys.* **149,** 373 (1991).

J.K. JESZKA, T. ENOKI, Z. SHI, K. IMAEDA, H. INOKUCHI, N. IWASAWA, H. YAMOCHI, and G. SAITO, "Thermal Properties of Tetrakis(Alkyltelluro)Tetrathiafulvalene (TTeC$_n$-TTF)", *Mol. Cryst. Liq. Cryst.* **196,** 167 (1991).

T. ASAHI, M. YUDASAKA, K. NAKANISHI, S. IWASHIMA, J. AOKI, N. SATO, and H. INOKUCHI, "Rectification Properties of In/Tetrabenzo[de,hi,op,st]Pentacene/Au Devices", *Phys. Status Solidi* A **122,** K97 (1990).

K. NAKASUJI, K. SUGIURA, T. KITAGAWA, J. TOYODA, H. OKAMOTO, K. OKANIWA, T. MITANI, H. YAMAMOTO, I. MURATA, A. KAWAMOTO, and J. TANAKA, "Exploration of New Cooperative Proton-Electron Transfer (PET) Systems. First Example of Extended Conjugated Quinhydrones: 1,5-Dihalo-2,6-naphthoquinhydrones", *J. Am. Chem. Soc.* **113,** 1862 (1991).

I. MURATA, S. SASAKI, K.-U. KLABUNDE, J. TOYODA, and K. NAKASUJI, "Synthesis of a Highly Amphoteric *s*-Indaceno[1,2,3-*cd*:5,6,7-*c'd'*]diphenalene: Switching between Diatropism and Paratropism Due to Charges in Oxidation Level", *Angew. Chem. Int. Ed. Engl.* **30,** 172 (1991).

K. NAKASUJI, J. TOYODA, K. IMAEDA, H. INOKUCHI, I. MURATA, A. ODA, A. KAWAMOTO, and J. TANAKA, "New Molecular Metals Composed of Peri-condensed Heterocycles", *Synthetic Metals* **42,** 2529 (1991).

K. YAMAGUCHI, M. OKUMURA, T. FUENO, and K. NAKASUJI, "New Models for Organic Magnetic Conductors or Organic Kondo and Dense Kondo Systems", *Synthetic Metals* **43,** 3631 (1991).

J. TOYODA, K. NAKASUJI, T. KOTANI, I. MURATA, A. KAWAMOTO, and J. TANAKA, "The Crystal Structure and Physical Properties of the 3:2 Charge Transfer Complex of Bis(ethylenedithio)dithiapyrene (ETDTPY) and Dibenzobarrelenotetracyanoquinodimethane (DBBTCNQ)", *Chem. Lett.* 1237 (1991).

K. NISHINO, M. TAKAGI, I. MURATA, J. INANAGA, and K. NAKASUJI, "(Thiepine)iron Tricarbonyl: Stabilization of Thermally Labile Parent Thipine by Transition-Metal Complexation", *J. Am. Chem. Stoc.* **113,** 5059 (1991).

M. HAGA, K. ISOBE, S.R. BOONE, and C.G. PIERPONT, "Comparative Studies on Charge Distribution for the Ruthenium and Osmium Quinone Complexes [M(bpy)$_2$(quinone)]^n (M=Ru, Os; n=0, +1, +2).", *Inorg. Chem.* **29,** 3795 (1990).

K. ASAKURA, K. KITAMURA-BANDO, Y. IWASAWA, H. ARAKAWA, and K. ISOBE, "Metal-Assisted Hydroformylation on a SiO$_2$-Attached Rh Dimer. In Situ EXAFS and FT-IR Observations of the Dynamic Behaviors of the Dimer Site.", *J. Am. Chem. Soc.* **112,** 249 (1990).

Y. HAYASHI, Y. OZAWA, and K. ISOBE, "Site-Selective Oxygen Exchange and Substitution of Organometallic Groups in an Amphiphilic Quadruple-Cubane-Type Cluster. Synthesis and Molecular Structure of [(MCp*)$_4$V$_6$O$_{19}$] (M=Rh, Ir).", *Inorg. Chem.* **30,** 1025 (1991).

Y. OZAWA, Y. HAYASHI, and K. ISOBE, "Structure of Triammonium Hexahydrogenhexamolybdorhodate (III) Hexahydrate.", *Acta Cryst.*, **C47,** 637 (1991).

Y. DO, X.-Z. YOU, C. ZHANG, Y. OZAWA, and K. ISOBE, "Trishomocubane-Type Methoxide Cluster as a Novel Mediator in the Extension of Cube Size in Organometallic Oxide Clusters: Synthesis and Structures of [(RhCp*)$_2$Mo$_3$O$_9$(OMe)$_4$] · MeOH and a Linear Quadruple Cubane-Type Cluster [(RhCp*)$_4$Mo$_6$O$_{22}$] · 4CH$_2$Cl$_2$ (Cp*=η^5–C$_5$Me$_5$).", *J. Am. Chem. Soc.* **113,** 5893 (1991).

H. OSHIO, "Ferromagnetic Interaction in Oxalate Bridged Complex [Cu(bpy)(ox)] · 2H$_2$O with Zigzag Chain Structure", *Chem. Lett.* 227 (1991).

Y. MAEDA, H. OSHIO, Y. TANIGUCHI, T. ONIKI, and Y. TAKASHIMA, "Physical Characteristic and Molecular Structure of Spin-Crossover Iron (III) Complexes of Monoclinic Form with Hexadentate Ligands Derived from Triethylenetetramine and Salicylaldehyde {Fe(sal$_2$trien)} Bph$_4$ acetone", *Bull. Chem. Soc. Jpn.* **64,** 1522 (1991).

Y. MAEDA, H. OSHIO, K. TORIUMI, and Y. TAKASHIMA, "Crystal Structures, Mössbauer Spectra, and Magnetic Properties of Spin-Crossover Complexes [Fe(bzpa)$_2$]ClO$_4$ and [Fe(acen)(3,4-lut)$_2$]BPh$_4$", *J. Chem. Soc. Dalton Trans.* 1277 (1991).

H. OSHIO, "Control of the Intramolecular Magnetic Interaction by the Spin Polarization of dπ-Electrons: Ferromagnetic Interaction between Iron Centres through an Organic Bridging Ligand.", *J. Chem. Soc. Chem. Comm.* 240 (1991).

H. OSHIO, K. TORIUMI, Y. MAEDA, and Y. TAKASHIMA, "Temperature Dependent Crystallographic Studies on Ferric Spin-Crossover Complexes with Different Spin Conversion Rates", *Inorg. Chem.* **30,** 4252 (1991).

M. MISHIMA, M. FUJIO, and Y. TSUNO, "Thermodynamic Stabilities of Phenonium Ions in the Gas Phase," *Chem. Lett.* 2277 (1990).

M. MISHIMA, Y. TSUNO, and M. FUJIO, "Substituent Effect on the Gas Phase Basicities of α, α, α-Trifluoromethylacetophenone. Intrinsic Nature of Resonance Demand," *Chem. Lett.* 2281 (1990).

M. FUJIO, Y. TSUJI, T. OTSU, and Y. TSUNO, "Substituent Effects on the Solvolysis of o-Methyl- and o,o'-Dimethyl α-t-Butylbenzyl Tosylates," *Tetrahedron Lett.* **32,** 1805 (1991).

S. IMAZU, N. SHIMIZU, and Y. TSUNO, "A Regiospecific Ene Reaction between γ-Alkylated Allyltrimethylsilanes and TCNE," *Chem. Lett.* 1845 (1990).

N. SHIMIZU, C. KINOSHITA, E. OSAJIMA, and Y. TSUNO, "Effects of Si-Si σ-Bonds on Stability of Adjacent Benzylic Cations," *Chem. Lett.* 1937 (1990).

N. SHIMIZU, M. SAKAI, and Y. TSUNO, "Butyllithium-Induced Syn β-Elimination of 2-Arylalkyl p-Toluenesulfonates," *Chem. Lett.* 2207 (1990).

N. SHIMIZU, S. IMAZU, F. SHIBATA, and Y. TSUNO, "Stereoselective Synthesis of (E)- and (Z)-2-Alkenyltrimethylsilanes from 1,2-Epoxy-1,3-bis(trimethylsilyl)propane," *Bull, Chem. Soc. Jpn.* **64,** 1122 (1991).

N. SHIMIZU, E. OSAJIMA, and Y. TSUNO, "Rates and Mechanism of the Solvolyses of 2,2-Dimethyl-2-sila-1-indanyl Bromide and α-Trialkylsilylbenzyl p-Toluenesulfonates. α-Silicon Effect on the Stability of Benzylic Cations in Solution," *Bull. Chem. Soc. Jpn.* **64,** 1145 (1991).

N. SHIMIZU, S. WATANABE, and Y. TSUNO, "Silicon Effects. II. Structure and Stability of 1-Phenyl-2-(trimethylsilyl)ethyl Cation in Solution," *Bull. Chem. Soc. Jpn.* **64,** 2249 (1991).

Y. MAEDA, M. GOTO, T. KOBAYASHI, M. MISHIMA, M. FUJIO, and Y. TSUNO, "The Substituent Effect on the Acetolysis of 2,2-Bis(aryl)ethyl Tosylates," *Memo. Fac. Sci., Kyushu Univ. Ser. C* **18 (1),** 63 (1991).

Y. MAEDA, M. GOTO M. MISHIMA, M. FUJIO, and Y. TSUNO, "The Substituent Effect on the Acetolysis of Monosubstituted 2,2-Diphenylethyl Tosylates," *Memo. Fac. Sci., Kyushu Univ. Ser. C* **18 (1),** 75 (1991).

M. GOTO, Y. MAEDA, T. KOBAYASHI, Y. SAEKI, M. MISHIMA, M. FUJIO, and Y. TSUNO, "The Substituent Effect on the Acetolysis of Unsymetrically Disubstituted 2,2-Diphenylethyl Tosylates," *Memo. Fac. Sci., Kyushu Univ. Ser. C* **18 (1),** 91 (1991).

K. YATSUGI, Y. TSUJI, M. FUJIO, and Y. TSUNO, "Solvolysis of 1,1,3,3-Tetramethylindan-2-yl Sulfonates," *Memo. Fac. Sci., Kyushu Univ. Ser. C* **18 (1),** 109 (1991).

Y. TSUJI, K. YATSUGI, M. FUJIO, and Y. TSUNO, "The Study of ^{18}O-Scrambling on the Solvolysis of α-t-Butylbenzyl Tosylate," *Memo. Fac. Sci., Kyushu Univ. Ser. C* **18 (1),** 121 (1991).

M. FUJIO, I. AKASAKA, S.-H. KIM, M. MISHIMA, Y. TSUJI, and Y. TSUNO, "Substituent Effects on the Solvolysis of Benzyl Chlorides," *Memo. Fac. Sci., Kyushu Univ. Ser. C* **18 (1),** 131 (1991).

G. BHASKAR REDDY, T. HANAMOTO, and T. HIYAMA, "Aluminium-Mediated [4+1] Cyclization Reaction: Novel Synthesis of 2,2,5,5-Tetramethylcyclopentanecarboxylic Acid", *Tetrahedron Lett.* **32,** 521 (1991).

J. INANAGA, O. UJIKAWA, and M. YAMAGUCHI, "SmI_2-Promoted Aryl Radical Cyclization. A New Synthetic Entry into Heterocycles", *Tetrahedron Lett.* **32,** 1737 (1991).

J. INANAGA, T. TABUCHI, and M. YAMAGUCHI, "Selective Formation of Allenyl- or Propargylstannanes via SmI_2-Induced Polarity Inversion of Allenyl Palladium Complexes", *Chem. Express* **6,** 419 (1991).

J. INANAGA, J. KATSUKI, and M. YAMAGUCHI, "SmI_2-Promoted Deacetoxylation of *O*-Acetylsugar Lactones. An Easy Access to Deoxysugar Lactones", *Chem. Lett.* 1025 (1991).

T. HANAMOTO and J. INANAGA, "SmI_2-Promoted Ketyl Radical Addition to *O*-Benzyl Formaldoxime. A New Aminomethylation", *Tetrahedron Lett.* **32,** 3555 (1991).

J. INANAGA, J. KATSUKI, O. UJIKAWA, and M. YAMAGUCHI, "Carbon-Carbon Bond Formation by Intermolecular Radical Reaction. SmI_2-Promoted Carbonyl-Alkyne Reductive Coupling", *Tetrahedron Lett.* **32,** 4921 (1991).

E.I. VON NAGY-FELSOBUKI and K. KIMURA, "Ab Initio Proton Affinities of HCOOH, CH_3COOH, CH_3OH and C_2H_5OH", *J. Phys. Chem.* **94,** 8041 (1990).

K. KIMURA, "Study of Electronic Autoionization of NO Molecule by Excited-State Photoelectron Spectroscopy", *Chinese J. Phys.* **29,** 97 (1991).

Y. ACHIBA and K. KIMURA, "Autoionization Mechanism of NO Molecule: Optical-Optical Double Resonance MPI Photoelectron Spectroscopy of *ns* and *nd* Rydberg Series", *Chinese J. Phys.* **29,** 223 (1991).

H. OZEKI, K. OKUYAMA, M. TAKAHASHI, and K. KIMURA, "MPI Ion-Current and Photoelectron Spectra of Jet-Cooled *p*-Phenylenediamines", *J. Phys. Chem.* **95,** 4308 (1991).

M. TAKAHASHI, H. OZEKI, and K. KIMURA, "A New High-Resolution Threshold Photoelectron Analyzer. Obsevation of Rotational Structure of NO^+ Cation", *Chem. Phys. Lett.* **181,** 255 (1991).

K. AWAZU, H. KAWAZOE, K. MUTA, T. IBUKI, K. TABAYASHI, and K. SHOBATAKE, "Characterization of Silica Glasses Sintered under Cl_2 Ambients", *J. Appl. Phys.* **69,** 1849 (1991).

T. NAGATA, T. KONDOW, K. KUCHITSU, K. TABAYASHI, and K. SHOBATAKE, "Collision Energy Dependence of the Cross Section for Production of $CN(B^2\Sigma^+)$ in the Reaction of $Ar(^3P_{0,2})$ and $Kr(^3P_{0,2})$ with BrCN", *J. Chem. Phys.* **95,** 1011 (1991).

K. MITSUKE, S. SUZUKI, T. IMAMURA, and I. KOYANO, "Negative-Ion Mass Spectrometric Study of Ion-Pair Formation in the Vacuum Ultraviolet. IV. $CH_4 \rightarrow H^- + CH_3^+$ and $CD_4 \rightarrow D^- + CD_3^+$", *J. Chem. Phys.* **94,** 6003 (1991).

K. MITSUKE, S. SUZUKI, T. IMAMURA, and I. KOYANO, "Negative-Ion Mass Spectrometric Study of Ion-Pair Formation in the Vacuum Ultraviolet. V. $CF_4 \rightarrow F^- + CF_3^+$", *J. Chem. Phys.* **95,** 2398 (1991).

S. SATO and T. OHMORI, "Photochemical Formation of $[HFe_3(CO)_{11}]^-$ and $[HFe(CO)_4]^-$ from $Fe(CO)_5$ adsorbed on Hydrated Alumina", *J. Chem. Soc. Chem. Commun.* 1032 (1990).

Y. UKISU, A. KAZUSAKA, and M. NOMURA, "Oxidative Dimerization of 1-Propyne on a 2-Pyridylethyl Copper Complex Fixed Silica Catalyst", *Bull. Chem. Soc. Jpn.* **64,** 293 (1991).

Y. OHNO and T. MATSUSHIMA, "Spatial Distribution of Reactive Carbon Dioxide Desorption on Palladium(100) Surfaces", *Surface Sci.* **239,** L521 (1991).

T. MATSUSHIMA, Y. OHNO, and K. NAGAI, "Spatial Distribution of Reactive Carbon Dioxide Desorption on Iridium(110)(1×2) Reconstructed Surfaces", *Surface Sci.* **239,** L561 (1990).

T. MATSUSHIMA, Y. OHNO, and K. NAGAI, "Transformation of Iridium(110)(1×1) into (1×2) and Spatial Distribution of Reactive Carbon Dioxide Desorption", *J. Chem. Phys.* **94,** 704 (1991).

Y. OHNO and T. MATSUSHIMA, "Dissociation of Oxygen Admolecules on Platinum(110)(1×2) Reconstructed Surfaces at Low Temperatures", *Surface Sci.* **241,** 47 (1991).

T. Matsushima, "Spatial Distribution of Reactive Carbon Dioxide Desorption on Pt(110)(1×2) Surface", *Surface Sci.* **242,** 489 (1991).

T. MATSUSHIMA, Y. OHNO, and K. NAGAI, "Orientation of Reaction Site and Spatial Distribution of Product Desorption; CO Oxidation on Pt, Ir(110)(1×2)", *Shokubai (Catalyst),* **32,** 340 (1990).

K. NAGAI, "Thermal Desorption Spectrum of Hard Hexagon Model", *Surface Sci.* **244,** L147 (1991).

T. MIZUTA, T. YAMAMOTO, K. MIYOSHI, and Y. KUSHI, "The Ligand Field Stabilization Effect on the Metal-ligand Bond Distances in Octahedral Metal Complexes with edta-type Ligands", *Inorg. Chim. Acta* **175,** 121 (1990).

H. SAKANE, I. WATANABE, K. ONO, S. IKEDA, S. KAIZAKI, and Y. KUSHI, "Structure of Fe(III) Complexes with EDTA and EDDDA in Aqueous Solution by EXAFS and XANES", *Inorg. Chim. Acta* **178,** 67 (1990).

F. KAWAIZUMI, Y. INOUE, and H. NOMURA, "Limiting Partial Molar Volumes of Ions in Water-Methanol and Water Acetonitrile.", *Bull. Chem. Soc. Jpn.* **64,** 510 (1991).

T. ARAGAKI, S. IWATA, H. TANGE, S. HIRAOKA, I. YAMADA, and F. KAWAIZUMI, "Theoretical Analysis of Turbulent Flow and Heat Transfer around a Surface-mounted Obstacle.", *J. Chem. Eng. Jpn.* **24,** 171 (1991).

F. KAWAIZUMI, H. HIRAKAWA, E. KUBOTA, and H. NOMURA, "Sedimentation Potential Measurements and Partial Molar Volumes of Univalent Ions in Water-Acetone Mixtures.", *Bull. Chem. Soc. Jpn.* **64,** 2607 (1991).

F. KAWAIZUMI and K.A. BURKOV, "Volume Changes Accompanying the Stepwise Complex Formation in Aqueous Solutions. Cu(II)-bpy Complexes.", *Chem. Lett.* 1755 (1991).

I. TANIGUCHI, T. SHIMPUKU, K. YAMASHITA, and H. OHTAKI, "Electrocatalytic Reduction of Nitrous Oxide to Dinitrogen at a Mercury Electrode Using Ni^{II} Complexes of Macrocyclic Polyamines", *J. Chem. Soc., Chem. Commun.* 915 (1990).

T. RADNAI, K. INOUE, and H. OHTAKI, "An X-Ray Diffraction Study on Zinc(II) Complexes with α-Alaninate Ion in Aqueous Solution", *Bull. Chem. Soc. Jpn.* **63,** 3420 (1990).

K. WAIZUMI, H. MASUDA, H. OHTAKI, K. TSUKAMOTO, and I. SUNAGAWA, "In Situ Observation of the Phase Transition among Cobalt(II) Dichloride Hydrates and Crystal Structures of the Tetra- and Hexahydrates", *Bull. Chem. Soc. Jpn.* **63,** 3426 (1990).

H. OHTAKI and H. SEKI, "The Structure of Nickel(II) and Copper(II) Complexes with 1,4,8,11-Tetraazacyclotetradecane in Aqueous Solution As Studied by the X-Ray Diffraction Method", *J. Macromol. Sci.-Chem.* **A27,** 1305 (1990).

K. WAIZUMI, H. MASUDA, H. OHTAKI, K.A. BURKOV, and M.Y. SCRIPKIN, "Structure of $MgCl_2 \cdot RbCl \cdot 6H_2O$", *Acta Cryst.* **C47,** 251 (1991).

N. FUKUSHIMA, Y. TAMURA, and H. OHTAKI, "Dissolution of Alkali Fluoride and Chloride Crystals in Water Studied by Molecular Dynamics Simulations", *Z. Naturforsch.,* **46a,** 193 (1991).

K. WAIZUMI, Y. TAMURA, H. MASUDA, and H. OHTAKI, "X-Ray Diffraction Studies on Ternary $MgCl_2$-KCl-H_2O and $MgCl_2$-CsCl-H_2O Solutions Saturated with the Corresponding Double Salts, *Z. Naturforsch.* **46a,** 307 (1991).

H. WAKITA, G. JOHANSSON, M. SANDSTRÖM, P.L. GOGGIN, and H. OHTAKI, "Structure Determination of Zinc Iodide Complexes Formed in Aqueous Solution", *J. Solution Chem.* **20,** 643 (1991).

G. JOHANSSON, H. YOKOYAMA, and H. OHTAKI, "Structure of the Solvated Metal Ions in Nitrate and Chloride Solutions of Erbium(III) and Yttrium(III) in Dimethyl Sulfoxide", *J. Solution Chem.* **20,** 859 (1991).

G. JOHANSSON, M. MAGINI, and H. OHTAKI, "Coordination Around Thorium(IV) in Aqueous Perchlorate, Chloride and Nitrate Solutions", *J. Solution Chem.* **20,** 775 (1991).

H. SUZUKI, N. FUKUSHIMA, S. ISHIGURO, H. MASUDA, and H. OHTAKI, "Structures of Zinc(II) and Copper(II) Chloride *N,N*-Dimethylformamide Solvates", *Acta Cryst.* **C47,** 1838 (1991).

C. SASAKI, K. NAKAJIMA, M. KOJIMA, and J. FUJITA, "Preparation and Characterization of Optically Active Quadridentate Schiff Base-Titanium (IV) Complexes and the Catalytic Properties of These Complexes on Asymmetric Oxidation of Methyl Phenyl Sulfide with Organic Hydroperoxides", *Bull. Chem. Soc. Jpn.* **64,** 1318 (1991).

E. KIMURA, T. KOIKE, T. SHIOTA, and Y. IITAKA, "Acid Properties of Zinc(II) and Cadmium(II) in Complexation with Macrocyclic Oxopolyamine Ligands", *Inorg. Chem.* **29,** 4621 (1990).

M. SHIONOYA, E. KIMURA, and Y. IITAKA, "Mono-, Di- and Tetrafluorinated Cyclams", *J. Am. Chem. Soc.* **112,** 9237 (1990).

E. KIMURA, Y. KOTAKE, T. KOIKE, M. SHIONOYA, and M. SHIRO, "A Novel Cyclam Appended with 3-Hydroxypyridine. An Ambident Donor Ligand Comprising a Pyridyl N and a Pyridinolate O- Donors", *Inorg. Chem.* **29,** 4991 (1990).

M. KODAMA, A.B. MAHATMA, T. KOIKE, and E. KIMURA, "Polarographic Study of the Rates of the Dissociation Reactions of the Eu(III)-HAHA Complex and of the Eu(III)-, Gd(III)-, and Ho(III)-PAPA Complexes", *Bull. Chem. Soc. Jpn.* **63,** 2639 (1990).

M. KODAMA, T. KOIKE, A.B. MAHATMA, and E. KIMURA, "Thermodynamic and Kinetic Studies of Lanthanide Complexes of 1,4,7,10,13-Pentaazacyclopentadecane-N,N′,N″,N‴,N⁗-pentaacetic Acid and 1,4,7,10,13,16-Hexaazacyclooctadecane-N,N′,N″,N‴,N⁗-hexaacetic Acid", *Inorg. Chem.* **30,** 1270 (1991).

E. KIMURA, Y. KUROGI, T. TOJO, M. SHIONOYA, and M. SHIRO, "Design of Discriminating Hosts for Nobel Metal Ions with Double Functions of Thia and Amide Donors in Macrocyclic Structures", *J. Am. Chem. Soc.* **113,** 4857 (1991).

E. KIMURA, M. SHIONOYA, T. YAMAUCHI, and M. SHIRO, "The Proximal Imidazole Effect on Manganese(III)-Cyclam Complex", *Chem. Lett,* 1217 (1991).

E. KIMURA and T. KOIKE, "Roles of Zinc(II) ion in Phosphatases. A Model Study with Zinc(II)-Macrocyclic Polyamine Complexes", *J. Am. Chem. Soc.* **113,** 8935 (1991).

E. KIMURA, H. KUROSAKI, T. KOIKE, and K. TORIUMI, "X-Ray Structural Study of Zinc(II) Inclusion Complex of a Phenolate-Pendant Cyclam", *J. Inclusion Phenomena,* (1991) in press.

E. KIMURA, Y. KUROGI, and T. TAKAHASHI, "The First Gold(III) Macrocyclic Polyamine Complexes and Application to Selective Gold(III) Uptake", *Inorg. Chem.* **30,** 4117 (1991).

E. KIMURA, Y. KUROGI, M. SHIONOYA, and M. SHIRO, "Synthesis, Properties and Complexation of a New Imidazole-pendant Macrocyclic 12-membered Triamine Ligand", *Inorg. Chem.* **30,** 4524 (1991).

K. OSAKADA, A. GROHMANN, and A. YAMAMOTO, "New Ruthenium Carboxylate Complexes Having a 1-5-η^5-Cyclooctadienyl Ligand.", *Organometallics,* **9,** 2092 (1990).

K. OSAKADA, M.-K. DOH, F. OZAWA, and A. YAMAMOTO, "Catalytic and Stoichiometric Carbonylation of β,γ-Unsaturated Carboxylic Acids to give Cyclic Anhydrides through Intermediate Palladium-Containing Cyclic Esters.", *Organometallics* **9,** 2197 (1990).

T. YAMAMOTO, K. SANO, K. OSAKADA, S. KOMIYA, A. YAMAMOTO, Y. KUSHI, and T. TADA, "Comparative Studies on Reactions of α,β- and β,γ-Unsaturated Amides and Acids with Nickel(0), Palladium(0), and Platinum(0) Complexes. Preparation of New Five- and Six-Membered Nickel- and Palladium-Containing Cyclic Amide and Ester Complexes.", *Organometallics,* **9,** 2396 (1990).

K. OSAKADA, Y. OZAWA, and A. YAMAMOTO "Preparation of $(Me_3P)_2Pd_2(\mu\text{-}\eta^3\text{-}C_3H_5)(\mu\text{-}SPh)$ by Reaction of Pd(0) Complex with Allyl Phenyl Sulfide.", *J. Organomet. Chem.,* **399,** 341 (1990).

K. OSAKADA, Y.-J. KIM, M. TANAKA, S. ISHIGURO, and A. YAMAMOTO, "Association of a Methylplatinum Fluoroalkoxide Complex with a Fluoro Alcohol through O-H · · · O Hydrogen Bonding.", *Inorg. Chem.,* **30,** 197 (1991).

K. OSAKADA, K. OHSHIRO, and A. YAMAMOTO, "Preparation, Structure, and Formation Mechanism of cis-$RuH(OAr)(PMe_3)_4$(Ar=C_6H_5, C_6H_4-p-Me) and cis-$RuH(OC_6H_4\text{-}p\text{-}CN)(PMe_3)_4$($HOC_6H_4$-p-CN).", *Organometallics* **10,** 404 (1991).

K. OSAKADA, Z.-H. ZHOU, and T. YAMAMOTO, "Structure of 5,5′-Dibromo-2,2′-bipyridine.", *Acta Cryst.* **C47,** 454 (1991).

K. OSAKADA, Y. OZAWA, and A. YAMAMOTO, "Preparation and Properties of Ethylpalladium Thiolate Complexes. Reaction with Organic Halides leading to C-S Bond Formation; Crystal Structure of trans-$[PdEt(Br)(PMe_3)_2]$.", *J. Chem. Soc. Dalton Trans.* 759 (1991).

K. OSAKADA and T. YAMAMOTO, "Preparation of ZnS and CdS by Thermal Degradation of (Methanethiolato)zinc and -cadmium Complexes, $[M(SMe)_2]_n$ (M=Zn, Cd).", *Inorg. Chem.* **30,** 2328 (1991).

K. OSAKADA, Y. OZAWA, and A. YAMAMOTO, "Molecular Structure and Carbonylation of Ethyl (benzenethiolato) palladium(II) Complex, trans-$PdEt(SPh)(PMe_3)_2$.", *Bull. Chem. Soc. Jpn.* **64,** 2002 (1991).

A. YAMAMOTO, F. OZAWA, K. OSAKADA, L. HUANG, T.-I. SON, N. KAWASAKI, and M.-K. DOH, "Mechanisms of Double and Single Carbonylation Reactions Catalyzed by Palladium Complexes.", *Pure & Appl. Chem.* **63,** 687 (1991).

T. TANAKA and K. TANAKA, "Simulation of the Nitrogen Cycle in Microbial Systems", *Pure & Appl. Chem.* **62,** 1059 (1990).

H. ISHIDA, T. TERADA, K. TANAKA, and T. TANAKA, "Photochemical CO_2 Reduction Catalyzed by $[Ru(bpy)_2(CO)_2]^{2+}$ Using Triethanolamine and 1-Benzyl-1,4-dihydronicotineamide as an Electron Donors", *Inorg. Chem.* **29,** 1059 (1990).

K. TANAKA and S. TANAKA, "Redox potential of Fe_4S_4 Cluster in Hydrophobic and Hydrophilic Spheres", *Bull. Chem. Soc. Jpn.* **64,** 1192 (1991).

H. NAGAO, H. MIYAMOTO, and K. TANAKA, "Carbon Dioxide Fixation Competed with Proton Addition to Methyl Acrylate", *Chem. Lett.* 322 (1991).

K. TANAKA, N. KOMEDA, and T. MATSUI, "Electrochemical Assimilatory and Dissimilatory Reductions of NO_3^- and NO_2^- *via* a Possible Free NO Intermediate", *Inorg. Chem.* **30,** 3282 (1991).

T. TAKAHASHI, T. SEKI, Y. NITTO, M. SABURI, C.J. ROUSSET, and E. NEGISHI, "Remarkably "Pair"-Selective and Regioselective Carbon-Carbon Bond Forming Reactions of Zirconacyclopentane Derivatives with Grignard Reagents", *J. Am. Chem. Soc.* **113,** 6266 (1991).

T. TAKAHASHI, N. SUZUKI, M. KAGEYAMA, Y. NITTO, M. SABURI, and E. NEGISHI, "Catalytic Hydrogenation of Alkenes Using Zirconocene-Alkene Complexes", *Chem. Lett.* 1579 (1991).

H. MIYAGI, Y. ISHII, T. AOSHIMA, Y. MIZOBE, and M. HIDAI, "Regioselective Complexes via Alkenyldiazenido Complexes", *Chem. Lett.* 611 (1991).

Y. ISHII, Y. KOBAYASHI, M. IWASAKI, and M. HIDAI, "Novel Ketene Formation by Reactions of Acid Chlorides with Low-Valent Platinum Complexes", *J. Organometal. Chem.* **405,** 133 (1991).

T. AOKI, Y. ISHII, Y. MIZOBE, and M. HIDAI, "Oxidative Addition of Chlorobenzene on an Iron Cyclopentadienyl Cation to a Low-valent Palladium Complex", *Chem. Lett.* 615 (1991).

M. IWASAKI, Y. KOBAYASHI, J.P. LI, H. MATSUZAKA, Y. ISHII, and M. HIDAI, "Palladium-Catalyzed Cyclocarbonylation of 3-(Heteroaryl)allyl Acetates", *J. Org. Chem.* **56,** 1922 (1991).

A.C. STREET, Y. MIZOBE, F. GOTOH, I. MEGA, H. OSHITA, and M. HIDAI, "Silylation of Coordinated Dinitrogen by Silylcobalt Complexes", *Chem. Lett.* 383 (1991).

Y. MIZOBE, T. ISHIDA, Y. EGAWA, K. OCHI, T. TANASE, and M. HIDAI, "Syntheses of Zero-Valent Molybdenum Complexes with the DMF Ligand", *J. Coord. Chem.* **23,** 57 (1991).

Y. ISHII, C. GAO, M. IWASAKI, and M. HIDAI, "Novel Synthesis of Phenol Derivatives by Palladium-Catalyzed Cyclocarbonylation of Penta-2,4-dienyl Acetates", *J. Chem. Soc. Chem. Commun.* 695 (1991).

T. ISHIDA, Y. MIZOBE, T. TANASE, and M. HIDAI, "A Series of Novel Carbonyl Complexes Derived from Dinitrogen Complex trans-$[W(N_2)_2(Ph_2PCH_2CH_2PPh_2)_2]$", *J. Organomet. Chem.* 409 (1991).

H. MATSUZAKA, Y. MIZOBE, M. NISHIO, and M. HIDAI, "Novel Reactions of Alkynes on Dinuclear Ruthenium Centers Bridged by Thiolate Ligands", *J. Chem. Soc. Chem. Commun.* 1011 (1991).

S. NAGAOKA, Y. OKAUTI, S. URANO, U. NAGASHIMA, and K. MUKAI, "Kinetic and Ab Initio Study of the Prooxidant Effect of Vitamin E. Hydrogen Abstraction from Fatty Acid Esters and Egg Yolk Lecithin", *J. Am. Chem. Soc.* **112,** 8921 (1990).

U. NAGASHIMA, S. NAGAOKA, and S. KATSUMATA, "Investigation of Dynamic Process in Low-lying Ionic States of o-hydroxybenzaldehyde", *J. Phys. Chem.* **95,** 3532 (1991).

T. KATOH, U. NAGASHIMA, and M. MIMURO, "Fluorescence Properties of the Allenic Carotenoid Fucoxanthin: Implimentation for Energy Transfer in Photosynthetic Pigment Systems", *Photosynthesis Research* **27,** 221 (1991).

K. HONDA, K. KITAURA, and K. NISHIMOTO, "Monte Carlo Simulation of Liquid Water and an Evaluation of Thermodynamic Properties", *Mol. Sim.* **6,** 275 (1991).

K. FUKE, F. MISAIZU, K. TUKAMOTO, and K. KAYA, "Picosecond Measurements of Vibrationally-Resolved Proton-Transfer Rate of Jet-Cooled 1-Azacarbazole Dimer", *J. Chem. Phys.* **95,** 4074 (1991).

A. NAKAJIMA, K. FUKE, K. TSUKAMOTO, Y. YOSHIDA, and K. KAYA, "Photodissociation Dynamics of NH_3, NH_2D, NHD_2, and ND_3: Rovibronic Absorption Analysis of the $\tilde{A}$-$\tilde{X}$ Transition", *J. Phys. Chem.* **95,** 571 (1991).

H. UMEMOTO, A. MASAKI, T. OHNUMA, F. MISAIZU, and K. FUKE, "The Intramultiplet Mixing of $Zn(4^3P_J)$ by Collision with Ar", *J. Phys. B: At. Mol. Opt. Phys.* **24,** 1639 (1991).

H. UMEMOTO, A. MASAKI, T. OHNUMA, K. KUWAHARA, Y. WADA, F. MISAIZU, and K. FUKE, "The Intramultiplet Relaxation of $Cd(5^3P_2)$ by H_2 and D_2", *J. Chem. Phys.* **94,** 7951 (1991).

A. MASAKI, T. OHNUMA, Y. WADA, H. UMEMOTO, F. MISAIZU, and K. FUKE, "The Intramultiplet Relaxation of $Cd(5^3P_2)$ Induced by Collision with N_2 and CO", *J. Chem. Phys.* **95,** 372 (1991).

F. MISAIZU, K. MITSUKE, T. KONDOW, and K. KUCHITSU, "Formation of Negative Ions from $(CO_2)_m$ in Collision with High-Rydberg Atoms", *J. Chem. Phys.* **94,** 243 (1991).

F. MISAIZU, T. KONDOW, and K. KUCHITSU, "Formation of Negative Ions of Water Clusters by Electron Transfer from High-Rydberg Atoms", *Chem. Phys. Lett.* **178,** 369 (1991).

S. BANDOW, "Structural Phase Transition of Ultrafine MnF_2 Particles Induced by Size Reduction", *Jpn. J. Appl. Phys.* **30,** 788 (1991).

S. BANDOW and K. KIMUIRA, "Disappearance of Long Range Spin-Order in Ultrafine Magnetite Particles", *Z. Phys. D* **19,** 271 (1991).

H. HASEGAWA, N. SATOH, K. TSUJII, and K. KIMURA, "Fractal Analysis of the Coalescence Process of Au Nano-Meter Particles Dispersed in 2-Propanol", *Z. Phys. D,* **20,** 325 (1991).

Y. YAMASHITA, M. TOMURA, and S. TANAKA, "A Facile Preparation of Tetrathiafuluvalenes having Alkylthio Groups from 1,3-Dithiole-2-thiones using a Hight-pressure Reaction", *J. Chem. Soc. Perkin Trans. 1,* 3358 (1990).

E. HASEGAWA, K. OKADA, H. IKEDA, Y. YAMASHITA, and T. MUKAI, "Photosensitized [2+2] Cycloreversion Reactions of Arylated Cage Compounds in Nonpolar Solvents. Highly Efficient Adiabatic Exciplex Isomerization", *J. Org. Chem.* **56,** 2170 (1991).

Y. YAMASHITA, S. TANAKA, K. IMAEDA, and H. INOKUCHI, "Tetrathio-Derivatives of p-Quinodimethanes Fused with 1,2,5-Thiadiazoles. A Novel Type of Organic Semiconductors", *Chem. Lett.* 1213 (1991).

Y. YAMASHITA, S. TANAKA, K. IMAEDA, H. INOKUCHI, and M. SANO, "5,8-Bis(1,3-dithiol-2-ylidene)-5,8-dihydroquinoxalines: Novel Electron Donors with Low Oxidation Potentials", *J. Chem. Soc. Chem. Commun.* 1132 (1991).

K. AWAGA and Y. MARUYAMA, "High-Pressure Effects on the Canted Ferromagnetism in Manganese(II) Phthalocyanine", *Phys. Rev. B* **44,** 2589 (1991).

K. AWAGA and Y. MARUYAMA, "Ferromagnetic Interaction in an α-Nitronyl Nitroxide under High Pressure", *Synth. Metals* **43,** 3249 (1991).

M. KINOSHITA, P. TUREK, M. TAMURA, K. NOZAWA, D. SHIOMI, Y. NAKAZAWA, M. ISHIKAWA, M. TAKAHASHI, K. AWAGA, T. INABE, and Y. MARUYAMA, "An Organic Radical Ferromagnet", *Chem. Lett.* 1225 (1991).

P. TUREK, K. NOZAWA, D. SHIOMI, K. AWAGA, T. INABE, Y. MARUYAMA, and M. KINOSHITA, "Ferromagnetic Coupling in a New Phase of the *p*-Nitrophenyl Nitronyl Nitroxide Radical", *Chem. Phys. Lett.* **180,** 327 (1991).

K. AWAGA and Y. MARUYAMA, "Pressure-Induced Enhancement of the Ferromagnetic Intermolecular Interaction of an α-Nitronyl Nitroxide Organic Radical", *Chem. Mater.* **2,** 535 (1990).

H. OKAMOTO, K. TORIUMI, T. MITANI, and M. YAMASHITA, "Optical and Magnetic Properties of the Halogen-Bridged Metal Complexes Modified by Hydrogen Bondings: {M(1R,2R-cyclohexanediamine)$_2$Br}Br$_2$(M=Pt, Pd, and Ni)", *Phys. Rev.* **B42,** 10381 (1990).

H. OKAMOTO, T. MITANI, Y. TOKURA, S. KOSHIHARA, T. KOMATSU, Y. IWASA, T. KODA, and G. SAITO, "Anomalous Dielectric Response in Tetrathiafulvalene-p-Chloranil as Observed in Temperature- and Pressure-Induced Neutral-to-Ionic Phase Transition", *Phys. Rev.* **B43,** 8224 (1991).

H. OKAMOTO, K. OKANIWA, T. MITANI, K. TORIUMI, and M. YAMASHITA, "Photo-Induced Gap State in the Mott-Hubbard System of Halogen-Bridged Ni^{3+} Complex ([Ni(chxn)$_2$Br]Br$_2$)", *Solid State Commun.* **77,** 465 (1991).

H. OKAMOTO, K. TORIUMI, K. OKANIWA, T. MITANI, and M. YAMASHITA, "A New 1-D Conducting State Stabilized by Strong H-Bondings in Halogen-Bridged Metal Complexes", *Synth. Met.* **42,** 2791 (1991).

K. OKANIWA, H. OKAMOTO, T. MITANI, K. TORIUMI, and M. YAMASHITA, "IR Study of the H-Bond Coupled with the Mixed-Valence State of Halogen-Bridged Metal Complexes", *J. Phys. Soc. Jpn.* **60,** 997 (1991).

S. KOSHIHARA, Y. TOKURA, Y. IWASA, T. KODA, G. SAITO, and T. MITANI, "Domain-Wall Excitations in Organic Charge-Transfer Compound Investigated by Photo-Reflectance Spectroscopy", *Synth. Met.* **41,** 2351 (1991).

K. FUKUI, T. SAITO, S. KONDO, Y. FUJII, Y. SAKISAKA, and M. WATANABE, "Core Absorption Spectra of Crystalline and Amorphous GeTe Thin Films", *J. Phys. Soc. Jpn.* **59,** 4161 (1990).

H. NAKAGAWA, M. FUJITA, T. MIYANAGA, H. MATSUMOTO, K. FUKUI, and M. WATANABE, "Photo-Induced Production of CN^--Ions on the Crystal Surface of KCl", *Rev. Solid State Sci.* **4,** 741 (1990).

H. NAKAGAWA, A. FUKUMOTO, A. OHNISHI, K. FUKUI, H. MATSUMOTO, M. FUJITA, T. MIYANAGA, and M. WATANABE, "Luminescence from Surface CN^- Centers Created Photochemically on Alkali Halide Crystals", *J. Lumi.* **48/49,** 811 (1991).

M. FUJITA, H. NAKAGAWA, N. KITAGATA, H. MATSUMOTO, T. MIYANAGA, K. FUKUI, and M. WATANABE, "Fine Structures of Cd_2^+ 4d Core Excitons in $CdCl_2$-$CdBr_2$ Mixed Crystals and CdI_2 Crystal", *J. Phys. Soc. Jpn.* **60,** 1792 (1991).

M. KAMADA and S. HIROSE, "Temperature Dependence of Ultraviolet Emission from CN^- in Surface Layers of NaCl and KCl", *J. Phys. Soc. Jpn.* **60,** 3178 (1991).

K. ICHIKAWA, O. AITA, M. KAMADA, and K. TSUTSUMI, "Surface Core Exciton in LiCl Studied by Photoelectron Spectroscopy", *Phys. Rev.* **B43,** 5063 (1991).

M. NISHIJIMA, S. TANAKA, N. TAKAGI, and M. ONCHI, "Chemical Reactivity of the Si(100)-K Surface", *Surf. Sci.* **242,** 498 (1991).

A. HIRAYA, K. FUKUI, P.-K. TSENG, T. MURATA, and M. WATANABE, "K-Absorption Spectrum of Solid Neon", *J. Phys. Soc. Jpn.* **59,** 1824 (1991).

A. HIRAYA and K. SHOBATAKE, "Direct Absorption Spectra of Jet-cooled Benzene in 130–260 nm", *J. Chem. Phys.* **94,** 7700 (1991).

A. HIRAYA and K. SHOBATAKE, "Direct Absorption Spectra of S_2 and S_3 States of Benzene Clusters", *Chem. Phys. Lett.* **178,** 543 (1991).

Review Articles and Textbooks

E. HIROTA, "Dynamical Molecular Structures Studied by High Resolution Spectroscopy", *J. Mol. Struct.* **223,** 149 (1990).

E. HIROTA, "An Elementary Aspect of Short-lived Molecules—Their Structures and Roles in Chemical Reactions", in "New Areas in Science Opened by Light and Beam (in Japanese)", *4th Open Symposium on "University and Science"*, Kubapuro, p.14 (1990).

E. HIROTA, "Topics Concerning Carbon", *Chemistry* (in Japanese) **46,** 508 (1991).

M. TAKAYANAGI and I. HANAZAKI, "Photochemical Processes in Weakly Bound Binary Complexes", *Chem Rev.* **91,** 1193 (1991).

N. NISHI, "Photochemical and Photophysical Processes of Surface Molecules on Condensed Molecular Solids" in "Chemistry of Excitation Processes on Solid Surfaces" *KIKAN KAGAKU SOSETSU* **12,** 57 (1991).

J. INANAGA, "Carbon-Carbon Bond-Formation via SmI_2-Promoted Electron Transfer Process", in "Trends in Organic Chemistry", **Vol. 1,** J. Menon Ed., Council of Scientific Research Integration, pp.23-30 (1990).

J. INANAGA, "Samarium-Mediated Acyclic Stereoselection in Radical Reaction", *Organometallic News* (in Japanese) 200 (1990).

J. INANAGA, "Preparation and Reaction of Organolanthanoid Complexes", *Kidorui* (in Japanese), 49 (1990).

J. INANAGA, "Lanthanide One-Electron Transfer Agent: Samarium Diiodide", *Yuki Gosei Kagaku Kyokaishi* (in Japanese) **48,** 1024 (1990).

S. TOMODA and K. KIMURA, "Proton Transfer in Ionic States of Hydrogen-Bonded Dimers. A Photoelectron Spectroscopic Approach", in "Vacuum Ultraviolet Photoionization and Photodissociation of Moleucles", ed. by C.-Y. Ng, World Scientific, p.101 (1991).

K. KIMURA, "Photoionization Spectroscopic Study of Molecules and Molecular Clusters by Synchrotron Radiation" (in Japanese), *Hyoumen,* Vol. **5,** p.328 (1990).

K. KIMURA, "Diagnostics of Molecules by Laser Photoelectron Spectroscopy" (in Japanese), *Gendai Kagaku,* Tokyo Kagaku Doujin, p.38 (1990).

K. SHOBATAKE, A. HIRAYA, K. TABAYASHI, and T. IBUKI, "Absorption and Fluorescence Studies of Molecules and Molecular Clusters," in "Vacuum Ultraviolet Photoionization and Photodissociation of Molecules and Clusters", ed. by C. Y. Ng, World Scientific Pub., p.503 (1991).

K. SHOBATAKE and T. URISU, "Surface Photochemical Reactions and their Applications to Semiconductor Process Technologies," in "Synchrotron Radiation — Applications to Chemistry", ed. by H. Inokuchi, Gakkai Shuppan (in Japanese), p.181 (1991).

S. SATO, "Photocatalytic Water Splitting over Powdered Semiconductors", *Shokubai (Catalyst)* (in Japanese) **33,** 209 (1991).

H. OHTAKI, "Looking at Dissolution and Nucleation Processes of Sodium Chloride Crystals", (in Japanese) *Suuri-Kagaku,* **334,** 42-47 (1991).

H. OHTAKI and H. MASUDA, "Local Structure of Macromolecule-Metal Complexes in Solution" in "Macromolecular Complexes — Dynamic Interactions and Electronic Processes" E. Tsuchida Ed., VCH, New York, USA, pp.175-210 (1991).

E. KIMURA and T. KOIKE, "Macrocyclic Polyamines as a Probe for Equibrium Study of the Acid Function of Zinc(II) ion in Hydrolysis Enzymes", *Comments Inorg. Chem.* **11,** 285 (1991).

K. OSAKADA and T. YAMAMOTO, "Transition Metal Complexes with Sulfur-Containing Ligands and their Relevance to Metal Sulfides.", *Yukagaku* (in Japanese) **39,** 831 (1990).

K. TANAKA, "Electrochemical CO_2 Reduction Catalyzed by Ru Metal Complexes", *Denki Kagaku* (in Japanese) **58,** 989-996 (1990).

K. TANAKA, "Chemical Simulation of Nitrogen Cycle Catalyzed by Coordination Compounds", *Yukagaku* (in Japanese) **39,** 777-783 (1990).

K. TANAKA, "CO_2 Fixation by Artificial Photosynthesis" *Kagaku* (in Japanese) **46,** 313-316 (1991).

T. TAKAHASHI, "Selective Preparation of Cu, Cu_2O or CuO from Organocopper Compounds at Low Temperature", *Ceramics* (in Japanese) **26,** 614 (1991).

Institute for Molecular Science, Myodaiji, Okazaki 444, Japan